



**UCL**

**Reconfiguration of amino acid  
biosynthesis in TGF- $\beta$ <sub>1</sub>-induced  
myofibroblasts**

**Mr Greg Contento**

**A thesis submitted to University College, London, for the  
degree of Doctor of Philosophy**

Centre for Inflammation and Tissue Repair

UCL Respiratory

Division of Medicine

University College London

## Acknowledgements

I would like to thank first and foremost my supervisor, Professor Rachel Chambers for her guidance, support and devotion to the success and growth of her students. If ever the commitment, rigor and deservedness of earning a PhD title comes into question, Prof Chambers should be consulted. Your attention to detail and consciousness to every biological possibility has taught me much about the foundations of the scientific process.

I would like to thank my parents for their unyielding support and love. In light of this PhD, I would like to thank my mother, Professor Guillermina Girardi, who was the first to show me the wonders and rewards of a scientific career. You helped embolden me to my every success and helped remedy my every failure. I would also like to thank my father, Rolando whose love of learning, debate and philosophy inspired me greatly. Thank you to my sisters, Julieta and Martina, for having supported me every step of the way.

Thank you to the members of UCL Respiratory for your willingness to help and assist one another and foster a comfortable environment for scientific research. I would like to thank my friend, Dr Anwen Brown for her invaluable emotional support throughout the ups and downs inherent to a PhD pursuit.

Thank you to GSK and the BBSRC for funding my studies and allowing me to explore the hypotheses I formed and giving me the tools to answer burning curiosities.

## **Declaration**

I confirm that the work contained in this thesis is entirely my own. Where information has been derived from other sources, I confirm that this has been indicated in this thesis.

## Abstract

At sites of tissue injury, the differentiation of fibroblasts into highly synthetic extracellular matrix (ECM)-producing myofibroblasts is essential for tissue repair and chiefly mediated by the pro-fibrotic cytokine, TGF- $\beta_1$ . In a fibrotic setting, these myofibroblasts fail to respond to pro-apoptotic signals during the resolution phase and relentlessly deposit ECM components, leading to destruction of healthy tissue and, in the case of lung fibrosis, respiratory failure and death. Differentiating myofibroblasts exhibit a reprogramming in their metabolic networks which, like cancer cells, is believed to support the biosynthetic and bioenergetic needs of a highly protein-synthesizing cell. Evidence suggests that the changes observed in glucose and glutamine metabolic networks are critical for fibrogenesis.

The present study shows that TGF- $\beta_1$  induces ATF4 protein levels via mTOR to upregulate the serine-glycine biosynthetic axis enzymes (PHGDH, PSAT1, PSPH, SHMT2) which are required for enhanced collagen synthesis. Pharmacological inhibition of PHGDH and siRNA-mediated silencing of PSAT1 both prevent TGF- $\beta_1$ -stimulated pHLFs from synthesizing enhanced levels of collagen protein.

Glycine is essential in the growth media for pHLFs to synthesize TGF- $\beta_1$ -enhanced collagen I levels. Glutamine, which supports the serine-glycine biosynthetic axis via its generation of glutamate, is critical for collagen synthesis and compensates for a withdrawal of glucose for pHLFs to synthesize TGF- $\beta_1$ -induced collagen I.

TGF- $\beta_1$  accelerates glutamine consumption and increases intracellular glutamate synthesis, an event facilitated by upregulating GLS1 and downregulating GLUL. GLS1-derived glutamate supports the biosynthetic pathways for alanine and proline, the latter mediated by GPT2 and required for TGF- $\beta_1$ -induced mTORC1 activation via a mechanism which is independent of the amino acid sensing Rag-GTPases. Furthermore, the group of enzymes to which GPT2 and PSAT1 belong, the aminotransferases, prevent TGF- $\beta_1$ -induced collagen synthesis upon pharmacological inhibition, an event rescued by exogenous addition of nonessential amino acids and  $\alpha$ -ketoglutarate.

Together, this work identifies the aminotransferases as a promising therapeutic target for fibrotic conditions by limiting the capacity for enhanced collagen synthesis

in fibroblasts. Further understanding the pro-fibrotic functions of the members of this enzyme family may yield promising results to aid in the development of therapeutic approaches and strategies.

## Impact Statement

The data presented in this thesis may educate therapeutic approaches aimed at targeting metabolic networks pivotal for myofibroblasts to deposit pathogenic levels of collagen. Targeting of the metabolic enzymes shown in this thesis to be required for TGF- $\beta_1$ -induced collagen synthesis in animal models could yield potential therapeutic value to be translated to the clinic for treating fibrotic diseases. Together, the data in this thesis support the notion that, much like in the oncology setting, targeting upregulated metabolic pathways can starve cells of metabolites necessary for meeting the biomolecular and bioenergetic demands of a highly protein-synthesizing cell, in this setting being a TGF- $\beta_1$ -stimulated myofibroblast, is a promising therapeutic approach.

Inside academia, this thesis established a method for quantifying nonessential amino acids intracellularly and extracellularly using HPLC. This methodology will help future projects characterise and validate the metabolic consequences of new compounds and conditions. This thesis further merged two cellular fractionation protocols to be able to immunoblot for chromatin-bound proteins, which confirmed the time-point at which the transcription factor ATF4 was likely initiating its gene regulatory functions. As such, this new method will allow quantification and detection of proteins (including transcription factors) in three intracellular fractions (cytosol, nucleus and chromatin-bound). This thesis highlights the resilience of metabolic networks in terms of compensatory pathways and bidirectional reactions which should be considered when analysing datasets that may educate a clinical strategy. Furthermore, the variance in growth medias among scientific labs reduces efficiency in replicating biological findings and increases the chances of generating artefactual data. This thesis stresses the importance of appropriate media selection and the significant effects on intracellular metabolic networks the concentration of two nutrients (glucose & glutamine) have. As such, a consensus may be reached whereby a more physiologically relevant growth media is used which may not only allow for a higher degree of cross-referencing between labs but also potentially enhance translational efficiency to the clinic.

## Table of contents

### Contents

Acknowledgements .....	2
Declaration .....	3
Abstract .....	4
Impact Statement .....	6
List of figures .....	11
List of tables .....	13
Abbreviations .....	14
Chapter 1: Introduction.....	17
1.1 Idiopathic Pulmonary Fibrosis. ....	17
1.1.1 Clinical manifestations.....	17
1.1.2 Treatments. ....	19
1.2 Pathogenesis of IPF. ....	20
1.2.1 Ageing. ....	20
1.2.2 Genetic predisposition. ....	21
1.2.3 Fibroblast differentiation. ....	21
1.2.4 Collagen biosynthesis. ....	22
1.3 TGF- $\beta_1$ signalling in IPF. ....	24
1.4 mTOR signalling.....	28
1.4.1 PI3K/Akt mTORC1 activation. ....	29
1.4.2 GTPases in mTORC1 activity.....	29
1.5 Metabolic reprogramming.....	32
1.6 Serine biosynthesis. ....	33
1.7 Glycine biosynthesis.....	35
1.8 Regulation of serine/glycine biosynthesis.....	35
1.9 Glutamine metabolism.....	39
1.9.1 Glutamine in nucleotide biosynthesis. ....	39
1.9.2 Glutaminolysis. ....	40
1.9.3 Glutamate in the mitochondria.....	41
1.10 Functions of $\alpha$ -ketoglutarate.....	45
1.11 Metabolic changes in pulmonary fibrosis.....	47
1.12 Summary, hypothesis and aims. ....	49
CHAPTER 2: Materials & Methods .....	50
Materials.....	50

2.1 Cell culture. ....	50
2.2 Cytokines. ....	50
2.3 Metabolites. ....	50
2.4 Pharmacological compounds. ....	51
2.5 Antibodies. ....	52
2.6 Primary human lung fibroblasts. ....	53
Methods ....	53
2.7 Cell culture conditions. ....	53
2.8 Preparation of cells for experiments. ....	54
2.9 Compound and metabolite preparation. ....	54
2.10 siRNA preparation. ....	55
2.11 Macromolecular crowding assay. ....	55
2.12 Immunoblotting. ....	56
2.13 Chromatin-bound protein fractionation. ....	57
2.14 qRT-PCR and analysis. ....	58
2.14.1 RNA isolation, purification and quantification. ....	58
2.14.2 DNase treatment. ....	58
2.14.3 cDNA synthesis. ....	59
2.14.4 Quantitative RT-PCR. ....	59
2.15 Quantification of hydroxyproline from cell supernatants. ....	60
2.16 Quantification of free amino acids. ....	62
2.17 Statistical analysis. ....	63
Chapter 3: Results. ....	64
Overview ....	64
3.1 The role of the serine biosynthetic pathway in mediating the pro-fibrotic effects of TGF- $\beta_1$ in human lung fibroblasts. ....	64
3.1.1 Introduction. ....	64
3.1.2 Physiological glucose and glutamine media supports TGF- $\beta_1$ -induced collagen I deposition. ....	66
3.1.3 TGF- $\beta_1$ increases the protein levels of the serine-glycine biosynthetic pathway via an mTOR-dependent mechanism. ....	69
3.1.4 TGF- $\beta_1$ increases ATF4 expression via an mTOR-dependent mechanism. ....	69
3.1.5 TGF- $\beta_1$ -induced <i>ATF4</i> mRNA levels are SMAD3-dependent. ....	71
3.1.6 TGF- $\beta_1$ induces ATF4 protein abundance from 8 hours onwards. ....	72
3.1.7 Loss of ATF4 via siRNA-mediated knockdown decreases pHLF cell viability. ....	76
3.1.8 PHGDH inhibition decreases TGF- $\beta_1$ -induced collagen I deposition. ....	78

3.1.9 HPLC optimised to detect and quantify nonessential amino acids. ....	80
3.1.10 TGF- $\beta_1$ increases intracellular glycine levels via an mTOR-dependent mechanism.....	83
3.1.11 Metabolite supplementation to siPSAT1-treated pHLFs does not rescue TGF- $\beta_1$ -induced collagen synthesis.....	86
3.1.12 Summary.....	88
3.2 The role of extracellular glycine, serine, glutamine and glucose in TGF- $\beta_1$ -induced collagen I deposition.....	89
3.2.1 Introduction.....	89
3.2.2 Glycine withdrawal decreases TGF- $\beta_1$ -induced collagen I deposition.....	89
3.2.3 Extracellular glycine is more valuable than serine for cells to mount a full TGF- $\beta_1$ -induced collagen response.....	92
3.2.4 Glutamine is critical for TGF- $\beta_1$ -induced collagen I deposition.....	92
3.2.5 Intracellular levels of glutamine, glutamate and proline are higher in TGF- $\beta_1$ -stimulated cells growing in supraphysiological levels of glucose and glutamine.....	95
3.2.6 Summary.....	100
3.3 The role of glutamine metabolism in TGF- $\beta_1$ -stimulated pHLFs.....	101
3.3.1 Introduction.....	101
3.3.2 Extracellular glutamine levels decrease at a faster rate in TGF- $\beta_1$ -stimulated cells.....	101
3.3.3 TGF- $\beta_1$ increases the mRNA levels of glutamine transporter genes.....	104
3.3.4 TGF- $\beta_1$ increases <i>GLS1</i> gene expression.....	106
3.3.5 TGF- $\beta_1$ modulates the mRNA levels of glutaminolysis pathway genes.....	108
3.3.6 TGF- $\beta_1$ modulates the protein abundance of GLS1, GPT2, GOT1, GOT2, GLUD1 and GLUL.....	110
3.3.7 GLS1 is critical for TGF- $\beta_1$ -induced collagen synthesis.....	110
3.3.8 Glutamate $\alpha$ -ketoglutarate supplementation rescue TGF- $\beta_1$ -induced collagen synthesis in CB-839-treated pHLFs.....	112
3.3.9 GLUD1 does not impact on TGF- $\beta_1$ -induced collagen synthesis.....	117
3.3.10 Supplementation of $\alpha$ -ketoglutarate regenerates intracellular glutamate levels following GLS1 inhibition in TGF- $\beta_1$ -stimulated cells.....	121
3.3.11 TGF- $\beta_1$ increases intracellular alanine and proline levels.....	123
3.3.12 Intracellular alanine, aspartate and proline levels are GLS1-dependent.....	123
3.3.13 Alanine supplementation rescues TGF- $\beta_1$ -induced collagen I deposition in CB-839-treated pHLFs.....	127
3.3.14 GPT2 regulates intracellular alanine levels.....	127
3.3.15 GPT2 is critical for TGF- $\beta_1$ -induced collagen synthesis.....	128

3.3.16 AOAA inhibits TGF- $\beta$ <sub>1</sub> -induced intracellular alanine levels and collagen synthesis. ....	136
3.3.17 AOAA and siGPT2 treatment inhibit TGF- $\beta$ <sub>1</sub> -induced mTORC1 activation. ....	136
3.3.18 Silencing of GOT1 and GOT2 does not impact on TGF- $\beta$ <sub>1</sub> -induced mTORC1 activation. ....	140
3.3.19 Silencing of RagA and RagB do not impact on TGF- $\beta$ <sub>1</sub> -induced mTORC1 activation. ....	140
3.3.20 Supplementation with nonessential amino acids and $\alpha$ -ketoglutarate rescues the inhibition on TGF- $\beta$ <sub>1</sub> -induced collagen synthesis in AOAA-treated pHLFs. ....	144
3.2.21 Summary. ....	147
Chapter 4: Discussion .....	148
Overview: .....	148
4.1 The role of the serine-glycine biosynthetic axis in mediating the pro-fibrotic effects of TGF- $\beta$ <sub>1</sub> in pHLFs.....	149
4.1.1 Introduction. ....	149
4.1.2 TGF- $\beta$ <sub>1</sub> -enhanced collagen synthesis and sensitivity to mTOR inhibition is maintained in physiological media.....	150
4.1.3 TGF- $\beta$ <sub>1</sub> increases the protein levels of the serine-glycine biosynthesis enzymes through an mTOR-dependent mechanism. ....	151
4.1.4 TGF- $\beta$ <sub>1</sub> increases ATF4 expression through an mTOR-independent and Smad3-dependent mechanism. ....	152
4.1.5 siRNA-mediated ATF4 silencing leads to cell death.....	154
4.1.6 Pharmacological inhibition of PHGDH attenuates TGF- $\beta$ <sub>1</sub> -induced collagen I deposition.....	155
4.1.7 TGF- $\beta$ <sub>1</sub> -increased intracellular glycine levels are mTOR and SHMT2 dependent. ....	157
4.1.8 Potential role for PSAT1 in TGF- $\beta$ <sub>1</sub> -induced collagen synthesis.....	159
4.2 Effect of extracellular serine, glycine, glucose and glutamine on TGF- $\beta$ <sub>1</sub> -induced collagen I deposition.....	160
4.2.1 Introduction. ....	160
4.2.2 Extracellular glycine is required for a full TGF- $\beta$ <sub>1</sub> -induced collagen I response. ....	160
4.2.3 Role of extracellular glutamine and glucose in TGF- $\beta$ <sub>1</sub> -induced collagen I deposition.....	161
4.3 Role of glutamine metabolism in TGF- $\beta$ <sub>1</sub> -induced pro-fibrotic parameters. ....	164
4.3.1 Introduction. ....	164
4.3.2 TGF- $\beta$ <sub>1</sub> increases extracellular glutamine depletion and glutamine transporter gene expression in pHLFs.....	164

4.3.3 TGF- $\beta_1$ increases the expression of the glutaminolysis pathway. ....	165
4.3.4 TGF- $\beta_1$ -induced GLS1-derived glutamate is critical for enhanced collagen I deposition.....	167
4.3.5 Alanine is conditionally essential for TGF- $\beta_1$ -induced collagen I deposition..	168
4.3.6 Alanine modulates TGF- $\beta_1$ -induced mTORC1 activation via a Rags-independent mechanism. ....	172
4.3.7 Aminotransferase-derived $\alpha$ -ketoglutarate and nonessential amino acids are both required for TGF- $\beta_1$ -induced collagen I deposition. ....	173
4.4 Conclusion. ....	175
4.6 Future work. ....	177
References.....	179

### List of figures

Figure 1. 1 Alveolar tissue architecture changes due to interstitial fibrosis. ....	18
Figure 1. 2 Canonical and non-canonical TGF- $\beta_1$ signalling. ....	27
Figure 1. 3 PI3K/Akt and amino acid sensing modulation in mTORC1 signalling. ...	31
Figure 1. 4 Serine-glycine biosynthetic axis. ....	38
Figure 1. 5 Glutamine metabolism.....	44
Figure 1. 6 Sources and functions of $\alpha$ -ketoglutarate.....	46
Figure 3. 1. TGF- $\beta_1$ concentration-dependently increases collagen I deposition in physiological DMEM.....	67
Figure 3. 2. ATP-competitive mTOR inhibition decreases TGF- $\beta_1$ -induced collagen I deposition.....	68
Figure 3. 3. TGF- $\beta_1$ increases the protein abundance of the serine-glycine biosynthetic axis via an mTOR-dependent mechanism.....	70
Figure 3. 4. mTOR regulates TGF- $\beta_1$ -induced ATF4 expression via a post-transcriptional mechanism.....	73
Figure 3. 5. TGF- $\beta_1$ -induced ATF4 mRNA levels are Smad3-dependent.....	74
Figure 3. 6. TGF- $\beta_1$ -induced ATF4 is chromatin-bound from 8 hours onwards. ....	75
Figure 3. 7. siATF4 treatment decreases cell count. ....	77
Figure 3. 8. NCT-503 decreases TGF- $\beta_1$ -induced collagen I expression. ....	79
Figure 3. 9. HPLC conditions and absorbance resolution of nonessential amino acids.....	81
Figure 3. 10. Absorbance measurements of amino acid standards in HPLC have linearity.....	82
Figure 3. 11. TGF- $\beta_1$ -induced intracellular glycine levels are mTOR-dependent. ....	84
Figure 3. 12. TGF- $\beta_1$ -induced intracellular glycine levels are SHMT2-dependent. ...	85
Figure 3. 13. Metabolite supplementation to siPSAT1-treated cells does not rescue TGF- $\beta_1$ -induced collagen synthesis. ....	87
Figure 3. 14. Glycine is required in the media for a full TGF- $\beta_1$ -induced collagen response. ....	91

Figure 3. 15. Supplementation with glycine but not serine rescues the reduced levels of TGF- $\beta_1$ -induced collagen I deposition following withdrawal of both amino acids. ....	94
Figure 3. 16. Glutamine is critical for TGF- $\beta_1$ -induced collagen synthesis. ....	96
Figure 3. 17. Intracellular levels of glutamine, glutamate and proline are higher in TGF- $\beta_1$ -stimulated pHLFs growing in standard DMEM. ....	97
Figure 3. 18. Extracellular glutamine levels decrease at a faster rate in TGF- $\beta_1$ -stimulated pHLFs. ....	103
Figure 3. 19. TGF- $\beta_1$ increases the mRNA levels of <i>SLC38A5</i> , <i>SLC38A1</i> , <i>SLC1A5</i> . ....	105
Figure 3. 20 TGF- $\beta_1$ increases the mRNA levels of GLS1 and splice variants GAC and KGA. ....	107
Figure 3. 21. TGF- $\beta_1$ modulates key glutaminolysis pathway gene mRNA levels over time. ....	109
Figure 3. 22. TGF- $\beta_1$ modulated the protein abundance of key glutaminolysis pathway enzymes. ....	111
Figure 3. 23. CB-839 concentration-dependently decreases TGF- $\beta_1$ -induced collagen I deposition. ....	114
Figure 3. 24. siGLS1 treatment decreases TGF- $\beta_1$ -induced collagen synthesis. ...	115
Figure 3. 25. Cell-permeable $\alpha$ -ketoglutarate does not affect collagen synthesis or cell count up to 3mM. ....	116
Figure 3. 26. Glutamate and $\alpha$ -ketoglutarate supplementation rescue CB-839-treated TGF- $\beta_1$ -stimulated collagen synthesis. ....	117
Figure 3. 27. GLUD1 inhibition with R162 does not impact on TGF- $\beta_1$ -induced collagen synthesis. ....	119
Figure 3. 28. siGLUD1 treatment does not impact on TGF- $\beta_1$ -induced collagen synthesis. ....	120
Figure 3. 29. $\alpha$ -ketoglutarate supplementation rescues intracellular glutamate levels in CB-839-treated and TGF- $\beta_1$ -stimulated cells. ....	122
Figure 3. 30. TGF- $\beta_1$ increases intracellular alanine and proline levels. ....	125
Figure 3. 31. $\alpha$ -ketoglutarate supplementation rescues CB-839-treated and TGF- $\beta_1$ -stimulated intracellular levels of alanine, aspartate and proline. ....	126
Figure 3. 32. Alanine supplementation rescues TGF- $\beta_1$ -induced collagen I deposition in GLS1-inhibited cells. ....	130
Figure 3. 33. Alanine supplementation increases intracellular proline levels in CB-839-treated cells. ....	131
Figure 3. 34. GPT2 is a major regulator of intracellular alanine levels. ....	132
Figure 3. 35. siGPT2-inhibited TGF- $\beta_1$ -induced collagen synthesis is rescued by alanine supplementation. ....	133
Figure 3. 36. TGF- $\beta_1$ -induced GPT2 protein abundance is independent of extracellular alanine concentrations. ....	134
Figure 3. 37. AOAA treatment depletes intracellular alanine levels. ....	135
Figure 3. 38. AOAA treatment inhibits TGF- $\beta_1$ -stimulated collagen synthesis. ....	138
Figure 3. 39. AOAA inhibits TGF- $\beta_1$ -induced mTORC1 activation as determined by assessing 4E-BP1 phosphorylation. ....	139
Figure 3. 40. Alanine supplementation rescues siGPT2-treated TGF- $\beta_1$ -induced mTORC1 activity. ....	141

Figure 3. 41. Dual silencing of GOT1 and GOT2 does not impact on TGF- $\beta_1$ -induced mTORC1 activation.....	142
Figure 3. 42. Dual silencing of RagA and RagB does not impact on TGF- $\beta_1$ -induced mTORC1 activation.....	143
Figure 3. 43. Alanine and nonessential amino acid supplementation do not impact on AOAA-treated TGF- $\beta_1$ -induced collagen I deposition.....	145
Figure 3. 44. Nonessential amino acid supplementation with $\alpha$ -ketoglutarate rescues AOAA-treated TGF- $\beta_1$ -induced collagen I deposition.....	146
Figure 4. 1. Proposed mechanism by which TGF- $\beta_1$ regulates collagen synthesis via metabolic pathways.....	176

### List of tables

Table 2. 1 Selectivity of AZD8055 data supplied by GSK in cell-free recombinant assays.....	51
Table 2. 2 Antibodies used for immunofluorescence in macromolecular crowding. .	52
Table 2. 3 Antibodies used for immunoblotting. ....	53
Table 2. 4 Preparation and storage conditions for inhibitors and metabolites. ....	55
Table 2. 5 Primer sequences for qRT-PCR.....	60
Table 2. 6 Conditions and buffers composition for HPLC detection of hydroxyproline. ....	62
Table 2. 7 Conditions and buffers composition for HPLC detection of amino acids. .	63
Table 3. 1. TGF- $\beta_1$ increases the expression of the serine-glycine biosynthetic pathway genes via an mTOR-dependent mechanism.....	65

## Abbreviations

**ADP**- Adenosine diphosphate

**AMPK**- AMP-activated protein kinase

**AOAA**- Aminoxyacetic acid

**ASNS**- Asparagine synthetase

**ATP**- Adenosine triphosphate

**ATF4**- Activating transcription factor 4

**AUC**- Area under curve

**BLM**- Bleomycin

**CRISPR**- Clustered regularly interspaced short palindromic repeats

**DAPI**- 4',6-diamidino-2-phenylindole

**DEPTOR**- DEP domain containing MTOR interacting protein

**DMEM**- Dulbecco's modified eagle medium

**ECM**- Extracellular matrix

**EDTA**- Ethylenediaminetetraacetic acid

**ETC**- Electron transport chain

**FBS**- Foetal bovine serum

**FDG**- Fluorodeoxyglucose

**FGFR**- Fibroblast growth factor receptor

**FTM**- Fibroblast to myofibroblast transition

**FVC**- Forced vital capacity

**GLS**- Glutaminase

**GLUD**- Glutamine dehydrogenase

**GLUL**- Glutamine synthetase

**GMP**- Guanosine monophosphate

**GOT**- Glutamic-oxaloacetic transaminase

**GPT**- Glutamic-pyruvic transaminase

**GTP**- Guanosine triphosphate

**HIF**- Hypoxia inducible factor  
**HK**- Hexokinase  
**HPLC**- High performance liquid chromatography  
**HRCT**- High-resolution computed tomography  
**HRP**- Horseradish peroxidase  
**ILD**- Interstitial lung disease  
**IMP**- Inosine monophosphate  
**IPF**- Idiopathic pulmonary fibrosis  
**IRES**- Internal ribosome entry site  
**ISR**- Integrated stress response  
**LAP**- Latency associated peptide  
**LDH**- Lactate dehydrogenase  
**LTBP**- Latent TGF- $\beta$  binding protein  
**ME**- Malic enzyme  
**MEM**- Minimum essential medium  
**MMP**- Matrix metalloproteinase  
**NAD**- Nicotinamide adenine dinucleotide  
**NADP**- Nicotinamide adenine dinucleotide phosphate  
**NASH**- Non-alcoholic steatohepatitis  
**NEAA**- Nonessential amino acids  
**NSCLC**- Non-small-cell lung cancer  
**OAT**- Ornithine aminotransferase  
**PDGF**- Platelet-derived growth factor  
**PHD**- Hypoxia-inducible factor prolyl hydroxylase  
**PHGDH**- Phosphoglycerate dehydrogenase  
**PHP**- Phosphohydroxypyruvate  
**PPP**- Pentose phosphate pathway  
**PS**- Phosphoserine  
**PSPH**- Phosphoserine phosphatase  
**PSAT**- Phosphoserine aminotransferase

**PTEN**- Phosphatase and tensin homolog  
**RAPTOR**- Regulatory-associated protein of mTOR  
**RHEB**- Ras homolog enriched in brain  
**ROS**- Reactive oxygen species  
**SAM**- S-adenosyl methionine  
**SHMT**- Serine hydroxymethyltransferase  
**TCA**- Tricarboxylic acid  
**TGF**- Transforming growth factor  
**THF**- Tetrahydrofolate  
**TIMPS**- Tissue inhibitor of metalloproteinase  
**TSC**- Tuberous sclerosis  
**UIP**- Usual interstitial pneumonia  
**UPR**- Unfolded protein response  
**UTR**- Untranslated region  
**XIAP**- X-linked inhibitor of apoptosis

# Chapter 1: Introduction

## 1.1 Idiopathic Pulmonary Fibrosis.

Idiopathic pulmonary fibrosis (IPF) is a life-threatening interstitial lung disease (ILD) caused by a progressive and chronic scarring of the lungs. It has unknown aetiology and carries a median survival of 3-5 years from diagnosis, a prognosis worse than that of breast or colon cancer [1]. While disease initiation is unknown, several risk factors have been identified such as cigarette smoking, gastroesophageal reflux and hepatitis C infection [2]. Indeed, patients with a smoking history have a 60% higher risk of developing IPF and are found to be 13-14 years younger at diagnosis compared with non-smokers [3]. IPF accounts for 55% of diagnoses of over 150 ILDs, with an estimated incidence rate of 4.6 cases per 100,000 people in the UK [3]. This rate is significantly higher in males and increases with age; less than 5% of cases are found in people aged below 50 years [1].

### 1.1.1 Clinical manifestations.

Patients with IPF usually suffer from chronic exertional dyspnoea, dry cough, inspiratory crackles and clubbing of the digits due to extended low blood oxygen levels [4]. The diagnostic procedure for IPF is complex as it requires exclusion of all other ILDs, involving the identification of a histopathological or radiologic pattern of usual interstitial pneumonia (UIP), as defined in the 2018 joint ATS/ERS/JRS/ALAT statement [2]. Radiologically, high-resolution computed tomography (HRCT) detects a basal sub-pleural reticulation in the lung with a heterogeneous net-like appearance of honeycombing [5]. Histologically, the presence of dense accumulations of myofibroblasts are the hallmark lesion of IPF, known as fibrotic foci. These myofibroblasts are typically enveloped in dense extracellular matrix (ECM) and are bound by irregularly shaped hyperplastic type II alveolar epithelial cells (Figure 1.1) [6]. Studies have shown that disease severity and progression correlate with the number of fibrotic foci [7].

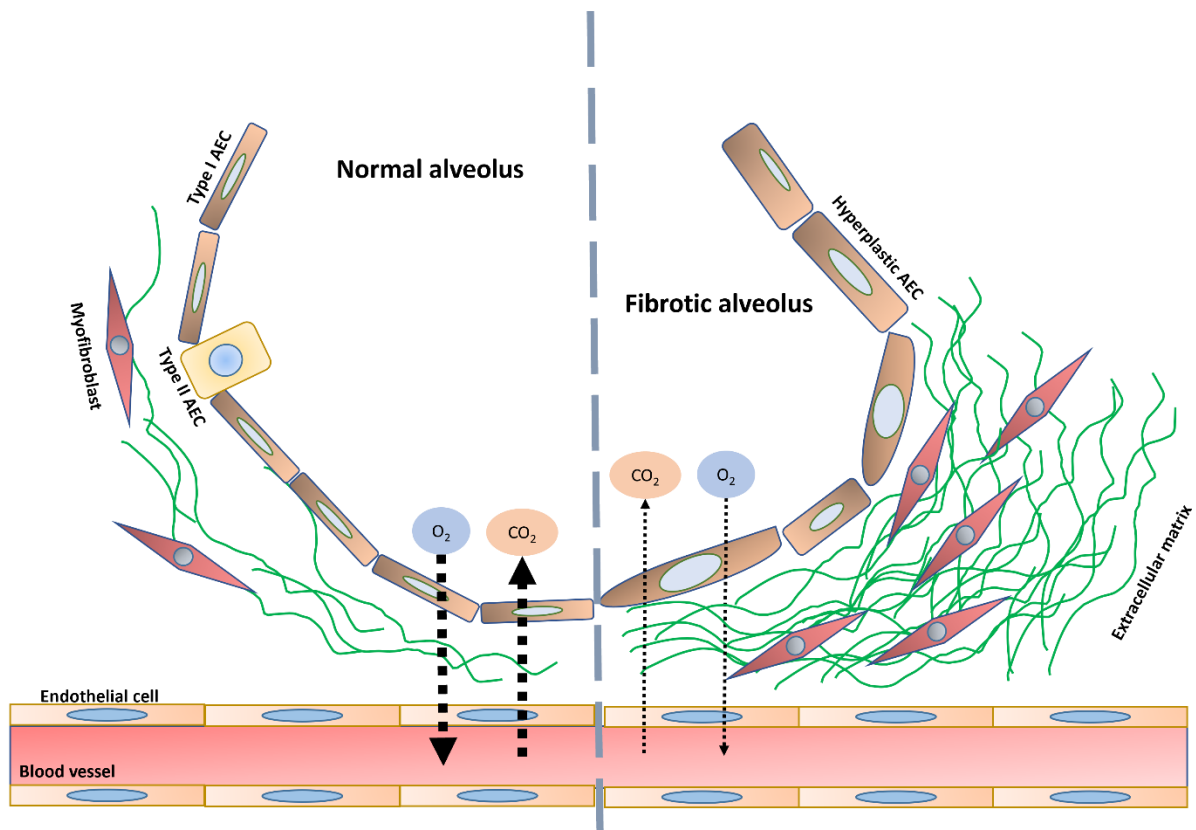


**Figure 1. 1 Alveolar tissue architecture changes due to interstitial fibrosis.**

Accumulation of myofibroblasts which deposit excessive amounts of extracellular matrix proteins leads to an impairment in gas exchange. Repetitive lung injury which is believed to start the fibrotic cascade results in the development of poorly differentiated and hyperplastic alveolar epithelial cells.

### 1.1.2 Treatments.

Until the 2010s, treatment options for patients with IPF were limited and were focused more on supportive measures such as oxygen therapy or lung transplantation. The commonly prescribed triple-therapy regime of azathioprine, N-acetyl-cysteine and prednisolone was shown to have minimal efficacy and even harmful effects and was thus abandoned following the PANTHER-IPF trial [8]. As of 2020 there are just two FDA-approved drugs for IPF which were shown to slow, but not halt, disease progression: nintedanib and pirfenidone. Both drugs produce an approximate 50% decrease in the rate of decline of forced vital capacity (FVC) in IPF patients [9]. Together, these drugs produce a small increase in survival compared to placebo as measured in the phase III international trials INPULSIS-1, INPULSIS-2 and ASCEND [9]. Both agents target aspects of the fibrotic cascade and were shown to decrease fibroblast and myofibroblast numbers and subsequently ECM accumulation *in vitro* [10]. Nintedanib is a triple receptor tyrosine kinase (RTK) inhibitor which targets the receptors for platelet-derived growth factor (PDGFR), fibroblast growth factor (FGFR) and vascular endothelial growth factor (VEGFR). *In vitro*, nintedanib was shown to limit fibroblast migration, fibroblast to myofibroblast differentiation (FTM) and fibroblast-mediated ECM deposition [11]. Pirfenidone has a poorly elucidated mechanism of action yet *in vivo* studies using the bleomycin-induced lung fibrosis model demonstrated a reduction in the levels of several cytokines and growth factors, including transforming growth factor  $\beta_1$  (TGF- $\beta_1$ ) [12]. While both agents offer the possibility of substantially limiting the rapid lung function decline in IPF patients, they may also produce significant gastrointestinal side effects. Patients prescribed nintedanib or pirfenidone opt for a reduction in dose or discontinuation of therapy roughly 50% and 40% of the time, respectively [13]. Therefore, while these current treatment options offer a degree of respite, the need for better therapeutics is pressing. Further research and a better understanding of the pathogenesis of IPF will aid in the development of new antifibrotic strategies.

## **1.2 Pathogenesis of IPF.**

IPF is accompanied by significant innate and adaptive immune response changes and whether these promote or are a consequence of fibrogenesis is actively debated [14]. The lack of efficacy of anti-inflammatory therapies such as corticosteroids, however, has largely disproved the thinking of chronic inflammation as a driver of disease progression [15, 16]. There have been recent calls to omit the term 'idiopathic' in IPF given the significant improvements to the understanding of the genetic, cellular and molecular mechanisms involved [17, 18]. The current understanding centres around a repetitive injury to the alveolar epithelium as the initiator of the disease. This injury occurs over decades of repetitive insults in the form of environmental factors, ageing and genetic predispositions. Chronic type II epithelial cell injury results in the increased release of pro-fibrotic mediators which lead to eventual fibroblast accumulation, fibrotic foci development and impaired lung function [19].

### **1.2.1 Ageing.**

Ageing, as a process in this disease context, can be viewed as impacting epithelial cell turnover which eventually reaches a limit, as a result of a failure in stem cell renewal efficiency which in turn culminates in abnormal reepithelization and hyperplastic cell formation [20]. Senescent cells are a consequence of ageing and have been shown to be in higher abundance in the IPF lung [21]. Senescent biomarkers p16, p21 and senescence-associated  $\beta$ -galactosidase activity (SA- $\beta$ -gal) have all been detected in epithelial cells of IPF tissue. Indeed, p16 expression was found to correlate with disease severity [21]. In the bleomycin lung fibrosis mouse model, treatment with the senolytic agents, dasatinib and quercetin, improved lung function and overall health, but did not decrease lung fibrosis [21]. Mitochondrial function also appears to decline with age and parameters such as biogenesis, ATP production, and respiration are all decreased in the IPF lung [22]. Protein synthesis quality additionally declines with age, leading to activation of the unfolded protein response (UPR), markers of which are elevated in epithelial cells in IPF tissue [23]. Together, these ageing processes promote epithelial cell dysfunction which in turn initiates the fibrotic cascade.

### 1.2.2 Genetic predisposition.

The genetic mutations which predispose to IPF offer great insight into its pathogenesis and further highlight the pulmonary epithelium as a likely initiator of the disease. A key genetic predisposition and the strongest known risk factor for developing IPF is the *MUC5B* promoter variant *rs35705950*, present in 41.9% of patients with IPF [24]. *MUC5B* encodes mucin secreted by epithelial cells which maintains the protective lining against potential irritants and pathogens. This variant leads to mucin overexpression and was shown to be actively transcribed in epithelial cells that are undergoing endoplasmic reticulum (ER) stress in IPF [25]. Another well-characterised mutation is in the surfactant protein C gene (*SFTPC*) which is expressed by type II alveolar epithelial cells. Surfactant proteins are essential for reducing surface tension in the alveoli to prevent structural collapse during expiration [26]. Mutations which affect the C-terminus are commonly found in IPF patients and impede post-translational modification efficiency of the surfactant, causing protein misfolding, aggregation and ER stress [27]. Mutations in the telomere genes *TERT* and *TERC* are also described in sporadic and familial IPF. Loss of function variants accelerate telomere shortening which may decrease mitotic capacity and hence repair of the epithelium [28].

Recently, a genome-wide association study (GWAS) identified three novel variants which increase the risk for developing IPF in the genes *DEPTOR*, *MAD1L1* and *KIF15* [29]. All resulted in decreased expression of their protein products. *DEPTOR* inhibits the kinase activity of mTOR, a protein shown to be critical for fibrogenesis in TGF- $\beta_1$ -stimulated lung fibroblasts [30]. Therefore, patients with this variant may have higher than normal levels of mTOR activation that may lead to an acceleration of fibrotic processes. *MAD1L1* and *KIF15* gene products are postulated to interfere with telomerase activity and mitotic spindle-assembly, respectively. These variants may promote fibrogenesis by decreasing the regenerative function of the epithelium and lead to senescent or apoptotic pathways.

### 1.2.3 Fibroblast differentiation.

A pivotal process in IPF development and progression is the differentiation of fibroblasts into myofibroblasts within the lung interstitium. Fibroblasts in healthy lung

tissue normally present in very low numbers. However, in response to repetitive epithelial injury, fibroblast numbers increase and these cells undergo differentiation into highly secretory and contractile myofibroblasts [31]. Normally, myofibroblasts undergo apoptosis once the injury has been repaired. In IPF, however, the injury is incessant and myofibroblasts appear to display evidence of being resistant to programmed cell death. Indeed, IPF myofibroblasts have been shown to overexpress the pro-survival protein BCL-2 as well as the cell cycle inhibitors p21 and p16, leading to a senescent, anti-proliferative and apoptosis-resistant cell still capable of its original extracellular matrix secretory functions [21]. Additionally, low expression of phosphatase and tensin homolog (PTEN), a negative regulator of the phosphoinositide-3-kinase (PI3K) pathway, was observed which leads to an inhibition of the pro-apoptotic and cell cycle arrest transcription factor regulator, FoxO3a [32].

The source of myofibroblasts in IPF is still not well defined and includes either resident fibroblasts, circulating CXCR4+ bone marrow derived fibrocytes and epithelial cells adopting mesenchymal properties [33]. Epithelial-mesenchymal transition (EMT) is a process where epithelial cells lose apical-basal polarity, N-cadherin junctions and exhibit morphological changes [34, 35]. Recent studies, however, showed that epithelial cells undergoing EMT produce much lower than expected levels of ECM components [36]. Additionally, lineage-tracing studies have shown these cells to contribute negligibly to the mesenchymal population [37]. Instead, epithelial cells undergoing EMT have been observed to contribute to increasing fibroblast numbers indirectly through the release of pro-fibrotic mediators that stimulate fibroblast recruitment, replication and differentiation such as TGF- $\beta_1$ , platelet-derived growth factor (PDGF) and connective tissue growth factor (CTGF) [36, 38]. The pro-fibrotic microenvironment is then maintained to allow myofibroblasts to be chronically activated and produce pathological levels of ECM components which ultimately destroy the normal alveolar architecture.

#### **1.2.4 Collagen biosynthesis.**

Collagens are a major component of the ECM alongside hydrating proteoglycans, hyaluronic acid and other matricellular proteins. Collagens are critical for tissue and organ stability and function. There are 28 known types of collagen and in the lung,

collagen types I and III account for nearly 95% of total lung collagen content [39, 40]. Collagen type IV and collagen type II are also found in the lung as components of basement membranes and cartilage supporting the airways, respectively. The ECM is constantly being laid down by fibroblasts and degraded by proteolytic enzymes such as matrix metalloproteinases (MMPs). In IPF, there is evidence of an imbalance in the levels of MMPs and its inhibitors, named tissue inhibitors of metalloproteinases (TIMPs), in favour of the TIMPS, which may accentuate the progressive deposition of pathological ECM [41].

ECM stiffness is also believed to play a role in IPF pathogenesis as it can promote fibroblast differentiation as well as activating the potent pro-fibrotic cytokine, TGF- $\beta_1$ , via the integrin  $\alpha\beta_5$  [42, 43]. Fibroblasts grown in pathologically relevant matrix stiffnesses *in vitro* have been shown to adopt functional changes similar to those of IPF-derived fibroblasts such as apoptosis resistance, increased proliferation and enhanced collagen synthesis [44]. This stiffening of the ECM may act as a threshold which, when exceeded, drives a positive-feedback fibrotic cascade leading to further ECM deposition and fibrosis.

Collagen I is the most abundant protein the human body and has been shown to be the dominant collagen type in the IPF lung [45]. It forms insoluble fibrils which aid in wound repair, tissue function and regeneration. Collagen I synthesis and deposition in the fibrotic lung is facilitated by myofibroblasts and this secretory rate is increased upon exposure to several mediators, chiefly TGF- $\beta_1$ . Collagen I is a heterotrimer of two  $\alpha_1(I)$  chains (encoded by the *COL1A1* gene) and one  $\alpha_2(I)$  chain (encoded by the *COL1A2* gene). Following transcription, collagen I mRNAs are capped at their 5' end and polyadenylated at their 3' end before engaging with ribosomes on the rough endoplasmic reticulum (rER) [45]. Translation then ensues with the growing polypeptide chain of 3,300 residues entering the lumen of the rER guided by a signal recognition domain which is later cleaved by a signal peptidase. The procollagen polypeptide, consisting mainly of glycine and proline repeats is then post-translationally modified by hydroxylation of its proline residues and glycosylation of its asparagine and lysine residues. Hydroxyproline residues may be further modified by addition of sugars such as galactose and galactosyl-glucose [46]. The hydroxylation reactions are critical for collagen helical stability and are facilitated by

Fe (II)- and  $\alpha$ -ketoglutarate-dependent dioxygenases which use  $O_2$ , vitamin C (ascorbic acid) and  $\alpha$ -ketoglutarate as substrates, releasing succinate and  $CO_2$ . Hydroxylation of proline at position 4, catalysed by prolyl 4-hydroxylase (P4HA), is particularly important for protein stability and triple helix formation via hydrogen bonding. Deficiency in vitamin C leads to inhibition of the activity of these crucial enzymes and hampers collagen biosynthesis, a defining feature of scurvy.

The completed polypeptides, known as procollagen, are eventually transported to the Golgi apparatus where they are packaged into secretory vesicles and secreted into the extracellular space. They are then proteolytically cleaved at their C-propeptide and N-propeptide terminals which causes spontaneous aggregation into collagen fibres. This aggregation is stabilised by the formation of covalent cross-links catalysed by lysyl oxidases.

### **1.3 TGF- $\beta_1$ signalling in IPF.**

TGF- $\beta_1$  is a pleiotropic cytokine with major functions in immune system regulation and cell growth. It is one of three TGF- $\beta$  isoforms and has been strongly implicated in the development of IPF [47]. In the development of lung fibrosis, TGF- $\beta_1$  is predominantly produced by alveolar macrophages, bronchial epithelial cells and type II alveolar epithelial cells [48]. By promoting the synthesis of ECM components, particularly of collagens, TGF- $\beta_1$  has also been implicated in, renal, cardiac and liver fibrosis and systemic conditions, such as scleroderma [49]. The central role of TGF- $\beta_1$  in driving fibrogenesis has been extensively demonstrated including attenuation of bleomycin-induced lung fibrosis through treatment of soluble TGF- $\beta_1$  receptors thus decreasing total amounts of active TGF- $\beta_1$  [50]. Overexpression of TGF- $\beta_1$  in the lungs of developing foetal monkeys led to a severe and progressive lung fibrosis [51]. TGF- $\beta_1$  greatly skews the balance towards ECM expansion by not only increasing the synthesis of ECM components but also by decreasing the expression of MMPs and increasing the expression of TIMPs [52]. Furthermore, TGF- $\beta_1$  promotes the release of other pro-fibrotic mediators, such as CTGF and PDGF, which may act synergistically to enhance fibroblast ECM synthesis [53]. Targeting TGF- $\beta_1$  has therefore been a much sought-after therapeutic strategy yet many concerns arise from global inhibition of TGF- $\beta_1$  signalling due to its importance in

controlling inflammation and promoting tumour suppression. Therefore, understanding the signalling pathways and changes induced by TGF- $\beta_1$  may allow selective targeting of the pro-fibrotic effects without dampening immune signalling and cancer suppressive roles.

TGF- $\beta_1$  is secreted in an inactive form complexed with the latency-associated peptide (LAP) and latent TGF- $\beta$  binding protein 1 (LTBP-1) which cross-link it to the ECM. Activation of TGF- $\beta_1$  can occur through several mechanisms including a low pH environment, proteolysis by MMPs (notably MMP-2 and MMP-9), reactive oxygen species (ROS) and mechanical forces induced by integrins which bind to the arginine-glycine-aspartate (RGD) domain in LAP (notably by  $\alpha\beta_5$  and epithelial  $\alpha\beta_6$  and  $\alpha\beta_8$ ) [54, 55]. Once released, TGF- $\beta_1$  binds to the type II TGF- $\beta$  (T $\beta$ RII) receptor homodimer which then forms a complex with a homodimer of type I TGF- $\beta$  (T $\beta$ RI) receptors, forming a heterotetrameric receptor complex. T $\beta$ RII has intrinsic serine/threonine kinase activity and is then able to phosphorylate T $\beta$ RI, which recruits and further phosphorylates the receptor-regulated Smads (R-Smads), Smad2 and Smad3. Once phosphorylated, the R-Smads bind to Smad4 and form a heterodimer which shuttles to the nucleus to modulate the expression of genes with Smad-binding element (SBE) regions [56]. TGF- $\beta_1$  has a refractory period where its receptor is internalized following stimulation, thus temporarily reducing cell responsiveness to further TGF- $\beta_1$  stimulation [57]. Smad proteins regulate the expression of multiple genes involved in ECM component synthesis, including collagen I [58]. In animal models, Smad3-null mice had greatly decreased radiation-induced fibrosis in the lungs, liver and kidney [59]. Interestingly, only knockdown of Smad3 and not of Smad2 reduced collagen I synthesis in TGF- $\beta_1$ -stimulated hepatic stellate cells [60]. Following target gene transcription, the Smad proteins are ubiquitinated and subsequently degraded by the proteasome [61].

TGF- $\beta_1$  additionally promotes other signalling pathways that are Smad-independent, or non-canonical (See Figure 1.2). T $\beta$ RII can be auto-phosphorylated on three tyrosine residues (Y259, Y336 and Y424) which can be bound by proteins with Src homology 2 (SH2) domains, such as growth factor receptor binding protein 2 (Grb2), leading to the activation of the MAPK cascade including MEK and ERK [62].

Recruitment of TGF- $\beta_1$ -activated kinase 1 (TAK1) leads to downstream activation of

JNK, p38 MAPK and NF- $\kappa$ B pathways [56]. Importantly, TGF- $\beta_1$  can activate the PI3K/mTOR axis which is commonly dysregulated in cancers and found to be active in IPF myofibroblasts as well as fibroblasts following TGF- $\beta_1$  stimulation *in vitro* [30]. The mTOR pathway downstream of TGF- $\beta_1$  will be a major focus of the work presented in this thesis and will therefore be discussed in further detail in the next section.

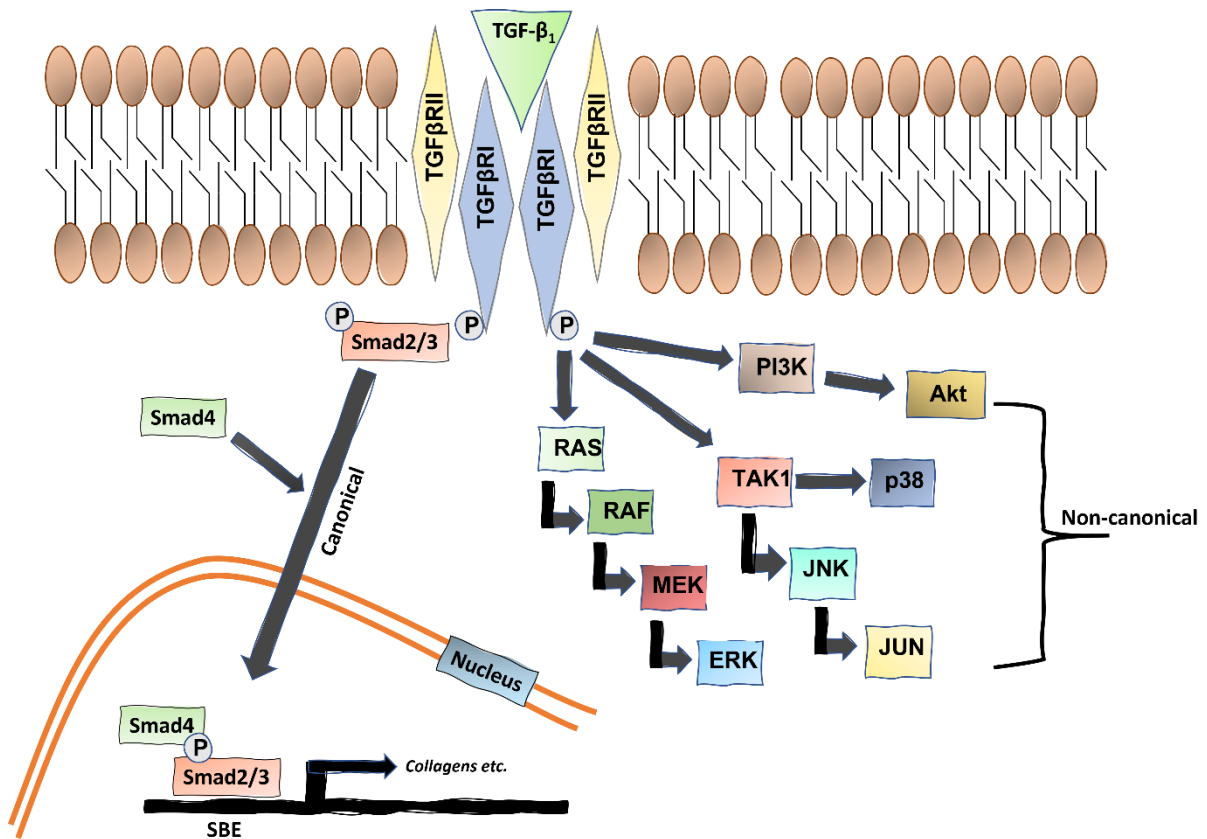


**Figure 1. 2 Canonical and non-canonical TGF-β<sub>1</sub> signalling.**

In canonical signalling, TGF-β<sub>1</sub> induces heterodimerization of the TGFβRI and TGFβRII receptors, leading to TGFβRI phosphorylation by TGFβRII. Smad2 or Smad3 are then phosphorylated and form a complex with Smad4, translocating to the nucleus and binding to smad binding element (SBE) regions of the DNA. In non-canonical signalling, phosphorylated TGFβRI receptors recruit signalling mediators such as phosphoinositide 3-kinase (PI3K), TGF-β<sub>1</sub>-activated kinase 1 (TAK1), extracellular signal-regulated kinase (ERK), Jun N-terminal kinase (JNK) or p38 mitogen-activated protein kinase (p38).

## 1.4 mTOR signalling.

The mammalian target of rapamycin (mTOR) is a serine/threonine protein kinase which belongs to the phosphoinositide 3-kinase-related kinase (PI3K) family. Together with different accessory proteins, mTOR forms either mTOR complex 1 (mTORC1) or mTOR complex 2 (mTORC2). These complexes regulate a host of biological processes such as protein synthesis, metabolism, autophagy, motility and cell growth [63]. Hyperactivation of mTOR is frequently detected in tumour cells with aberrant signalling of the upstream pathway activators, PI3K and Akt [64]. An inhibitor of this pathway, phosphatase and tensin homolog (PTEN) is frequently mutated in a loss-of-function manner to allow chronic activation of mTOR [65].

mTORC1 is formed by mTOR, rapamycin-sensitive adapter protein of mTOR (Raptor), mammalian lethal with Sec-13 protein 8 (mLST8), proline-rich AKT substrate 40kDa (PRAS40) and DEP domain TOR-binding protein (Deptor). This complex regulates cell growth, proliferation and survival and is activated by a host of stimuli, including growth factors, amino acids, intracellular energy, oxygen levels and stress signals [66]. A major function of mTORC1 is regulating protein translation via phosphorylation of eukaryotic translation initiation factor 4E (eIF4E)-binding protein 1 (4E-BP1) which dissociates it from eIF4E, a protein required for ribosome assembly and translation initiation. Once phosphorylated, 4E-BP1 dissociates from eIF4E and allows for cap-dependent translation initiation [67]. Another prominent function of mTORC1 is regulation of autophagy through phosphorylation and inhibition of autophagy-initiating kinase (ULK1) and phosphorylation of ATG14, a component of PIK3C3 which is critical for autophagosome nucleation and maturation.

mTORC2 is formed by mTOR, rapamycin-insensitive companion of mTOR (Rictor), mLST8, Deptor, stress-activate protein kinase-interacting protein 1 (mSin1) and protein-binding Rictor (Protor-1). It is best described as a regulator of the actin cytoskeleton and aspects of metabolism and proliferation through phosphorylating AGC kinases such as Akt, serum and glucocorticoid-induced protein kinase (SGK) and protein kinase C (PKC).

Both mTOR complexes have been found to be activated in lung fibroblasts following TGF- $\beta_1$  stimulation and pharmacological inhibition of the mTOR kinase prevented TGF- $\beta_1$  induced collagen synthesis [30, 68]. Furthermore, it was observed that

knocking out the mTORC1 component, Raptor, decreased TGF- $\beta$ <sub>1</sub>-induced collagen I deposition in pHLFs, an effect not replicated by knocking out the mTORC2 component, Rictor [30]. Additionally, mTORC1-induced phosphorylation of 4E-BP1 was demonstrated to be the critical pathway downstream of mTORC1 for TGF- $\beta$ <sub>1</sub>-induced collagen I deposition.

#### **1.4.1 PI3K/Akt mTORC1 activation.**

mTORC1 can be activated via the PI3K/Akt signalling cascade and is dysregulated in IPF [68, 69]. PI3K refers to class 1 PI3 kinases which are composed of a single p110 $\alpha$ - $\delta$  catalytic subunit and a p85 regulatory subunit that binds to phosphorylated tyrosine residues via SH2 and SH3 domains. The p110 subunit phosphorylates phosphatidylinositol-4,5-bisphosphate (PIP<sub>2</sub>) to produce phosphatidylinositol-3,4,5-triphosphate (PIP<sub>3</sub>), which is able to recruit and bind to cell membrane protein with pleckstrin homology (PH) domains, such as the serine/threonine kinase Akt [70]. In immunoprecipitation studies, p85 was found to be constitutively bound to T $\beta$ RII and later associated with T $\beta$ RI upon TGF- $\beta$ <sub>1</sub> binding [71]. Once Akt binds via its PH domain to PIP<sub>3</sub>, it undergoes a conformational change which exposes its T308 residue for phosphorylation by phosphoinositide-dependent kinase-1 (PDK1) [70]. Akt can then be further phosphorylated by mTORC2 at its S473 residue to fully activate it. Once its T308 residue is phosphorylated, Akt can activate mTORC1 by phosphorylating and therefore inactivating tuberous sclerosis complex 2 (TSC2), a suppressor of Ras homolog enriched in brain (RHEB) which activates mTORC1 [72]. Akt can also aid in mTORC1 activation via phosphorylating PRAS40, a component of mTORC1 (Figure 1.1).

#### **1.4.2 GTPases in mTORC1 activity.**

Activation of mTORC1 occurs at the lysosomal surface where it encounters RHEB which is weakly-bound to the lysosomal membrane via its farnesylated C-terminal [73]. The activity of RHEB is determined by whether it is GTP or GDP-loaded, a state controlled by the GTPase-activating protein (GAP) complex TSC, a heterodimer consisting of TSC1 and TSC2. TSC has numerous serine and threonine residues

which may be phosphorylated to impact the GTP-loading function of RHEB, thus activating it [74]. Energy stress signals leading to 5' AMP-activated protein kinase (AMPK) activity promote TSC inhibition, an off-mechanism to prevent mTORC1 activity in times of low cellular energy [75]. Conversely, TSC is activated by Akt, a common event in growth factor signalling and an indication to enable active cellular growth.

mTORC1 interacts with another critical GTPase at the lysosomal surface, the obligate heterodimeric Rag proteins, with RagA or RagB pairing with RagC or RagD [76, 77]. While the exact mechanism is still under investigation, the Rag GTPases activate mTORC1 by binding to the subunit RAPTOR. However, recent work has shown that RagA/RagB binding to mTORC1 causes no conformational changes and likely induces mTORC1 activation by localising it to the lysosomes to be allosterically activated by RHEB [76]. Like RHEB, the activity of these heterodimers is dependent on whether they are GTP or GDP-loaded, a state controlled by GAPs such as GATOR1 or guanine exchange factors (GEFs) like SLC38A9 and Ragulator. The Rag GTPases are responsive to amino acid levels and have been shown to be modulated by levels of intracellular leucine, arginine and S-adenosylmethionine (SAM), sensed by Sestrin2, cytosolic arginine sensor for mTORC1 subunit 1 (CASTOR1) and SAMTOR, respectively [78]. These three proteins influence Rag GTP-loading by interacting with either GATOR2 (Sestrin2/CASTOR1) or GATOR1 (SAMTOR) (Figure 1.1) [79]. SLC38A9 is a transmembrane transporter found on the lysosomal surface which has a large N-terminal domain allowing for binding to the Rag-Ragulator complex. It senses arginine and its overexpression has been shown to activate mTORC1 in the absence of an amino acid input [80]. Additionally, cells expressing a RagB mutant constitutively bound to GTP resulted in amino acid insensitive-mTORC1 activation [78]. These findings illustrate the dominant role the Rag-Ragulator complex plays in mTORC1 regulation.

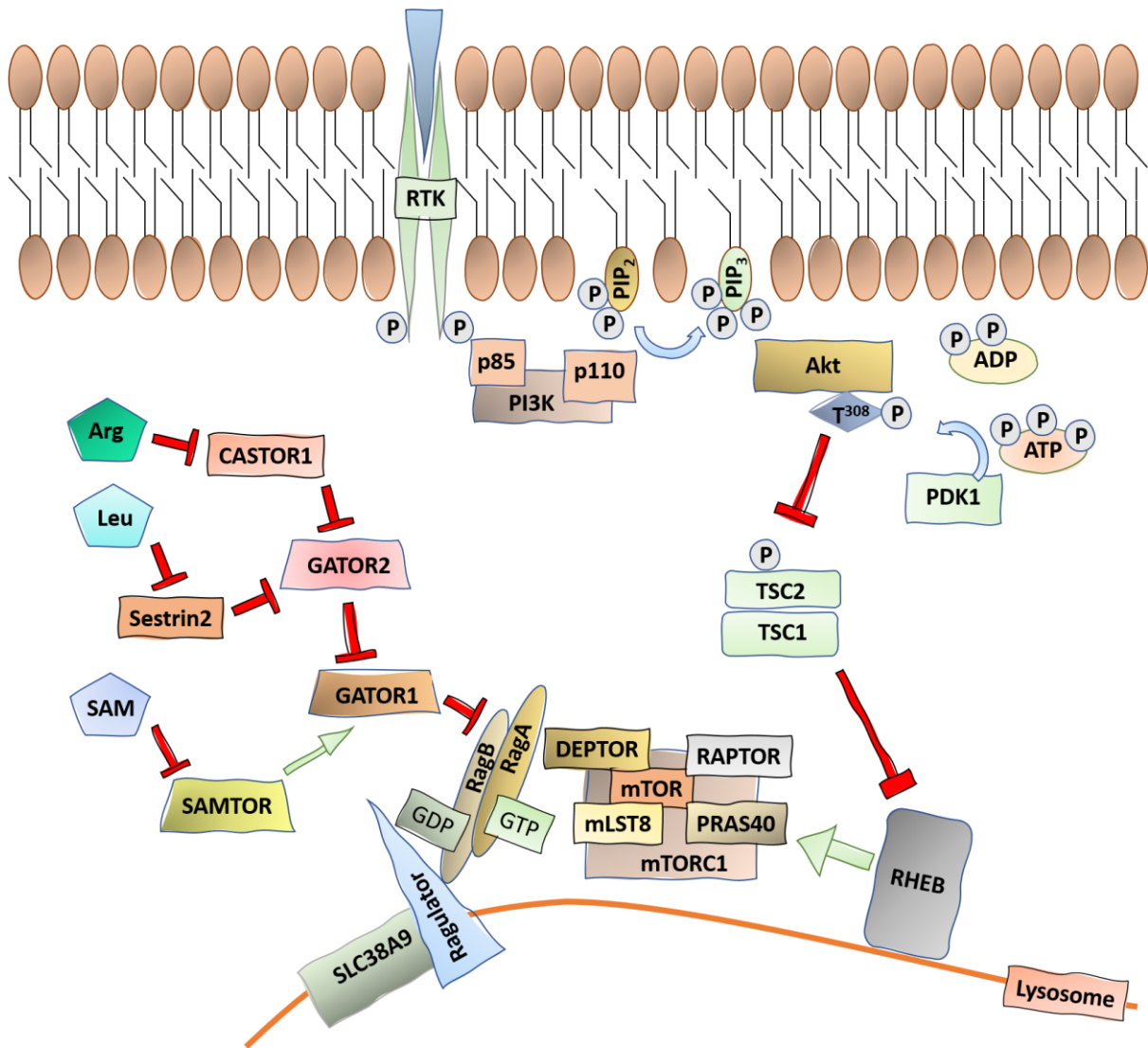


**Figure 1. 3 PI3K/Akt and amino acid sensing modulation in mTORC1 signalling.**

Receptor tyrosine kinases (RTKs) auto-phosphorylate upon ligand binding, recruiting PI3K to the cell membrane. PI3K then phosphorylates PIP<sub>2</sub> to PIP<sub>3</sub> which recruits Akt via its PH domain where it is then phosphorylated and activated by PDK1, leading to suppression of TSC activity via an inhibitory phosphorylation event on TSC2 by Akt. TSC inactivation relieves its inhibition on RHEB, found on the lysosomal surface, which is a potent activator of mTORC1. Amino acids can regulate this activation event via a cascade of inhibitory proteins that culminate on the GTPase GATOR1 which removes the necessary GTP bound to the Rags required for mTORC1 activation.

## 1.5 Metabolic reprogramming.

Metabolism is a highly fluctuating landscape of chemical reactions that supports nearly all aspects of cellular biology. The role of metabolism in cancer progression has been continuously investigated since the famous experiments of Otto Warburg describing a preference for glycolysis instead of oxidative phosphorylation as an ATP-generating source for cancer cells in the presence of oxygen. Since then, great advancements have been made in understanding the functions of metabolism in the oncology setting yet the role of metabolism in the fibrotic setting is only at the beginning. There is a high degree of overlap between the metabolic characteristics detected in cancer and those beginning to be found in lung fibrosis and other fibrotic conditions. Both cancer cells and myofibroblasts exhibit stark metabolic changes which support the biomolecular and bioenergetic demands of a highly protein-synthesizing cell [81, 82]. Metabolic reprogramming of fibroblasts in fibrotic diseases has been detected in chronic kidney disease (CKD), systemic sclerosis (SSc) and alcoholic liver disease (ALD) [83-85]. Pharmacological inhibition of pyruvate dehydrogenase kinase (PDK) with dichloroacetate ameliorated kidney fibrosis in mouse models [86]. Glucose consumption is frequently increased in tumour cells and this can be detected clinically using positron-emission tomography (PET) following administration of the radiopharmaceutical glucose analogue, <sup>18</sup>fluoro-deoxyglucose (<sup>18</sup>FDG) [87]. In an IPF patient, <sup>18</sup>FDG-PET showed areas of high signal intensity (more glucose consumption) overlapping with areas of fibrosis [88]. Increased glucose consumption can result in enhanced glycolysis, providing higher levels of the intermediates required for the synthesis of macromolecules necessary for cell division or in the setting of IPF, ECM component synthesis and fibroblast proliferation. This observation of increased glucose consumption in the fibrotic lung raised the possibility that fibroblastic foci may be more metabolically active than previous thought and a distinct metabolic profile of the IPF lung existed. Indeed, a subsequent metabolomics study on IPF lung tissue and control donor lung found the levels of 108 metabolites are altered in IPF [89]. As examples, amino acids like glutamine, glutamate and hydroxyproline were found to be elevated in the IPF lung as well as long-chain and medium-chain fatty acids when compared with normal lung tissue [89, 90]. Drawbacks from this study include the lack of cell-specificity and thus certain fibroblast-specific metabolic signatures may have been missed.

## 1.6 Serine biosynthesis.

The serine biosynthetic pathway is of high interest in the cancer setting due to its variable metabolic functions and has not been extensively examined in the context of fibrosis [91, 92]. Serine biosynthesis uses the glycolysis intermediate 3-phosphoglycerate (3-PG) which is converted to serine through a series of linear enzymatic reactions mediated by three enzymes: phosphoglycerate dehydrogenase (PHGDH), phosphoserine aminotransferase 1 (PSAT1) and phosphoserine phosphatase (PSPH) (Figure 1.2) [93]. Serine is critical for the biosynthesis of cysteine, glycine and choline and supports one-carbon metabolism via its conversion to glycine, transferring a carbon to tetrahydrofolate (THF) [92].

PHGDH exists as a tetramer of four identical subunits which converts 3-PG to phosphohydroxypyruvate (PHP) concomitant with NAD<sup>+</sup> reduction, forming NADH as a by-product [94]. PHGDH is frequently upregulated in cancer and was found to be amplified in ~6% of breast cancers (reaching as high as 70% in oestrogen receptor (ER)-negative breast tumours) and ~40% of melanomas [95]. Pharmacological inhibition of PHGDH *in vitro* has been shown to strongly decrease proliferation of tumour cells, even in cells grown in media containing serine [96]. This observation along with the abundance in extracellular availability of glycine and serine made it unclear why tumour cells would increase serine synthesis, a pathway which diverts glycolysis. Another product in this pathway is  $\alpha$ -ketoglutarate, generated in the processing of PHP by PSAT1 and using glutamate as the nitrogen donor. Indeed, a recent study found that PHGDH suppression did not impact intracellular serine levels in cells with high PHGDH expression but instead decreased  $\alpha$ -ketoglutarate levels by roughly 50% [97]. Additionally, PHGDH inhibition has been observed to activate SHMT1 activity and reduce the incorporation of exogenous serine into nucleotides [98]. Furthermore, PHGDH inhibition decreased nucleotide synthesis through disrupting central carbon metabolism and the pentose phosphate pathway [98]. As an enzyme at the interface between glycolysis and serine biosynthesis, PHGDH

activity regulated the flux of a host of metabolites in a serine-independent fashion. The antitumorigenic effect of inhibiting PHGDH was found to be reversed by exogenous supplementation of nucleosides and  $\alpha$ -ketoglutarate [96].

PSAT1 is the second enzyme in serine biosynthesis and is a pyridoxal-phosphate (PLP)-dependent enzyme that mediates the transfer of the amino group of glutamate to PHP, creating 3-phosphoserine (3-PS) and  $\alpha$ -ketoglutarate. PSAT1 has been found to be upregulated in various cancers and been referred to as an oncogene whose expression correlates with disease severity [99]. Knockdown of PSAT1 in lung adenocarcinoma cells dramatically decreased their metastatic potential *in vitro* and *in vivo* [100]. Additionally, altering the levels of glucose or glutamine did not affect PSAT1-enhanced cell invasiveness, indicating a non-enzymatic mechanism by which PSAT1 promoted tumourigenesis. In non-small cell lung cancer (NSCLC) cells, PSAT1 was found to be overexpressed and to regulate the levels of the oncogene, cyclin D1 through a GSK-3 $\beta$  mechanism [101]. In colorectal cancer cells, ectopic expression of PSAT1 promoted cell growth and increased their resistance to oxaliplatin [102]. A recent study identified *PSAT1*, among 9 other metabolic genes, as capable predictors of prognosis and progression in clear cell renal cell carcinoma (ccRCC) [103]. PSAT1 has also been identified as a critical regulator of embryonic stem cell renewal and pluripotency by controlling intracellular levels of  $\alpha$ -ketoglutarate which impacted on DNA and histone methylation states [104].

The final enzyme of serine biosynthesis is PSPH which removes the phosphate group ( $P_i$ ) from 3-PS through hydrolysis, producing serine. Like PHGDH and PSAT1, PSPH has also been positively linked to cancer progression. In breast and colon cancers, the pro-tumorigenic effects of PSPH activity were shown to be through its serine synthesis functions [105, 106]. Additionally, the pro-survival effects induced by PSPH in lung cancer cells were shown to continue even in the presence of extracellular serine, identifying a serine biosynthesis-independent function for PSPH as a regulator for insulin receptor substrate 1 (IRS-1) activity [107]. Another study found the decrease in proliferation following PSPH knockdown of squamous cell carcinoma cells was independent of its serine-synthesis functions [108]. A further investigation showed PSPH regulated MAPK signalling and thereby impacting on the tumorigenic potential of NSCLC cells [109].

## 1.7 Glycine biosynthesis.

Glycine is required in the biosynthetic pathways of purines, creatine, porphyrins and the antioxidant protein glutathione. It is also a major amino acid constituent of collagens, amounting to roughly a third of the polypeptide sequence. Glycine biosynthesis is regulated by serine hydroxymethyltransferase (SHMT) which catalyses the conversion of serine and glycine and exists as an obligate dimer which is functionally active as a tetramer upon binding to pyridoxal 5'-phosphate (PLP), the active form of vitamin B<sub>6</sub> [110, 111]. It has three isoforms; two in the cytosol or nucleus (SHMT1/SHMT2 $\alpha$ ) and one in the mitochondria (SHMT2) [112]. The reaction induces retro-aldol cleavage of serine, transferring the carbon unit to THF and thereby producing 5,10-methylene tetrahydrofolate (5,10-CH<sub>2</sub>-THF) [113]. The generation of 5,10-CH<sub>2</sub>-THF through SHMT is the main source of activated one-carbon units required for purine and pyrimidine synthesis and methylation reactions [114]. Glycine can then provide further one-carbon units to THF via the glycine cleavage system (GCS) which is activated at high intracellular glycine concentrations and produces 5,10-CH<sub>2</sub>-THF, NH<sub>3</sub>, CO<sub>2</sub>, NADH and H<sup>+</sup> [115]. The enzymes which then use 5,10-CH<sub>2</sub>-THF for *de novo* nucleotide synthesis have been key targets for cancer therapeutics, termed antifolates. A famous example is methotrexate which inhibits dihydrofolate reductase (DHFR), the enzyme responsible for THF synthesis [116]. Given the success of antifolates, recent attention has moved to targeting SHMT, where SHMT2 is often found overexpressed in tumours [117]. A recent study found the SHMT inhibitor SHIN2 to function synergistically with methotrexate in mouse T-cell acute lymphoblastic leukaemia [118]. In models of diffuse B-cell lymphoma, a study found SHMT inhibition to be cytotoxic via reduced glycine levels in cancer cells with defective glycine uptake [119].

## 1.8 Regulation of serine/glycine biosynthesis.

One of the most established regulators of the serine and glycine biosynthetic axis genes is the basic leucine zipper transcription factor (TF) activating transcription factor 4 (ATF4). ATF4 is a master regulator of a host of genes able to increase the

adaptive properties of a cell to overcome internal stresses. These include viral infection, nutrient deprivation (ATP, glucose, amino acids), endoplasmic reticulum stress and hypoxia [120]. These stress signals are detected by a group of four kinases which phosphorylate eukaryotic translation initiation factor 2 $\alpha$  (eIF2 $\alpha$ ) on its Ser<sup>51</sup> residue, resulting in a translational decrease of most mRNAs by preventing Met-tRNA recruitment to the initiation complex [121]. However, ATF4 mRNA contains two upstream open reading frames in its 5' UTR which allow for it to be translated in a cap-independent manner [121]. Under normal non-stressed conditions, these two mRNA elements of ATF4 prevent it from being translated. General control non-depressible 2 (GCN2) is the kinase that senses nutrient deprivation through uncharged tRNAs, leading to an ATF4-dependent upregulation in expression of amino acid metabolism genes, such as PHGDH, PSAT1, PSPH and SHMT2 [122]. GCN2 knockout mice only showed phenotypic abnormalities if fed a diet lacking in any amino acid, otherwise appearing healthy and fertile [123, 124]. Tampering with intracellular serine levels, such as through inhibition of lactate dehydrogenase A (LDHA), which provides NAD<sup>+</sup> used in serine biosynthesis, has also been shown to activate the GCN2-eIF2 $\alpha$ -ATF4 axis [125].

Several DNA-modifying and transcription factors have been observed to work cooperatively with ATF4 to ensure maximal gene transcription. These include the demethylase lysine-specific demethylase 4C (KDM4C), the methyltransferase G9A and the transcription factors nuclear factor erythroid 2-related factor 2 (NRF2) and c-Myc. In several cancer cell lines, KDM4C epigenetically activates serine biosynthesis genes through removal of repressive histone H3 lysine 9 (H3K9) trimethylations [126]. This requires ATF4 binding and KDM4C was further shown to induce transcription of the ATF4 gene. G9A upregulation has been detected in several cancer types and its inhibition shown to decrease proliferation [127]. G9A enhanced the transcription of the serine pathway genes by adding single methyl groups at H3K9, a modification associated with active chromatin. Loss of G9A using shRNA and pharmacological inhibition with the compound BIX01294 significantly reduced global H2K9me<sub>1</sub> levels, serine biosynthesis gene expression and proliferation in bone, breast, colon and lung cancer cell lines [127]. NRF2 regulates cytoprotective genes such as detoxifying enzymes and antioxidant proteins and is ubiquitously and constitutively expressed in all cells, allowing for a prompt gene transcriptional

program to be induced [128, 129]. It has a high turnover, being constantly degraded by the ubiquitin proteasome 26S through binding with the E3 ligase adapter Kelch-like ECH-associated protein 1 (KEAP1) [130, 131]. KEAP1 is able to sense the redox state of the cell through its 27 cysteine residues which distort quaternary structure and thus binding to NRF2 if oxidized by unacceptable levels of ROS not mitigated by the endogenous presence of antioxidant molecules like glutathione [130, 132]. The role of NRF2 in regulating the serine biosynthetic pathway genes has only relatively recently been observed [122]. It is classically known as a master regulator of cytoprotective genes involved in redox homeostasis, glutathione synthesis and antioxidant defence. NRF2 frequently carries mutations in several cancers which impact on its binding affinity to KEAP1, allowing for constitutive NRF2 activity which enhances resistance to chemo and radiotherapy and results in a poorer prognosis [133]. In NSCLC cells, silencing of NRF2 led to a complete loss of ATF4 protein levels as well as a significant decrease in gene expression of *PHGDH*, *PSAT1*, *PSPH*, *SHMT1* and *SHMT2* [122]. C-Myc has also been shown to upregulate the expression of these enzymes through ATF4 mRNA induction and that this transcriptional event is critical for tumour growth under nutrient deprivation [134-136].

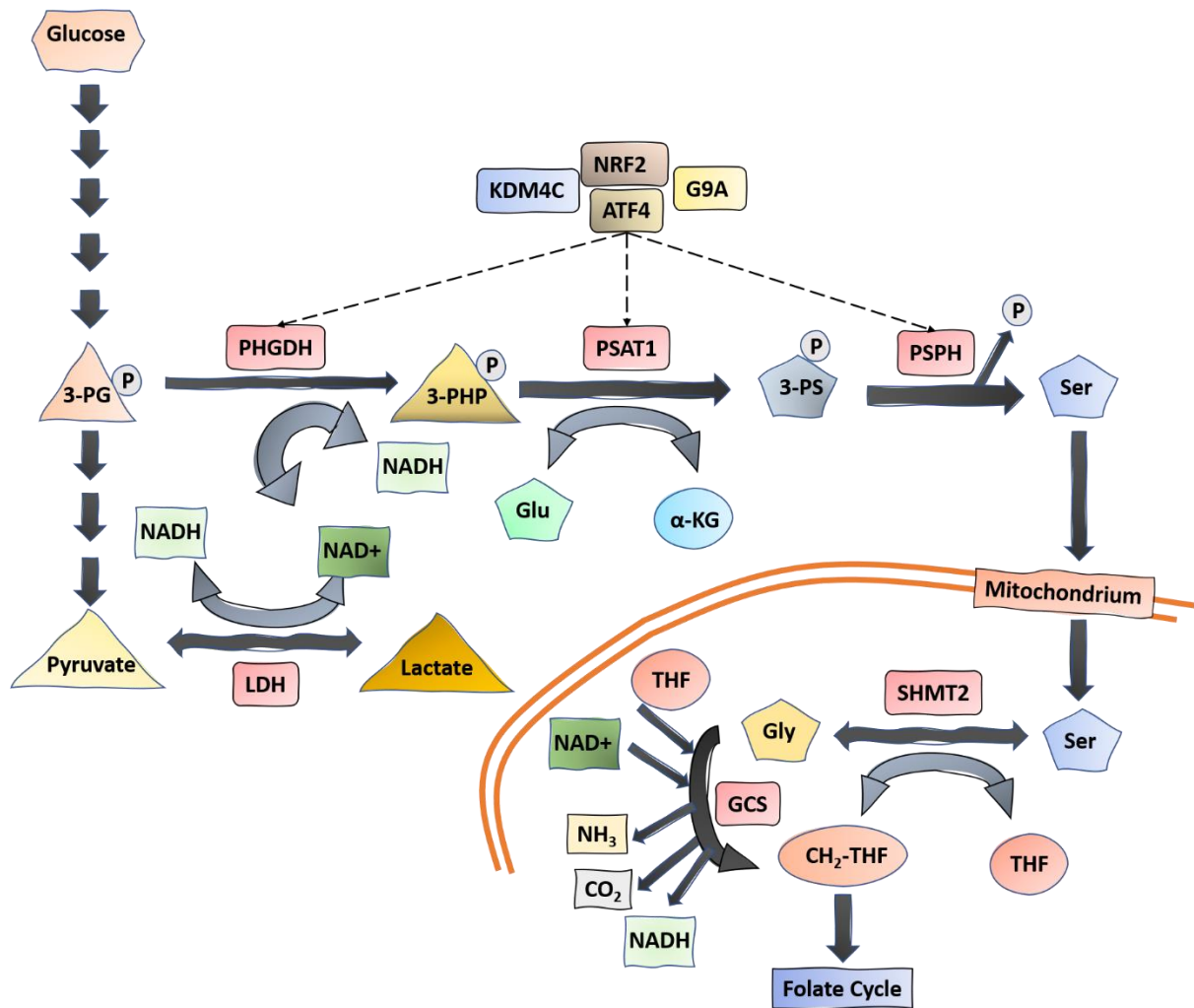


**Figure 1. 4 Serine-glycine biosynthetic axis.**

Serine biosynthesis branches from the glycolytic intermediate 3-phosphoglycerate (3-PG), which is used by PHGDH to produce 3-phosphohydroxypyruvate (3-PHP) in a NAD<sup>+</sup> dependent reaction. Downstream of glycolysis lies lactate production via LDH which produces cytosolic NAD<sup>+</sup>. 3-PHP is then converted to 3-phosphoserine (3-PS) by PSAT1 which transfers an amino group from glutamate, leaving  $\alpha$ -ketoglutarate. 3-PS is then used by PSPH which removes an inorganic phosphate group to produce serine. The expression levels of these three enzymes which make up serine biosynthesis is modulated by ATF4, KDM4C, NRF2 and G9A. Serine can then produce mitochondrial glycine via SHMT2 which removes a carbon unit and transfers it to THF, producing 5,10-CH<sub>2</sub>-THF. Glycine can also further provide one-carbon units to THF via the glycine cleavage system (GCS).

## 1.9 Glutamine metabolism.

Glutamine is the most abundant amino acid in blood and is involved in many biological functions including antioxidant defence, redox homeostasis, nonessential amino acid synthesis, nucleotide synthesis, fatty acid synthesis and anaplerosis (Figure 1.3). Due to its wide range of functions, it is not surprising that this amino acid is avidly consumed by cancerous cells which greatly enhances their proliferative and growing capabilities [137]. Intravenous administration of asparaginase is one of the most successful metabolic therapies for cancer and its therapeutic benefit was recently shown to be heavily reliant on being able to degrade glutamine as well as asparagine, thus starving leukemic cells of essential nutrients [138]. Circulating glutamine is between 500-800 $\mu$ M and maintained largely by skeletal muscle as well as the lungs in times of stress [139, 140].

Glutamine is the major cellular source of ammonia production through its metabolism by glutaminase (GLS) and glutamate dehydrogenase (GLUD), yielding ammonia, ammonium and  $\alpha$ -ketoglutarate. The reaction of ammonia ( $\text{NH}_3$ ) to ammonium ( $\text{NH}_4^+$ ) has a  $\text{PK}_a$  of 9.15 and therefore under physiological conditions (pH 7.4), 98.3% of these species exist as  $\text{NH}_4$  [141]. Ammonia is generally regarded as a toxic by-product that is secreted from cells to be neutralised in the liver through conversion to urea. However, recent work has shown that breast cancer cells use circulating ammonia for amino acid biosynthesis through glutamate dehydrogenase (GLUD)-dependent assimilation with  $\alpha$ -ketoglutarate, yielding glutamate [142].

### 1.9.1 Glutamine in nucleotide biosynthesis.

Glutamine plays an indispensable role in the biosynthetic pathways for purines and pyrimidines. Purine synthesis stems from the early glycolysis intermediate glucose-6-phosphate (G6P) in what is known as the pentose phosphate pathway (PPP). This pathway requires 3 ATP molecules to produce phosphoribosyl pyrophosphate (PRPP) which undergoes a series of enzymatic reactions involving three molecules of ATP, two of glutamine, one of glycine and one of aspartate (the biosynthesis of these amino acids is dependent on glutamine) to yield inosine monophosphate (IMP) [143]. A committed step in the biosynthetic pathway for purines is the first utilizing

PRPP which is catalysed by amidophosphoribosyltransferase (PPAT), an enzyme frequently overexpressed in cancer [144]. IMP can then be processed into AMP using aspartate and GMP using another molecule of glutamine.

Pyrimidine biosynthesis is regulated by carbamoyl-phosphate synthetase 2, aspartate transcarbamylase and dihydroorotase (CAD), a 243 kDa protein which is formed by the convergence of four enzymes and self-assembles into a roughly 1.5 MDa hexamer [145]. CAD oligomerization can be promoted by phosphorylation of its Ser<sup>1859</sup> residue by S6 kinase (S6K), an mTORC1-regulated protein [146]. The first step involves carbamoyl phosphate synthase II (CPSII) and glutaminase which use glutamine, bicarbonate and two ATP molecules to produce carbamoyl phosphate (CP). Aspartate is then added to CP by aspartate transcarbamoylase (ATC), yielding carbamoyl aspartate and lastly condensed to dihydroorotate which is the cyclic precursor to the pyrimidine ring by dihydroorotase (DHO) [147]. Following three further enzymatic reactions involving NAD<sup>+</sup> and PRPP, uridine monophosphate (UMP) is produced [148]. Phosphorylation reactions of UMP can produce UDP and UTP, the latter of which can be converted to UTP by addition of an amino group from glutamine [149].

### **1.9.2 Glutaminolysis.**

Glutaminolysis defines the downstream catabolic reactions that convert glutamine into the tricarboxylic acid (TCA) cycle intermediate  $\alpha$ -ketoglutarate. Glutamine is considered a nitrogen reservoir as it can donate its two amino groups to convert keto-acids into amino acids. Once deaminated, glutamine becomes glutamate and one further deamination yields  $\alpha$ -ketoglutarate. Glutamate is directly involved in the biosynthetic pathways of the nonessential amino acids (NEAAs) alanine, aspartate, serine (and by extension glycine), cysteine and proline. Asparagine biosynthesis uses the ATP-dependent transfer of the glutamine R-group amine to aspartate by asparagine synthetase (ASNS), producing asparagine and glutamate.

The rate of glutaminolysis is regulated by glutaminase, which removes the R-group amine of glutamine, releasing ammonia and producing glutamate [150]. Glutaminase is encoded by two genes, kidney-type *GLS1* and liver-type *GLS2*. *GLS1* is

expressed more globally than GLS2, which is only found in the liver, brain, pituitary gland and pancreas [150]. GLS1 mRNA can be alternatively spliced to produce two isoforms: glutaminase C (GAC) or kidney-type glutaminase (KGA). The former isoform is more active than KGA and increased in several cancers [150]. Conversely, GLS2 is often found silenced via promoter methylation in liver cancer and has been shown to be tumour suppressive and a confirmed p53-target gene [151]. The catalytic activity of both glutaminases is enhanced by inorganic phosphate binding near the active site, though GAC shows a greater increase in enzymatic activity [152, 153]. GLS2 is activated by its by-product, ammonia, while GLS1 is inhibited. Furthermore, the subcellular localisations of these enzymes vary; GLS2 is often found in the mitochondria and has been shown to translocate to the nucleus while KGA is found in the cytosol and GAC in the mitochondria [151].

A recently developed nanomolar GLS1 inhibitor, CB-839/Telaglenastat, has reached phase 2 clinical trials as a treatment for NSCLC (clinical trials.gov identifier NCT04265534). This compound is also being used in clinical trials employing synergistic strategies with other agents to limit cancer progression. These include the DNA/RNA synthesis inhibitor capecitabine, the hypomethylating agent azacytidine and the CDK4/6 inhibitor palbociclib (clinical trials.gov identifiers NCT02861300/NCT03047993/NCT03965845). CB-839 was also found to synergize with the mTORC1 inhibitor AZD8055 to reduce triple-negative breast cancer growth *in vitro* and *in vivo* [154]. In the setting of fibrosis, CB-839 was shown to ameliorate BLM-induced lung fibrosis in mouse models as well as reducing fibrotic endpoints in non-alcoholic steatohepatitis (NASH) fibrosis mouse models [155, 156].

### **1.9.3 Glutamate in the mitochondria.**

Glutamine-derived glutamate in the mitochondria can be used in the biosynthesis of alanine via glutamic-pyruvic transaminase 2 (GPT2), aspartate via glutamic-oxaloacetic transaminase 2 (GOT2),  $\alpha$ -ketoglutarate via GLUD (as well as GPT2 and GOT2), and proline via firstly delta-1-pyrroline-5-carboxylate synthase (P5CS) and then pyrroline-5-carboxylate reductase 1 (PYCR1). Glutamate is furthermore used in the synthesis of the antioxidant glutathione, a tripeptide of glutamate, cysteine and glycine.

GPT2 and GOT2 are part of the aminotransferase family which convert glutamate to  $\alpha$ -ketoglutarate in the process of generating alanine and aspartate, respectively. These two enzymes are highly expressed in the liver and are frequently measured in clinical blood samples to assess potential liver damage or dysfunction [157]. Both enzymes have cytosolic isoforms, GPT1 and GOT1. The GPTs regulate a cross-organ cycle known as the Cahill cycle where glycolysis in skeletal muscle produces pyruvate that is then converted to alanine via GPT activity, secreted and carried by the blood to the liver and deaminated back to pyruvate by the hepatic GPTs for gluconeogenesis. In colon cancer cells, GPT2 was shown to control the utilization of glutamine as a TCA cycle carbon source (generating  $\alpha$ -ketoglutarate) when oncogenic transformations such as LDHA induction were present, indicating a prominent role in orchestrating pro-tumorigenic metabolism [158]. In breast cancer cells, GPT2 was observed to function in reverse and deplete  $\alpha$ -ketoglutarate levels, leading to proline hydroxylase 2 (PHD) inhibition and subsequent HIF1 $\alpha$  stability [159]. In several cancer cell lines, GPT2 was found to compensate and restore cell proliferation following GLS1 inhibition, indicating a therapeutic need for dual inhibition of these two mitochondrial enzymes [160]. The GOTs regulate the malate-aspartate shuttle which uses oxaloacetate as an electron acceptor from NADH in the intermembrane space of the mitochondria to generate malate, which can then enter the matrix (the inner membrane is impermeable to NADH) via the malate- $\alpha$ -ketoglutarate antiporter. Additionally, the GOTs produce aspartate which is required in the urea cycle for the ATP-dependent fusion with citrulline, forming arginosuccinate through the hepatocyte-expressed arginosuccinate synthase (ASS1). In pancreatic ductal adenocarcinoma (PDA), GOT1 is frequently overexpressed and knockdown studies showed decreased cell proliferation and disrupted glycolysis, nucleotide metabolism and redox homeostasis [161, 162].

Conversion of glutamate to  $\alpha$ -ketoglutarate can also be mediated by GLUD, which seemingly wastes the amino group by releasing it as ammonia. Highly proliferative tumours show high transaminase (GPT2/GOT2) and low GLUD expression while the opposite is seen for quiescent cells [163]. GLUD is a hexameric enzyme that sits at the junction between nitrogen and carbon metabolism, using NADP<sup>+</sup> or NAD<sup>+</sup> as an electron donor to deaminate glutamate to  $\alpha$ -ketoglutarate and is negatively regulated by GTP and positively regulated by ADP and leucine [164, 165]. Therefore, in times

of low cellular energy, GLUD activity will be skewed towards  $\alpha$ -ketoglutarate synthesis and therefore TCA cycle operation. The reaction catalysed by GLUD is reversible and can reach equilibrium in the liver [165]. However, the  $K_m$  for ammonia is around 20-30 mM which is rare in non-hepatic cells and therefore the reaction is expected to proceed towards glutamate deamination in most other tissues [165]. As glutamate is a neurotransmitter, GLUD has been implicated in the pathogenesis of the neurological diseases Alzheimer's and Parkinson's [166]. GLUD has also been observed as a critical source for  $\alpha$ -ketoglutarate in cells with isocitrate dehydrogenase (IDH) mutations which leads to generation of the oncometabolite 2-hydroxyglutarate (2-HG), an  $\alpha$ -ketoglutarate-dependent enzyme inhibitor [167].

Proline biosynthesis occurs in the mitochondria and therefore is reliant on mitochondrial glutamate availability. As a major constituent of collagens, proline comprises nearly 10% of amino acid mass of proteins in humans [168]. While proline has been found to influence gene expression and act as an antioxidant, its primary biological function appears to be proteogenic [169]. The precursor to proline synthesis is P5C which can be synthesized from ornithine or glutamate and is converted to proline via PYRC1 in an NADH-dependent reaction [170]. Ornithine is an intermediate in the urea cycle and can be produced from arginine via arginase activity. Ornithine can then be converted to P5C via ornithine aminotransferase (OAT) which uses  $\alpha$ -ketoglutarate and produces glutamate in a reversible reaction. As stated earlier in this section, P5C can be produced via P5CS using glutamate in a NADPH-dependent reaction. A recent study found that fibroblasts stimulated with TGF- $\beta_1$  used proline biosynthesis as a sink for excess NAD(P)H production through the TCA cycle [170]. This study also reported TGF- $\beta_1$ -induced an increase in reactive oxygen species (ROS) and stabilised HIF1 $\alpha$  prior to increasing to proline biosynthesis, an effect that was reversed once intracellular proline levels increased [170].

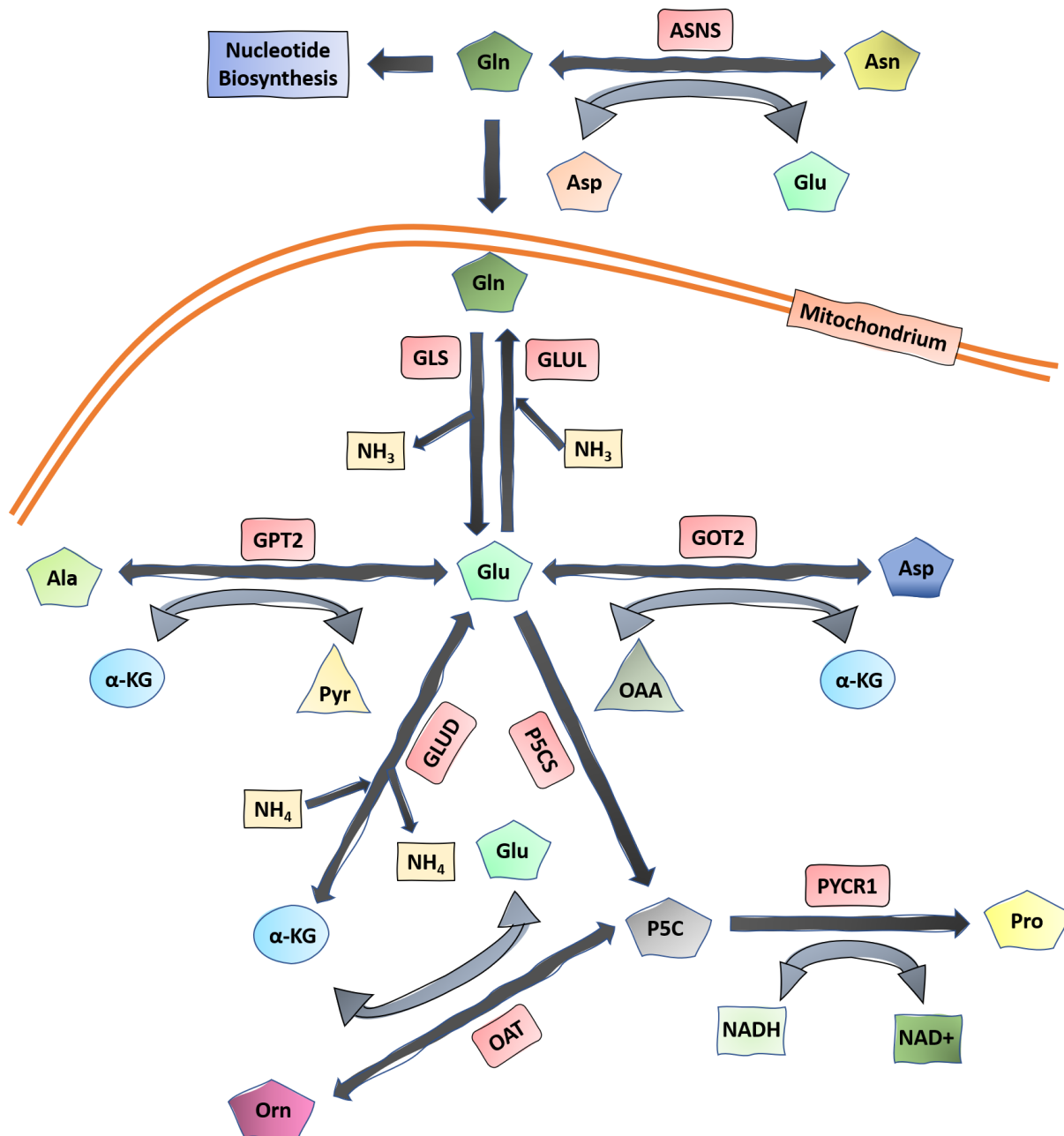


**Figure 1. 5 Glutamine metabolism.**

Glutamine is critical for nucleotide biosynthesis and is used in asparagine biosynthesis via ASNS which transfers an amino group from glutamine to aspartate, producing asparagine and glutamate. In the mitochondria, glutamine is deaminated by GLS to produce glutamate and the reverse reaction catalysed by GLUL. Glutamate can then provide an amino group to pyruvate and oxaloacetate to produce alanine and aspartate via GPT2 and GOT2, respectively. The deamination product of glutamate yields  $\alpha$ -ketoglutarate. Glutamate can be directly deaminated by GLUD, producing  $\alpha$ -ketoglutarate and ammonia (which in physiological conditions becomes ammonium). Glutamate can then produce proline via conversion to P5C via P5CS and then proline via PYCR1 in a NADH-dependent reaction. Proline can also be synthesized from ornithine via OAT which transfers an amino group from ornithine to  $\alpha$ -ketoglutarate, producing P5C and glutamate.

## 1.10 Functions of $\alpha$ -ketoglutarate.

$\alpha$ -ketoglutarate is best known as one of the 10 metabolites that constitute the TCA cycle which produces the reducing equivalents NADH and FADH<sub>2</sub> required for electron-transport chain (ETC) function and subsequent ATP production. It can be produced through glutaminolysis and aminotransferase reactions as previously described and through the IDH family, which consists of three isozymes (IDH1-3) using isocitrate and releasing a molecule of CO<sub>2</sub> [171]. IDH1 is cytosolic while IDH2 and IDH3 are mitochondrial. IDH1 and IDH2 use NADP<sup>+</sup> as a cofactor to produce NADPH while IDH3 uses NAD<sup>+</sup> to produce NADH for ETC-derived ATP synthesis. NADPH is an essential reducing factor in glutathione and thioredoxin functioning as well as a cofactor for lipid and nucleic acid synthesis [172, 173]. Mutations in IDH1/2 are frequently observed in numerous cancer types and are found in 20% of acute myeloid leukaemia (AML) cases [174, 175].

Aside from fuelling the TCA cycle,  $\alpha$ -ketoglutarate supports hydroxylation and demethylation reactions. There is a close link between metabolism and epigenetic remodelling. The role of  $\alpha$ -ketoglutarate in gene expression by modulating histone methylation states has been shown to be exploited by cancer cells, which synthesize an altered version of  $\alpha$ -ketoglutarate known as 2-HG (termed an 'oncometabolite') which inhibits demethylases, thus impacting on gene transcription [176]. Acetyl-coA fuels the TCA cycle and fatty acid synthesis and is required for histone acetylation reactions. This connection ensures gene expression changes only occur during times of adequate nutrient availability [177]. Demethylation (and methylation) also affects non-histone proteins, with 1,005 lysine sites in 974 human proteins and 2,159 arginine sites in 896 human proteins identified [178]. Hydroxylation reactions are critical for collagen protein stability as mentioned in section 1.2.4. In hypoxic signalling, HIF1 $\alpha$  is constantly being hydroxylated by prolyl hydroxylase domain proteins (PHDs) which mark it for degradation. As this reaction is dependent on O<sub>2</sub>, it does not function when O<sub>2</sub> levels are below a threshold, resulting in HIF1 $\alpha$  stabilisation, nuclear translocation and active gene transcription. Extracellular  $\alpha$ -ketoglutarate was also found to act as an antioxidant by reacting with H<sub>2</sub>O<sub>2</sub>, a common ROS which can be produced through ascorbic acid oxidation in cell medias, producing succinate [179].

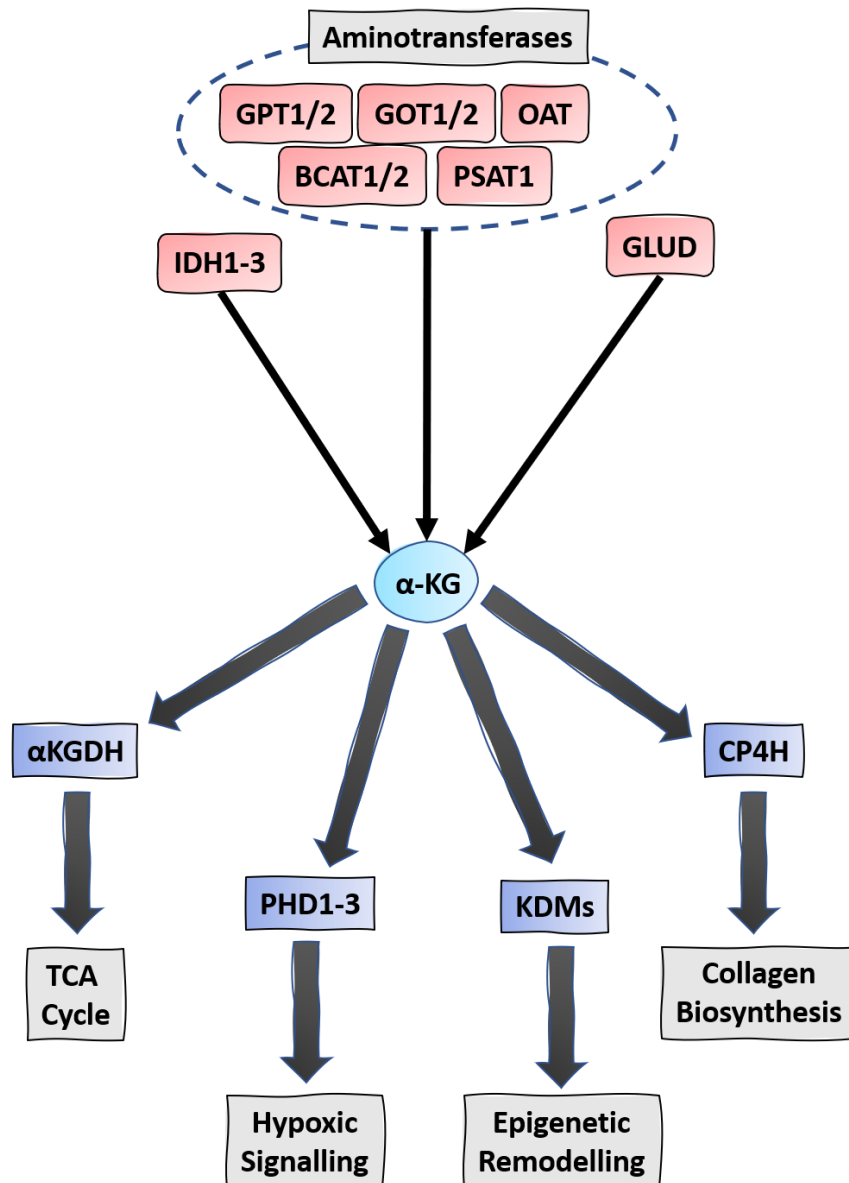


**Figure 1. 6 Sources and functions of  $\alpha$ -ketoglutarate.**

$\alpha$ -ketoglutarate ( $\alpha$ -KG) can be generated via the IDHs, aminotransferases and GLUD. It is a component of the TCA cycle used by  $\alpha$ -ketoglutarate dehydrogenase ( $\alpha$ KGDH) and thus generates reducing equivalents for the ETC to produce ATP. It is a substrate for hydroxylation reactions and is required for PHD1-3 activity which leads to HIF-1 $\alpha$  hydroxylation and degradation. It is also a substrate required for demethylation reactions and thus required for histone demethylation. Hydroxylation reactions are furthermore crucial in collagen polypeptide stability via proline hydroxylation.

## 1.11 Metabolic changes in pulmonary fibrosis.

Lung fibroblast studies performed *in vitro* have shown multiple metabolic changes induced following TGF- $\beta_1$  stimulation. The most prominent to date highlight the importance for glycolysis, fatty acid synthesis and glutamine metabolism in supporting TGF- $\beta_1$ -induced fibrotic functions, such as fibroblast to myofibroblast differentiation and ECM component synthesis.

In terms of glucose metabolism, TGF- $\beta_1$  has been shown to increase the expression of glucose transporter 1 (GLUT1) and the glycolytic flux enzymes hexokinase 2 (HK2), phosphofructokinase-1 (PFK-1), 6-phosphofructo-2-kinase/fructose-2,6-biphosphatase 3 (PFKFB3) [180-182]. Pharmacological inhibition of PFKFB3 with 3-PO was shown to attenuate bleomycin-induced (BLM) lung fibrosis in mice [182]. A recent study showed a similar attenuation in the BLM lung fibrosis mouse model with the HK2 inhibitor, lonidamine [181]. Both studies showed a similar *in vitro* effect of reduced TGF- $\beta_1$ -induced expression of pro-fibrotic endpoints with 3-PO and lonidamine. The expression of the enzymes in the biosynthesis of serine, which stems from the glycolytic intermediate 3-phosphoglycerate (3-PG), have been shown to be increased with TGF- $\beta_1$  stimulation in lung fibroblasts [81]. Additionally, inhibiting the first enzyme of the pathway, phosphoglycerate dehydrogenase (PHGDH), with the compound NCT-503 attenuated BLM-induced lung fibrosis [183].

In terms of fatty acid synthesis, fatty acid synthase (FASN) was shown to be increased by TGF- $\beta_1$  and its inhibition with the compound C75 decreased TGF- $\beta_1$ -induced collagen I synthesis, an effect able to be rescued by exogenous addition of palmitate [184]. While this study found C75 reduced BLM-induced mouse lung fibrosis, another group showed conflicting results with an increase in fibrosis severity following C75 administration, citing a reduced capacity for monocyte-driven collagen resorption [185].

In terms of glutamine metabolism, TGF- $\beta_1$  was shown to enhance glutamine consumption, glutamate synthesis, and the expression of GLS1, the main enzyme responsible for glutamine catabolism [186]. Furthermore, the GLS1 inhibitor, CB-839 decreased BLM-induced lung fibrosis in mice [155]. The mechanism of action of CB-839 was concluded to be by limiting the synthesis of glutamate-dependent  $\alpha$ -ketoglutarate, required for mTORC1 activation and proline hydroxylation [187]. The

functional implications of glutamine metabolism with respect to supporting TGF- $\beta$ <sub>1</sub>-induced fibrotic endpoints remain unclear as contradictory evidence exists. A study found GLS1 inhibition reduced the expression of the myofibroblast differentiation marker,  $\alpha$ -smooth muscle actin, though this was not replicated in a later study [186, 188]. Additionally, another investigation concluded that the functional role of glutamine metabolism is to synthesise amino acids such as proline and glycine, and not for the synthesis of  $\alpha$ -ketoglutarate [187, 188]. Together these studies have highlighted the pivotal role of the pleiotropic amino acid glutamine as well as the need to expand our understanding of its numerous metabolic fates during TGF- $\beta$ <sub>1</sub>-induced fibroblast ECM synthesis.

## **1.12 Summary, hypothesis and aims.**

Idiopathic pulmonary fibrosis is a rapidly progressing fatal lung disease in which activated myofibroblasts in the pulmonary interstitium produce excessive levels of extracellular matrix components leading to obliteration of airspaces and destruction of alveolar tissue architecture. As the effector cells of the fibrogenic response, understanding the mechanisms the myofibroblast utilizes to support enhanced extracellular matrix synthesis could aid in the identification of novel opportunities for therapeutic exploitation. There is emerging evidence that myofibroblasts rewire their metabolic pathways to support and mitigate the vast changes induced following activation into highly contractile and synthetic cells. One of the most well-studied pathways is glutamine metabolism which influences a wide range of processes such as ATP production, redox maintenance, nucleotide and amino acid biosynthesis. The precise function(s) of glutamine metabolism which support enhanced extracellular matrix synthesis still remain unclear.

This thesis will therefore address the following hypothesis:

**TGF- $\beta_1$ -induced changes in cellular metabolism are critical to support enhanced collagen synthesis.**

The specific aims of this thesis are to:

1. Evaluate the effect of TGF- $\beta_1$  on the expression of the serine and glycine biosynthetic pathway and its role in enhanced collagen synthesis.
2. Define the functional impact of extracellular glucose, glutamine, glycine and serine on TGF- $\beta_1$ -enhanced collagen synthesis.
3. Investigate the role of glutamine metabolism in TGF- $\beta_1$ -enhanced collagen synthesis.

## CHAPTER 2: Materials & Methods

### Materials.

#### 2.1 Cell culture.

For the majority of experiments in this thesis, cells were grown in Dulbecco's modified eagle's medium (DMEM) (ThermoFisher #A144301-01) which was supplemented with 5mM D-(+)-glucose (Sigma-Aldrich #G8270) and 700 $\mu$ M L-glutamine (ThermoFisher #25030-024). Media labelled as 'supraphysiological' was DMEM (ThermoFisher #21969035). Experiments in serine and glycine-free media used MEM (ThermoFisher #21090022). All medias were supplemented with penicillin and streptomycin (ThermoFisher #15070063). Where specified, foetal bovine serum (FBS) (ThermoFisher #10270106) was supplemented at 0, 0.4 or 10% (v/v). Where appropriate, compounds were solubilised in either media or dimethyl sulfoxide (DMSO) (Sigma-Aldrich #D2650). Cell layer detachment for passaging and plating used trypsin-EDTA (ThermoFisher #25300062) and DPBS for washes (ThermoFisher #BR0014G). For macromolecular crowding experiments, Ficoll PM 70 (Sigma-Aldrich #F2878), Ficoll PM 400 (Sigma-Aldrich #F4375), ascorbic acid 2-phosphate sesquimagnesium salt hydrate (Sigma-Aldrich #A8960), and 96-well flat clear-bottom black microplates (Corning #3603) were used. Cells were grown in sterile T175 flasks (ThermoFisher #159910).

#### 2.2 Cytokines.

Transforming growth factor  $\beta_1$  (TGF- $\beta_1$ ) (R&D Biosystems #101-B1/CF) was reconstituted in a 4mM HCl and 0.1% BSA (w/v) solution to 10 $\mu$ g/ml and stored in aliquots at -20°C.

#### 2.3 Metabolites.

For rescue experiments, L-serine (Sigma-Aldrich #S4311), glycine (Sigma-Aldrich #G8790), dimethyl 2-oxoglutarate (Sigma-Aldrich #349631), L-glutamic acid monosodium salt monohydrate (Sigma-Aldrich #49621), L-alanine (Sigma-Aldrich

#A7469), sodium pyruvate (Sigma-Aldrich #P5280) and MEM non-essential amino acid solution (100x) (Sigma-Aldrich #M7145) were used.

## 2.4 Pharmacological compounds.

The commercially available mTOR inhibitor, AZD8055 was obtained from GlaxoSmithKline (GSK) (compound identifier code GSK2976031). Cell-free pIC<sub>50</sub> data for several kinases were provided by GSK (Table 2.1).

AZD8055	mTORC1/2	PI3K $\alpha$	PI3K $\beta$	PI3K $\gamma$	PI3K $\delta$	DNA-PK
pIC <sub>50</sub>	>9.1	5.6	4.7	5.3	5.9	6

**Table 2. 1 Selectivity of AZD8055 data supplied by GSK in cell-free recombinant assays.**

The PHGDH inhibitor, NCT-503 was purchased from Sigma-Aldrich (#SML1659) and has a cell-free IC<sub>50</sub> of 2.5 $\mu$ M for PHGDH [98].

The GLS1 inhibitor, CB-839/Telaglenastat was purchased from Selleckchem (#S7655) and has a cell-free IC<sub>50</sub> of 24nM for GLS1 [189].

The GLUD1 inhibitor, R162 was purchased from Sigma-Aldrich/Calbiochem (#5.38098) and has an IC<sub>50</sub> of 23 $\mu$ M for GLUD1 [190].

The aminotransferase inhibitor, O-(carboxymethyl)hydroxylamine hemihydrochloride (AOAA) was purchased from Sigma-Aldrich (#C13408). As a nonselective inhibitor for PLP-dependent enzymes, no IC<sub>50</sub> data is available.

## 2.5 Antibodies.

The antibodies used in the macromolecular crowding experiments are described below, in Table 2.2. DAPI was used to stain nuclei (ThermoFisher #D1306).

Antibody	Host species	Cat. #	Conjugate	Dilution
Collagen I	Mouse	Sigma-Aldrich (2456)	-	1/1000
Anti-mouse	Mouse	Thermo-Fisher (A-11001)	AF488	1/1000

**Table 2. 2 Antibodies used for immunofluorescence in macromolecular crowding.**

The antibodies used for immunoblotting are described below, in Table 2.3. Luminata Crescendo Western HRP substrate (#WBLUR0500) was used for chemiluminescent detection of bands.

Antibody	Host species	Cat. #	Dilution
PHGDH	Rabbit	CST (#13428)	1/1000
PSAT1	Rabbit	ThermoFisher (#PA5-22124)	1/1000
PSPH	Rabbit	ThermoFisher (#PA5-19113)	1/1000
SHMT2	Rabbit	CST (#11815)	1/1000
ATF4	Rabbit	CST (#9202)	1/1000
p-Smad3 (S <sup>423/425</sup> )	Rabbit	CST (#9520)	1/1000
Histone H3	Rabbit	Abcam (ab16483)	1/1000
GLS1	Rabbit	Abcam (ab156876)	1/1000
GPT2	Rabbit	Atlas (HPA051514)	1/1000
GOT1	Rabbit	CST (#34423)	1/1000
GOT2	Rabbit	ThermoFisher (#PA5-27572)	1/1000

GLUD1	Rabbit	Abcam (ab166618)	1/1000
GLUL	Rabbit	Abcam (ab49873)	1/1000
p-4E-BP1 (S <sup>65</sup> )	Rabbit	CST (#9451)	1/1000
4E-BP1	Rabbit	CST (#9644)	1/1000
RagA	Rabbit	CST (#4357)	1/1000
RagB	Rabbit	CST (#8150)	1/1000
$\alpha$ -tubulin	Rabbit	CST (#9099)	1/5000

**Table 2. 3 Antibodies used for immunoblotting.**

## 2.6 Primary human lung fibroblasts.

Human samples were obtained with informed and signed consent and with research ethics committee approval (10/H0504/9, 10/H0720/12 & 12/EM/0058). Primary human lung fibroblast cell lines were produced through explant culture. Purity of the lines was confirmed by immunohistochemical analysis using antibody markers for epithelial, mesothelial, endothelial and smooth muscle cells. Over 95% of cells in the lines stained positive for the mesenchymal marker vimentin. Fibroblasts were stored in 20% FBS and 10% DMSO (v/v) DMEM at liquid nitrogen temperature. Cells from cell line 0311 (54 year old, male) were only used between passage numbers four and eight.

## Methods

### 2.7 Cell culture conditions.

Primary human lung fibroblasts (pHLFs) were maintained in DMEM supplemented with 10% FBS, 5mM glucose, 700 $\mu$ M glutamine and 50 units/ml of penicillin and streptomycin in T175 flasks. Cells were incubated in a 37°C and 10% CO<sub>2</sub> humidified incubator and routinely tested for mycoplasma contamination. Upon reaching 80-90% confluency, cell monolayers were washed once with PBS and then incubated with 7mls of 0.05% trypsin-EDTA until detachment was observed. 14mls of 10% FBS DMEM was then added to neutralise the trypsin and the cell suspension centrifuged

at 300g for 5 minutes at room temperature using a bench centrifuge (MSE Mistral 3000, UK). The supernatant was subsequently discarded, and the cell pellet resuspended in 10% FBS DMEM. A fourth of the resuspension was transferred to a new tube and topped up to 20mls of 10% FBS DMEM which was then transferred once more to a new T175 flask for further expansion. The following section describes the procedure if the cells after resuspension were to be used for an experiment.

## 2.8 Preparation of cells for experiments.

An aliquot of the resuspension was taken and used for cell counting with a Scepter 2.0 Handheld Automatic Cell Counter (Millipore). pHLFs were seeded at a density of  $1 \times 10^5$ /ml and allowed to grow for 24-48 hours (dependent on experimental procedure). For 6-well plates, 2mls of cell suspension was added per well; for 12-well plates, 1ml of cell suspension was added per well; for 96-well plates, 100 $\mu$ l of cell suspension was added per well (avoiding the perimeter wells which received 100 $\mu$ l DMEM). Following 48 hours, media was replaced with serum-starved media (0% or 0.4% FBS DMEM) and left for a further 16-24 hours. This serum starvation step ensured limited interference with other cytokines and growth factors present in FBS prior to treating with TGF- $\beta_1$ . Before experiments, the media was replaced with fresh serum-starved media which was left for an hour to allow cells to acclimate metabolically.

## 2.9 Compound and metabolite preparation.

Compound/Metabolite	Received as a	Solubilised in	Stock concentration	Storage temperature
AZD8055	Powder	DMSO	10mM	-20°C
NCT-503	Powder	DMSO	20mM	4°C
R162	Powder	DMSO	30mM	-20°C
CB-839	Liquid	DMSO	10mM	-80°C
AOAA	Powder	DMEM	10mM	RT
L-serine	Powder	DMEM	5mM	RT

Glycine	Powder	DMEM	5mM	RT
L-glutamic acid	Powder	DMEM	5mM	RT
L-alanine	Powder	DMEM	5mM	RT
Dimethyl 2-oxoglutarate	Liquid	DMEM	6.9M	RT
Nonessential amino acids	Liquid	DMEM	10mM	4°C
Pyruvate	Liquid	DMEM	10mM	4°C

**Table 2. 4** Preparation and storage conditions for inhibitors and metabolites.

Amino acid solutions were filtered using 0.2µm filters prior to cell administration.

### 2.10 siRNA preparation.

5nmol of silencing RNA (siRNA) containing four different target sequences was received from Dharmacon™ and resuspended in 500µl nuclease-free water to produce a stock concentration of 10µM which was then aliquoted and stored at -20°C. All siRNA studies utilized pHLFs grown on 12-well plates. Following 24 hours from cell seeding, the media was replaced with 0% FBS DMEM without penicillin and streptomycin. The lipid vector, Lipofectamine® RNAiMAX (ThermoFisher, USA) was incubated with the siRNA or the non-targeting siRNA control (siNT) for 15 minutes to ensure optimal uptake of the RNA by the lipid vectors. Cells were then treated with the siRNA/siNT for a final concentration of 20nM for 6 hours before half of the media was removed and 1.5mls 0.4% FBS DMEM added. After 24 hours, the media was removed and replaced with fresh 0 or 0.4% FBS DMEM for the start of the experiment.

### 2.11 Macromolecular crowding assay.

Collagen I deposition was measured in a 96-well format using a high-content imaging based macromolecular crowding assay. The macromolecular components allow for close proximity of collagen cross-linking enzymes to the cell surface which are able to effectively cleave secreted procollagen peptides and establish an insoluble collagen matrix within the 48-hour timeframe of the experiment. This allows

for visualisation and quantification of the complete collagen maturation process. A limitation is the inherent dynamic range restrictions of antibody-based fluorescent techniques which prevents absolute quantification in methods such as HPLC.

pHLFs were seeded in a black-walled 96-well plate (Corning, USA) in 10% FBS DMEM. After 48 hours, cells were observed for confluency and the media replaced with 0.4% FBS DMEM. The next day, macromolecular crowding media was made in 0.2µm-filtered 0.4% FBS DMEM containing Ficoll PM 400 (25mg/ml), Ficoll PM 70 (37.5mg/ml) and 17µg/ml ascorbic acid. After an hour, inhibitors were added (if applicable) and cells left undisturbed for 1-2 hours. Metabolites were then added (if applicable) and cells left undisturbed for 30 minutes. Lastly, 1ng/ml of TGF-β<sub>1</sub> or control was added. All inhibitors, metabolites and cytokines were solubilised in the macromolecular crowding media.

pHLFs were then left in the incubator for 48 hours before receiving a PBS wash, fixation with -20°C methanol (VWR, UK), permeabilised with 0.1% (v/v) Triton-X-100 (Sigma-Aldrich, UK) in PBS and then stained with primary collagen I antibody and left overnight at 4°C. Plates were washed three times with 0.05% Tween-20 (v/v) (Sigma-Aldrich, UK) following fixation, permeabilization and antibody staining. The fluorescent secondary antibody (AF 488) and DAPI in PBS were then added and plates incubated at room temperature for 90 minutes before a final three washes with PBS-T and storage with 200µl/well of PBS at 4°C if not immediately imaged afterwards. Fluorescent signal was measured using the high content imaging platform ImageXpress (Molecular Devices, USA) and subsequent images collected were analysed using the Meta Xpress software. Mean fluorescent intensity per well was calculated with reads from four fields of view and data normalised to cell count. Data was analysed, expressed as the mean ± SEM and presented using GraphPad Prism 8. IC<sub>50</sub> values were calculated using four-parameter non-linear regression, where applicable.

## **2.12 Immunoblotting.**

Cells grown in 6-well or 12-well plates were lysed with 70µl or 120µl of PhosphoSafe (Novagen, USA) supplemented with Complete mini protease inhibitor (Roche,

Germany), respectively. Lysates were then scraped and transferred to microcentrifuge tubes and protein quantified using the bicinchoninic acid (BCA) protein assay (Pierce, USA) before storage at -20°C. Following the manufacturer's instructions, samples were read at 562nm and a standard curve using bovine serum albumin from 20µg/ml to 2mg/ml was used to quantify protein concentrations. For all immunoblotting experiments, 7.5µg of protein was used per well. Protein samples were treated with Bolt sample reducing agent 10x (ThermoFisher, USA) and Bolt LDS sample reducing buffer (ThermoFisher, USA) and then incubated for 10 minutes at 95°C. Tubes were then spun down to recapture condensation and loaded onto a 4-12% Bis-Tris gel (ThermoFisher, USA) and run at 150V for 45-60 minutes or until sufficient ladder separation. Gel transfer onto a nitrocellulose membrane was performed using an iBlot® 2 dry blotting system (ThermoFisher, USA) at 20V for 7 minutes. Membranes were then transferred onto small trays with 0.01% (v/v) Tween-20 in TBS (TBS-T) and then incubated at room temperature for one hour with 5% milk in TBS-T. Afterwards, membranes were transferred to 50ml Falcon® conical tubes with 5mls of 5% BSA in TBS-T and incubated overnight at 4°C with a primary antibody (listed in Table 2.3). Membranes were then washed with TBS-T three times before being incubated at room temperature for two hours with a horseradish peroxidase (HRP)-linked secondary antibody (Dako, UK). Afterwards, membranes were washed with TBS-T three times and developed by adding a layer of HRP substrate and waiting one minute before imaging using an ImageQuant™ LAS 4000 system (GE Healthcare Life Sciences, UK). Quantification analysis was performed using ImageQuant™ TL software (GE Healthcare Life Sciences, UK).

### **2.13 Chromatin-bound protein fractionation.**

Cells were seeded in T175 flasks and given 0.4% FBS DMEM media 24 hours prior to TGF-β<sub>1</sub> stimulation and subsequent cell lysis at 8 hours and 24 hours. Cell lysis and cytosolic extraction were performed using NE-PER™ following the manufacturer's instructions (ThermoFisher, USA). The pellet containing the nuclear fraction was then lysed for 30 minutes in Buffer B (3mM EDTA, 0.2mM EGTA and 1mM DTT with protease inhibitor) and followed by centrifugation at 1,700g at 4°C for 5 minutes. At this stage, nucleosoluble proteins remained in the supernatant and the

chromatin-bound proteins in the pellet, which was then washed once with Buffer B and resuspended in Laemmli buffer (4% SDS, 20% glycerol, 10% 2-ME, 0.004% bromophenol blue and 0.125M Tris-HCl).

## **2.14 qRT-PCR and analysis.**

### **2.14.1 RNA isolation, purification and quantification.**

All reagents were of molecular biology grade and DEPC-treated deionised water was used where applicable. Equipment, gloves and surfaces were routinely treated with RNaseZap (Sigma-Aldrich, UK) to reduce the chances of RNase contamination.

Cells were seeded in 6-well plates as previously described and cellular RNA extracted using a Qiagen RNeasy Mini Kit (QIAGEN, USA) which consists of the following steps. 350µl of buffer RLT was added to plate wells and scraped before being transferred to microcentrifuge tubes. 350µl of 70% ethanol (VWR, UK) was then added to each sample and mixed thoroughly by pipetting up and down several times. The sample was then transferred to a RNeasy Mini spin column and centrifuged at 10,000g for 15 seconds at room temperature. The flow-through was discarded and 700µl of Buffer RW1 was added to the column and centrifuged at 10,000g for 15 seconds at room temperature. The flow-through was discarded and 500µl of Buffer RPE was added to the column and centrifuged as before. The flow-through was discarded and the above step repeated. Finally, 50µl of RNase-free water (supplied by the kit) was added directly onto the column membrane and left for 1 minutes before centrifugation at 15,000g for 15s. This last step was repeated once more with 25µl of RNase-free water, reaching a total volume of 75µl of extract.

### **2.14.2 DNase treatment.**

Sample genomic DNA was removed from the eluted samples by DNase (ThermoFisher, USA) treatment which involved incubation at 37°C for 10 minutes before being heat-inactivated at 60°C for another 10 minutes using a DNA Engine thermal cycler (Bio-Rad, USA). RNA concentration and protein contamination were assessed using a Nanodrop spectrophotometer (ThermoFisher, USA) by measuring

the  $A_{260}$  and  $A_{260/280}$  ratio, respectively. Samples with ratios between 1.7 and 2.0 were considered appropriate quality for subsequent cDNA conversion.

### **2.14.3 cDNA synthesis.**

cDNA was created by reverse transcription of the purified RNA samples using a qScript cDNA supermix kit (Quanta Biosciences, USA). Between 500ng-1 $\mu$ g of RNA was added to 4 $\mu$ l of qScript cDNA Supermix (5x reaction buffer containing optimized concentrations of  $MgCl_2$ , dNTPs, recombinant RNase inhibitor protein, qScript reverse transcriptase, random primers and oligo (dT) primers). Nuclease-free water was added to achieve a final volume of 20 $\mu$ l. Samples were then incubated for 5 minutes at 25°C followed by 30 minutes at 42°C and finally 5 minutes at 85°C.

### **2.14.4 Quantitative RT-PCR.**

Quantitative real-time polymerase chain reaction (qRT-PCR) was performed using a Power SYBR® Green PCR Master Mix (ThermoFisher, UK). The reaction consisted of 5 $\mu$ l of the SYBR Green PCR mix, 2 $\mu$ l of cDNA and 800nM of forward and reverse primers. Samples were run as triplicates on a Mastercycler EP Realplex (Eppendorf, Germany). Cycling conditions: 95°C for 10 minutes for SYBR Green activation, 95°C for 15 seconds and 60°C for one minute for 40 cycles. Product specificity was assessed with a melting curve analysis which confirmed a single melting curve indicated a single PCR product. Cycle threshold (Ct) values were defined as the earliest point of the linear region of the logarithmic amplification plot reaching a threshold level of detection. Ct values were normalised by subtracting the average of the Ct values of the two housekeeping (HK) genes used (ATP synthase 5B (*ATP5B*) and  $\beta_2$  macroglobulin (*B2M*)). These two HK genes were identified by GeNorm analysis as the most stable genes for TGF- $\beta_1$  studies. Relative expression was calculated using the  $2^{-\Delta Ct}$  approach. Primer sequences are listed below, in Table 2.4. Primer sequences for *ATP5B* and *B2M* are proprietary and not available (Primer Design, UK).

Gene	Forward sequence	Reverse sequence
<i>COL1A1</i>	ATGTAGGCCACGCTGTTCTT	GAGAGCATGACCGATGGATT
<i>ATF4</i>	TTCTCCAGCGACAAGGCTAAGG	CTCCAACATCCAATCTGTCCCG
<i>SLC38A1</i>	CTTTTGCCACCTTTCCCTTT	GAGAGAAACAAACATGCTCCAA
<i>SLC38A2</i>	ATGAGTTGCCTTTGGTGATCC	ACAGGACACGGAACCTGAAAT
<i>SLC38A5</i>	CAGGCATCCGAGCCTATGAG	CCC CAACATTGTGCAGACAG
<i>SLC1A5</i>	CATCATCCTCGAAGCAGTCA	CTCCGTACGGTCCACGTAAT
<i>GLS1</i>	AGTTGCTGGGGG CATTCT TTTAGTT	CCTTTGATCACCACCTTCTCTTCGA
<i>GAC</i>	CCTCGAAGAGAAGGTGGTGATC	GTCTCATTGACTCAGGTGAC
<i>KGA</i>	CTGGAAGCCTGCAAAGTAAAC	TGA GGT GTGTA CTGG ACTTGG
<i>GLUL</i>	GGGAGGAGAATGGTCTGAAGT	GGG AGG AGA ATGGTCTGAAGT
<i>GLUD1</i>	CTCCAAACCCTGGTGTTCATT	CACACGCCTGTGTTACTGGT
<i>GPT2</i>	TCCTCACGCTGGAGTCCATGA	ATGTTGGCTCGGATGACCTCTG
<i>GOT1</i>	GGACCTGGAACCACATCACTGA	ACCACTTGGCAGCAGGTAGATG
<i>GOT2</i>	AAGAGGGACACCAATAGCAAAAA	GCAGAACGTAAGGCTTTCCAT

**Table 2. 5 Primer sequences for qRT-PCR.**

## 2.15 Quantification of hydroxyproline from cell supernatants.

Hydroxyproline present in cell supernatants was used as a proxy marker for pro-collagen secreted by the pHLFs. Hydroxyproline represents approximately 12% of the procollagen primary sequence and it is not found in significant quantities in other proteins. Quantification used reverse-phase high performance liquid chromatography (HPLC) which detected hydroxyproline covalently bound to the derivatization agent 7-chloro-4-nitrobenzo-oxa-1,2-diazole (NBD-Cl) using absorbance at 490nm. NBD-Cl preferentially reacts with secondary amino acids one order of magnitude faster than with primary amino acids and thus a derivatisation time of 20 minutes allows for maximal hydroxyproline conversion whilst limiting potential interference from primary amino acids.

Cells were grown in 12-well plates and 48 hours post-TGF- $\beta_1$  stimulation, 1ml of supernatants were transferred to 15ml tubes and mixed with 2mls of 100% ethanol (VWR, UK) and left overnight at 4°C to precipitate proteins. Extraction of the proteins

was performed using 0.45µm filters under a vacuum. Proteins were then hydrolysed by heating the filters in glass tubes with 2mls of 6M HCl at 110°C for 16-24 hours. 180µl of the hydrolysates was then transferred to 1.5ml tubes and evaporated to dryness via heating for 2-3 hours at 100°C. Samples were then reconstituted with 100µl of Milli-Q water (Millipore, UK), buffered with 100µl of 0.4M potassium tetraborate and reacted with 100µl 36mM NBD-Cl (in methanol). Samples were then heated to 37°C for 20 minutes and the reaction stopped by addition of 50µl 1.5M HCl and then 150µl of 167mM sodium acetate and 26% acetonitrile (v/v) at pH 6.4. Samples were then vortexed and filtered using low dead volume 0.22µm filters (ThermoFisher, UK) into polypropylene tube inserts within an Amber Snap Seal vial (Sigma-Aldrich, UK). Vials were then loaded onto an Agilent 1100 series HPLC (Agilent Technologies, USA) and injected into the column running with a mixture of buffers A and B as described below, in Table 2.5. Absorbance monitoring at 495nm was used to detect the hydroxyproline peak and elution time (4-6 minutes) from the column. Quantification of peaks was gathered from area under the curve (AUC) analysis and using a standard curve of known hydroxyproline concentrations.

<b>Column</b>	<b>LiChrospher, 100 RP-18, 250 x 4mm, 5µm</b>	
<b>Mobile phase</b>	<b>Buffer A-</b> aqueous acetonitrile (8% v/v) 82.9mM sodium acetate, pH 6.4 <b>Buffer B-</b> aqueous acetonitrile (75% v/v)	
<b>Column flow rate</b>	1.0ml/min	
<b>Column temperature</b>	40°C	
<b>Detection wavelength</b>	495nm	
<b>Elution gradient</b>	Time (min)	Buffer B (%)
	0	0
	5	5
	6	80
	12	80

	12.5	0
	25	0

**Table 2. 6 Conditions and buffers composition for HPLC detection of hydroxyproline.**

## 2.16 Quantification of free amino acids.

Free amino acids were quantified using reverse-phase high performance liquid chromatography (HPLC). For extracellular amino acids, 500µl of cell supernatants were deproteinated using 3kDa protein-filter columns (Sigma-Aldrich, UK) which were centrifuged at 12,000g for 45 minutes and the flow-through evaporated to dryness under vacuum and centrifugation at 45°C. For intracellular amino acids, cell monolayers were washed once with ice-cold PBS before being lysed with ice-cold RIPA buffer (ThermoFisher, UK) supplemented with protease inhibitor. Lysates were then transferred to 1.5ml tubes and vortexed vigorously for 30 seconds before being centrifuged at 21,000g for 10 minutes at 2°C. Supernatants were then transferred to 3 kDa columns and the process repeated as described above for extracellular amino acids. Samples were then reconstituted with 100µl of Milli-Q water and the process repeated as described for hydroxyproline in section 2.15. Derivatization time was extended to 60 minutes and a standard curve was made using nonessential amino acids mix supplemented with L-glutamine. Mobile phase and gradient were different to hydroxyproline settings and are listed below, in Table 2.6.

<b>Column</b>	<b>LiChrospher, 100 RP-18, 250 x 4mm, 5µm</b>
<b>Mobile phase</b>	<b>Buffer A-</b> aqueous acetonitrile (2% v/v) 82.9mM sodium acetate, pH 6.4 <b>Buffer B-</b> aqueous acetonitrile (75% v/v)
<b>Column flow rate</b>	1.0ml/min
<b>Column temperature</b>	40°C
<b>Detection wavelength</b>	495nm

<b>Elution gradient</b>	<b>Time (min)</b>	<b>Buffer B (%)</b>
	0	0
	12	0
	20	3
	26	5
	50	26
	50	80
	56	80
	56	0
	69	0

**Table 2. 7 Conditions and buffers composition for HPLC detection of amino acids.**

### **2.17 Statistical analysis.**

All data are expressed as the means  $\pm$  SEM and generated using GraphPad Prism 8. Statistical differences between groups were determined using one-way or two-way analysis of variance (ANOVA) with Tukey post-hoc test. Four-parameter and non-linear regression analysis was used to produce IC<sub>50</sub> values from compound concentration curves. The  $\alpha$  level was 0.05 for all tests.

## Chapter 3: Results

### Overview

The experimental results begin with an explanation of the preliminary work which initiated the subsequent studies of this thesis. It has been divided into three sections. The first section investigates the role of the serine and glycine biosynthetic pathways in mediating the pro-fibrotic functions of TGF- $\beta_1$  in primary human lung fibroblasts (pHLFs). The second section defines the functional impact of extracellular glucose, glutamine, glycine and serine concentrations on TGF- $\beta_1$ -induced collagen synthesis. The third and last section investigates the roles of glutamine metabolism in supporting TGF- $\beta_1$ -induced collagen synthesis.

### 3.1 The role of the serine biosynthetic pathway in mediating the pro-fibrotic effects of TGF- $\beta_1$ in human lung fibroblasts.

#### 3.1.1 Introduction.

Studies into the therapeutic potential of targeting the metabolic changes induced by TGF- $\beta_1$  in fibroblasts are relatively recent and limited in numbers. To obtain a more comprehensive image of these changes, ongoing studies in our centre employed RNA sequencing and demonstrated that the expression levels of many metabolic genes and pathways were significantly modulated by TGF- $\beta_1$  in primary human lung fibroblasts (pHLFs). One of these highly modulated pathways was the serine and glycine biosynthetic axis comprising the enzymes PHGDH, PSAT1, PSPH and SHMT2 (Table 3.1). The multifunctional kinase mTOR was further shown to be critical in mediating these transcriptional changes through pharmacological inhibition with the compound AZD8055. The studies described in the following section investigate the expression profiles, transcriptional regulation and role in TGF- $\beta_1$ -induced fibrotic parameters of this metabolic pathway.

**Hypothesis:** TGF- $\beta_1$  increases the expression of the serine-glycine biosynthetic axis to supply metabolites necessary to synthesize enhanced levels of collagen.

<b>Gene</b>	<b>Fold change with TGF-<math>\beta_1</math></b>	<b>Fold change with TGF-<math>\beta_1</math> and AZD8055</b>
<i>PHGDH</i>	6.8	-8.9
<i>PSAT1</i>	18.7	-30.5
<i>PSPH</i>	3.7	n.a.
<i>SHMT2</i>	4	-4

**Table 3. 1. TGF- $\beta_1$  increases the expression of the serine-glycine biosynthetic pathway genes via an mTOR-dependent mechanism.**

RNA sequencing data showing fold changes of serine-glycine biosynthesis genes in pHLFs 24 hours following TGF- $\beta_1$  stimulation compared to (second column) unstimulated and (third column) TGF- $\beta_1$ -stimulated and AZD8055 (mTOR inhibitor)-treated. n.a. means no fold change was measured. Data presented with permission [81].

### 3.1.2 Physiological glucose and glutamine media support TGF- $\beta_1$ -induced collagen I deposition.

Mounting evidence shows a concerning loss of metabolic fidelity between the *in vitro* and *in vivo* setting depending on the composition of the cell culture media, often containing supraphysiological levels of the pleiotropic nutrients glucose and glutamine. The transcriptomic work mentioned in Section 3.1.1 was performed in pHLFs grown in standard DMEM with 25mM glucose and 2mM glutamine. Average levels of these nutrients in the blood are much lower; 4-6mM for glucose and 500-800 $\mu$ M for glutamine. Therefore, the media was changed to acknowledge this discrepancy, adopting a concentration of 5mM for glucose and 700 $\mu$ M for glutamine. Deposition of collagen I, a core component of the ECM in lung fibrosis, was then measured by pHLFs grown in this altered media using a macromolecular crowding assay to confirm an adequate TGF- $\beta_1$  response. TGF- $\beta_1$  increased collagen deposition in a concentration-dependent manner with an EC<sub>50</sub> of 75pg/ml (95% CI 58-92pg/ml) (Figure 3.1). Fluorescent quantification was normalised to cell count and no significant change in cell numbers with TGF- $\beta_1$  stimulation was observed. To ensure a maximal response and maintain a degree of comparison with other studies and works, all stimulations with TGF- $\beta_1$  throughout this thesis were kept at 1ng/ml, unless stated otherwise.

Previous work has highlighted a pivotal role for the protein complex mTORC1 in regulating the pro-fibrotic functions of TGF- $\beta_1$ , including collagen I deposition. Indeed, the transcriptomic analysis mentioned in Section 3.1.1 showed the top modulated metabolic axis by TGF- $\beta_1$  (*PHGDH*, *PSAT1*, *PSPH* and *SHMT2*) to be mTOR-dependent. The requirement for this complex in supporting TGF- $\beta_1$ -induced collagen I deposition in pHLFs was then confirmed pharmacologically in the new media using a potent ATP-binding site competitive inhibitor, AZD8055. Treatment with this compound resulted in a concentration-dependent inhibition of TGF- $\beta_1$ -induced collagen I deposition with an IC<sub>50</sub> of 219nM (95% CI 168-288nM) (Figure 3.2). To ensure appropriate inhibition of mTOR activity, 1 $\mu$ M concentration of AZD8055 was chosen for all future experiments.

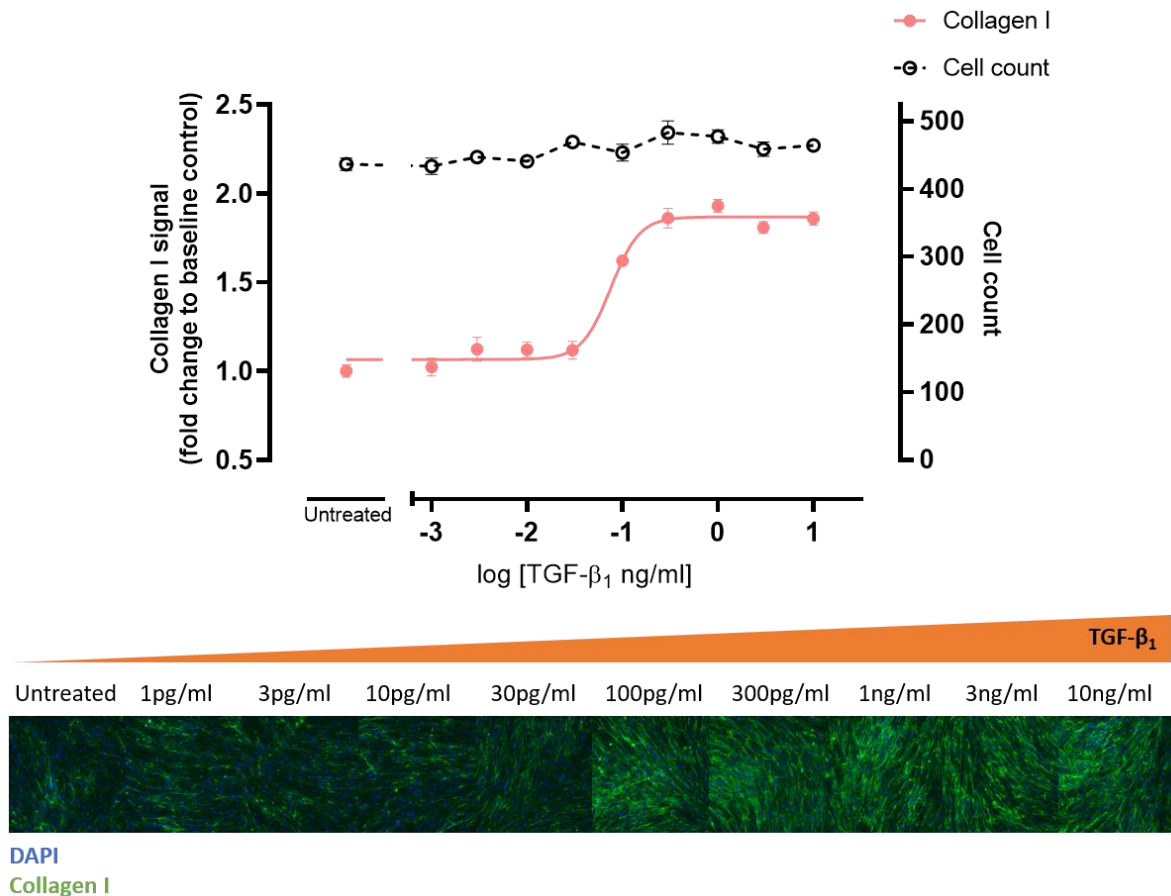


**Figure 3. 1. TGF- $\beta_1$  concentration-dependently increases collagen I deposition in physiological DMEM.**

Confluent pHLFs were stimulated with increasing concentrations of TGF- $\beta_1$  (1pg/ml to 10ng/ml) in macromolecular crowding conditions for 48 hours, prior to fixation and staining for collagen I and with DAPI. The mean fluorescent intensity and cell count per well (4 reads per well) was calculated and data expressed as mean  $\pm$  SEM of n=3 biological replicates with each biological replicate being an average of 6 technical replicates wells per condition. EC<sub>50</sub> value was calculated using four-parameter non-linear regression. Representative images from each condition are shown in the lower panel.

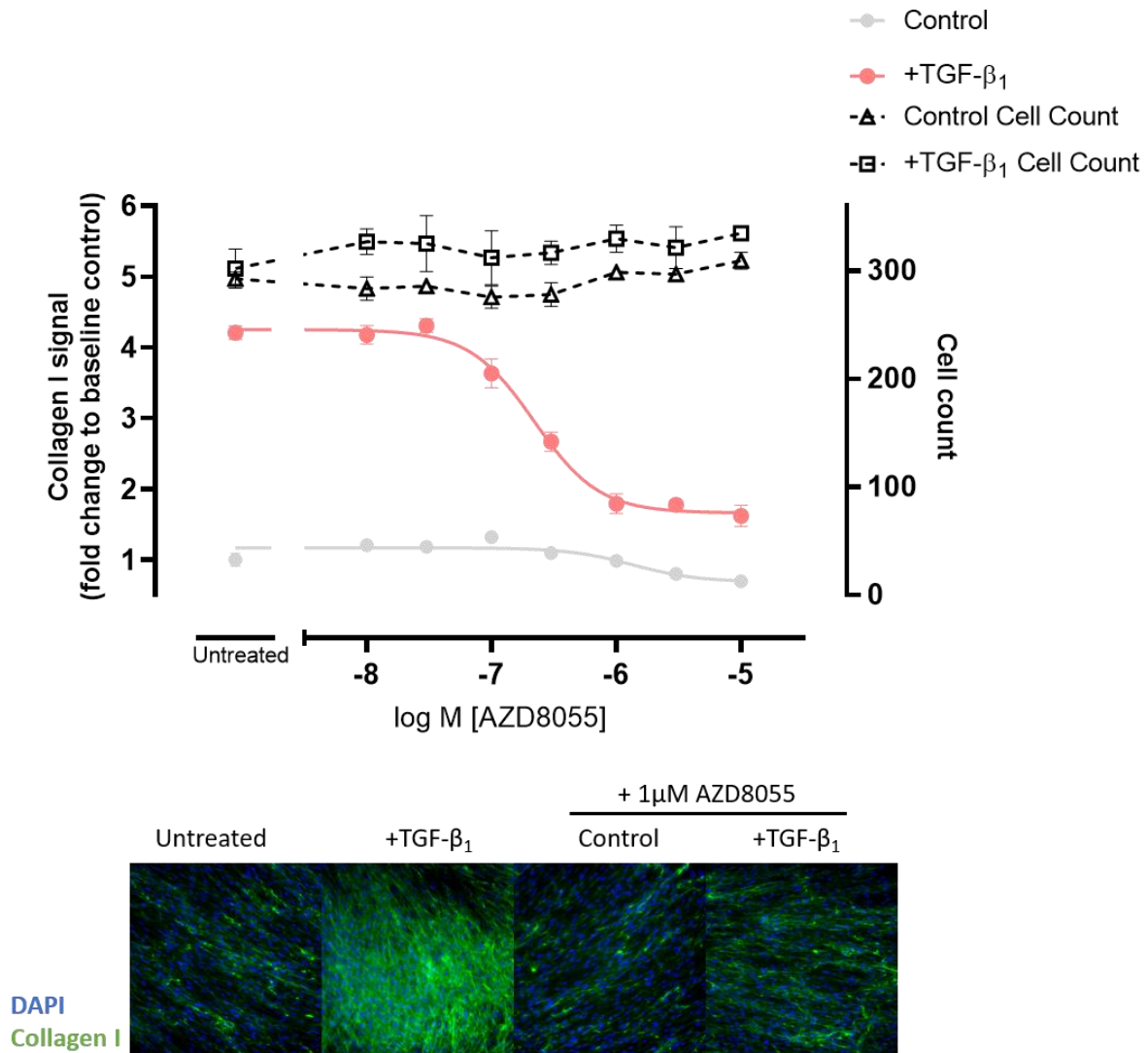


**Figure 3. 2. ATP-competitive mTOR inhibition decreases TGF- $\beta_1$ -induced collagen I deposition.**

Confluent pHLFs were stimulated with increasing concentrations of AZD8055 and stimulated with TGF- $\beta_1$  in macromolecular crowding conditions for 48 hours, prior to fixation and staining for collagen I and with DAPI. The mean fluorescent intensity and cell count per well (4 technical reads per well) was calculated and data expressed as mean  $\pm$  SEM of  $n=3$  biological replicates with each biological replicate being an average of 6 technical replicates wells per condition. IC<sub>50</sub> value was calculated using four-parameter non-linear regression. Representative images from each condition are shown in the lower panel.

In summary, these data show an induction in collagen I deposition following TGF- $\beta_1$  stimulation and the critical role of mTOR in mediating this pro-fibrotic effect in physiological DMEM. This is in agreement with other studies from our centre which assessed these pro-fibrotic parameters in high glucose and glutamine DMEM. All subsequent experiments were carried out in pHLFs grown in this 'physiological' media, henceforth known as 'DMEM' or 'media', unless stated otherwise.

### **3.1.3 TGF- $\beta_1$ increases the protein levels of the serine-glycine biosynthetic pathway via an mTOR-dependent mechanism.**

The RNA sequencing dataset showed a significant increase in the mRNA levels of PHGDH, PSAT1, PSPH and SHMT2 upon TGF- $\beta_1$  stimulation, which were all dependent on mTORC1 activity (Table 3.1). These changes were then assessed at the protein level at the same 24-hour time-point following TGF- $\beta_1$  stimulation using immunoblotting. Protein levels of all four enzymes were increased with TGF- $\beta_1$  stimulation and these increases were inhibited by AZD8055, mirroring the transcriptional signature seen in the RNA sequencing data (Fig. 3.3). Unexpectedly, SHMT2 protein levels were moderately increased with AZD8055 treatment alone, indicating an mTOR-dependent mechanism outside of TGF- $\beta_1$  signalling which may negatively regulate the protein abundance of this enzyme (Fig. 3.3D).

These data confirm that the serine-glycine biosynthetic axis proteins PHGDH, PSAT1, PSPH and SHMT2 are TGF- $\beta_1$ -responsive genes and that TGF- $\beta_1$ -induced expression is mTOR-dependent.

### **3.1.4 TGF- $\beta_1$ increases ATF4 expression via an mTOR-dependent mechanism.**

The next line of investigation aimed to elucidate the mTOR-dependent factor which was responsible for the transcriptional upregulation of this axis following TGF- $\beta_1$  stimulation. ATF4 is a known mTOR-responsive transcription factor that is integral for cellular stress adaptation, orchestrating the transcription of a host of genes, including all enzymes of the serine-glycine biosynthetic axis. Levels of *ATF4* mRNA

were then quantified by qPCR and observed to be significantly upregulated at 24 hours following TGF- $\beta_1$  stimulation ( $p < 0.001$ ,  $n = 3$ ) (Fig. 3.4A).

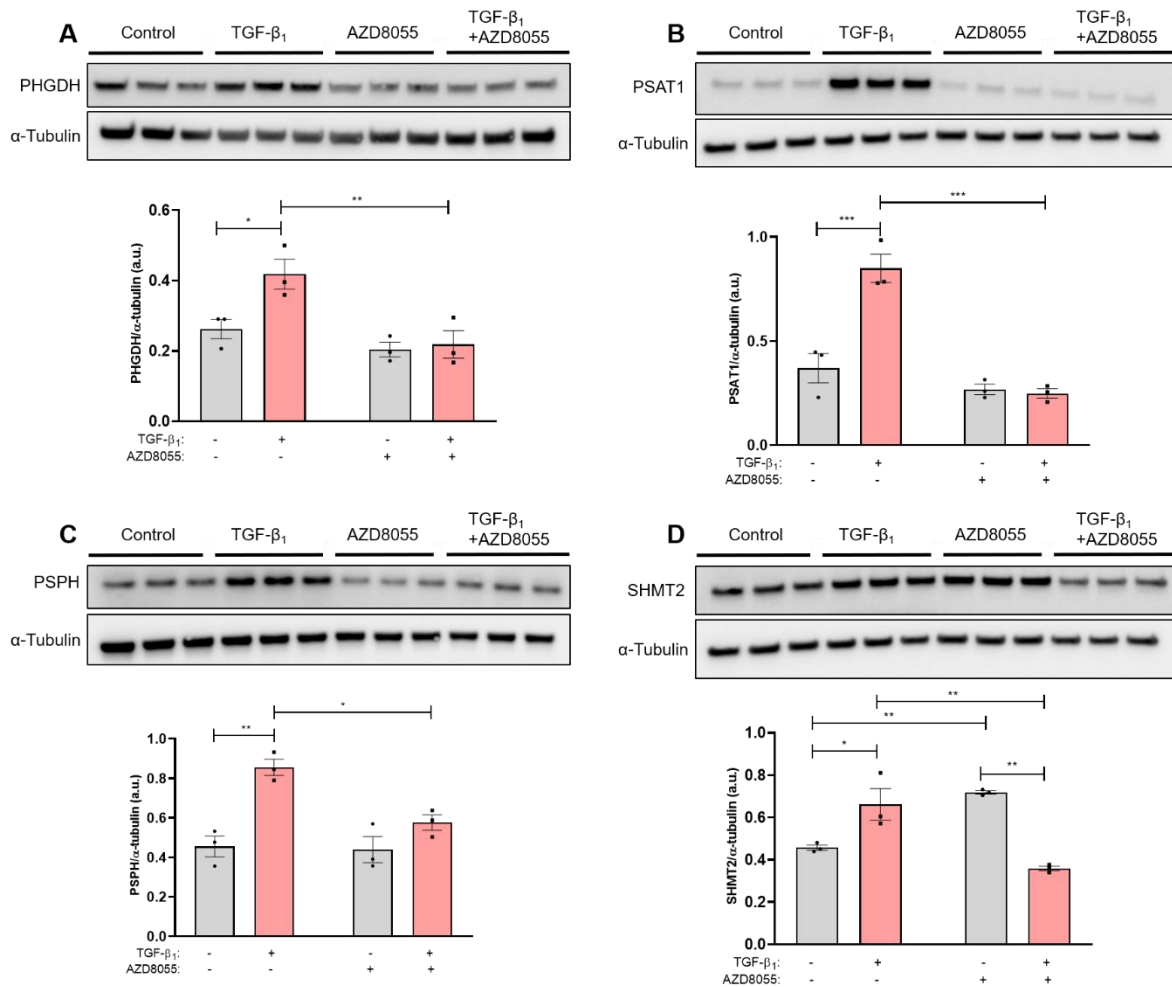


**Figure 3. 3. TGF- $\beta_1$  increases the protein abundance of the serine-glycine biosynthetic axis via an mTOR-dependent mechanism.**

pHLFs were serum starved for 24 hours prior to pre-incubation with 1  $\mu$ M AZD8055 or 0.1% DMSO control and stimulation with 1 ng/ml TGF- $\beta_1$ . Lysates were collected at 24 hours and PHGDH, PSAT1, PSPH and SHMT2 were assessed by immunoblotting and normalised to  $\alpha$ -tubulin. Comparisons between groups were performed by two-way ANOVA followed by Tukey post-hoc test. In all cases,  $p < 0.05$  was considered statistically significant. Data are presented as mean  $\pm$  S.E.M. of  $n = 3$  biological replicates \*= $p < 0.05$ , \*\*= $p < 0.01$ , \*\*\*= $p < 0.001$  [81].

Treatment with AZD8055 had no effect on *ATF4* mRNA levels. This indicated that TGF- $\beta_1$  transcriptionally modulates ATF4 via an mTOR-independent mechanism. In contrast, TGF- $\beta_1$  significantly increased ATF4 at the protein level and this effect was dependent on mTOR activity (Fig. 3.4B). This result was replicated using a further mTOR inhibitor, Torin-1 (Fig. 3.4C). Together, these results define a mechanism for ATF4 regulation which is mTOR-independent at the transcriptional level but mTOR-dependent at the post-transcriptional level.

### **3.1.5 TGF- $\beta_1$ -induced *ATF4* mRNA levels are SMAD3-dependent.**

The TGF- $\beta_1$  receptor bound to its ligand can promote signalling cascades through the canonical pathway involving the Smad proteins as well as several non-canonical pathways such as PI3K, TRAF4/6 and Ras signalling.

The previous section demonstrated that the increase in *ATF4* mRNA abundance was mTOR-independent. The following step was to determine whether this increase in *ATF4* mRNA levels is mediated through Smad signalling. After being phosphorylated and activated by the TGF- $\beta_1$ RI/II complex, Smad2 and Smad3 form a heterodimer which then associates with Smad4 and then translocates to the nucleus. Smad3 is phosphorylated at its serine 423 and 425 site and this mark is indicative of active Smad signalling. To assess the role of Smad signalling, an siRNA approach was used to silence Smad3 and therefore prevent the Smad2/3 heterodimer from forming and preventing a phosphorylation event (Smad3<sup>S423/425</sup>) and therefore activation of Smad signalling. Immunoblotting at 1-hour post-TGF- $\beta_1$  stimulation showed a complete loss of Smad3 phosphorylation at Ser<sup>423/425</sup> following treatment with siSmad3 which confirmed that the functional properties of this protein relating to TGF- $\beta_1$  signalling were inhibited (Fig. 3.5A). Furthermore, silencing of Smad3 completely inhibited the increase in *ATF4* mRNA abundance induced by TGF- $\beta_1$  stimulation (Fig. 3.5B). There was no baseline effect of *ATF4* mRNA levels observed

with siSmad3 which confirmed that the Smads signalling pathway is utilized to regulate ATF4 only in a TGF- $\beta_1$ -specific context.

Collectively, these data demonstrate that ATF4 is Smad3-dependent at the transcriptional level and mTOR-dependent at the post-transcriptional level.

### **3.1.6 TGF- $\beta_1$ induces ATF4 protein abundance from 8 hours onwards.**

The regulation of ATF4 was shown to be predominantly at the protein level 24 hours following TGF- $\beta_1$  stimulation (Fig. 3.4). To further investigate the temporal protein abundance profile of ATF4 in TGF- $\beta_1$ -stimulated pHLFs, a time-course was performed where cell proteins were extracted 3, 8, 24 and 48 hours following stimulation with TGF- $\beta_1$ . ATF4 protein levels were strongly increased beginning from 8 hours post TGF- $\beta_1$  stimulation (Fig. 3.6A). This was maintained up to 48 hours following TGF- $\beta_1$  stimulation. Echoing previous data, ATF4 was not detected in TGF- $\beta_1$ -stimulated cells treated with AZD8055.

To investigate ATF4 nuclear translocation, cellular proteins were separated into cytoplasmic, nuclear and chromatin-bound fractions using lyses buffers of different strengths. This confirmed ATF4 was very strongly associated with the chromatin-bound fraction at the 8-hour and 24-hour time-points following TGF- $\beta_1$  stimulation (Fig. 3.6B).

Taken together, these data show ATF4 to be induced by TGF- $\beta_1$  and bound to chromatin from 8 hours following stimulation. Furthermore, ATF4 protein abundance is maintained at similar levels up to 48 hours post TGF- $\beta_1$  stimulation.

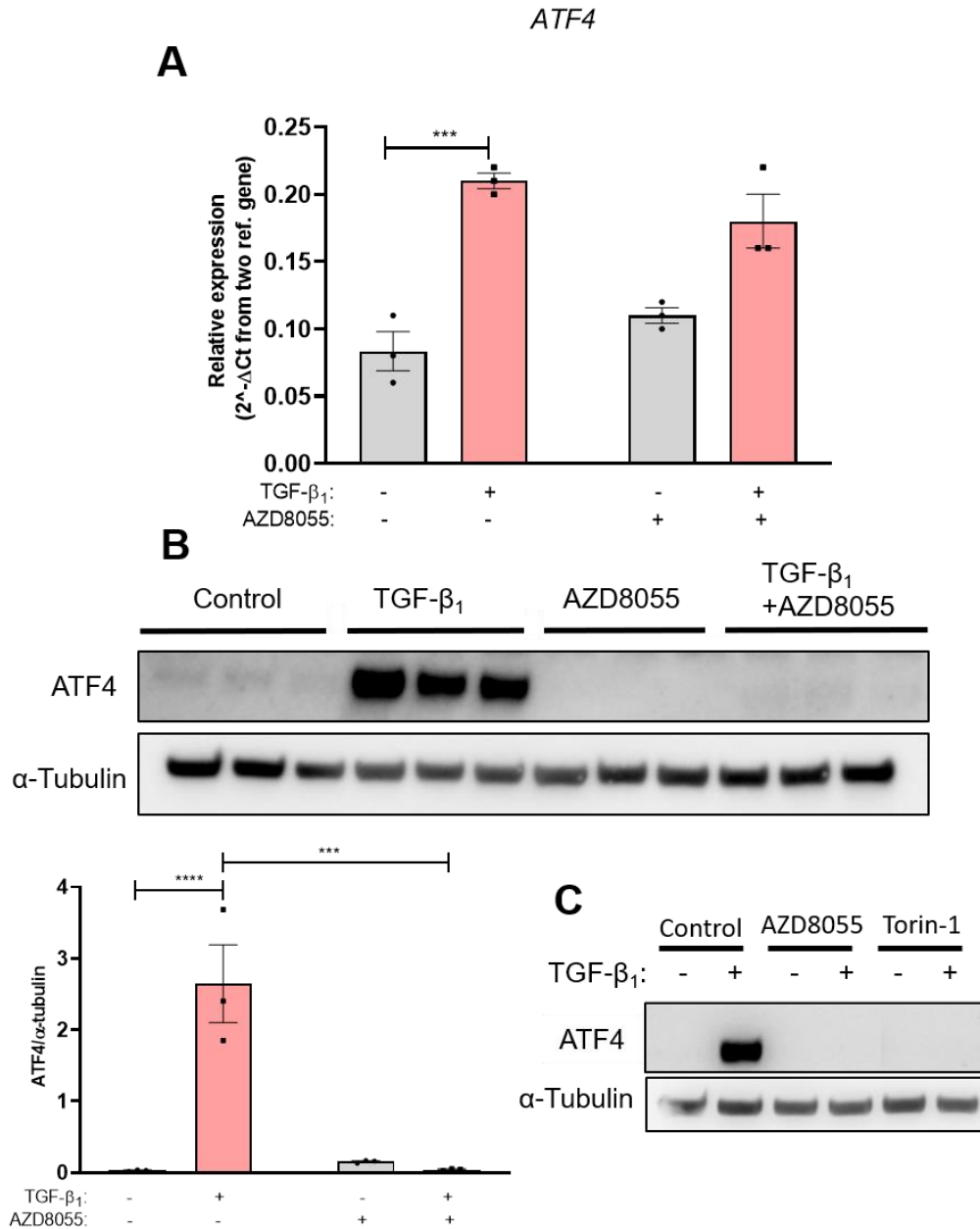


**Figure 3. 4. mTOR regulates TGF- $\beta_1$ -induced ATF4 expression via a post-transcriptional mechanism.**

pHLFs were serum starved for 24 hours prior to pre-incubation with 1 $\mu$ M AZD8055, 1 $\mu$ M Torin-1 or 0.1% DMSO control and stimulation with 1ng/ml TGF- $\beta_1$ . (A) mRNA or (B-C) protein lysates were collected at 24 hours. (A) *ATF4* gene expression quantified by qRT-PCR and expressed relative to the mean of two housekeeping genes. (B-C) Immunoblotting assessed ATF4 protein abundance and quantification expressed relative to  $\alpha$ -tubulin. Comparisons between groups were performed by two-way ANOVA followed by Tukey post-hoc test. In all cases,  $p < 0.05$  was considered statistically significant. Data expressed as mean  $\pm$  S.E.M. of  $n = 3$  biological replicates \*= $p < 0.05$ , \*\*\*= $p < 0.001$  [81].

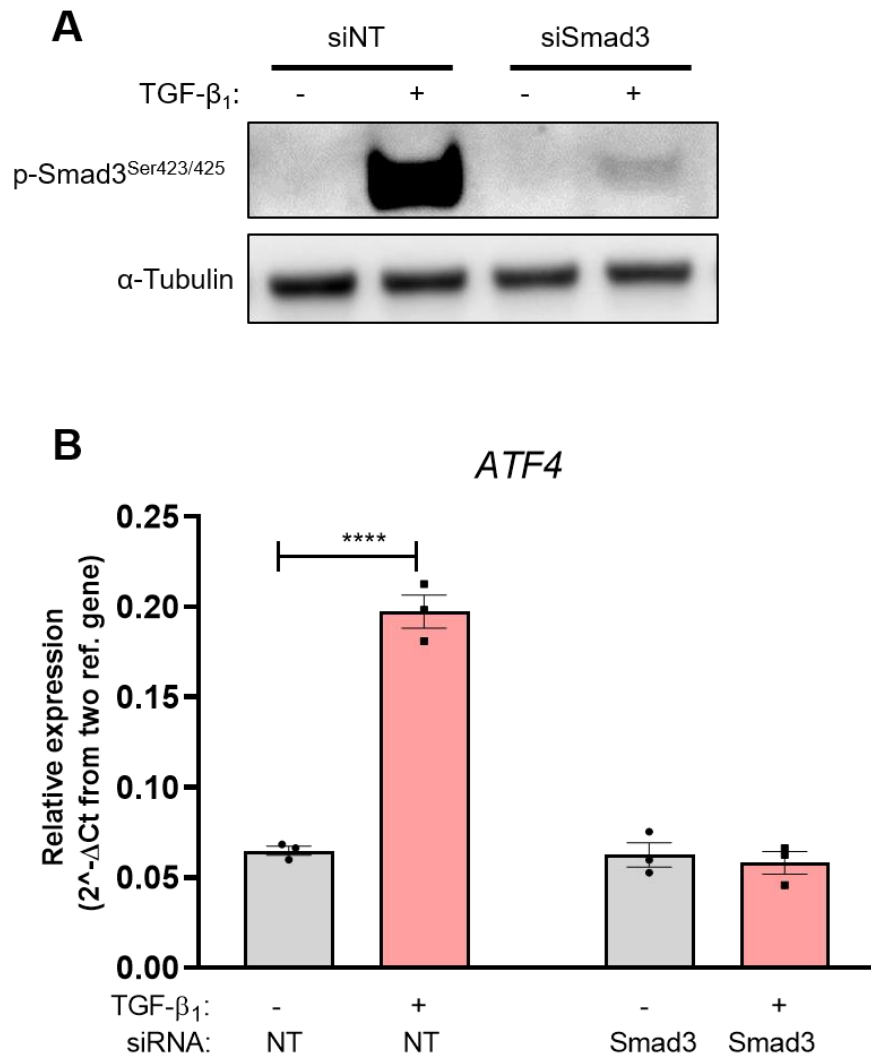


**Figure 3. 5. TGF- $\beta_1$ -induced ATF4 mRNA levels are Smad3-dependent.**

pHLFs were transfected with siSmad3 or non-targeting siRNA (siNT) as described in section 2.10. (A) Immunoblotting was used to assess knockdown efficiency at 3 hours post-TGF- $\beta_1$  stimulation. (B) *ATF4* gene expression was assessed by qRT-PCR 24 hours post-TGF- $\beta_1$  stimulation and expressed relative to the mean of two housekeeping genes. Comparisons between groups were performed by two-way ANOVA followed by Tukey post-hoc test. In all cases,  $p < 0.05$  was considered statistically significant. Data expressed as mean  $\pm$  S.E.M. of  $n=3$  biological replicates. \*\*\*\*= $p < 0.0001$  [81].

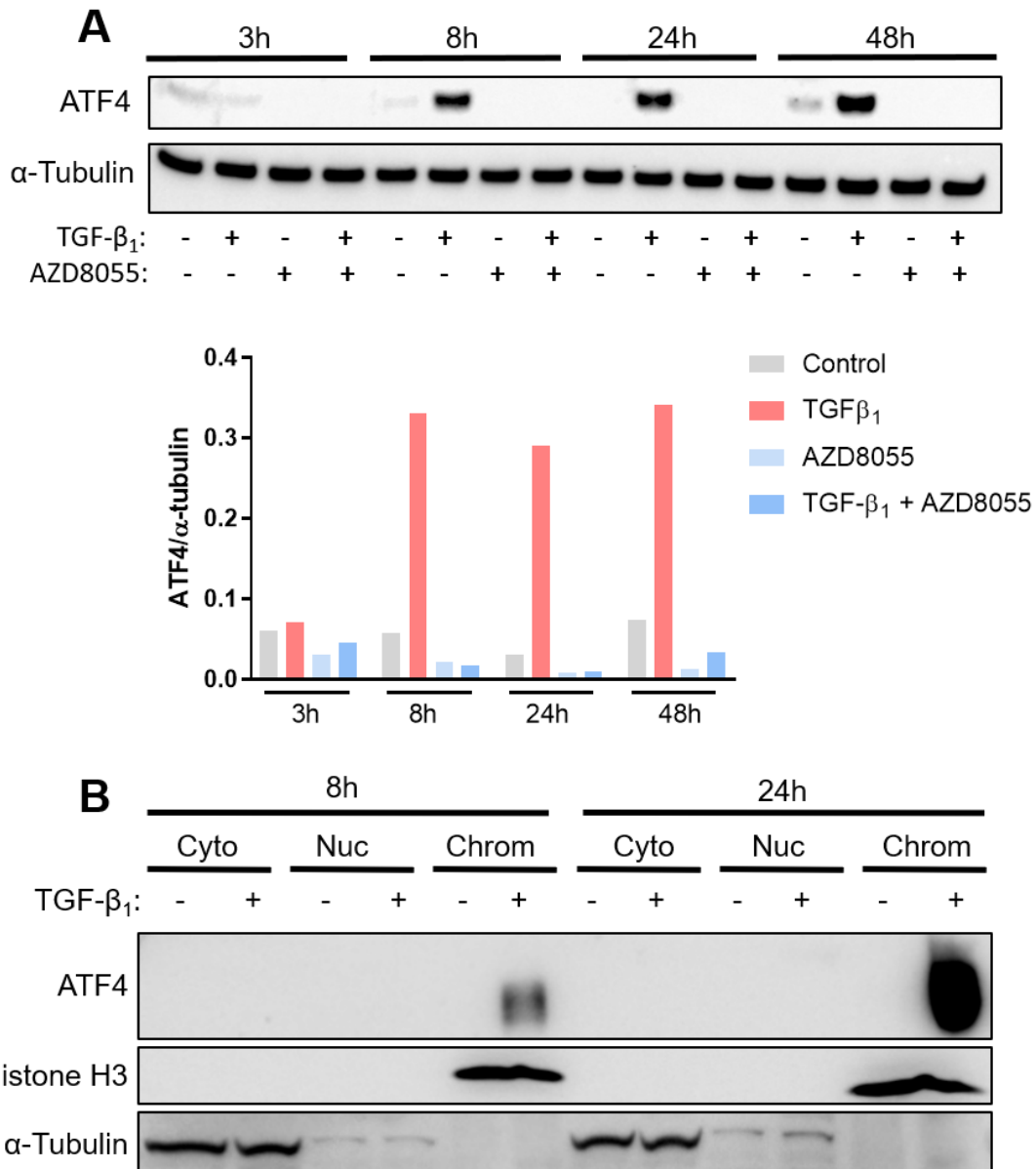


**Figure 3. 6. TGF- $\beta_1$ -induced ATF4 is chromatin-bound from 8 hours onwards.**

pHLFs were serum starved for 24 hours prior to pre-incubation with 1 $\mu$ M AZD8055 or 0.1% DMSO control and stimulation with 1ng/ml TGF- $\beta_1$ . (A) Proteins were collected at indicated timepoints, assessed by immunoblotting and quantification expressed relative to  $\alpha$ -tubulin. (B) Proteins were collected at indicated timepoints and fractionated as described in section 2.13 and assessed by immunoblotting. Data is from one independent experiment with single densitometry values shown and blots representative of n=3 biological replicates [81].

### **3.1.7 Loss of ATF4 via siRNA-mediated knockdown decreases pHLF cell viability.**

Previous data showed TGF- $\beta_1$  strongly increased ATF4 protein and mRNA levels. Furthermore, studies from the host centre found silencing of ATF4 inhibited the TGF- $\beta_1$ -dependent increases in the serine-glycine biosynthetic axis genes (Fig. 3.3) [81]. The following step was to evaluate the role of ATF4 in TGF- $\beta_1$ -induced collagen synthesis. To date, there is no commercially available small-molecule inhibitor for ATF4 and therefore an siRNA approach was taken. However, silencing of ATF4 over the 48-hour post-TGF- $\beta_1$  stimulation experimental timeframe resulted in significant cell death (Fig. 3.7A). pHLFs treated with siATF4 exhibited an approximate 20% decrease in cell count compared to those treated with siNT in both groups ( $p < 0.005$ ,  $n = 5$ ). This was confirmed through immunoblotting at 24 hours post-TGF- $\beta_1$  stimulation (Fig. 3.7B).

This cell viability effect prevented accurate collagen measurements as the pHLFs ceased to be confluent. However, a CRISPR-Cas9 approach overcame initial cell death as HLFs were able to achieve confluency throughout the protocol timeline of two weeks, much longer than the two days in the siRNA protocol [82]. It is not known if the knockdown efficiency of siATF4 would remain as high as observed in figure 3.7B if cells were allowed a similar timeframe to overcome the initial cell death following loss of ATF4 expression. Moreover, crATF4 cells displayed a complete reduction in TGF- $\beta_1$ -induced collagen deposition [81].

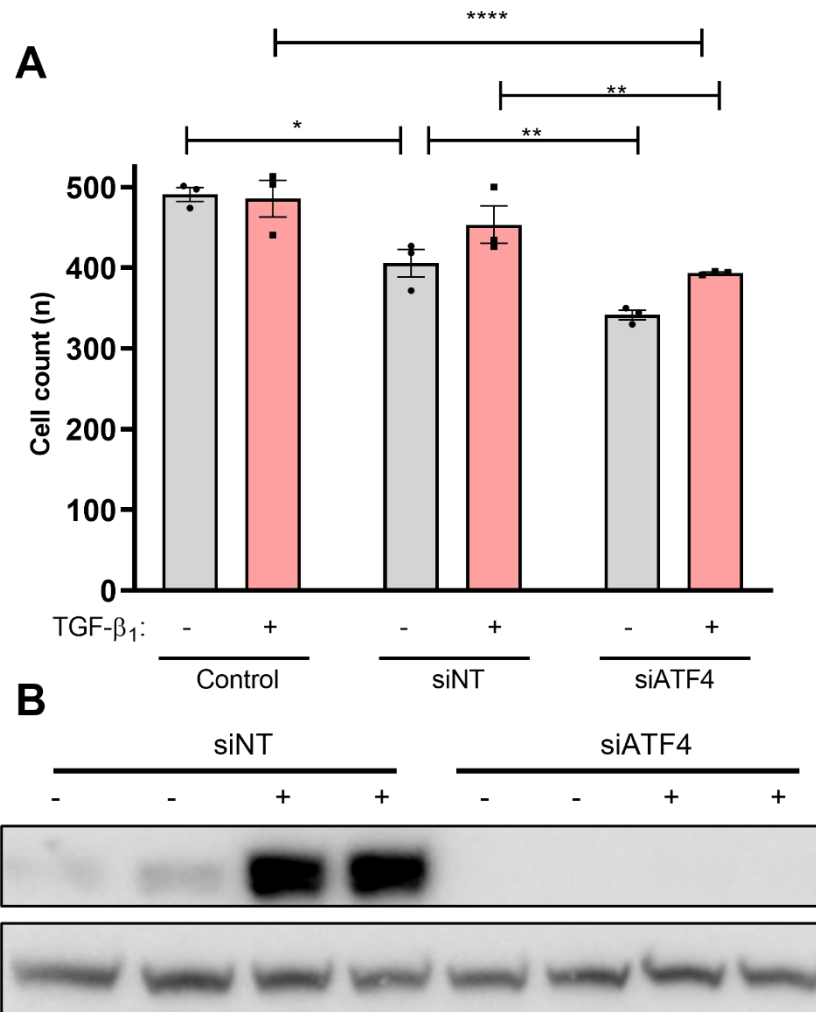


**Figure 3. 7. siATF4 treatment decreases cell count.**

pHLFs were transfected with siATF4 or siNT as described in section 2.10. (A) Cell count was measured using the macromolecular crowding assay 48 hours following TGF- $\beta_1$  (1ng/ml) stimulation. (B) ATF4 protein abundance was assessed by immunoblotting 24 hours following TGF- $\beta_1$  (1ng/ml) stimulation. Comparisons between groups were performed by two-way ANOVA followed by Tukey post-hoc test. In all cases,  $p < 0.05$  was considered statistically significant. Data expressed mean  $\pm$  S.E.M. of 3 biological replicates \*= $p < 0.05$ , \*\*= $p < 0.01$ , \*\*\*\*= $p < 0.0001$ .

### **3.1.8 PHGDH inhibition decreases TGF- $\beta$ <sub>1</sub>-induced collagen I deposition.**

The functional role of the serine biosynthetic pathway was next assessed using a pharmacological approach with a small-molecule inhibitor for PHGDH, NCT-503. This compound is non-competitive with the PHGDH substrates 3-PG and NAD<sup>+</sup> and has high stability after 48 hours in aqueous solution.

NCT-503 treatment completely inhibited TGF- $\beta$ <sub>1</sub>-induced collagen I deposition at 30 $\mu$ M but this effect was not concentration-dependent (Fig. 3.8A). No significant effect was detected in unstimulated pHLFs at this concentration of NCT-503 which indicated specific engagement of a TGF- $\beta$ <sub>1</sub>-mediated mechanism. Moreover, no cell count changes were measured at the highest concentration of NCT-503 used (Fig 3.8B).

*COL1A1* gene expression was then assessed 24 hours following TGF- $\beta$ <sub>1</sub> stimulation to gain further insight into the mechanism of action of PHGDH inhibition in reducing TGF- $\beta$ <sub>1</sub>-induced collagen I deposition. As expected, TGF- $\beta$ <sub>1</sub> significantly increased *COL1A1* mRNA levels by 7.2-fold ( $p < 0.0001$ ,  $n = 3$ ). Interestingly, 30 $\mu$ M NCT-503 treatment reduced *COL1A1* mRNA by approximately 50% in TGF- $\beta$ <sub>1</sub>-treated pHLFs compared to stimulation alone ( $p < 0.01$ ,  $n = 3$ ) (Fig. 3.8C).

Collectively, these data suggest PHGDH acts at both the transcriptional and post-transcriptional level to inhibit TGF- $\beta$ <sub>1</sub>-induced collagen I deposition.

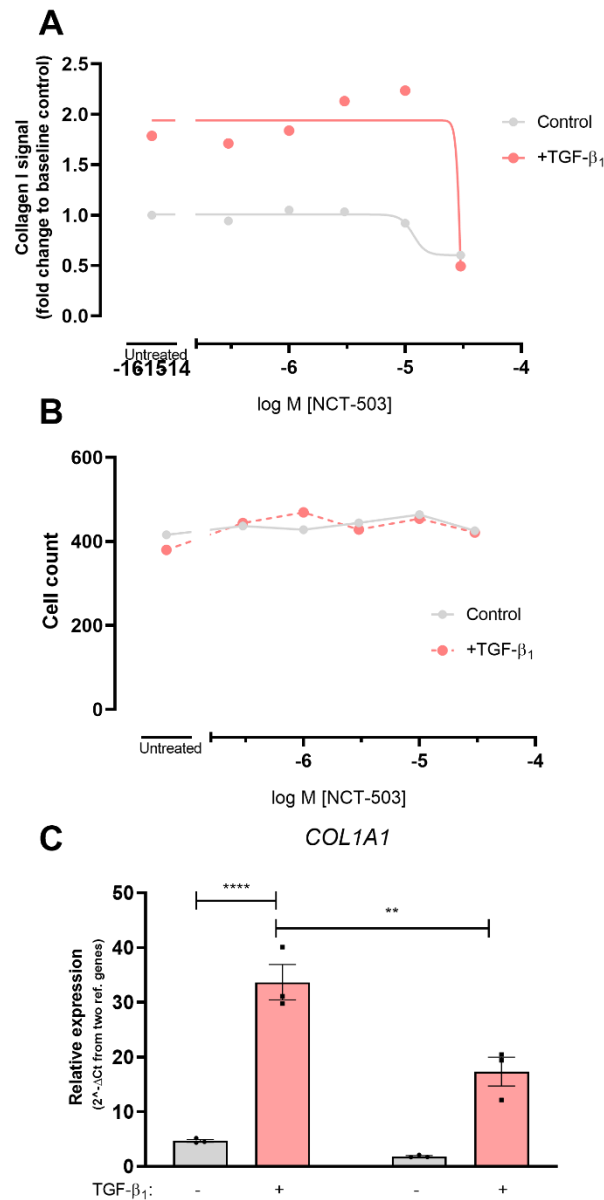


**Figure 3. 8. NCT-503 decreases TGF- $\beta_1$ -induced collagen I expression.**

pHLFs were serum-starved 24 hours prior to pre-incubation with (A) increasing concentrations of NCT-503 (300nM to 30 $\mu$ M) or (B) 30 $\mu$ M NCT-503 and 1ng/ml of TGF- $\beta_1$ . (A) collagen I deposition assessed by macromolecular crowding assay 48 hours post-TGF- $\beta_1$  stimulation. (B) *COL1A1* gene expression was assessed by qRT-PCR 24 hours post-TGF- $\beta_1$  stimulation and expressed relative to the mean of two housekeeping genes. Comparisons between groups were performed by two-way ANOVA followed by Tukey post-hoc test. In all cases,  $p < 0.05$  was considered statistically significant. (A,B) Figures are representative of  $n=3$  independent experiments and (C) presented as mean  $\pm$  S.E.M. of  $n=3$  biological replicates. \*\*= $p < 0.01$ , \*\*\*\*= $p < 0.0001$ .

### 3.1.9 HPLC optimised to detect and quantify nonessential amino acids.

High-performance liquid chromatography allows for the separation and quantification of small molecules which are solubilised in a flowing solvent through an adsorbent column. Factors such as size and charge affect the time each molecule interacts with and passes through the column, thereby allowing for separation upon passing the detector system. Specific isolation of small molecules with similar structures, such as amino acids, can be achieved using derivatization agents which react preferentially with a functional group, such as the compound NBD-Cl with amines. As PHGDH is the first and rate-limiting enzyme in the serine-glycine biosynthetic axis, the following step was to develop a technique for quantifying glycine and assessing whether TGF- $\beta_1$  modulated intracellular levels of this amino acid. Therefore, I developed and optimised a protocol to isolate and quantify glycine as well as glutamine, glutamate, proline, serine, aspartate and alanine using HPLC.

NBD-Cl preferentially reacts with secondary amino acids such as proline and hydroxyproline. Protocols for quantifying these amino acids set the derivatization time for 20 minutes and therefore this was extended to 69 minutes to allow for sufficient derivatization of the primary amino acids (Fig 3.9A). The organic solvent (acetonitrile) concentration was set low at 2% to reduce solubility and maximise adsorption of all amino acids to ensure they did not elute all at once. This separation aspect was further enhanced by imposing a gradual increase in acetonitrile throughout the 65 minutes of the HPLC run. These parameters were then used to derivatize the amino acids in media (DMEM) which were supplemented with a nonessential amino acid (NEAA) mix containing aspartate, glutamate, serine, glycine, proline and alanine. These parameters allowed for specific absorbance peaks to develop using a 495nm wavelength detector (Fig. 3.9B-C).

To assess the fidelity of the absorbance values with respect to changing concentrations, 5-point standard curves were produced ranging from 190nM to 95 $\mu$ M (Fig. 3.10). All 6 amino acids had  $R^2$  values higher than 0.999, indicating efficient translation between input amino acid concentration and output value generated using area under the curve (AUC) quantification.

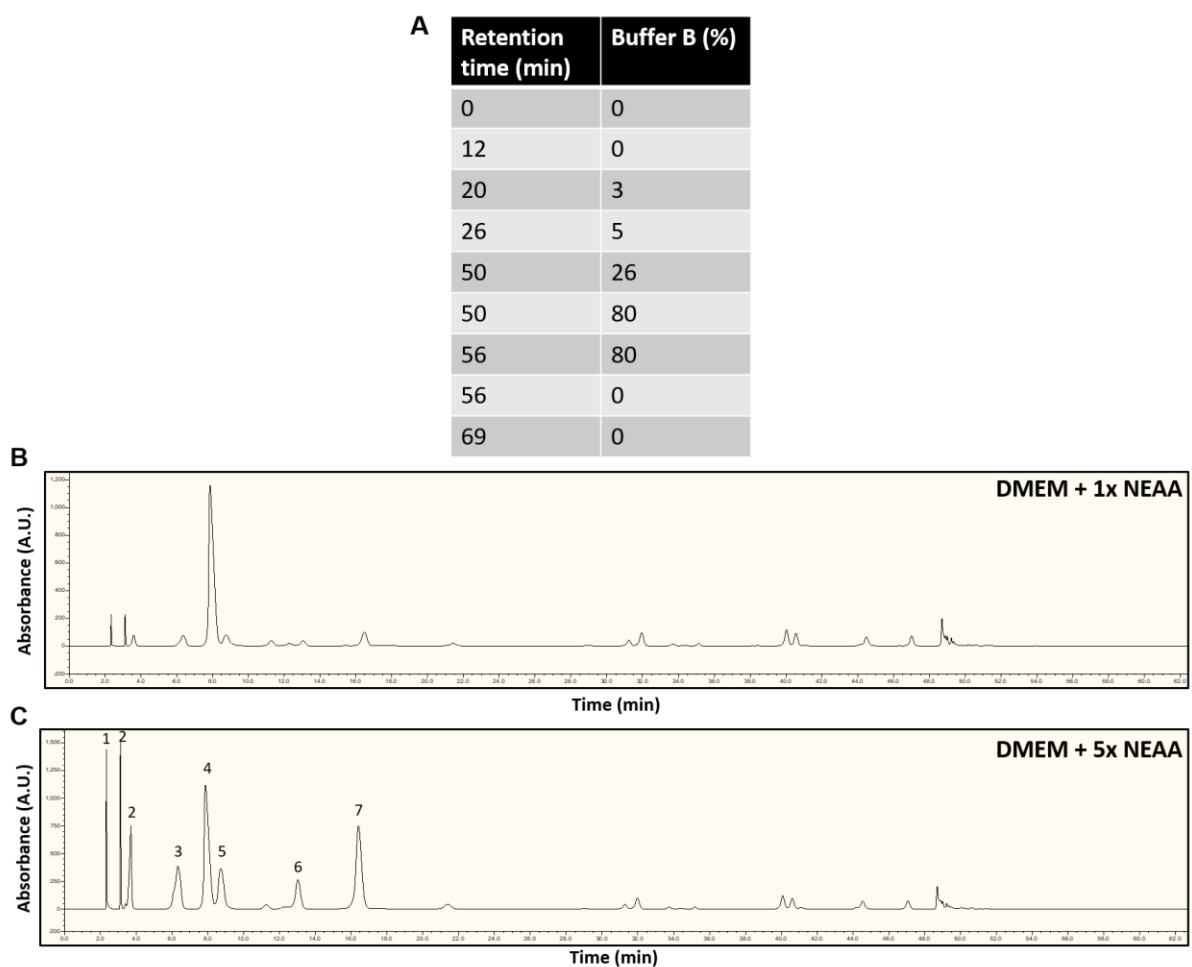


**Figure 3. 9. HPLC conditions and absorbance resolution of nonessential amino acids.**

(A) HPLC gradient conditions over the 69-minute run as described in section 2.16. (B-C) Chromatograph at 495nm absorbance of (B) 10 $\mu$ M and (C) 50 $\mu$ M nonessential amino acids. Peaks are: 1; Aspartate, 2; Glutamate, 3; Glycine, 4; NBD-Cl, 5; Glutamine, 6; Alanine, 7; Proline. Data is representative of n=3 independent experiments.

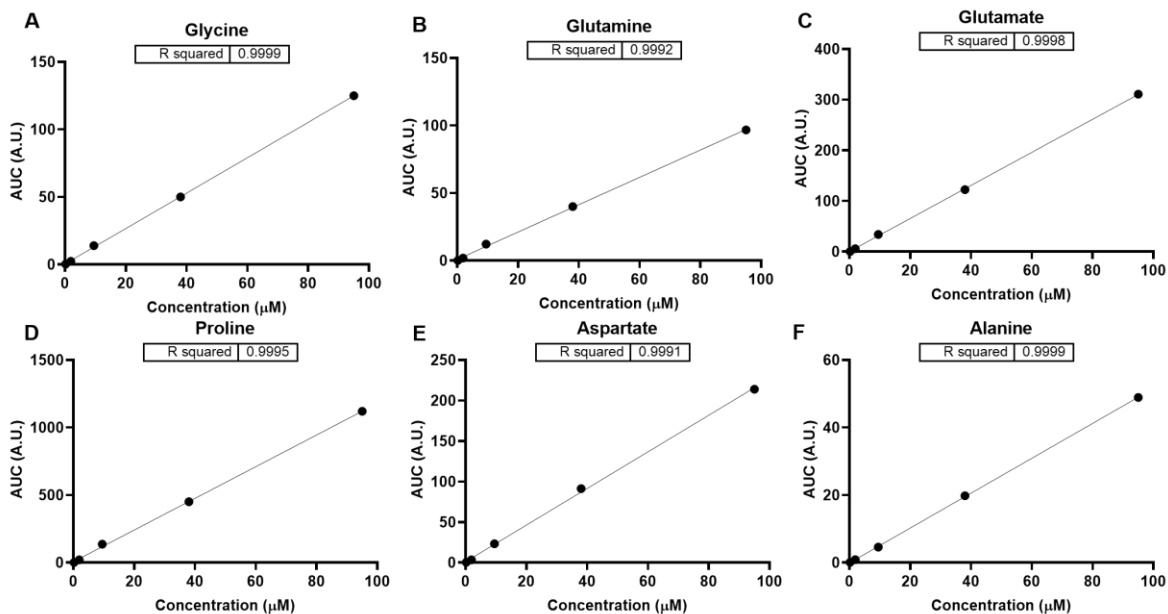


**Figure 3. 10. Absorbance measurements of amino acid standards in HPLC have linearity.**

A 5-point standard curve (0.19 $\mu\text{M}$ , 1.9 $\mu\text{M}$ , 9.5 $\mu\text{M}$ , 38 $\mu\text{M}$  and 95 $\mu\text{M}$ ) was run on the HPLC as described in section 2.16 for (A-F) of the specified amino acid. Data is representative of n=3 independent experiments.

### **3.1.10 TGF- $\beta$ <sub>1</sub> increases intracellular glycine levels via an mTOR-dependent mechanism.**

Previous findings identified PHGDH as a critical enzyme for TGF- $\beta$ <sub>1</sub>-induced collagen deposition. To gain insight into the mechanism of action, the intracellular levels of glycine, a major amino acid constituent of collagen I and downstream product of PHGDH, were quantified following TGF- $\beta$ <sub>1</sub> stimulation. As the increase in PHGDH expression following TGF- $\beta$ <sub>1</sub> was shown to be mTOR-dependent, the levels of glycine were further measured in pHLFs treated with the mTOR inhibitor AZD8055 prior to stimulation with TGF- $\beta$ <sub>1</sub>. Glycine levels were increased 1.66-fold with TGF- $\beta$ <sub>1</sub>, and this increase was completely inhibited by mTOR inhibition with AZD8055 (Fig. 3.11).

I next investigated whether this increase in intracellular glycine was dependent on the *de novo* serine-glycine axis by selectively silencing PHGDH and SHMT2, the first and last enzymes of this pathway, individually. The knockdown efficiency using siRNA targeted against these enzymes was assessed using immunoblotting and showed a near-total loss in protein abundance (Fig. 3.12A-B). Surprisingly, silencing PHGDH did not lead to a significant change in glycine levels (Fig. 3.12C). Silencing of SHMT2, however, significantly decreased TGF- $\beta$ <sub>1</sub>-induced glycine levels by roughly 60% (Fig. 3.12C).

Collectively, these data show TGF- $\beta$ <sub>1</sub> increases intracellular glycine through an mTOR-dependent mechanism. PHGDH does not appear to play a role in TGF- $\beta$ <sub>1</sub>-induced glycine levels while SHMT2 is critical for the TGF- $\beta$ <sub>1</sub>-induced increases in intracellular glycine levels.

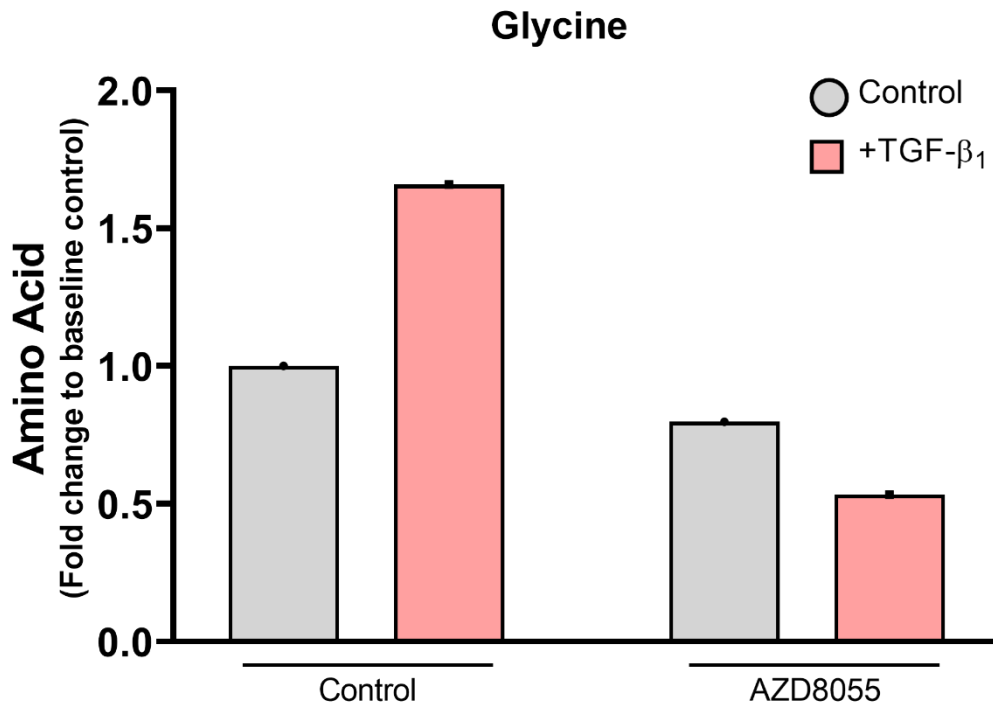


**Figure 3. 11. TGF- $\beta_1$ -induced intracellular glycine levels are mTOR-dependent.**

pHLFs were serum-starved 24 hours prior to pre-incubation with 1 $\mu$ M of AZD8055 and stimulated with 1ng/ml TGF- $\beta_1$ . Intracellular glycine levels were measured 48 hours following stimulated. Data is shown as an average of n=2 independent experiments.

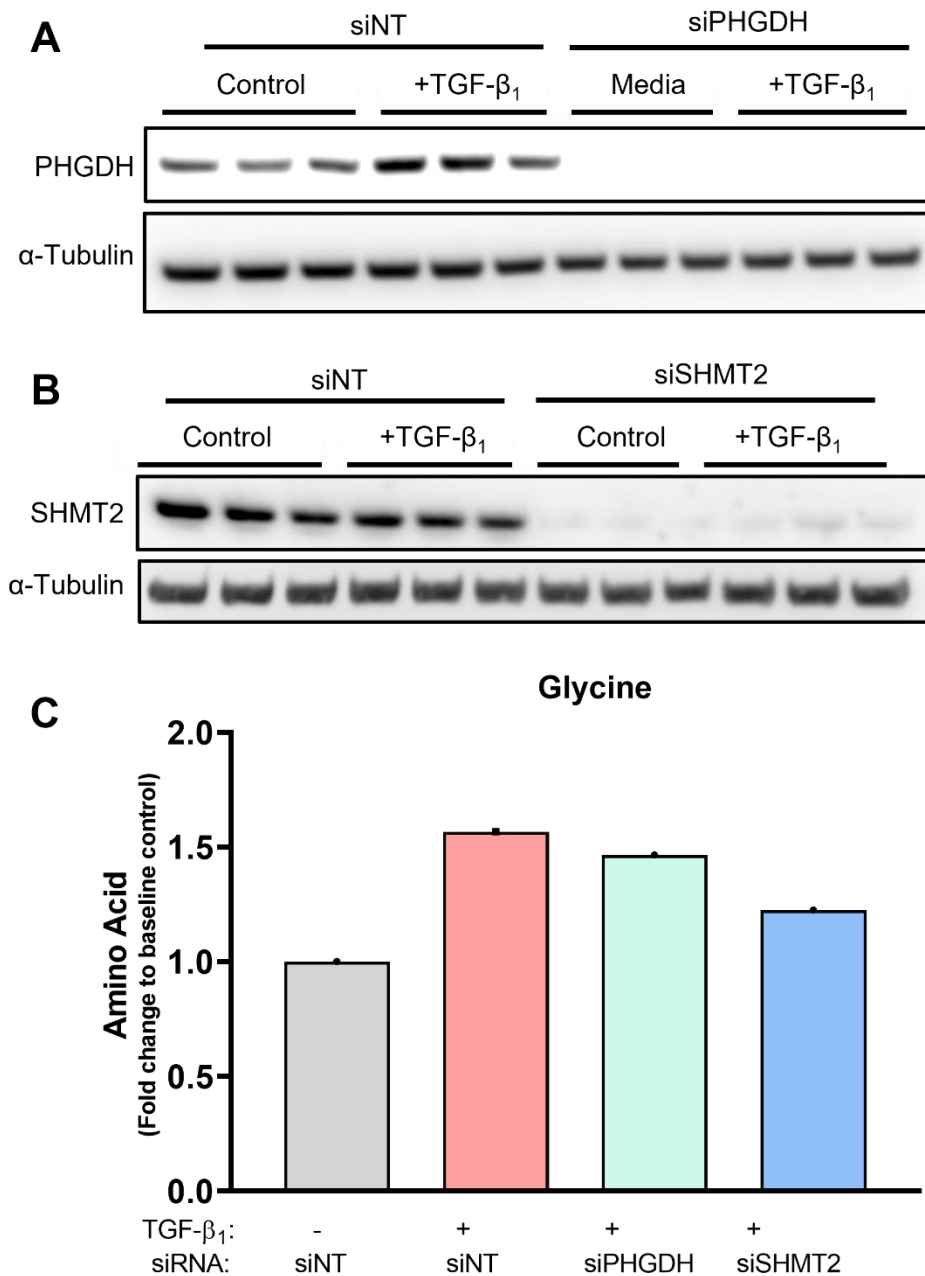


**Figure 3. 12. TGF- $\beta_1$ -induced intracellular glycine levels are SHMT2-dependent.**

pHLFs were transfected with siPHGDH, siSHMT2 or siNT as described in section 2.10 and stimulated with 1 ng/ml TGF- $\beta_1$ . (A-B) Immunoblots assessing (A) PHGDH and (B) SHMT2 knockdown efficiency 24 hours post-TGF- $\beta_1$  stimulation. (C) Intracellular glycine levels measured 48 hours post-TGF- $\beta_1$  stimulation. Blots are representative of n=3 biological replicates and glycine quantification values an average of n=2 independent experiments.

### **3.1.11 Metabolite supplementation to siPSAT1-treated pHLFs does not rescue TGF- $\beta$ <sub>1</sub>-induced collagen synthesis.**

The previous section suggested that PHGDH-derived serine was not necessary for the TGF- $\beta$ <sub>1</sub>-induced *de novo* synthesis of glycine. PSAT1 facilitates the middle step of the serine biosynthetic pathway and is dependent on both glucose and glutamine metabolic pathways for its enzymatic activity and to produce 3-PHP (which subsequently becomes serine) and  $\alpha$ -ketoglutarate. Due to these two functions and high increase in protein levels induced by TGF- $\beta$ <sub>1</sub>, PSAT1 was silenced to further interrogate the role of the serine biosynthetic pathway in TGF- $\beta$ <sub>1</sub>-induced collagen synthesis. Collagen synthesis for siRNA experiments was determined using HPLC-based quantification of hydroxyproline in 12-well plates to allow for sufficient cell numbers and protein lysates to validate knockdown efficiency using immunoblotting, a feature not possible using the 96-well macromolecular crowding assay previously used due to smaller well sizes. Treating pHLFs with siPSAT1 completely abolished PSAT1 protein abundance (Fig. 3.13A).

Silencing of PSAT1 prevented pHLFs from synthesizing TGF- $\beta$ <sub>1</sub>-induced levels of collagen, which were brought down to unstimulated levels (Fig 3.13B). Surprisingly, neither addition of serine, glycine nor  $\alpha$ -ketoglutarate, the metabolites whose biosynthesis is dependent on PSAT1 activity, was able to rescue the inhibitory effects of siPSAT1 on TGF- $\beta$ <sub>1</sub>-enhanced collagen synthesis. Addition of both serine and  $\alpha$ -ketoglutarate further failed to rescue this effect. These data suggest a possible mechanism of action for PSAT1 in supporting TGF- $\beta$ <sub>1</sub>-induced collagen synthesis which may be independent of its classical biosynthetic functions.

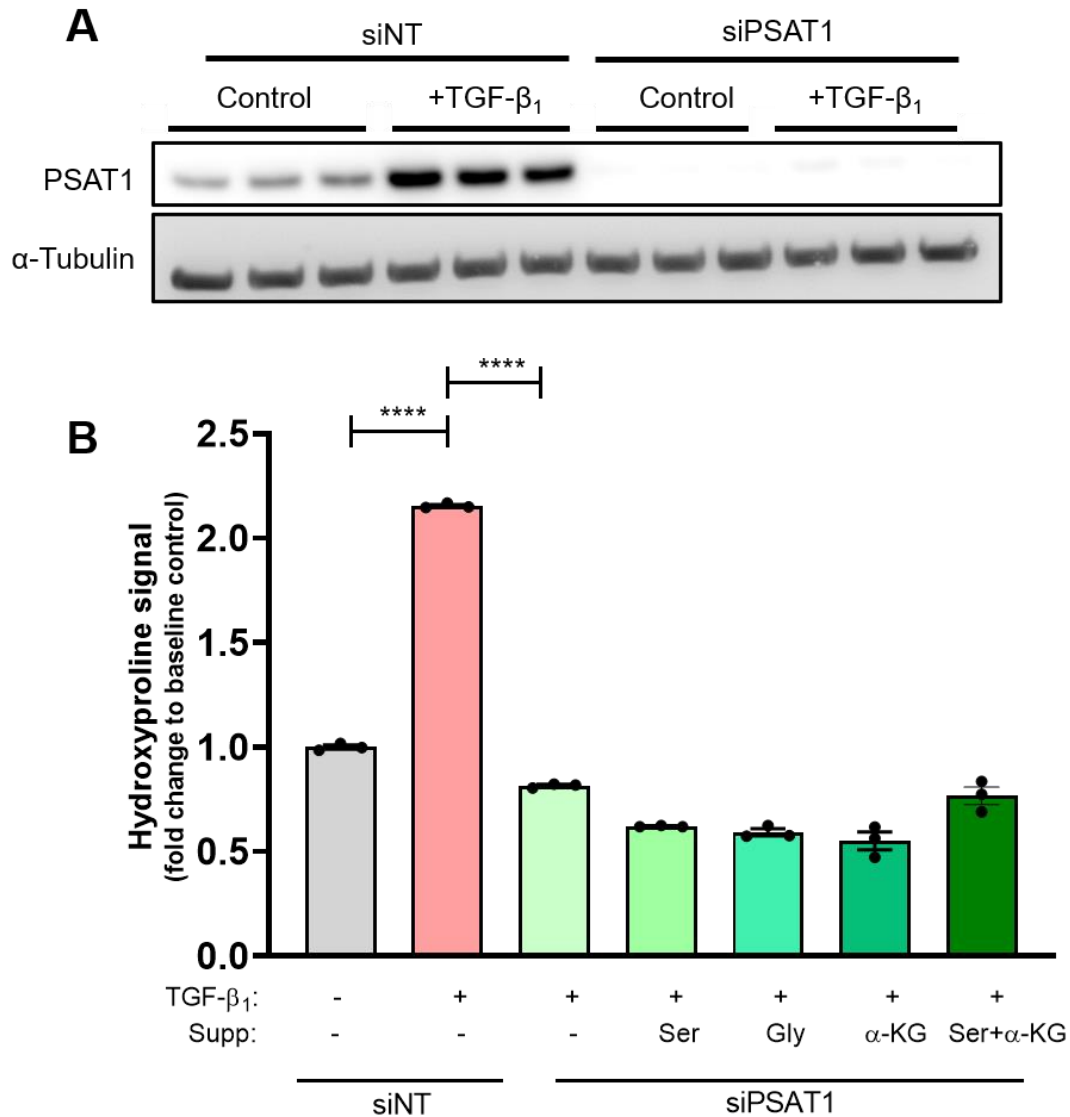


**Figure 3. 13. Metabolite supplementation to siPSAT1-treated cells does not rescue TGF- $\beta_1$ -induced collagen synthesis.**

pHLFs were transfected with siPSAT1 or siNT as described in section 2.10 and stimulated with 1ng/ml TGF- $\beta_1$ . (A) Immunoblot assessing PSAT1 knockdown efficiency 24 hours post-TGF- $\beta_1$  stimulation. (B) Pro-collagen levels quantified as described in section 2.15. Supplements (500 $\mu$ M serine or glycine and 4mM dimethyl 2-oxoglutarate) were given an hour prior to TGF- $\beta_1$  stimulation and pro-collagen quantified after 48 hours. Comparisons between groups were performed by two-way ANOVA followed by Tukey post-hoc test. In all cases,  $p < 0.05$  was considered statistically significant. Data are presented as mean  $\pm$  S.E.M. of  $n=3$  biological replicates \*\*\*\*= $p < 0.0001$ .

### **3.1.12 Summary.**

The results described in this section show that the serine-glycine biosynthetic axis enzymes (PHGDH, PSAT1, PSPH and SHMT2) are upregulated following TGF- $\beta_1$  stimulation through an mTOR-dependent mechanism. This mechanism is likely through mTOR regulating the post-transcriptional levels of the master amino acid biosynthesis transcription factor, ATF4. Pharmacological inhibition of PHGDH (the first enzyme in serine biosynthesis) showed a complete attenuation in TGF- $\beta_1$ -induced collagen I deposition levels. Levels of glycine, the end-product of the serine-glycine biosynthetic axis, were increased by TGF- $\beta_1$  and dependent on SHMT2. However, supplementation of the media with pathway products glycine, serine or  $\alpha$ -ketoglutarate was unable to rescue the effects of serine biosynthesis inhibition via silencing of PSAT1.

Taken together, these data are potentially supportive of previous reports describing a non-enzymatic as well as serine-independent role for the serine biosynthetic pathway in tumour cells. These data furthermore highlight PHGDH and PSAT1 as potential targets for the development of anti-fibrotic therapeutic strategies.

## **3.2 The role of extracellular glycine, serine, glutamine and glucose in TGF- $\beta_1$ -induced collagen I deposition.**

### **3.2.1 Introduction.**

The data presented in section 3.1 profiled the role of the serine-glycine biosynthetic axis in TGF- $\beta_1$ -induced collagen I deposition. The data further showed TGF- $\beta_1$ -responsiveness in a media with physiological levels of the multifunctional nutrients glucose and glutamine, thereby possibly limiting the introduction of metabolic artefacts. The next steps were to better understand the role of these nutrients in the cell culture media with respect to TGF- $\beta_1$ -induced collagen I deposition.

**Hypothesis:** Extracellular glycine, serine, glutamine and glucose are required for TGF- $\beta_1$ -induced collagen I deposition.

### **3.2.2 Glycine withdrawal decreases collagen I deposition.**

The previous section showed the TGF- $\beta_1$ -dependent increase in intracellular glycine levels in pHLFs was SHMT2-dependent. This observation was made in cells growing in media with 400 $\mu$ M glycine which is on the higher end of the physiological blood range. To gain insight into whether extracellular glycine modulates TGF- $\beta_1$ -induced collagen I deposition or if pHLFs depend entirely on *de novo* glycine synthesis via SHMT2, TGF- $\beta_1$ -induced collagen I deposition was assessed in cells grown in media devoid of glycine.

TGF- $\beta_1$  increased collagen I deposition in pHLFs grown in 400 $\mu$ M glycine by 68% ( $p < 0.0001$ ,  $n = 3$ ) and this increase was reduced to 40% in TGF- $\beta_1$ -stimulated cells grown in media lacking glycine (Fig. 3.14). However, baseline collagen I levels were similarly reduced by 34% ( $p = 0.043$ ), indicating a TGF- $\beta_1$ -independent effect which glycine withdrawal has on collagen I synthesis. The reduction in TGF- $\beta_1$ -stimulated collagen deposition measured with 0 $\mu$ M glycine was rescued by the addition of

200 $\mu$ M glycine and upwards, indicating that extracellular glycine at physiological blood concentration is required for a full collagen I response.

These data led to the conclusion that pHLFs require extracellular glycine to mount a full collagen I response and subsequently a full TGF- $\beta_1$ -induced collagen I response. However, with no exogenous glycine, TGF- $\beta_1$ -stimulated pHLFs are still able to reach 58% of a full TGF- $\beta_1$ -induced collagen I response.

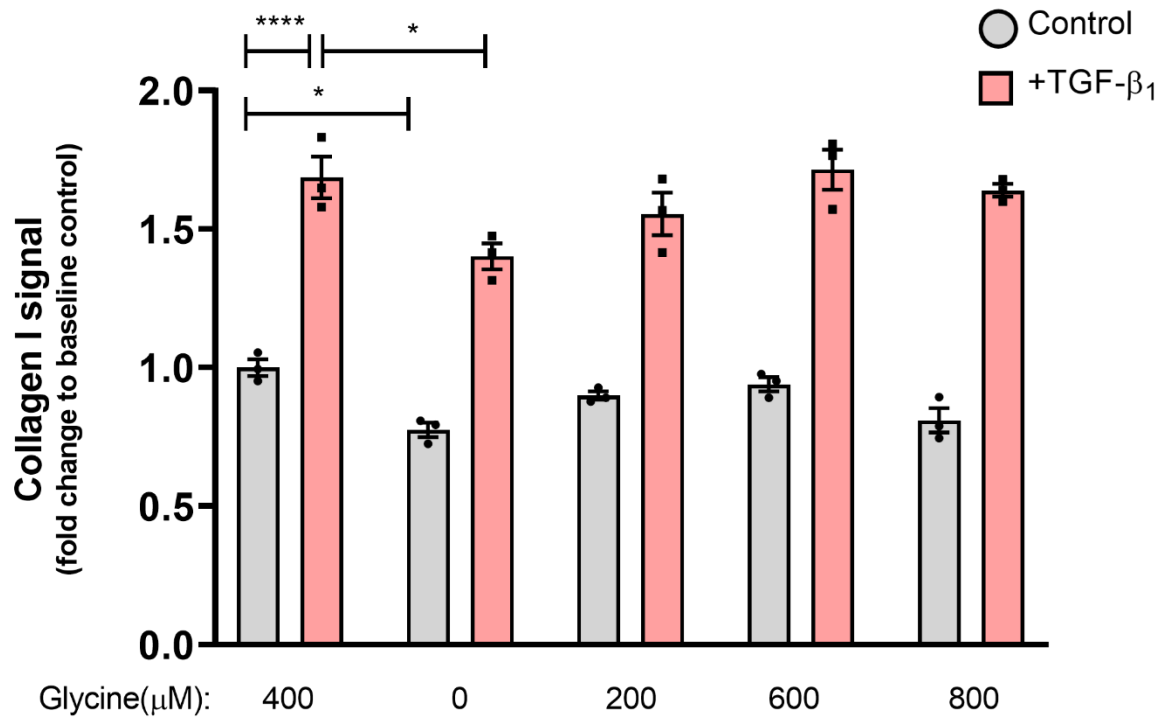


**Figure 3. 14. Glycine is required in the media for a full collagen response.**

pHLFs were grown in serine and glycine free DMEM (see section 2.1) and were serum-starved 24 hours prior to being given an increasing concentration of glycine (0-800μM) and then stimulated (1ng/ml) by TGF-β<sub>1</sub>. Collagen I deposition was measured using the macromolecular crowding assay 48 hours following stimulation. Comparisons between groups were performed by two-way ANOVA followed by Tukey post-hoc test. In all cases,  $p < 0.05$  was considered statistically significant. Data are presented as mean  $\pm$  S.E.M. of  $n=3$  biological replicates \*= $p < 0.05$ , \*\*\*\*= $p < 0.0001$ .

### **3.2.3 Extracellular glycine is more valuable than serine for cells to mount a full TGF- $\beta_1$ -induced collagen response.**

As serine and glycine can be interconverted via the SHMT isozymes, the effect of simultaneous serine and glycine depletion on TGF- $\beta_1$ -induced collagen I deposition was investigated next. pHLFs grown in media lacking these two amino acids exhibited a 60% decrease in TGF- $\beta_1$ -induced collagen levels ( $p < 0.001$ ,  $n = 3$ ) and a 34% decrease in baseline collagen levels ( $p < 0.05$ ,  $n = 3$ ) (Fig. 3.15). Interestingly, this decrease in both TGF- $\beta_1$ -stimulated and unstimulated collagen levels was rescued by addition of 400 $\mu$ M glycine but not by 400 $\mu$ M serine to the media.

Whilst the decrease in TGF- $\beta_1$ -stimulated cells was greater than control cells, this data suggests that glycine and serine both play a role in maintaining baseline levels of collagen synthesis outside of TGF- $\beta_1$  stimulation. Additionally, removal of both glycine and serine suggest an additive effect in reducing collagen synthesis when compared to sole glycine removal measured in figure 3.14.

### **3.2.4 Glutamine is critical for TGF- $\beta_1$ -induced collagen I deposition.**

The previous section confirmed pro-fibrotic TGF- $\beta_1$  responsiveness in pHLFs grown in media with physiological levels of glucose and glutamine (Fig. 3.1). As these two nutrients are critical for *de novo* serine and glycine biosynthesis, their functional impact on TGF- $\beta_1$ -induced collagen I deposition was assessed by varying their concentrations in the media. Glucose is a major source of cellular energy by supplying the key TCA cycle generator pyruvate, supports nucleotide biosynthesis and provides the carbon backbone for the synthesis of several amino acids, such as serine. Glutamine is a major nitrogen-source for cells and is highly diversified in its functions ranging from antioxidant synthesis, pH balance, TCA cycle fuelling and amino acid synthesis. During *de novo* serine synthesis, the amino group from glutamine-derived glutamate becomes the amino group in the newly synthesized serine.

pHLFs were grown in normal media (5mM glucose and 0.7mM glutamine) and an hour prior to stimulation with TGF- $\beta_1$  the media was replaced with fresh media of varying glucose and glutamine concentrations. Without glutamine present in the

media, glucose at physiological concentration (5mM) was not able to maintain TGF- $\beta_1$ -induced collagen I deposition (Fig. 3.16A). However, glucose at a concentration of 25mM was able to overcome this glutamine deficiency and allow pHLFs to mount a full TGF- $\beta_1$ -induced collagen I response. Interestingly, glucose withdrawal in media with at least 0.7mM glutamine had no impact on TGF- $\beta_1$ -induced collagen I deposition. Furthermore, 2mM of glutamine did not further increase TGF- $\beta_1$ -induced collagen I deposition when compared to 0.7mM glutamine. To ensure these effects were not due to changes in cell number, cell count via DAPI staining was measured and found to be unaffected throughout all conditions (Fig. 3.16B).

Together, these results highlight glutamine as a critical nutrient in the cell culture media for supporting TGF- $\beta_1$ -induced collagen I deposition. Glucose is only able to compensate for glutamine deficiency and support this response at a supraphysiological concentration of 25mM. These data show that physiological glutamine levels are sufficient in the absence of glucose in supporting TGF- $\beta_1$ -induced collagen I deposition.

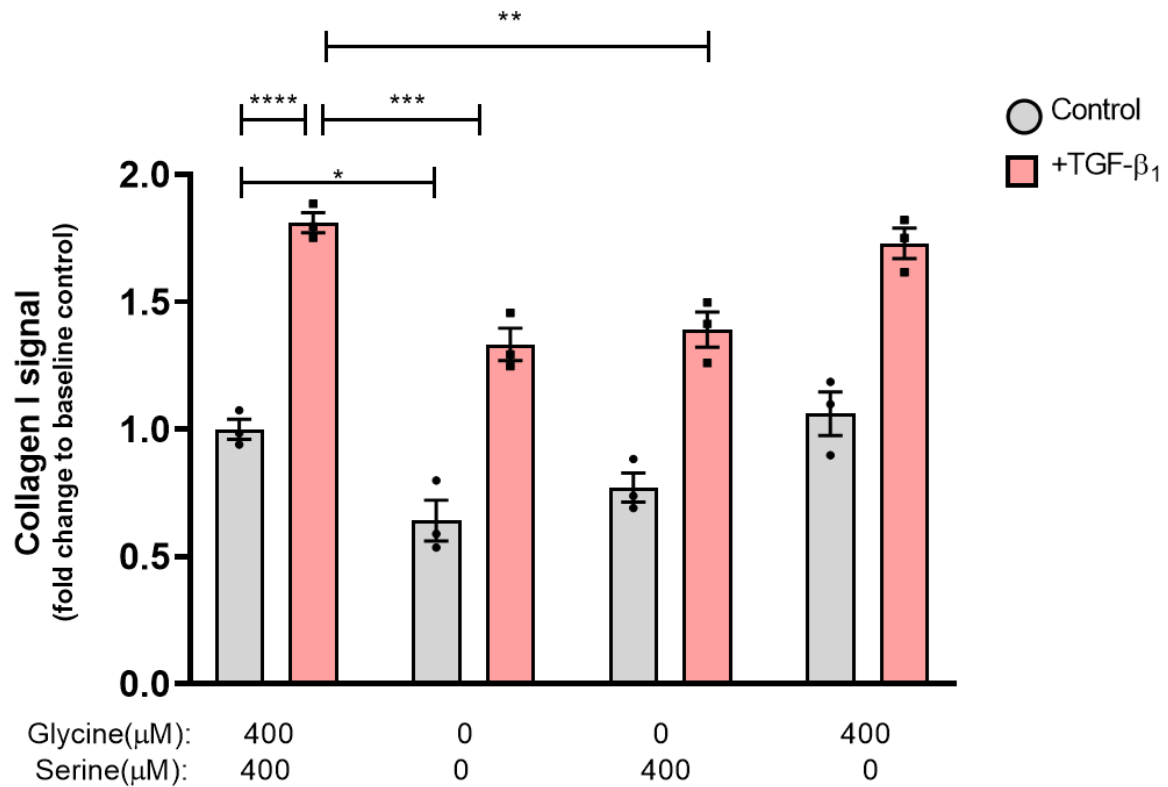


**Figure 3. 15. Supplementation with glycine but not serine rescues the reduced levels of TGF-β<sub>1</sub>-induced collagen I deposition following withdrawal of both amino acids.**

pHLFs were grown in serine and glycine free DMEM (see section 2.1) and were serum-starved 24 hours prior to being given the stated concentrations of glycine or serine and then stimulated (1ng/ml) by TGF-β<sub>1</sub>. Collagen I deposition was measured using the macromolecular crowding assay 48 hours following stimulation. Comparisons between groups were performed by two-way ANOVA followed by Tukey post-hoc test. In all cases, p<0.05 was considered statistically significant. Data are presented as mean ± S.E.M. of n=3 biological replicates \* =p<0.05, \*\* =p<0.01, \*\*\* =p<0.001, \*\*\*\* =p<0.0001.

### **3.2.5 Intracellular levels of glutamine, glutamate and proline are higher in TGF- $\beta_1$ -stimulated cells growing in supraphysiological levels of glucose and glutamine.**

The previous section suggested a metabolic event occurs in pHLFs grown in supraphysiological levels of glucose (25mM) which can compensate for glutamine withdrawal with respect to supporting TGF- $\beta_1$ -induced collagen I deposition. This raised the possibility that high levels of extracellular glucose may 'flood' the intracellular pool of glucose-dependent metabolites, thereby producing artificially high levels of components necessary for TGF- $\beta_1$ -induced collagen synthesis otherwise synthesized via glutamine metabolism in physiological conditions. Furthermore, standard DMEM contains 2mM glutamine which may also lead to supraphysiological intracellular metabolite levels since glutamine metabolism produces the glutamate necessary for the *de novo* synthesis of glycine and proline, two major amino acid components of collagen I. The impact on the intracellular concentrations of these amino acids in pHLFs grown in standard DMEM (25mM glucose, 2mM glutamine) and physiological DMEM (5mM glucose, 0.7mM glutamine) was therefore investigated. To allow for cross-comparison between medias, absolute amounts of these amino acids were quantified against a standard curve.

#### **Intracellular glutamine levels**

pHLFs grown in physiological DMEM and stimulated with TGF- $\beta_1$  had 14.7-times lower intracellular glutamine levels than unstimulated cells ( $0 < 0.05$ ,  $n=3$ ) (Fig. 3.17A). Strikingly, this effect was lost in pHLFs grown in standard DMEM, with similar levels of intracellular glutamine between TGF- $\beta_1$ -stimulated and unstimulated cells. Furthermore, unstimulated pHLFs grown in standard DMEM had 3.6-times higher glutamine levels than pHLFs grown in physiological DMEM media.

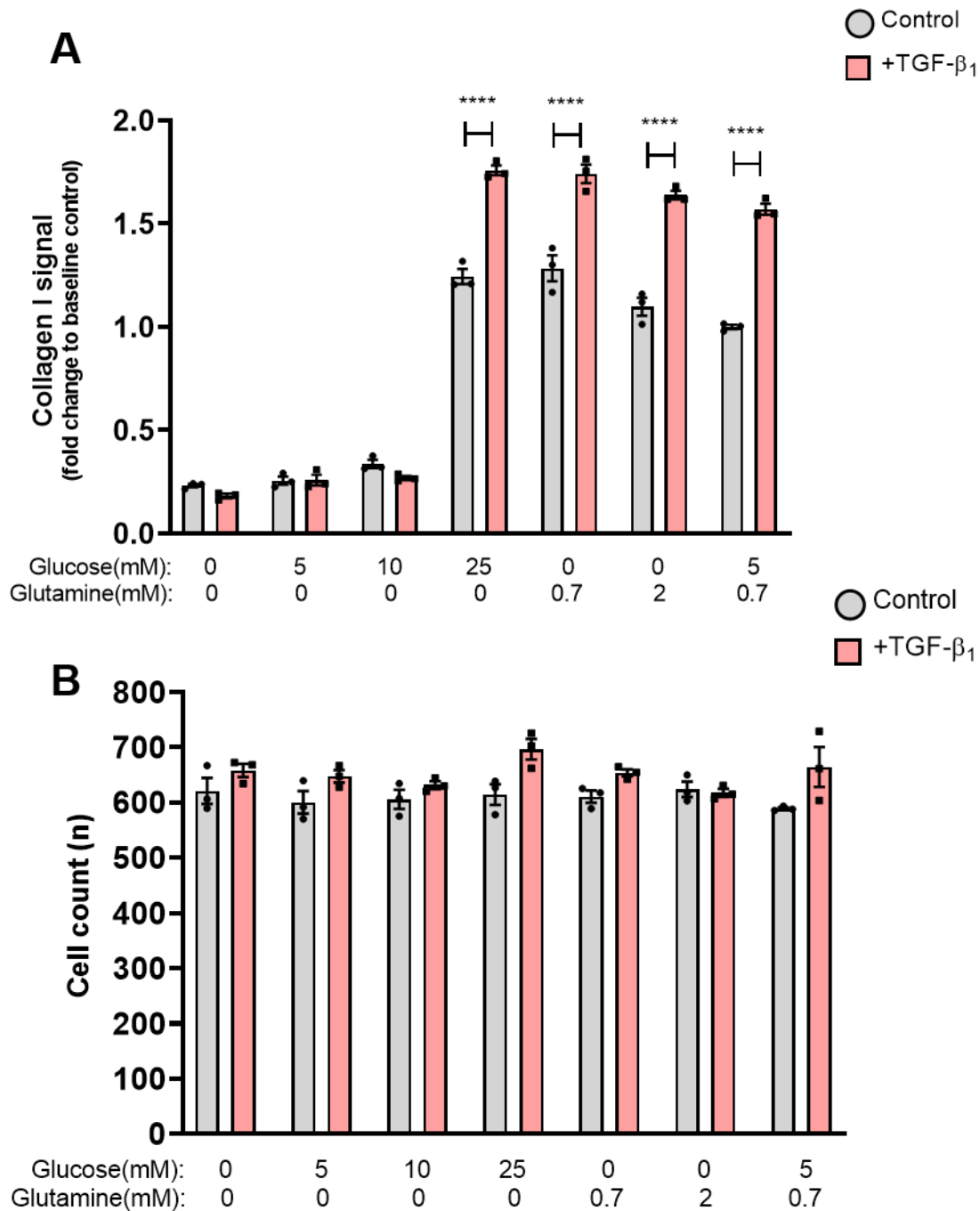


**Figure 3. 16. Glutamine is critical for TGF-β<sub>1</sub>-induced collagen synthesis.**

pHLFs were grown in physiological DMEM lacking glutamine and glucose (see section 2.1) and were serum-starved 24 hours prior to being given the stated concentrations of glutamine and glucose and then stimulated (1ng/ml) by TGF-β<sub>1</sub>. (A) Collagen I deposition was measured using the macromolecular crowding assay 48 hours following stimulation. (B) Cell count was measured from the macromolecular crowding assay. Comparisons between groups were performed by two-way ANOVA followed by Tukey post-hoc test. In all cases,  $p < 0.05$  was considered statistically significant. Data are presented as mean  $\pm$  S.E.M. of  $n=3$  biological replicates \*\*\*\*= $p < 0.0001$ .

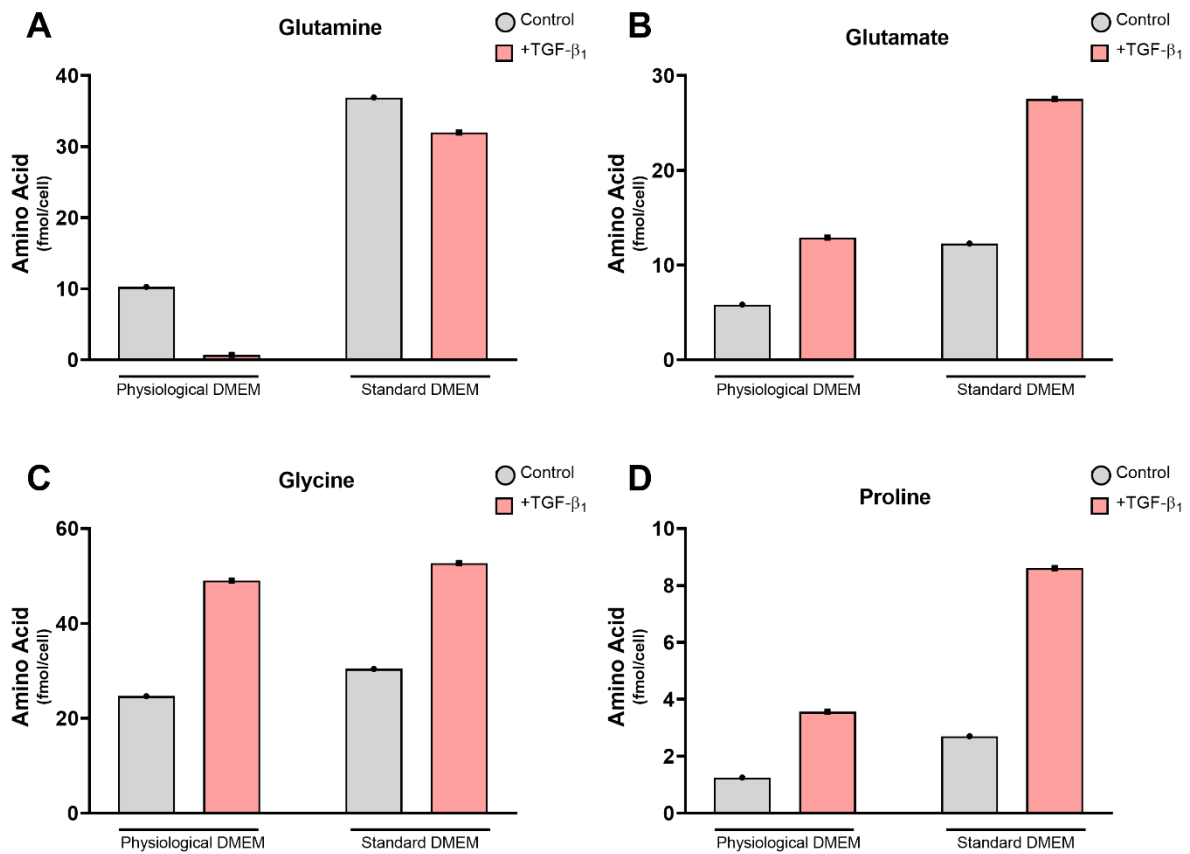


**Figure 3. 17. Intracellular levels of glutamine, glutamate and proline are higher in TGF- $\beta_1$ -stimulated pHLFs growing in standard DMEM.**

pHLFs were grown in physiological DMEM or standard DMEM (see section 2.1) and were serum-starved 24 hours prior to being stimulated by TGF- $\beta_1$  (1 ng/ml). Intracellular levels of (A) glutamine, (B) glutamate, (C) glycine and (D) proline were measured 48 hours following stimulation. Data is shown as an average of n=2 independent experiments.

These data show that intracellular glutamine levels following TGF- $\beta_1$  stimulation differ significantly depending on glucose and glutamine concentration within the media. In physiological DMEM, TGF- $\beta_1$  stimulated pHLFs exhibit a significant decrease in intracellular glutamine levels, which reflects either decreasing glutamine uptake or increasing glutamine catabolism. In contrast, pHLFs grown in standard DMEM showed no changes in intracellular glutamine levels following TGF- $\beta_1$  stimulation. Lastly, intracellular glutamine concentrations were around 3-fold higher in unstimulated cells grown in standard DMEM compared to physiological DMEM, suggesting that pHLFs may consume more glutamine if higher extracellular concentrations are provided.

### **Intracellular glutamate levels**

Glutamate is a highly functional amino acid, necessary for the biosynthesis of nearly all nonessential amino acids and is the immediate downstream product of glutamine metabolism. Fig 3.17A raised the possibility that TGF- $\beta_1$ -activated pHLFs increase glutamine metabolism instead of limiting glutamine uptake, leading to a TGF- $\beta_1$ -induced increase in intracellular glutamate levels. Indeed, TGF- $\beta_1$  stimulation led to an increase in intracellular levels of glutamate by approximately 2-fold for pHLFs grown in either media (Fig. 3.17B). Additionally, unstimulated pHLFs grown in standard DMEM had similar levels of intracellular glutamate as TGF- $\beta_1$ -stimulated pHLFs grown in physiological DMEM.

These data show that intracellular glutamate levels are increased by TGF- $\beta_1$  in pHLFs grown in either media. Furthermore, pHLFs in standard DMEM exhibit higher levels of intracellular glutamate.

### **Intracellular glycine levels**

The *de novo* glycine biosynthetic pathway has been shown to be highly upregulated in response to TGF- $\beta_1$  via an mTOR-dependent mechanism. Glycine is predominantly synthesized through the catabolism of serine, with the amino group

provided by glutamate. I therefore also measured glycine levels in both medias to determine if there were increased glycine levels when higher amounts of glutamine and glucose were present. As expected, intracellular glycine levels were increased by TGF- $\beta_1$ . Interestingly, intracellular glycine levels were similar for pHLFs grown in either media (Fig. 3.17C). These data indicate that intracellular glycine levels are not impacted by higher availability of glutamine and glucose as found in standard DMEM.

### **Intracellular proline levels**

Proline is a major component of the collagen polypeptide and its hydroxylation to form hydroxyproline is critical for protein stability and subsequent deposition into the ECM. Aside from the urea cycle, proline is synthesized through a series of enzymatic reactions beginning with glutamate. In my experiments, proline levels followed the same pattern as glutamate levels under TGF- $\beta_1$  stimulation in both media compositions (Fig. 3.17D). TGF- $\beta_1$  induced a significant increase in intracellular proline in both medias. Furthermore, proline levels at baseline in pHLFs grown in standard DMEM were equivalent to those measured in TGF- $\beta_1$ -stimulated levels in pHLFs grown in physiological DMEM. TGF- $\beta_1$  further increased these levels in standard DMEM by 3-fold compared with the corresponding media-alone stimulated cells.

Collectively, these results show a significant altered profile of important intracellular amino acid levels in response to TGF- $\beta_1$ . They show a capacity for pHLFs to contain higher intracellular levels of glutamine, glutamate and proline when grown in supraphysiological levels of glucose and glutamine. These data furthermore suggest that in physiological DMEM, TGF- $\beta_1$ -activated pHLFs enhance their metabolism of glutamine, leading to a reduction in glutamine abundance but an increase in glutamate and proline.

### **3.2.6 Summary.**

The results described in this section explore the role of extracellular concentrations of glycine, serine, glutamine and glucose in TGF- $\beta_1$ -induced collagen deposition. Glycine and not serine was found to be required for a full TGF- $\beta_1$  collagen I response and glutamine was essential in supporting both unstimulated and TGF- $\beta_1$ -stimulated collagen levels. Supraphysiological levels of extracellular glucose (25mM) were capable of rescuing glutamine withdrawal, indicating a possible flooding of intracellular metabolic networks and metabolites. Indeed, in media with high levels of glucose and glutamine (standard DMEM), intracellular levels of glutamate and proline were similar to the levels of these amino acids in TGF- $\beta_1$ -stimulated pHLFs grown in physiological levels of glucose and glutamine. Under physiological conditions, intracellular glutamine levels were significantly depleted following TGF- $\beta_1$  stimulation, indicating that glutamine was being secreted or metabolised.

Taken together, these data highlight the complex issue of media composition and its role in influencing intracellular metabolic networks. These data further highlight the critical need for extracellular glutamine for pHLFs to mount a TGF- $\beta_1$ -induced collagen response in cells grown in physiological concentrations of glucose.

## **3.3 The role of glutamine metabolism in TGF- $\beta_1$ -stimulated pHLFs**

### **3.3.1 Introduction.**

The data presented in section 3.2 defined glutamine as a key extracellular component required for TGF- $\beta_1$ -enhanced collagen synthesis in physiological concentrations of glucose. Under these physiological conditions, pHLFs appear to enhance their metabolism of intracellular glutamine, as evidenced by depleted intracellular levels and increased levels of its metabolic product, glutamate (Fig. 3.17A-B). The experiments presented in this in section further investigate the role of glutamine metabolism in TGF- $\beta_1$ -induced collagen synthesis.

**Hypothesis:** Extracellular glutamine supports intracellular metabolic pathways which are critical for TGF- $\beta_1$ -induced collagen synthesis.

### **3.3.2 Extracellular glutamine levels decrease at a faster rate in TGF- $\beta_1$ -stimulated cells.**

At 48 hours following TGF- $\beta_1$  stimulation, pHLFs exhibited drastically lower levels of intracellular glutamine compared to unstimulated cells (Fig. 3.17A). This effect could be due to enhanced glutamine metabolism or increased glutamine efflux back into the media. To investigate these two possibilities, extracellular glutamine levels were compared at three time-points in cell supernatants from unstimulated pHLFs and from pHLFs stimulated with TGF- $\beta_1$ .

Extracellular glutamine levels decreased over the 48 hours of the experiment in both experimental groups (Fig. 3.18). At 24 hours, a decrease was measured in TGF- $\beta_1$ -stimulated cell supernatants, indicating an increase in glutamine uptake by pHLFs. The difference in extracellular glutamine concentrations between unstimulated and TGF- $\beta_1$ -stimulated groups widened by the 48-hour time-point. Unstimulated

supernatants contained nearly double the amount of glutamine as TGF- $\beta_1$ -stimulated supernatants ( $p < 0.0001$ ,  $n = 3$ ).

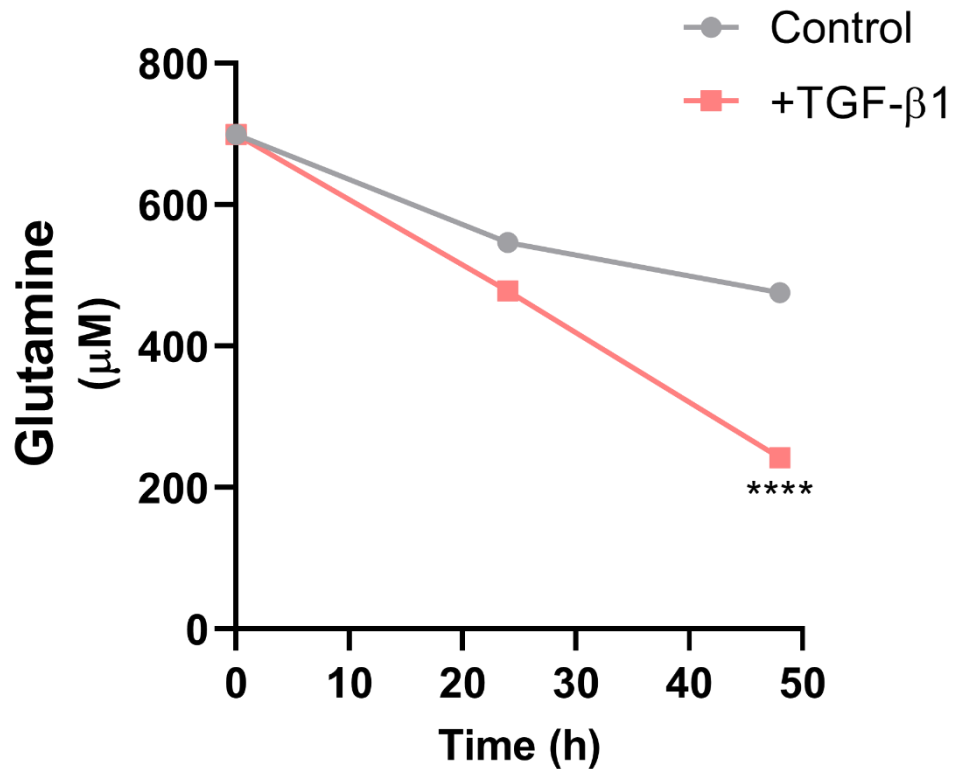


**Figure 3. 18. Extracellular glutamine levels decrease at a faster rate in TGF-β<sub>1</sub>-stimulated pHLFs.**

pHLFs were serum-starved 24 hours prior to being stimulated (1ng/ml) by TGF-β<sub>1</sub>. Cell supernatants were collected at 0-, 24- and 48 hours following stimulation and glutamine levels were quantified as described in section 2. 16. Significance values correspond to control and TGF-β<sub>1</sub> groups compared at the same time-point. Comparisons between groups were performed by two-way ANOVA followed by Tukey post-hoc test for the 48-hour timepoint which is shown as mean of n=3 biological replicates. The 24-hour timepoint is expressed as a mean of n=2 biological replicates. In all cases, p<0.05 was considered statistically significant. \*\*\*\*=p<0.0001.

These data show that extracellular glutamine levels decrease over time yet decrease at a faster rate in TGF- $\beta_1$ -stimulated cells.

### **3.3.3 TGF- $\beta_1$ increases the mRNA levels of glutamine transporter genes.**

Glutamine can be imported into the cell via various transporters. The observation that extracellular glutamine levels decrease faster with TGF- $\beta_1$  suggested an increased uptake. To better understand this, the expression levels of key glutamine transporters were measured. Lysates were collected at a very early (1-hour), early (3 hours), middle (12 hours) and late (24 hours) time point post-TGF- $\beta_1$  stimulation and mRNA levels of the major glutamine uptake transporters described in the literature, *SLC38A1*, *SLC38A2*, *SLC38A5* and *SLC1A5* were measured. To allow cross-comparison of the different transporters, mRNA levels for TGF- $\beta_1$ -stimulated pHLFs were normalised to their respective untreated levels at each time-point.

Figure 3.19A shows that *SLC38A5* was the only gene to be upregulated at 3 hours following TGF- $\beta_1$  stimulation. By 12-hours *SLC38A1* and *SLC38A5* showed an increase in mRNA levels. Interestingly, the transporter widely recognized as being critical for glutamine uptake, *SLC1A5* or *ASCT2*, was not increased until 24 hours by 2.35-fold ( $p < 0.05$ ,  $n = 3$ ) (Fig. 3.19B). *SLC38A5* and *SLC38A1* were still upregulated at 24-hours by 6.41 and 4.57-fold, respectively ( $p < 0.01$ ). The *SLC38A2* transporter was not upregulated at any time-point and its expression was not significantly different to that of unstimulated cells.

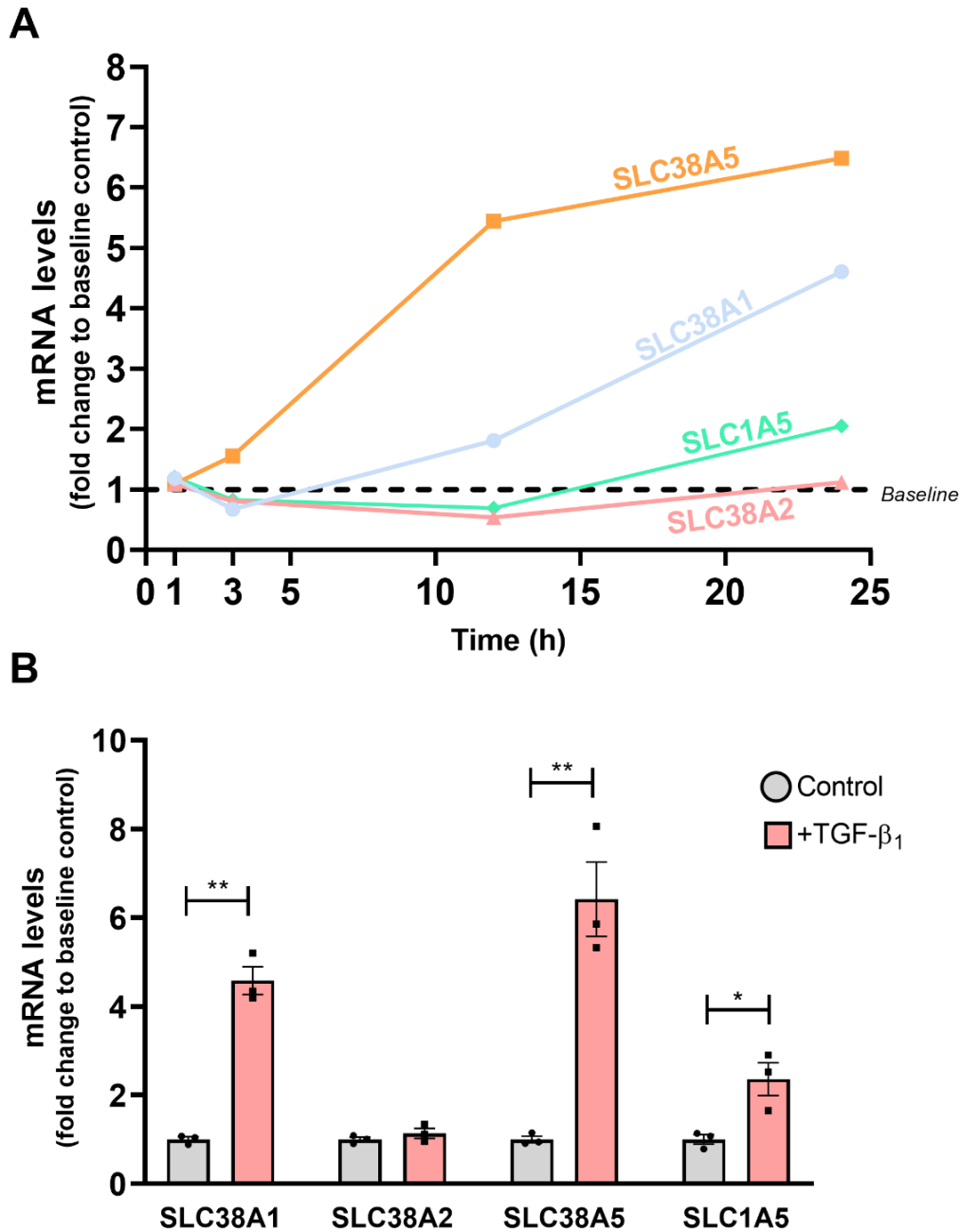


**Figure 3. 19. TGF- $\beta_1$  increases the mRNA levels of *SLC38A5*, *SLC38A1*, *SLC1A5*.**

pHLFs were serum-starved 24 hours prior to being stimulated (1ng/ml) by TGF- $\beta_1$ . RNA was extracted at indicated timepoints (1-, 3-, 12- and 24 hours following stimulation) and gene expression of *SLC38A1*, *SLC38A2*, *SLC38A5* and *SLC1A5* assessed by qRT-PCR and expressed relative to the mean of two housekeeping genes. Data expressed as a fold-change between TGF- $\beta_1$ -stimulated and unstimulated pHLFs (A) Time course experiment performed n=1. (B) 24-hours comparisons between groups were performed by two-way ANOVA followed by Tukey post-hoc test. In all cases, p<0.05 was considered statistically significant. Data are presented as mean  $\pm$  S.E.M. of n=3 biological replicates \* =p<0.05, \*\* =p<0.01.

Together, these results show that several glutamine transporters are modulated by TGF- $\beta_1$  and may be acting collectively to increase glutamine uptake as evidenced by the data reported in Figure 3.18. Collectively, these data support the concept that under TGF- $\beta_1$ , pHLFs increase their glutamine transporters to allow for an increased consumption of glutamine which is then metabolised to support TGF- $\beta_1$ -induced collagen synthesis.

### **3.3.4 TGF- $\beta_1$ increases *GLS1* gene expression.**

Previous data shows TGF- $\beta_1$  stimulation increased glutamine consumption, decreased intracellular glutamine levels and increased intracellular glutamate levels. These findings suggest that TGF- $\beta_1$  enhances glutamine catabolism in pHLFs. The process of converting glutamine to glutamate is primarily performed by the enzyme glutaminase, of which there are two isoforms in humans, *GLS1* and *GLS2*. *GLS1* has two splice variant isoforms, *KGA* and *GAC* which differ in their carboxy-terminus, but both retain their glutaminase enzyme domains.

The next experiments aimed to determine if GLS and its isoforms were modulated by TGF- $\beta_1$  at the transcriptional level, in order to identify which enzymes might be responsible for enhanced glutamine catabolism in TGF- $\beta_1$ -stimulated pHLFs. Given that *GLS2* expression has mainly been reported in brain and liver tissue, it was not surprising that *GLS2* was not detected. However, mRNA levels of *GLS1* and its two isoforms, *KGA* and *GAC* all were all significantly upregulated following TGF- $\beta_1$  stimulation ( $p < 0.0001$ ,  $n=4$ ) (Fig. 3.20). These data show that *GLS1* is not

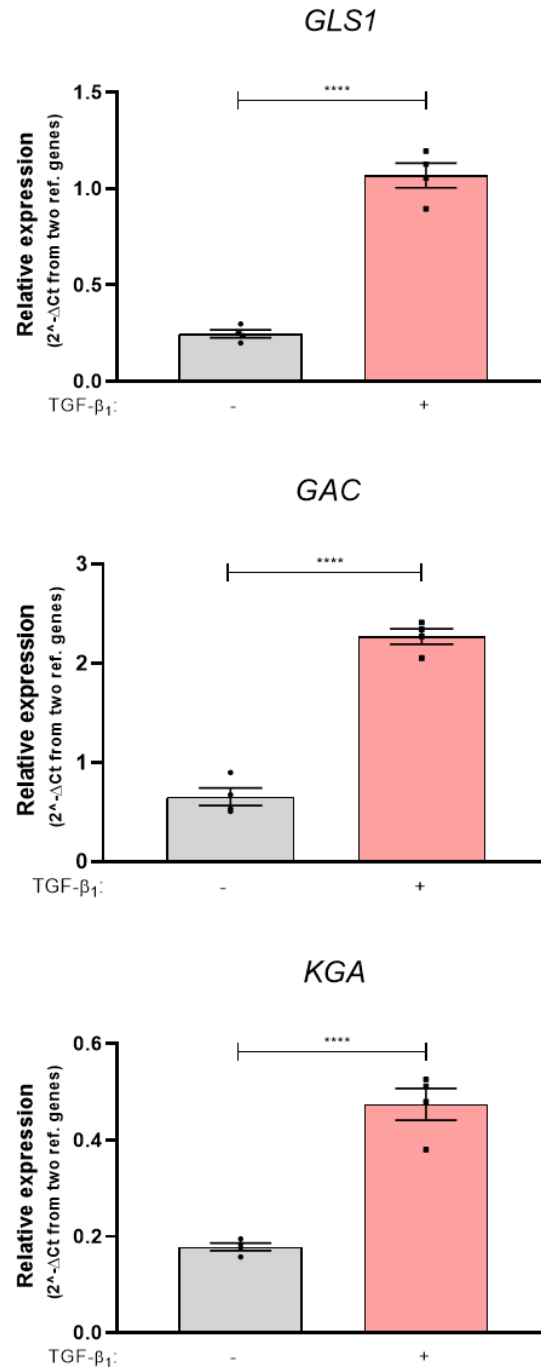


**Figure 3. 20** TGF-β<sub>1</sub> increases the mRNA levels of GLS1 and splice variants GAC and KGA.

pHLFs were serum-starved 24 hours prior to being stimulated (1ng/ml) by TGF-β<sub>1</sub>. *GLS1*, *GAC* and *KGA* gene expression was assessed by qRT-PCR 24 hours post-TGF-β<sub>1</sub> stimulation and expressed relative to the mean of two housekeeping genes. Comparisons between groups were performed by two-way ANOVA followed by Tukey post-hoc test. In all cases, p<0.05 was considered statistically significant. Data are presented as mean ± S.E.M. of n=3 biological replicates \*\*\*\*=p<0.0001.

only expressed but TGF- $\beta_1$ -modulated, highlighting a potential role in TGF- $\beta_1$ -induced glutamine catabolism as well as collagen synthesis.

### **3.3.5 TGF- $\beta_1$ modulates the mRNA levels of glutaminolysis pathway genes.**

Glutaminolysis defines the glutamine catabolic pathways which lead to  $\alpha$ -ketoglutarate generation. Throughout these series of enzymatic reactions, the nonessential amino acids aspartic acid, alanine and glutamate are produced through GOT1/2, GPT1/2 and GLS1, respectively. Glutamate can then produce  $\alpha$ -ketoglutarate through direct deamination by GLUD1 or be converted back to glutamine by GLUL. Glutaminolysis has gained much attention in the oncology setting as a highly pro-tumorigenic metabolic pathway due to its bioenergetic and biomolecular synthesis functions.

Expression of all glutaminolysis genes was found to be modulated by TGF- $\beta_1$ , with *GLS1*, *GPT2* and *GOT1* significantly upregulated and *GLUL*, *GLUD1* and *GOT2* downregulated following TGF- $\beta_1$  stimulation (Fig. 3.21; mRNA levels; Fig 3.22; protein levels). *GLS1* which catabolises glutamine and *GLUL* which anabolises glutamine had inverse temporal expression profiles which were significantly modulated from 3 hours onwards (Fig. 3.21A-B). This may indicate an early-induction and retained need for glutamine catabolism rather than re-synthesis in TGF- $\beta_1$ -stimulated fibroblasts. Expression of *GLUD1*, which further catabolises glutamate, was downregulated at 12 hours by approximately 59% ( $p < 0.01$ ,  $n = 3$ ), although by 24 hours this softened to 14% ( $p < 0.05$ ,  $n = 3$ ) (Fig. 3.21C). Of the two isoforms of *GPT*, only *GPT2* was found to be expressed by pHLFs (Fig. 3.21D). Initially *GPT2* was found to be decreased by 25% ( $p < 0.05$ ,  $n = 3$ ) at 3 hours but this changed to a 74% increase at 12 hours ( $p < 0.01$ ,  $n = 3$ ) and 141% at 24 hours ( $p < 0.01$ ,  $n = 3$ ). Of the two isoforms of *GOT*, only *GOT1* expression was increased by TGF- $\beta_1$ , which almost doubled at 24 hours following TGF- $\beta_1$  stimulation (Fig. 3.21E); whereas *GOT2* was decreased.

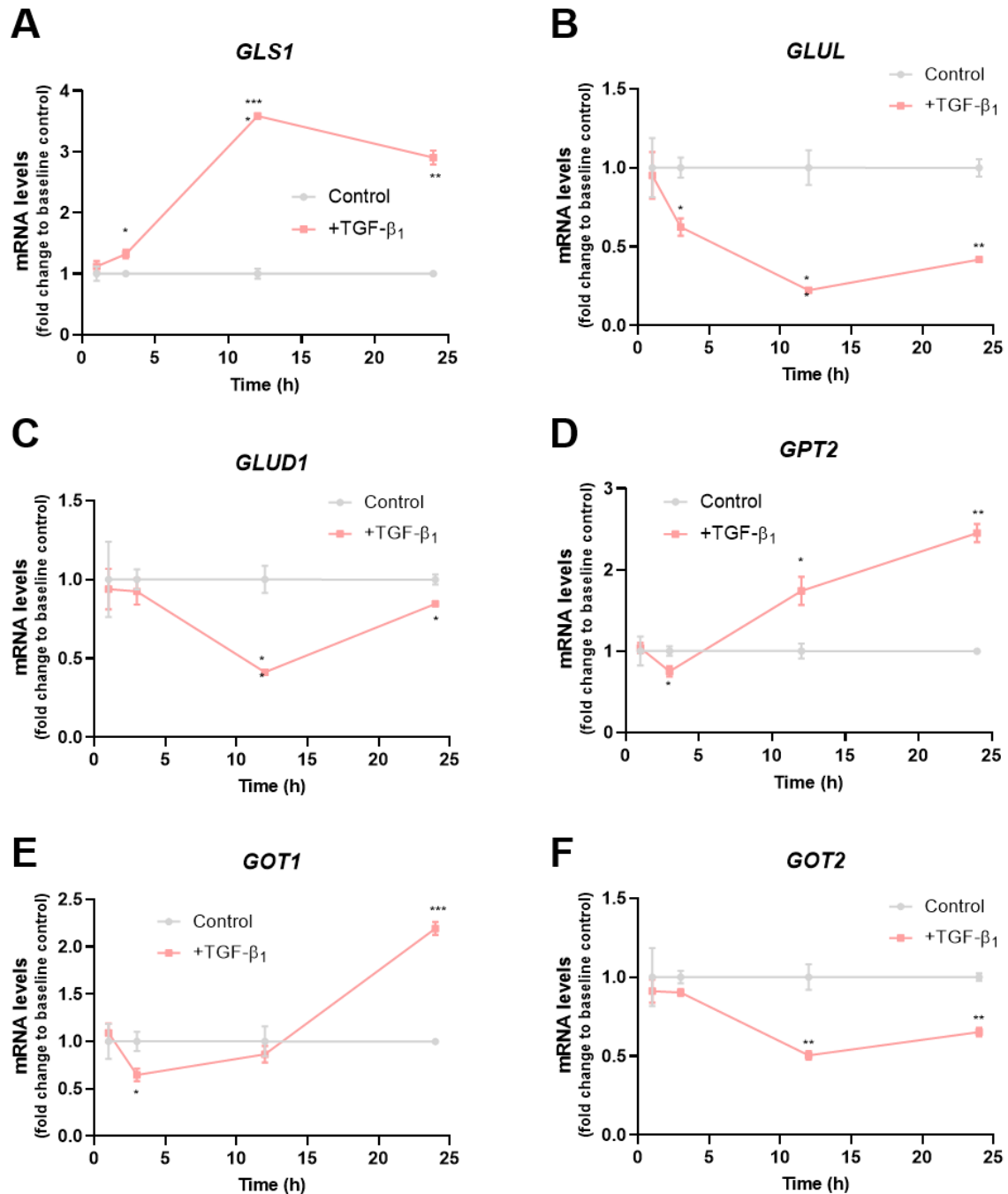


**Figure 3. 21. TGF- $\beta_1$  modulates key glutaminolysis pathway gene mRNA levels over time.**

pHLFs were serum-starved 24 hours prior to being stimulated (1ng/ml) by TGF- $\beta_1$ . RNA was extracted at indicated timepoints (1-, 3-, 12- and 24 hours following stimulation) and mRNA levels of (A) *GLS1*, (B) *GLUL*, (C) *GLUD1*, (D) *GPT2*, (E) *GOT1* and (F) *GOT2* assessed by qRT-PCR and expressed relative to the mean of two housekeeping genes. Comparisons between groups were performed by two-way ANOVA followed by Tukey post-hoc test. In all cases,  $p < 0.05$  was considered statistically significant. Data are representative of N=2 independent experiments and 24-hour and 3-hour time-points repeated N=3. Data are presented as mean  $\pm$  S.E.M. \*= $p < 0.05$ , \*\*= $p < 0.01$ , \*\*\*= $p < 0.001$ , \*\*\*\*= $p < 0.0001$ .

In contrast, *GOT2* expression decreased at both 12 and 24 hour time-points ( $p < 0.01$ ,  $n = 3$ ) (Fig. 3.21F). This suggested a distinct modulation in the compartmentalisation of aspartate synthesis by TGF- $\beta_1$ , potentially supporting cytosolic aspartate synthesis.

Collectively, these temporal profiles of changes in gene expression would be consistent with enhanced glutamine-dependent amino acid synthesis as seen by increased mRNA levels of *GLS1*, *GPT2* and *GOT1* and similarly downregulated expression of *GLUL*, *GLUD1* and *GOT2*. These expression profiles may indicate a potential need for the synthesis of glutamate, aspartic acid and alanine in TGF- $\beta_1$ -stimulated pHLFs.

### **3.3.6 TGF- $\beta_1$ modulates the protein abundance of GLS1, GPT2, GOT1, GOT2, GLUD1 and GLUL.**

I next sought to evaluate whether the transcriptional changes for *GLS1*, *GPT2*, *GOT1*, *GOT2*, *GLUD1* and *GLUL* induced by TGF- $\beta_1$  (Fig. 3.21) followed a similar trend at the protein level by immunoblotting cell lysates 24 hours following TGF- $\beta_1$  stimulation. This revealed that the patterns observed at the mRNA level were mirrored at the protein level (Fig. 3.22). Notably, the *GLS1* isoform GAC was found in higher abundance than KGA. TGF- $\beta_1$  strongly maintained the upregulation of *GPT2* and the downregulation of *GLUL* protein levels at 24 hours.

### **3.3.7 GLS1 is critical for TGF- $\beta_1$ -induced collagen synthesis.**

Having observed a significant TGF- $\beta_1$ -mediated increase in glutamine consumption (Fig 3.21), glutamate synthesis (Fig 3.17) and *GLS1* gene and protein levels (Fig. 3.20: mRNA levels, 3.22: protein levels), the role of this enzyme was next evaluated in TGF- $\beta_1$ -stimulated collagen synthesis using the pharmacological inhibitor, CB-839.

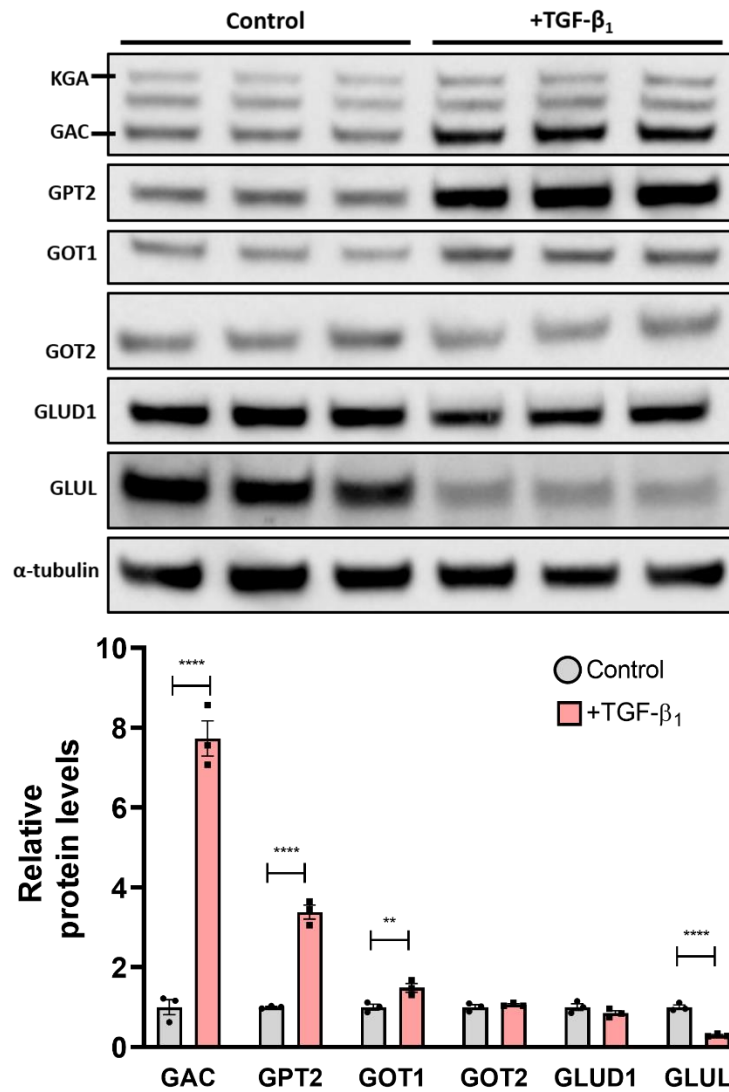


**Figure 3. 22. TGF-β<sub>1</sub> modulated the protein abundance of key glutaminolysis pathway enzymes.**

pHLFs were serum-starved 24 hours prior to being stimulated (1ng/ml) by TGF-β<sub>1</sub> and lysates collected at 24 hours. Protein levels assessed by immunoblotting. Blot is representative of N=3 independent experiments.

CB-839 promoted a concentration-dependent decrease in TGF- $\beta_1$ -induced collagen I deposition from 10nM (log -8) onwards ( $p < 0.001$ ,  $n = 3$ ) (Fig. 3.23). From 100nM (log -7) the reduction in TGF- $\beta_1$ -enhanced collagen I deposition was returned to baseline levels. From these data, the IC<sub>50</sub> of CB-839 was calculated to be 11nM (95% CI 7.7-15.5nM).

To further explore the role of GLS1 in supporting increased collagen I synthesis, an siRNA gene silencing approach to deplete GLS1 protein levels was used. Effective silencing of both GLS1 isoforms, KGA and GAC, was confirmed using immunoblotting (Fig. 3.24A). Treatment with siGLS1 significantly reduced TGF- $\beta_1$ -enhanced collagen I deposition (Fig. 3.24B). To ensure this effect was not a consequence of siRNA treatment, non-targeting siRNA (siNT) was used as a control for siGLS1.

Together, these data identify GLS1 as being critical for TGF- $\beta_1$ -induced collagen I deposition.

### **3.3.8 Glutamate $\alpha$ -ketoglutarate supplementation rescue TGF- $\beta_1$ -induced collagen synthesis in CB-839-treated pHLFs.**

Pharmacological and siRNA-mediated targeting approaches defined GLS1 as a critical enzyme for TGF- $\beta_1$ -increased collagen I deposition (Fig. 3.23-3.24). To interrogate the mechanism of action, the media of pHLFs treated with CB-839 was supplemented with glutamine, glutamate and the downstream metabolite of glutaminolysis,  $\alpha$ -ketoglutarate. The functional role for collagen I deposition of a cell-permeable form of  $\alpha$ -ketoglutarate, dimethyl  $\alpha$ -ketoglutarate was firstly assessed throughout a range of concentrations. Dimethyl  $\alpha$ -ketoglutarate was well-tolerated by pHLFs up to 3mM, with a sudden inhibition in collagen I deposition observed at 10mM and complete cell death at 30mM (Fig. 3.25). These concentrations are high considering the supplement contains a dimethyl group, which allows for passive diffusion into the cytoplasm and may therefore increase intracellular  $\alpha$ -ketoglutarate to levels the cell is unable to stabilise metabolically and lead to cell death. In TGF- $\beta_1$ -unstimulated pHLFs, dimethyl  $\alpha$ -ketoglutarate appeared to increase baseline collagen synthesis from 100 $\mu$ M, though this was not statistically significant ( $p = 0.12$ ,

n=3). For the supplementation concentration, 4mM was chosen which is in line with other studies that have used this metabolite [104].

Increasing the extracellular concentration of glutamine did not rescue the inhibitory effects of CB-839 on TGF- $\beta_1$ -induced collagen I deposition (Fig. 3.26). In contrast, glutamate or  $\alpha$ -ketoglutarate supplementation completely rescued TGF- $\beta_1$ -induced collagen I deposition. Collectively, these results identify GLS1-derived glutamate and  $\alpha$ -ketoglutarate as critical metabolites necessary for TGF- $\beta_1$ -increased collagen I deposition.

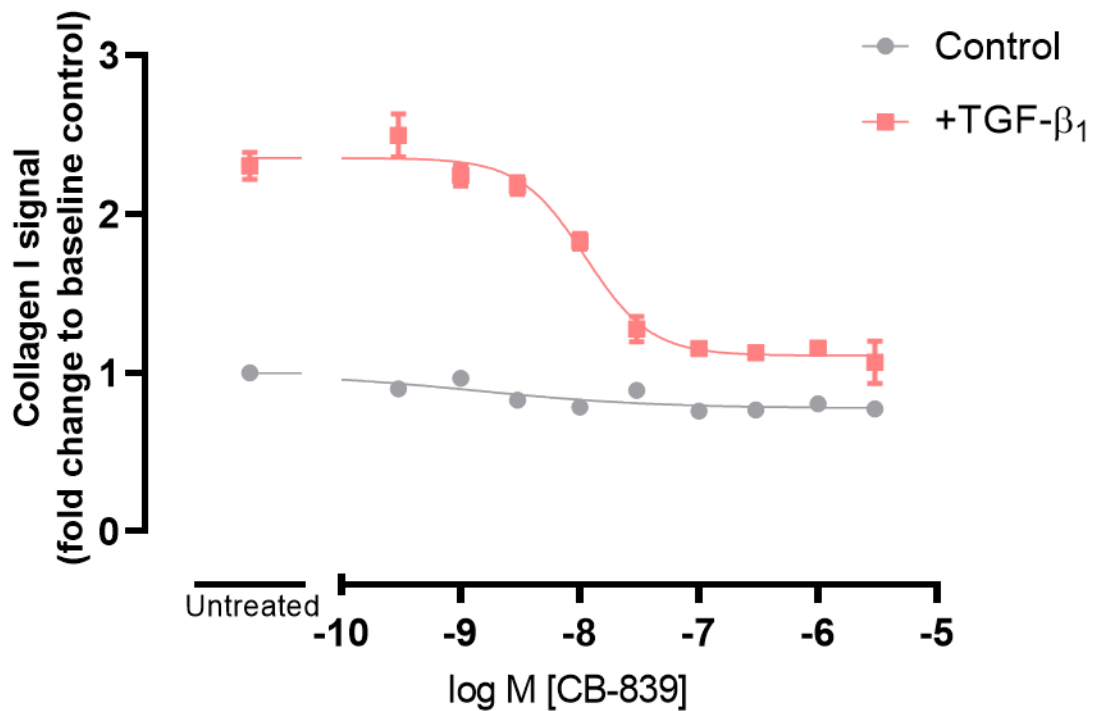


**Figure 3. 23. CB-839 concentration-dependently decreases TGF- $\beta_1$ -induced collagen I deposition.**

Confluent pHLFs were treated with increasing concentrations of CB-839 (300pM to 3 $\mu$ M) and stimulated with TGF- $\beta_1$  (1ng/ml) in macromolecular crowding conditions for 48 hours, prior to fixation and staining for collagen I and with DAPI. The mean fluorescent intensity and cell count per well (n=4 reads per well) was calculated and data expressed as mean  $\pm$  SEM of n=3 biological replicates. IC<sub>50</sub> value was calculated using four-parameter non-linear regression.



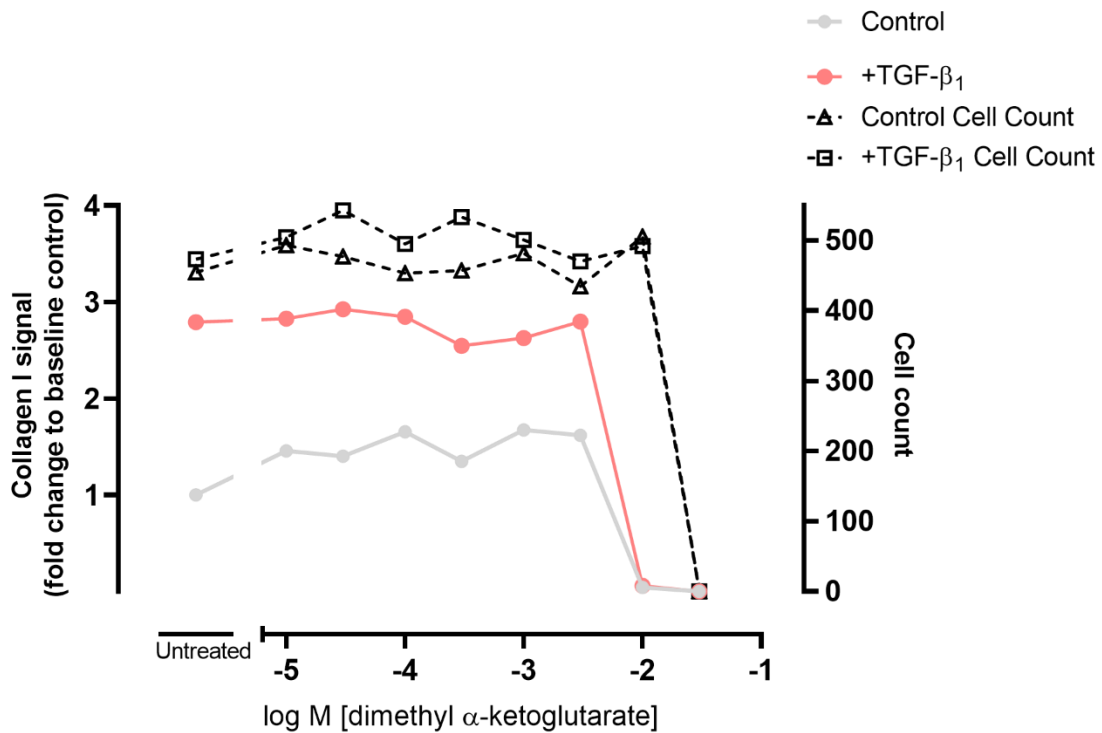


**Figure 3. 25. Cell-permeable α-ketoglutarate does not affect collagen synthesis or cell count up to 3mM.**

Confluent pHLFs were stimulated with increasing concentrations of dimethyl α-ketoglutarate (10μM to 30mM) and stimulated with TGF-β<sub>1</sub> in macromolecular crowding conditions for 48 hours, prior to fixation and staining for collagen I and with DAPI. The mean fluorescent intensity and cell count per well (4 reads per well) was calculated and data expressed as average per condition. Data is from one experiment and is representative of n=2 independent experiments.

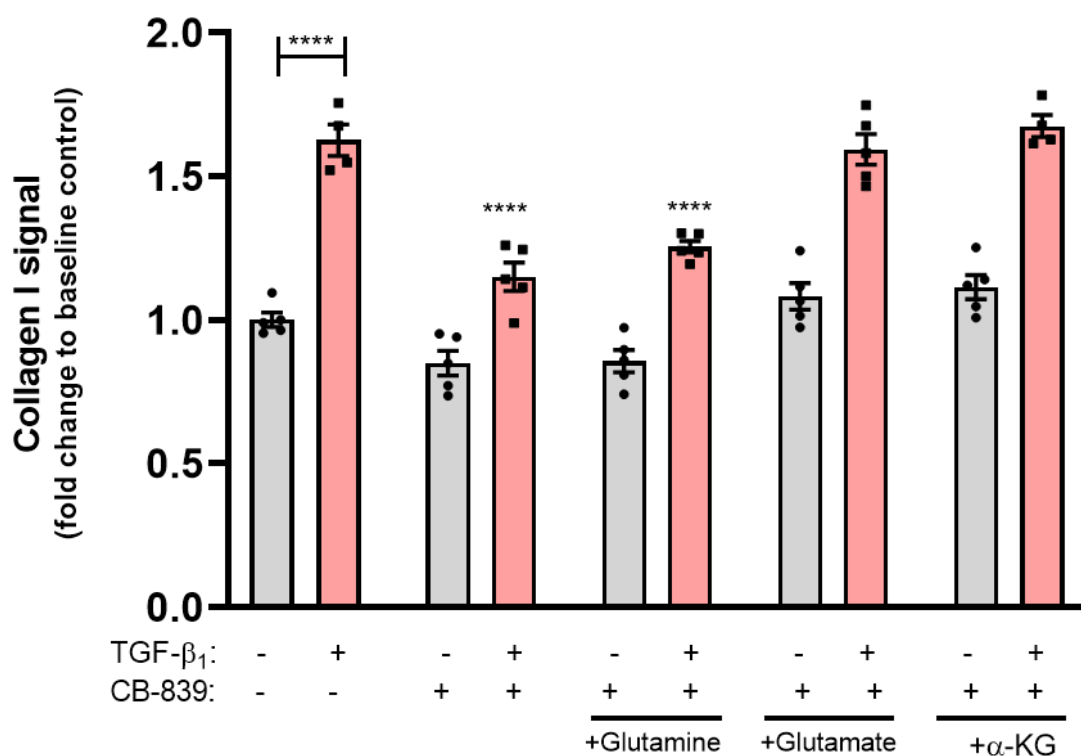


**Figure 3. 26. Glutamate and  $\alpha$ -ketoglutarate supplementation rescue CB-839-treated TGF- $\beta_1$ -stimulated collagen synthesis.**

pHLFs were serum-starved 24 hours prior to pre-treatment under macromolecular crowding conditions with 1 $\mu$ M CB-839 followed by supplementation (where applicable) of indicated metabolite and TGF- $\beta_1$  (1ng/ml) stimulation. The mean fluorescent intensity and cell count per well (n=4 reads per well) was calculated and data expressed as mean  $\pm$  SEM of n=4 replicate wells per condition. Comparisons between groups were performed by two-way ANOVA followed by Tukey post-hoc test. In all cases, p<0.05 was considered statistically significant. Data are presented as mean  $\pm$  S.E.M. of n=3 biological replicates \*\*\*\*=p<0.0001.

### **3.3.9 GLUD1 does not impact on TGF- $\beta$ <sub>1</sub>-induced collagen synthesis.**

As previously mentioned,  $\alpha$ -ketoglutarate can be produced by direct deamination of glutamate via GLUD1 or as a by-product in alanine and aspartate biosynthesis via GPT2 and GOT2, respectively. As supplementation of  $\alpha$ -ketoglutarate completely restored TGF- $\beta$ <sub>1</sub>-induced collagen deposition in CB-839-treated cells, this suggested that glutaminolysis is enhanced by TGF- $\beta$ <sub>1</sub> for the purpose of  $\alpha$ -ketoglutarate generation. GLUD1 has been identified as a key source of  $\alpha$ -ketoglutarate in tumour cells, so I therefore next investigated whether GLS1-derived glutamate was required for TGF- $\beta$ <sub>1</sub>-induced collagen synthesis by allowing GLUD1 to produce  $\alpha$ -ketoglutarate.

Pharmacological inhibition of GLUD1 with R162 had no effect on TGF- $\beta$ <sub>1</sub>-induced collagen I deposition (Fig. 3.27). Interestingly, R162 treatment increased collagen synthesis in baseline pHLFs from 10 $\mu$ M ( $p < 0.05$ ,  $n = 5$ ) and both TGF- $\beta$ <sub>1</sub>-stimulated and unstimulated cells at 30 $\mu$ M ( $p < 0.0001$ ,  $n = 5$ ). This baseline effect, however, was not observed in pHLFs treated with siGLUD1 (Fig 3.28). Furthermore, silencing of GLUD1 did not affect TGF- $\beta$ <sub>1</sub>-induced collagen I deposition, agreeing with the pharmacological data and supporting the dispensable role for this enzyme in TGF- $\beta$ <sub>1</sub>-induced collagen I deposition (Fig. 3.28). These results indicate that if  $\alpha$ -ketoglutarate generation is a critical function downstream of GLS1-derived glutamate, it is not facilitated by GLUD1 and this enzyme is not required for TGF- $\beta$ <sub>1</sub>-induced collagen I deposition.

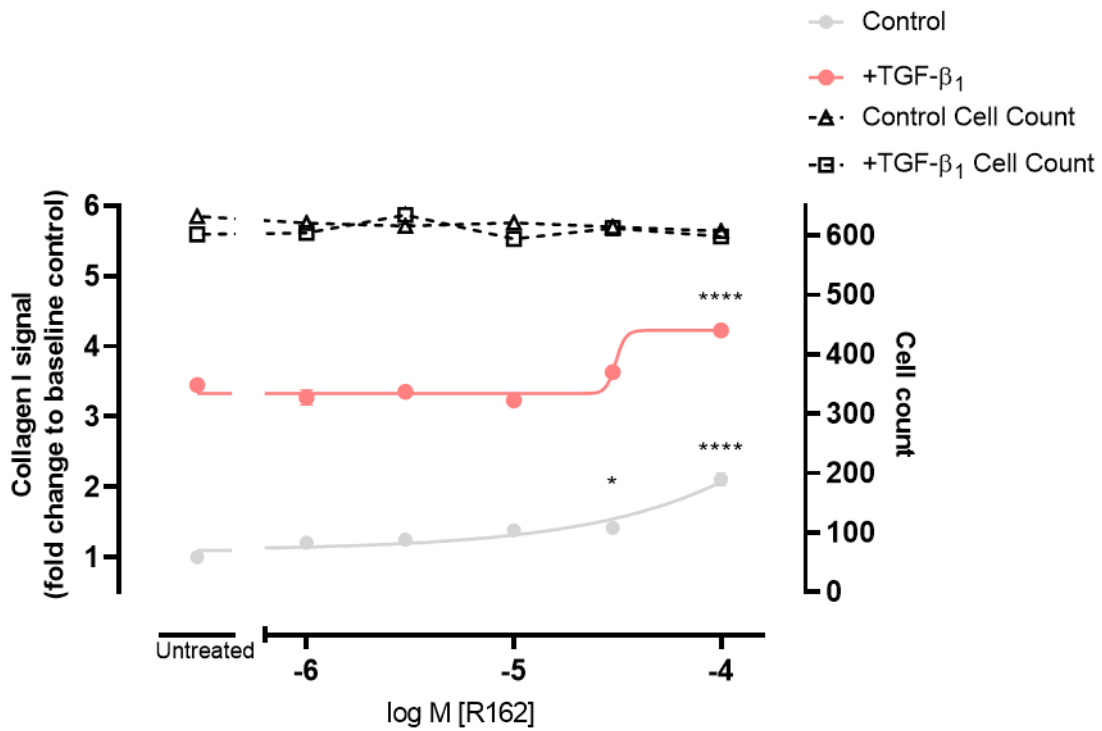


**Figure 3. 27. GLUD1 inhibition with R162 does not impact on TGF-β<sub>1</sub>-induced collagen synthesis.**

Confluent pHLFs were stimulated with increasing concentrations of R162 (1 μM to 100 μM) and stimulated with TGF-β<sub>1</sub> in macromolecular crowding conditions for 48 hours, prior to fixation and staining for collagen I and with DAPI. The mean fluorescent intensity and cell count per well (4 reads per well) was calculated and data expressed as mean ± SEM of n=3 biological replicates \* = p < 0.05, \*\*\*\* = p < 0.0001.

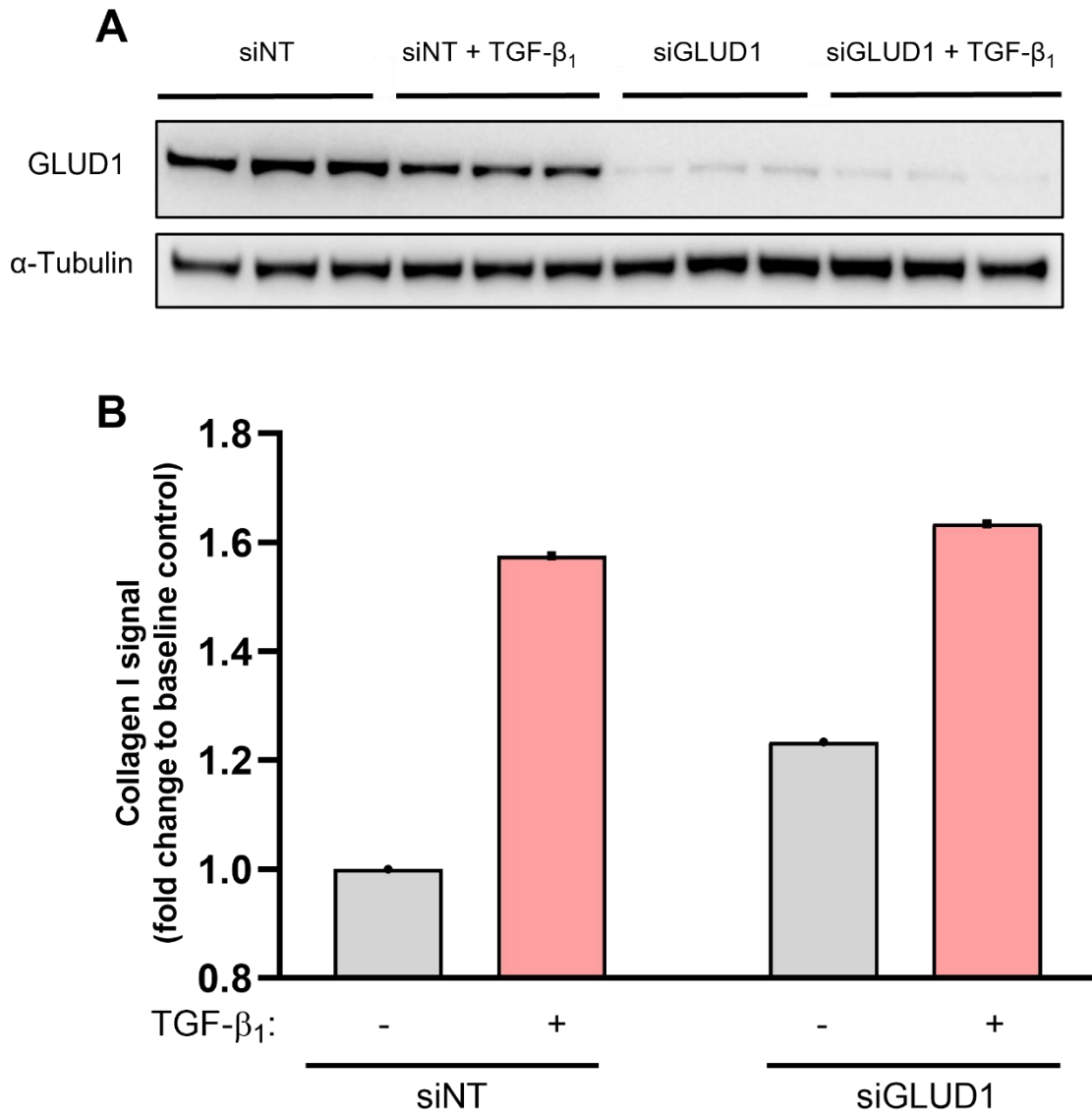


**Figure 3. 28. siGLUD1 treatment does not impact on TGF- $\beta_1$ -induced collagen synthesis.**

pHLFs were transfected with siGLUD1 or siNT as described in section 2.10. pHLFs were serum-starved 24 hours prior to stimulation with TGF- $\beta_1$  (1ng/ml). (A) GLUD1 protein abundance was assessed by immunoblotting 24 hours following TGF- $\beta_1$  (1ng/ml) stimulation (B) Collagen I deposition was measured using the macromolecular crowding assay 48 hours following TGF- $\beta_1$  (1ng/ml) stimulation. Blot is representative of n=3 biological replicates. Data is shown as an average of n=2 independent experiments.

### **3.3.10 Supplementation of $\alpha$ -ketoglutarate regenerates intracellular glutamate levels following GLS1 inhibition in TGF- $\beta_1$ -stimulated cells.**

The enzymatic reactions in the mitochondria which remove an amino group from glutamate to produce  $\alpha$ -ketoglutarate are all reversible. Therefore, it remained a possibility that supplying exogenous  $\alpha$ -ketoglutarate to GLS1-inhibited cells lead to *de novo* glutamate synthesis independent of GLS1 activity. Intracellular glutamate levels 48 hours following TGF- $\beta_1$  stimulation were then measured in cells treated with CB-839 and supplemented with  $\alpha$ -ketoglutarate, a condition which rescued inhibited-collagen I deposition (Fig. 3.26). As previously observed in Fig 3.17, TGF- $\beta_1$  stimulation increased intracellular glutamate levels by approximately 50% ( $p < 0.0001$ ,  $n = 3$ ) (Fig. 3.29). This increase, however, was completely abolished in cells treated with CB-839 and both TGF- $\beta_1$ -stimulated and unstimulated pHLFs exhibited glutamate levels of around 50% that of the baseline. As suspected, addition of  $\alpha$ -ketoglutarate to the media completely prevented these reductions and rescued TGF- $\beta_1$ -induced glutamate levels.

Taken together, these data show that  $\alpha$ -ketoglutarate supplementation regenerates intracellular glutamate levels decreased by GLS1 inhibition. These results further underline the role of GLS1-derived glutamate in supporting enhanced collagen I deposition induced by TGF- $\beta_1$ .

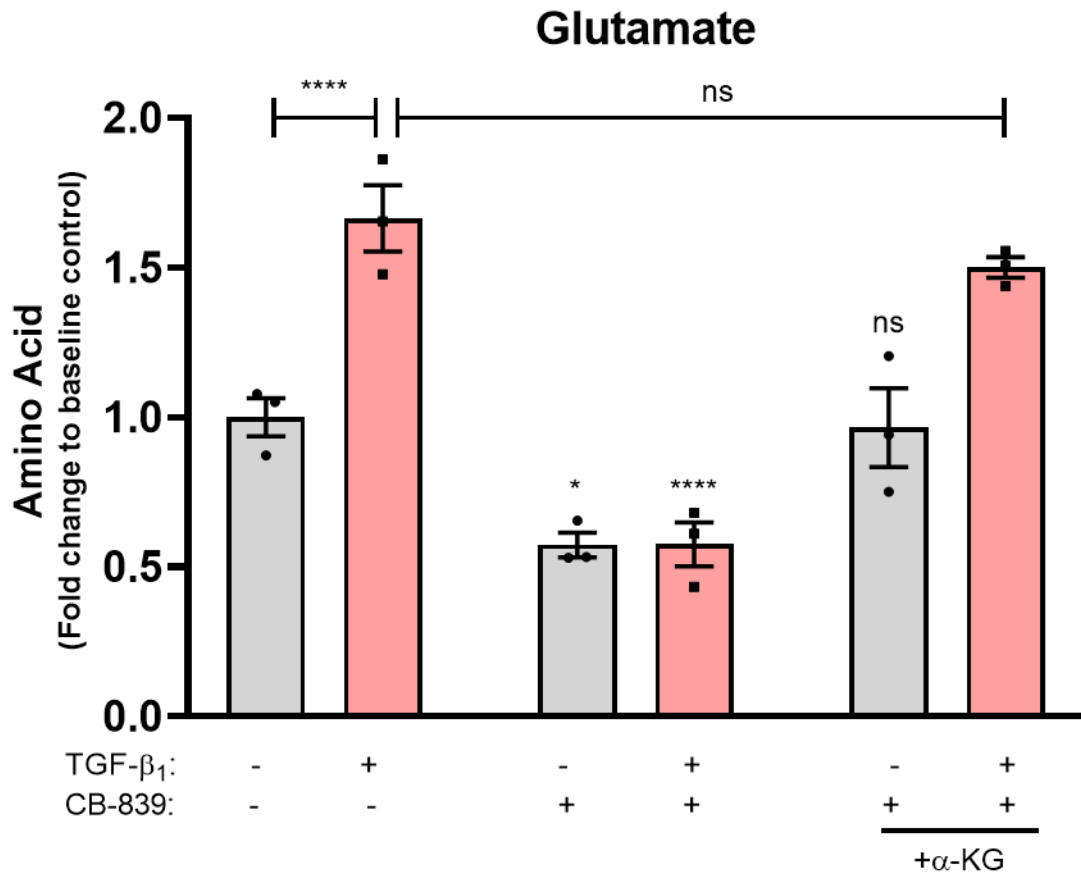


**Figure 3. 29.  $\alpha$ -ketoglutarate supplementation rescues intracellular glutamate levels in CB-839-treated and TGF- $\beta_1$ -stimulated cells.**

pHLFs were serum-starved 24 hours prior to pre-treatment with 1  $\mu$ M CB-839 followed by supplementation (where stated) of 4mM  $\alpha$ -ketoglutarate and TGF- $\beta_1$  (1ng/ml) stimulation. Intracellular glutamate levels were quantified as described in section 2.16 48 hours following stimulation. Comparisons between groups were performed by two-way ANOVA followed by Tukey post-hoc test. In all cases,  $p < 0.05$  was considered statistically significant. Data are presented as mean  $\pm$  S.E.M. of  $n=3$  biological replicates \*= $p < 0.05$ , \*\*\*\*= $p < 0.0001$ .

### **3.3.11 TGF- $\beta$ <sub>1</sub> increases intracellular alanine and proline levels.**

As the pro-fibrotic function(s) of GLS1-derived glutamate remained undefined, I next investigated whether the levels of the amino acids which are dependent on GLS1-derived glutamate (alanine, aspartate and proline) for their synthesis were also modulated by TGF- $\beta$ <sub>1</sub>. To this end, intracellular levels of these three amino acids were quantified over a 4-point time-course of 3, 12, 24 and 48 hours. Intracellular aspartate levels were decreased at 3 hours and 12 hours following TGF- $\beta$ <sub>1</sub> stimulation but showed no significant difference at 24 hours or 48 hours (Fig. 3.30A). In contrast, alanine and proline levels were increased from 24 hours (Fig. 3.30B-C).

Together, these results show pHLFs increase intracellular levels of alanine and proline, but not aspartate, following TGF- $\beta$ <sub>1</sub> stimulation with a maximal increase at 48 hours.

### **3.3.12 Intracellular alanine, aspartate and proline levels are GLS1-dependent.**

The biosynthesis of alanine, aspartate and proline are all dependent on glutamate availability. Alanine can be synthesized by GPT1/2, which transfer an amino group from glutamate to pyruvate, forming alanine and  $\alpha$ -ketoglutarate. Aspartate can be synthesized by GOT1/2, which transfer an amino group from glutamate to oxaloacetate, forming aspartate and  $\alpha$ -ketoglutarate. Glutamate can be converted to proline through a series of reactions facilitated by PYCR1 and P5CS. As GLS1 inhibition decreased glutamate levels, I next assessed whether GLS1-derived glutamate impacted on the synthesis of alanine, aspartate and proline. Additionally, having shown that  $\alpha$ -ketoglutarate supplementation rescued CB-839-decreased TGF- $\beta$ <sub>1</sub>-induced collagen I deposition and glutamate levels, the potential rescue effect of  $\alpha$ -ketoglutarate was also investigated as it may be due to enhanced amino acid biosynthesis.

As expected, TGF- $\beta$ <sub>1</sub> increased the intracellular levels of alanine, aspartate and proline (Fig. 3.31). The levels of these three amino acids were highly dependent on GLS1 activity, reaching below-baseline levels following GLS1 inhibition by CB-839. Interestingly,  $\alpha$ -ketoglutarate supplementation completely rescued alanine and

proline levels in TGF- $\beta$ <sub>1</sub>-stimulated and CB-839-treated pHLFs. In contrast, aspartate levels were not affected by  $\alpha$ -ketoglutarate supplementation and remained low in GLS1-inhibited cells, suggesting a dispensable role for this amino acid in TGF- $\beta$ <sub>1</sub>-induced collagen I deposition.

Together, these data show that in GLS1-inhibited pHLFs, exogenous  $\alpha$ -ketoglutarate supplementation regenerates intracellular TGF- $\beta$ <sub>1</sub>-increased levels of alanine and proline but not aspartate.

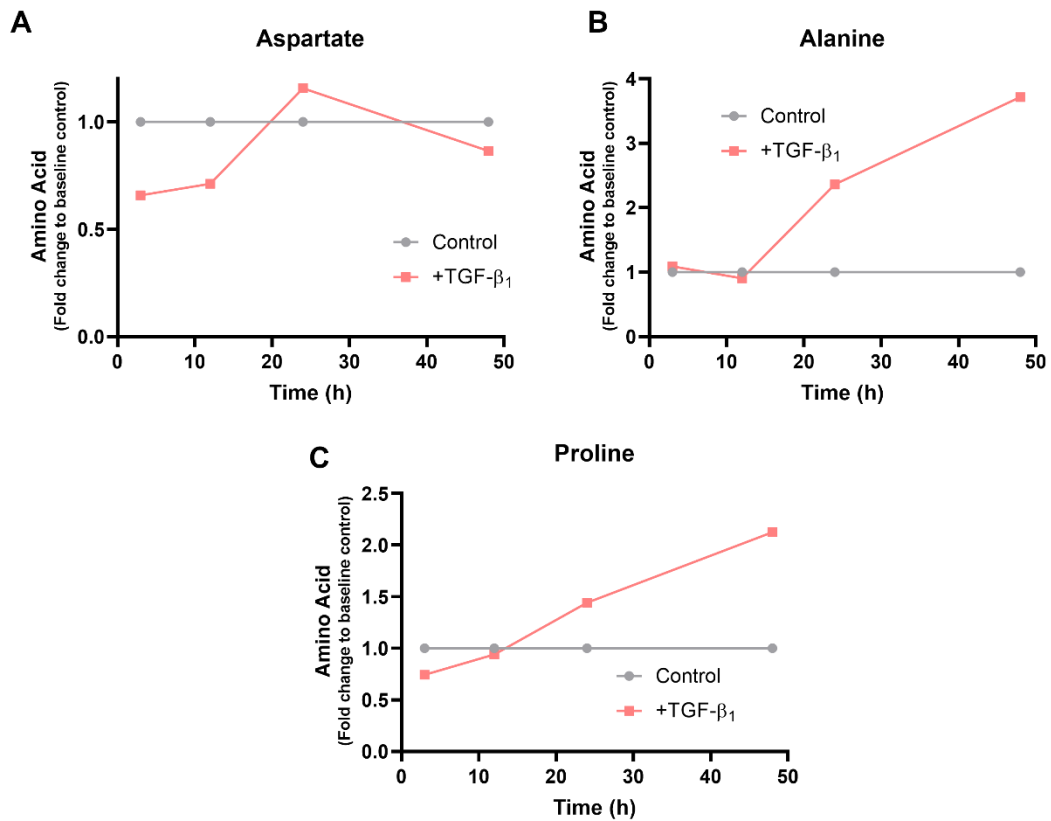


**Figure 3.30. TGF- $\beta_1$  increases intracellular alanine and proline levels.**

pHLFs were serum-starved 24 hours prior to TGF- $\beta_1$  (1ng/ml) stimulation. Intracellular amino acids for (A) aspartate, (B) alanine and (C) proline were quantified at indicated timepoints (3-, 12-, 24- and 48 hours) as described in section 2.16. Data are shown as an average of n=2 independent experiments.

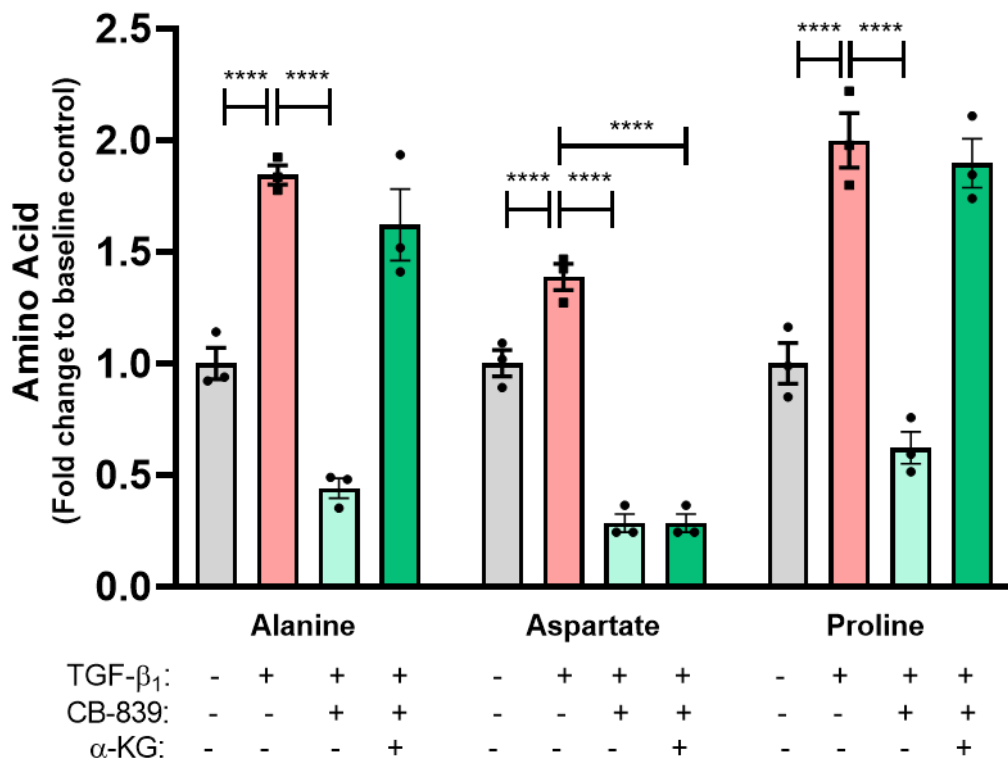


**Figure 3. 31.  $\alpha$ -ketoglutarate supplementation rescues CB-839-treated and TGF- $\beta_1$ -stimulated intracellular levels of alanine, aspartate and proline.**

pHLFs were serum-starved 24 hours prior to pre-treatment with 1  $\mu$ M CB-839 followed by supplementation (where stated) of 4mM  $\alpha$ -ketoglutarate and TGF- $\beta_1$  (1ng/ml) stimulation. Intracellular alanine, aspartate and proline levels were quantified as described in section 2.16 48 hours following stimulation. Comparisons between groups were performed by two-way ANOVA followed by Tukey post-hoc test. In all cases,  $p < 0.05$  was considered statistically significant. Data are presented as mean  $\pm$  S.E.M. of  $n=3$  biological replicates  
 \*\*\*\*= $p < 0.0001$ .

### **3.3.13 Alanine supplementation rescues TGF- $\beta$ <sub>1</sub>-induced collagen I deposition in CB-839-treated pHLFs.**

Having shown that  $\alpha$ -ketoglutarate regenerates glutamate, alanine and proline levels in CB-839-treated and TGF- $\beta$ <sub>1</sub>-stimulated pHLFs (Fig. 3.31), I next questioned whether the decrease in collagen I deposition could be remedied by addition of one of these TGF- $\beta$ <sub>1</sub>-regulated amino acids. Supplementation with 100 $\mu$ M alanine was able to fully rescue TGF- $\beta$ <sub>1</sub>-induced collagen I deposition in GLS1-inhibited pHLFs (Fig. 3.32). As proline is a major constituent amino acid in collagen I, this result brought into question how cells could synthesize collagen with such a marked reduction in intracellular proline levels following GLS1 inhibition (Fig. 3.31). Interestingly, alanine supplementation in CB-839-treated pHLFs stimulated with TGF- $\beta$ <sub>1</sub> significantly increased proline levels by almost 3-fold (Fig. 3.33). Alanine supplementation to CB-839-treated and TGF- $\beta$ <sub>1</sub>-stimulated cells produced approximately 46% of TGF- $\beta$ <sub>1</sub>-induced proline levels.

Taken together, these data suggest a critical role for alanine availability in regulating TGF- $\beta$ <sub>1</sub>-induced collagen I deposition and proline levels when GLS1 is inhibited.

### **3.3.14 GPT2 regulates intracellular alanine levels.**

Alanine can be synthesized by GLS1-derived glutamate through the GPT enzymes. Out of the cytosolic GPT1 and mitochondrial GPT2, only the latter was expressed in pHLFs and found to be modulated by TGF- $\beta$ <sub>1</sub> stimulation (Fig. 3.21/3.22). The previous section showed alanine supplementation rescues the inhibitory effects of CB-839 on TGF- $\beta$ <sub>1</sub>-induced collagen I deposition. Collectively, the previous results of this section suggested TGF- $\beta$ <sub>1</sub> enhances GLS1 activity to produce increased glutamate levels which GPT2 utilizes for increased alanine biosynthesis. To test whether GPT2 regulates *de novo* alanine biosynthesis, selective silencing of GPT2 using siRNA was employed and alanine levels were measured. Silencing of GPT2 drastically reduced intracellular alanine levels in both TGF- $\beta$ <sub>1</sub>-unstimulated and

stimulated cells (Fig. 3.34). These data lead to the conclusion that *de novo* alanine biosynthesis and alanine levels are entirely dependent on GPT2 activity.

### **3.3.15 GPT2 is critical for TGF- $\beta_1$ -induced collagen synthesis.**

Having shown that GLS1 and GPT2 regulate alanine levels, the functional impact of alanine biosynthesis in TGF- $\beta_1$ -induced collagen synthesis was next investigated. pHLFs were treated with GPT2 siRNA and grown in media supplemented with the products and substrates of the GPT reaction:  $\alpha$ -ketoglutarate, alanine, pyruvate and glutamate.

Silencing of GPT2 resulted in a complete inhibition in TGF- $\beta_1$ -induced collagen synthesis (Fig. 3.35A). No significant decrease in collagen levels was observed in unstimulated pHLFs, highlighting GPT2 as a TGF- $\beta_1$ -regulated enzyme for supporting enhanced collagen synthesis. Supplementation with 100 $\mu$ M alanine rescued the TGF- $\beta_1$  collagen response in GPT2-silenced cells by approximately 70% ( $p < 0.0001$ ,  $n=3$ ); whereas supplementation with either  $\alpha$ -ketoglutarate or glutamate did not rescue this response. Addition of pyruvate was able to significantly rescue siGPT2-decreased levels of collagen synthesis by approximately 37% ( $p < 0.0001$ ,  $n=3$ ). Interestingly and for unknown reasons, supplementation with any of the four metabolites produced a small but significant decrease in baseline collagen synthesis.

I next sought to investigate whether a complete rescue of siGPT2-reduced TGF- $\beta_1$ -induced collagen levels could be achieved by increasing the concentration of supplemented alanine. Interestingly, the baseline decrease observed in figure 3.35A following metabolite supplementation was not replicated and thus suggests an experimental artefact. Addition of 30 $\mu$ M alanine alleviated the reduction in TGF- $\beta_1$ -treated collagen levels by approximately 42% when compared to the TGF- $\beta_1$  stimulated control (Fig. 35B). This alleviation was further increased to approximately 82% with 100 $\mu$ M alanine (a similar rescue degree as in Fig. 3.35A) ( $p < 0.05$ ,  $n=3$ ) and a complete rescue was achieved from 300 $\mu$ M onwards of alanine supplementation. To ensure that the upregulation in GPT2 protein levels were due to TGF- $\beta_1$  signalling and not from a need to synthesize alanine in cells growing in an

alanine-free media, GPT2 protein levels were assessed across various alanine concentrations and its TGF- $\beta_1$ -induction was maintained (Fig. 3.36).

Taken together, these data identify GPT2-derived alanine as a critical amino acid required for TGF- $\beta_1$ -induced collagen synthesis.

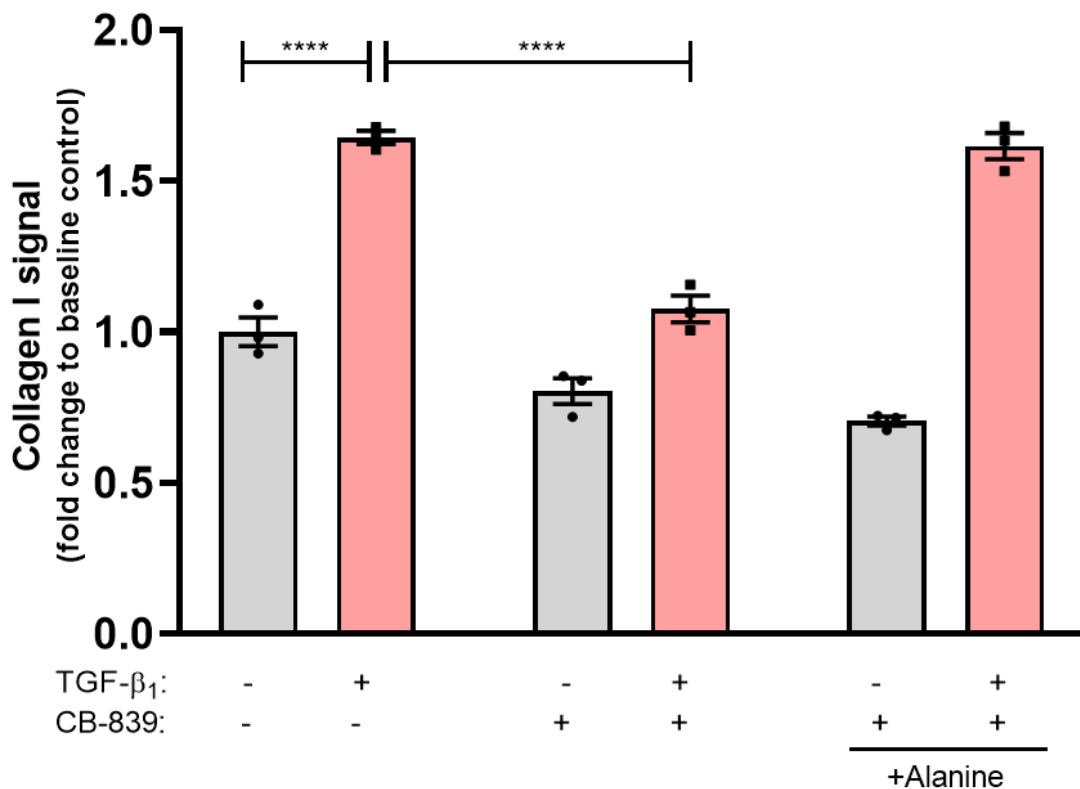


**Figure 3. 32. Alanine supplementation rescues TGF- $\beta_1$ -induced collagen I deposition in GLS1-inhibited cells.**

pHLFs were serum-starved 24 hours prior to pre-treatment under macromolecular crowding conditions with 1 $\mu$ M CB-839 followed by supplementation (where stated) of 500 $\mu$ M L-alanine and TGF- $\beta_1$  (1ng/ml) stimulation. The mean fluorescent intensity and cell count per well (n=4 reads per well) was calculated and data expressed as mean  $\pm$  SEM of n=3 replicate wells per condition. Comparisons between groups were performed by two-way ANOVA followed by Tukey post-hoc test. In all cases, p<0.05 was considered statistically significant. Data are presented as mean  $\pm$  S.E.M. of n=3 biological replicates \*\*\*\*=p<0.0001.

## Proline

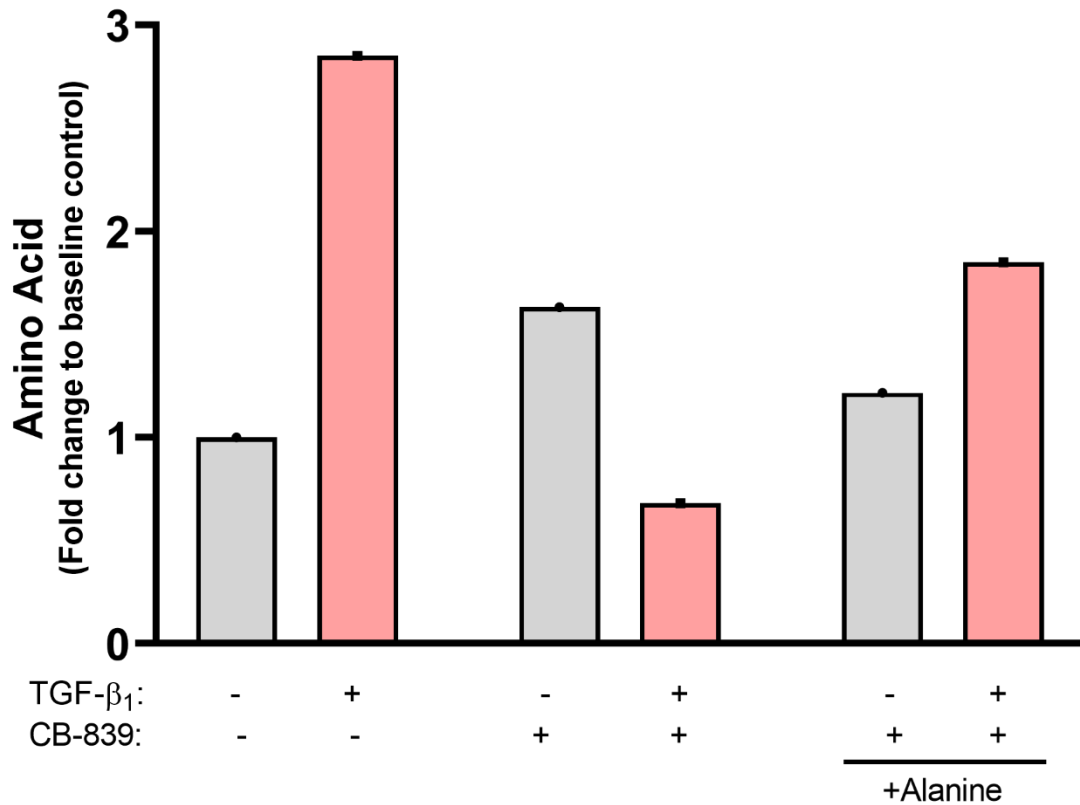


**Figure 3. 33. Alanine supplementation increases intracellular proline levels in CB-839-treated cells.**

pHLFs were serum-starved 24 hours prior to pre-treatment with 1 μM CB-839 followed by supplementation (where stated) of 500 μM L-alanine and TGF-β<sub>1</sub> (1 ng/ml) stimulation. Intracellular proline levels were quantified as described in section 2.16 48 hours following stimulation. Data are shown as the average of n=2 independent experiments.

## Alanine

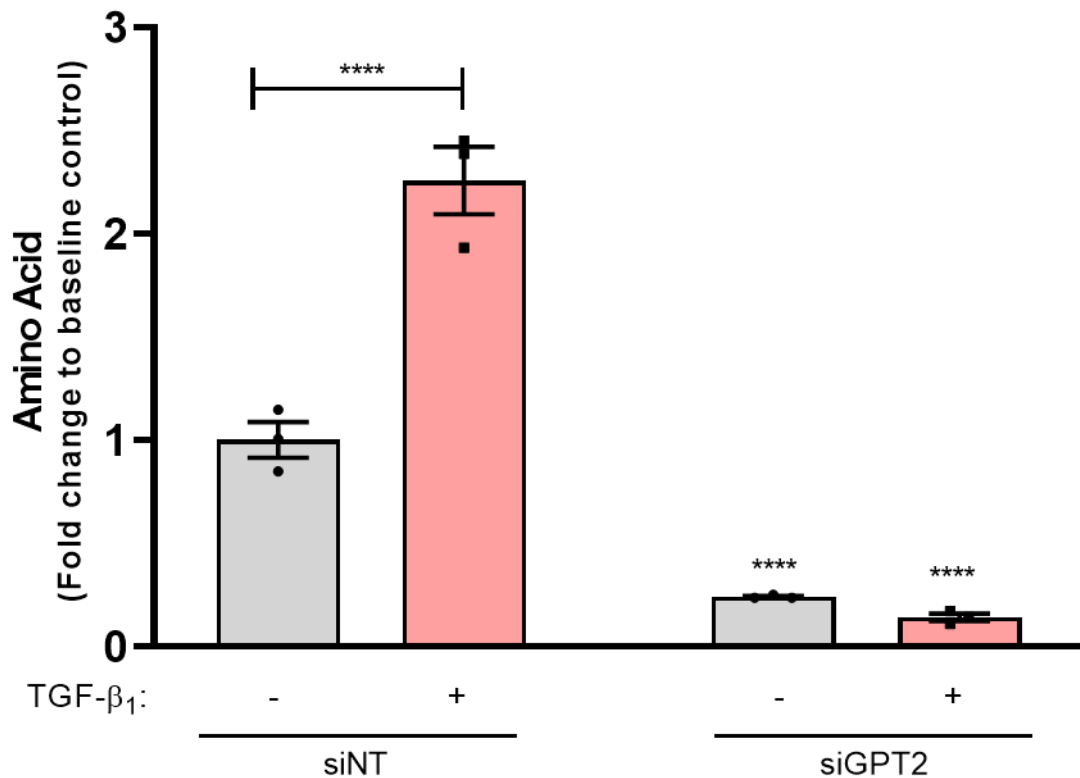


**Figure 3. 34. GPT2 is a major regulator of intracellular alanine levels.**

pHLFs were transfected with siGPT2 or siNT as described in section 2.10. pHLFs were serum-starved 24 hours prior to stimulation with TGF-β<sub>1</sub> (1ng/ml). Intracellular alanine levels were quantified as described in section 2.16 48 hours following stimulation. Comparisons between groups were performed by two-way ANOVA followed by Tukey post-hoc test. In all cases,  $p < 0.05$  was considered statistically significant. Data are presented as mean  $\pm$  S.E.M. of  $n=3$  biological replicates \*\*\*\*= $p < 0.0001$ .

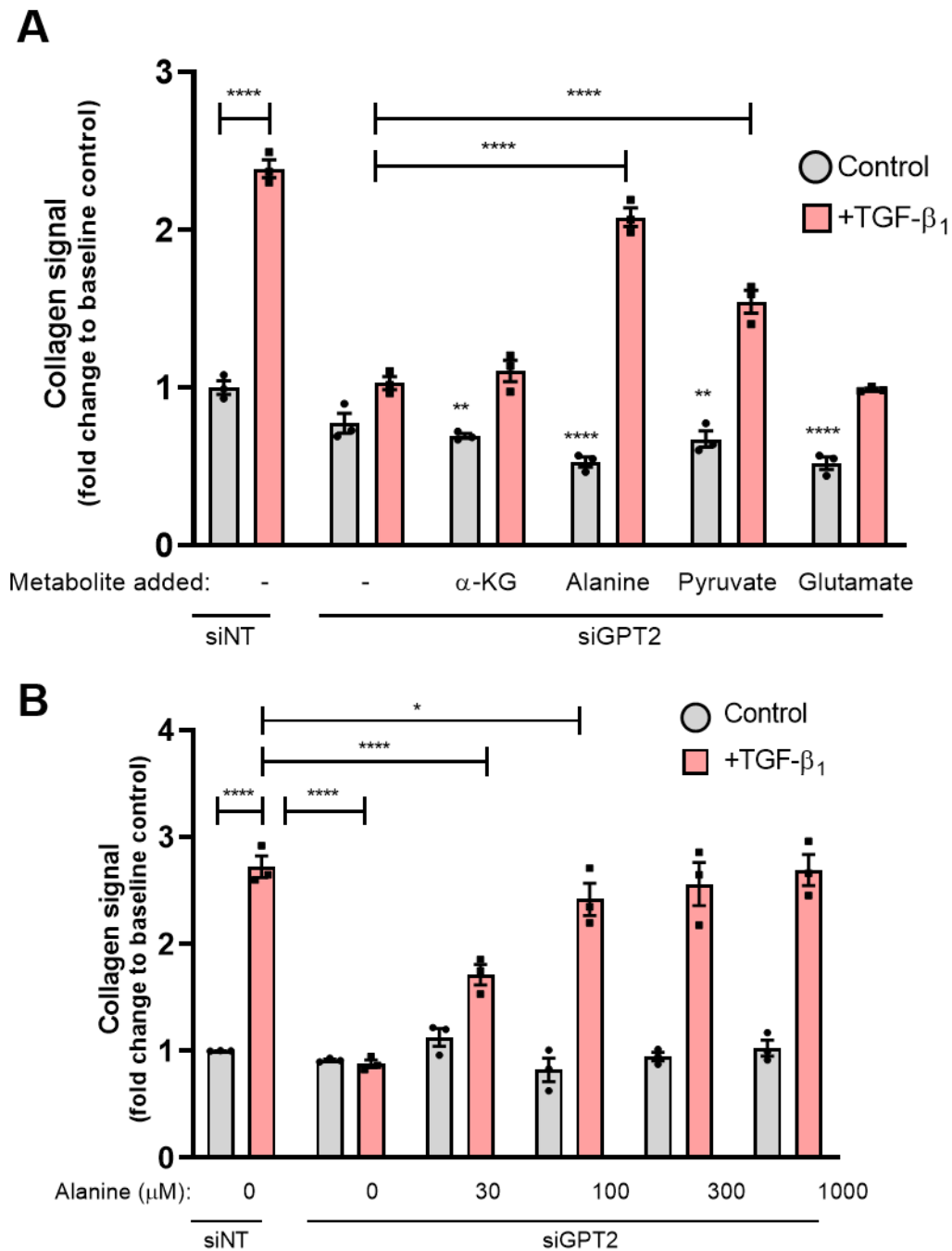


**Figure 3.35. siGPT2-inhibited TGF-β<sub>1</sub>-induced collagen synthesis is rescued by alanine supplementation.**

pHLFs were transfected with siGPT2 or siNT as described in section 2.10 and procollagen quantified as described in section 2.15. pHLFs were serum-starved 24 hours prior to (A) supplementation (where applicable) of (A) indicated metabolite (4mM α-ketoglutarate, 100μM alanine, 1mM pyruvate, 3mM glutamate) or (B) increasing concentration of alanine and TGF-β<sub>1</sub> (1ng/ml) stimulation. Comparisons between groups were performed by two-way ANOVA followed by Tukey post-hoc test. In all cases,  $p < 0.05$  was considered statistically significant. Data are presented as mean  $\pm$  S.E.M. of  $n=3$  biological replicates \*= $p < 0.05$ , \*\*= $p < 0.01$ , \*\*\*\*= $p < 0.0001$ .

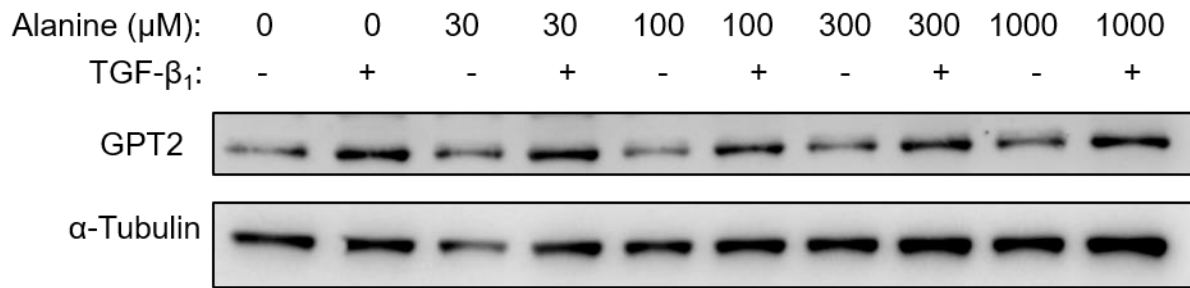


**Figure 3. 36. TGF- $\beta_1$ -induced GPT2 protein abundance is independent of extracellular alanine concentrations.**

pHLFs were serum starved for 24 hours prior to pre-incubation with an increasing concentration of alanine (0 to 1mM) and stimulation with 1ng/ml TGF- $\beta_1$ . Proteins were collected at 24 hours and GPT2 assessed by immunoblotting. Blot is representative of n=3 independent experiments.

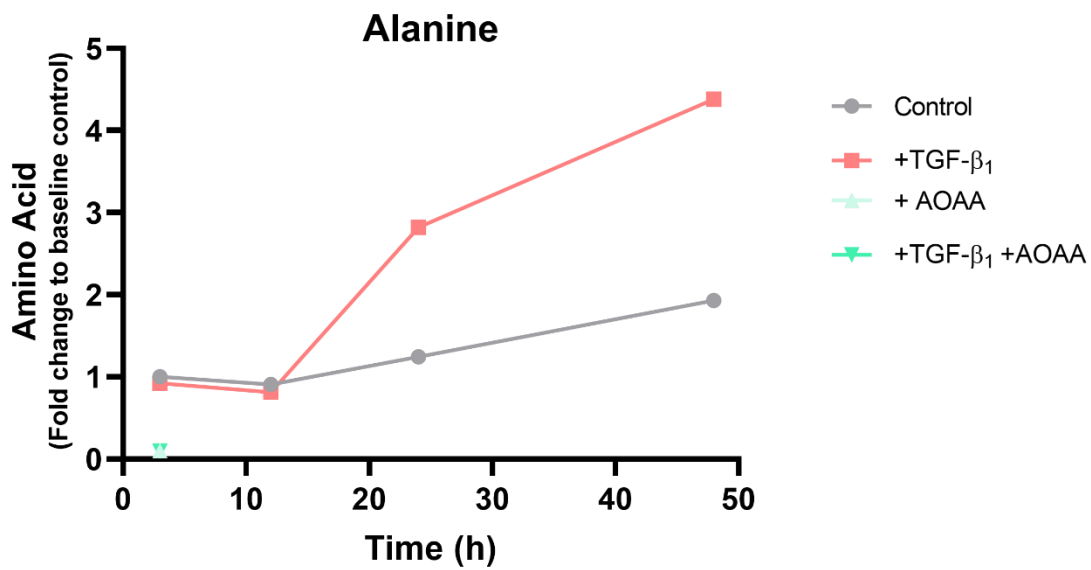


**Figure 3. 37. AOAA treatment depletes intracellular alanine levels.**

pHLFs were serum-starved 24 hours prior to pre-treatment with 1mM AOAA and TGF- $\beta_1$  (1ng/ml) stimulation. Intracellular alanine levels were quantified at indicated timepoints (3-, 12-, 24- and 48 hours) as described in section 2.16. Data is expressed as an average of n=2 biological replicates.

### **3.3.16 AOAA inhibits TGF- $\beta_1$ -induced intracellular alanine levels and collagen synthesis.**

The critical role of GPT2 for TGF- $\beta_1$ -induced collagen synthesis was next assessed pharmacologically. As there is no selective pharmacological agent for GPT2, I used aminooxyacetic acid (AOAA). AOAA is an inhibitor of pyridoxal phosphate (PLP)-dependent enzymes, which include aminotransferases involved in amino acid metabolism. To confirm AOAA impacted on the activity of GPT2, intracellular alanine levels were measured through an identical time-course as used in experiments described in Fig. 3.30.

As previously measured, TGF- $\beta_1$  increased alanine levels from 24 hours following stimulation (Fig. 3.37). Treatment with 500 $\mu$ M AOAA completely abolished intracellular alanine levels in both TGF- $\beta_1$ -stimulated and unstimulated pHLFs at 3 hours and alanine was undetectable by HPLC at further time-points. This time-course data confirmed that AOAA decreased intracellular alanine levels.

Collagen synthesis of pHLFs treated with AOAA was then measured and total inhibition of TGF- $\beta_1$ -induced collagen levels was observed (Fig. 3.38). Mirroring the effect of siGPT2 on baseline collagen levels, no significant effect was observed on baseline collagen levels with AOAA.

Together, these results confirm that pharmacological targeting of GPT2 with AOAA replicates the anti-fibrotic effects induced by GPT2 silencing with respect to enhanced collagen synthesis following TGF- $\beta_1$  stimulation.

### **3.3.17 AOAA and siGPT2 treatment inhibit TGF- $\beta_1$ -induced mTORC1 activation.**

mTORC1 activation has been shown to be a critical event for TGF- $\beta_1$ -enhanced collagen synthesis and occurs as early as 1-hour following TGF- $\beta_1$  stimulation [30]. Studies into the mechanisms leading to mTORC1 activation have highlighted the influential roles certain amino acids, such as leucine play. Upon activation, mTORC1 phosphorylates 4E-BP1 at several sites. Phosphorylation of the S65 site results in its dissociation from eIF4E and activation of cap-dependent mRNA translation. The

observation that AOAA treatment abolished alanine levels at the early time-point of 3 hours raised the question of whether alanine may affect TGF- $\beta_1$ -induced mTORC1 activation. To this end, pHLFs were treated with AOAA for 3 hours and mTORC1 activity was assessed through immunoblotting of 4E-BP1<sup>S65</sup> phosphorylation.

AOAA treatment completely abolished TGF- $\beta_1$ -induced mTORC1 activation, returning 4E-BP1 phosphorylation back to unstimulated levels (Fig. 3.39A). To investigate the mechanism of action, exogenous alanine at two concentrations of 100 $\mu$ M and 300 $\mu$ M was added to the media with AOAA and 4E-BP1<sup>S65</sup> phosphorylation measured. 300 $\mu$ M of alanine was able to rescue the decreased levels of 4E-BP1<sup>S65</sup> phosphorylation induced by AOAA treatment in TGF- $\beta_1$ -stimulated cells (Fig. 3.39B).

To determine whether these data indicated that GPT2-derived alanine was required for TGF- $\beta_1$ -induced mTORC1 activation, GPT2 was silenced using siRNA and 4E-BP1<sup>S65</sup> phosphorylation measured. Treatment with siGPT2 replicated the inhibitory effects on 4E-BP1<sup>S65</sup> phosphorylation induced by AOAA treatment (Fig. 3.40). Addition of exogenous alanine rescued this reduction by approximately 80%, as measured through band density quantification ( $p < 0.001$ ,  $n = 3$ ). Additionally, silencing of GPT2 led to an increase in total 4E-BP1, indicating a decrease in mTORC1 activity as a result of limited availability of alanine which is required for general protein synthesis.

Collectively, these results identify GPT2-derived alanine as critical for TGF- $\beta_1$ -induced mTORC1 activation.

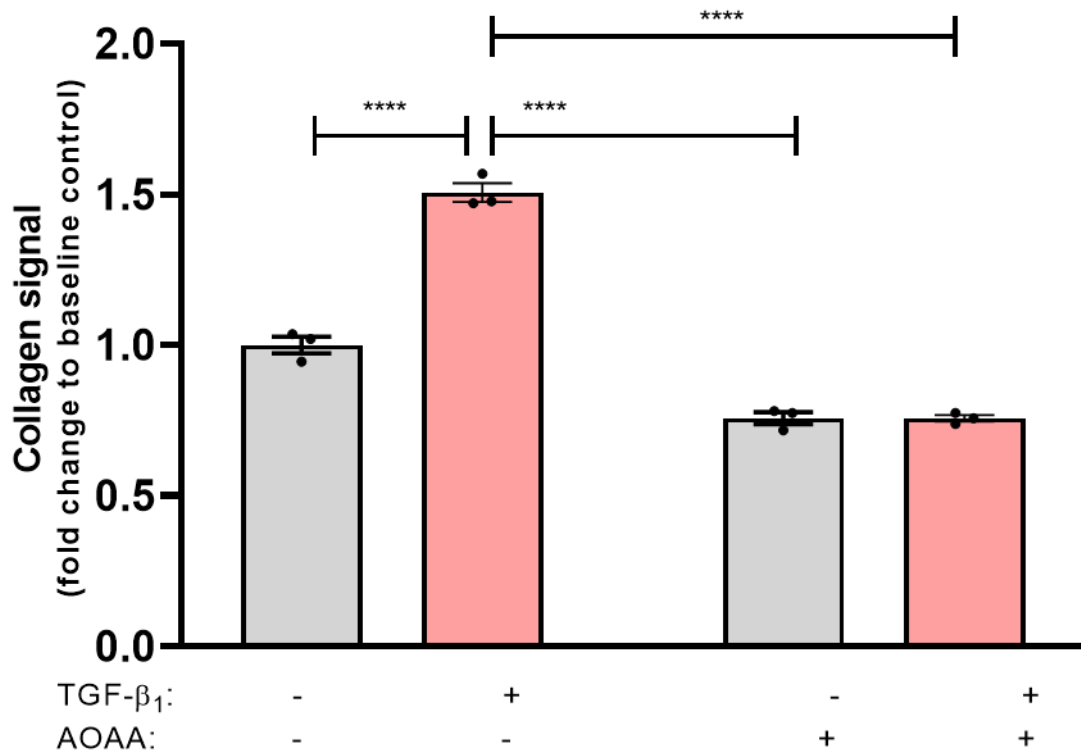


**Figure 3. 38. AOAA treatment inhibits TGF- $\beta_1$ -stimulated collagen synthesis.**

pHLFs were serum-starved 24 hours prior to pre-treatment with 1mM AOAA and TGF- $\beta_1$  (1ng/ml) stimulation. Procollagen was quantified as described in section 2.15. Comparisons between groups were performed by two-way ANOVA followed by Tukey post-hoc test. In all cases,  $p < 0.05$  was considered statistically significant. Data are presented as mean  $\pm$  S.E.M. of  $n=3$  biological replicates \*\*\*\*= $p < 0.0001$ .

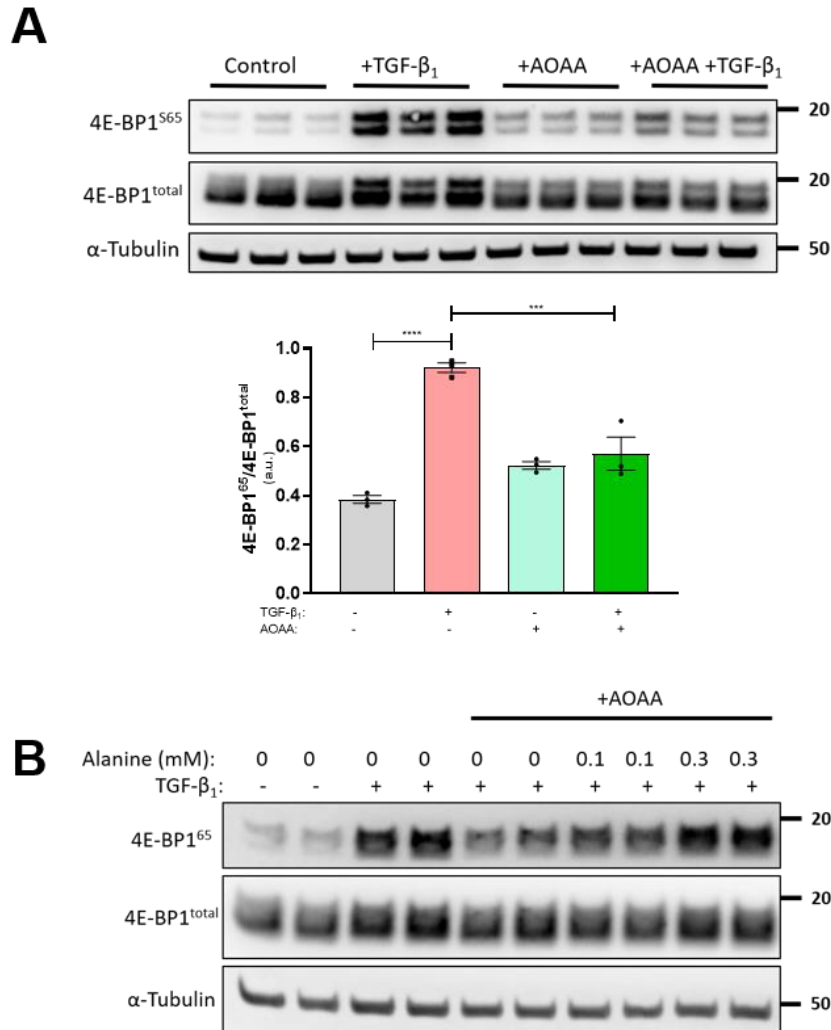


**Figure 3. 39. AOAA inhibits TGF-β<sub>1</sub>-induced mTORC1 activation as determined by assessing 4E-BP1 phosphorylation.**

pHLFs were serum starved for 24 hours prior to pre-incubation with 1mM AOAA. (A) Lysates collected at 3 hours (n=3). (B) pHLFs supplemented with 0mM, 0.1mM or 0.3mM alanine prior to stimulation and lysates collected at 3 hours (n=2). 4E-BP1<sup>S65</sup> and 4E-BP1 were assessed by immunoblotting and normalised to α-tubulin. Comparisons between groups were performed by two-way ANOVA followed by Tukey post-hoc test. In all cases, p<0.05 was considered statistically significant. Data are presented as mean ± S.E.M. of n=3 biological replicates \*\*\*\*=p<0.0001.

### **3.3.18 Silencing of GOT1 and GOT2 does not impact on TGF- $\beta$ <sub>1</sub>-induced mTORC1 activation.**

As an inhibitor for PLP-dependent reactions, AOAA can also inhibit GOT1 and GOT2, the enzymes responsible for aspartate biosynthesis. To assess whether these enzymes and the biosynthesis of aspartate also modulate TGF- $\beta$ <sub>1</sub>-induced mTORC1 activation, GOT1 and GOT2 were simultaneously silenced using siRNA.

However, dual silencing of both enzymes had no effect on the activation of mTORC1 following TGF- $\beta$ <sub>1</sub> stimulation (Fig. 3.41). These data allowed me to rule out a role for aspartate biosynthesis in TGF- $\beta$ <sub>1</sub>-induced mTORC1 activation and conclude that AOAA is likely acting by influencing GPT2-derived alanine biosynthesis to regulate mTORC1 activation.

### **3.3.19 Silencing of RagA and RagB do not impact on TGF- $\beta$ <sub>1</sub>-induced mTORC1 activation.**

A well-defined molecular mechanism for amino acid sensing by mTORC1 involves the family of Rag GTPases. The four Rag proteins (RagA, RagB, RagC and RagD) form heterodimers where RagA or RagB bind to RagC or RagD. Amino acids promote RagA/B GTP-loading which enables mTORC1 to directly interact with raptor and subsequently become capable of being activated. To assess whether TGF- $\beta$ <sub>1</sub>-induced mTORC1 activation was dependent on these amino acid sensing proteins, I treated pHLFs with siRNA to RagA and siRagB simultaneously which would prevent heterodimerization of the Rags. Knockdown efficiency was high, however silencing of RagA did not completely reduce its protein abundance (Fig. 3.42). Dual silencing of RagA and RagB had no significant effect on TGF- $\beta$ <sub>1</sub>-induced 4E-BP1<sup>S65</sup> phosphorylation (Fig. 3.42).

These findings indicate that amino acid sensing through the Rags is not required for TGF- $\beta$ <sub>1</sub>-induced mTORC1 activation and that alanine may be sensed by mTORC1 via a Rags-independent mechanism.

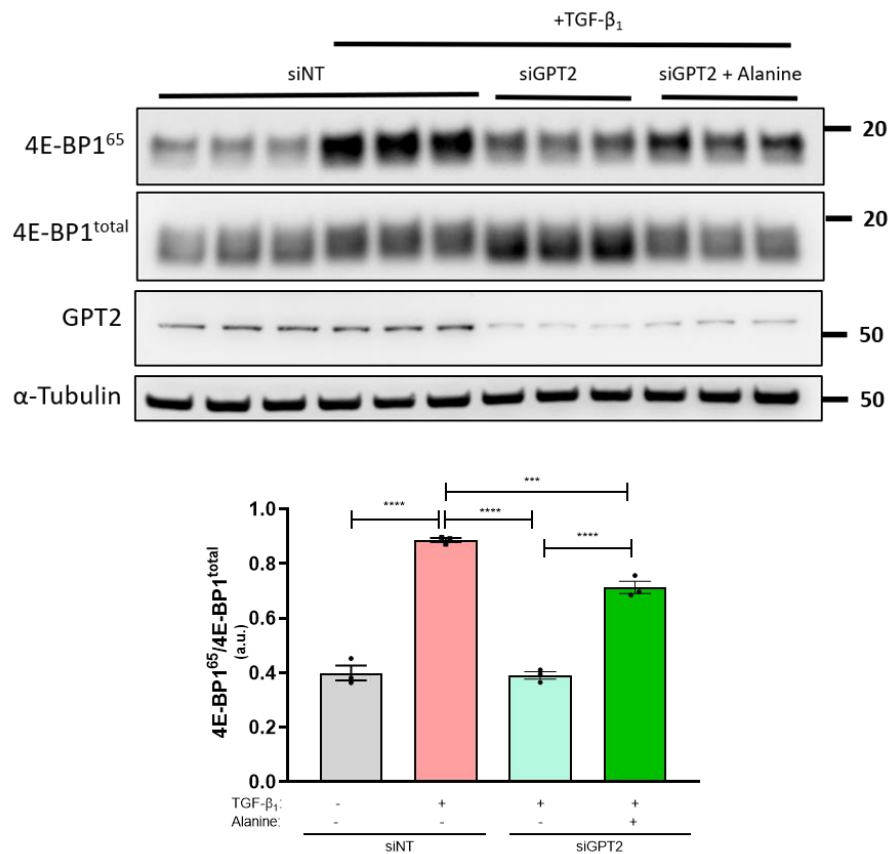


**Figure 3. 40. Alanine supplementation rescues siGPT2-treated TGF- $\beta_1$ -induced mTORC1 activity.**

pHLFs were transfected with siGPT2 or siNT as described in section 2.10. pHLFs were serum starved for 24 hours prior to pre-incubation with 500 $\mu$ M alanine and subsequent TGF- $\beta_1$  (1ng/ml) stimulation. Lysates were collected at 3 hours and 4E-BP1<sup>s65</sup>, 4E-BP1 and GPT2 were assessed by immunoblotting and normalised to  $\alpha$ -tubulin. Comparisons between groups were performed by two-way ANOVA followed by Tukey post-hoc test. In all cases,  $p < 0.05$  was considered statistically significant. Data are presented as mean  $\pm$  S.E.M. of  $n=3$  biological replicates \*\*\*\*= $p < 0.0001$ .

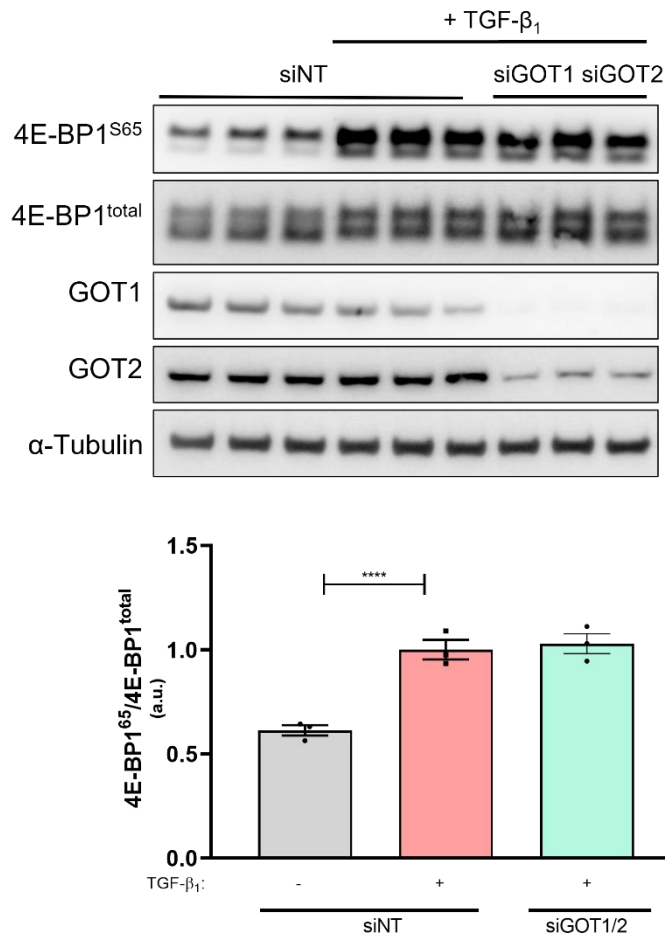


**Figure 3. 41. Dual silencing of GOT1 and GOT2 does not impact on TGF-β<sub>1</sub>-induced mTORC1 activation.**

pHLFs were transfected with siGOT1 and siGOT2 or siNT as described in section 2.10. pHLFs were serum starved for 24 hours prior to TGF-β<sub>1</sub> stimulation (1ng/ml). Lysates were collected at 3 hours and 4E-BP1<sup>S65</sup>, 4E-BP1, GOT1 and GOT2 were assessed by immunoblotting. Comparisons between groups were performed by two-way ANOVA followed by Tukey post-hoc test. In all cases,  $p < 0.05$  was considered statistically significant. Data are presented as mean  $\pm$  S.E.M. of  $n=3$  biological replicates \*\*\*\*= $p < 0.0001$ . Blots are representative of  $n=3$  independent experiments.

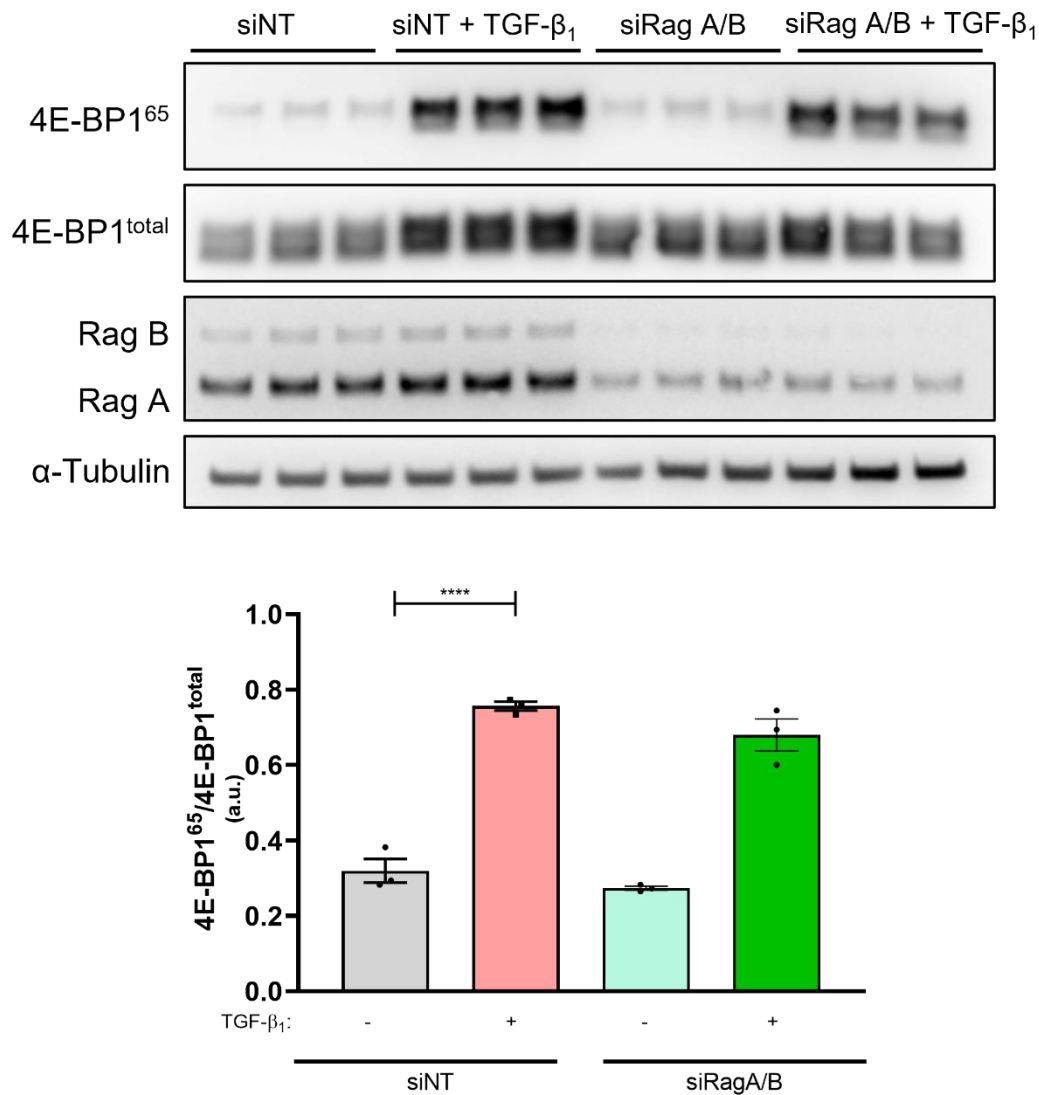


**Figure 3. 42. Dual silencing of RagA and RagB does not impact on TGF- $\beta_1$ -induced mTORC1 activation.**

pHLFs were transfected with siRagA and siRagB or siNT as described in section 2.10. pHLFs were serum starved for 24 hours prior to TGF- $\beta_1$  stimulation (1ng/ml). Lysates were collected at 3 hours and 4E-BP1<sup>s65</sup>, 4E-BP1, RagA and RagB were assessed by immunoblotting. Comparisons between groups were performed by two-way ANOVA followed by Tukey post-hoc test. In all cases,  $p < 0.05$  was considered statistically significant. Data are presented as mean  $\pm$  S.E.M. of  $n=3$  biological replicates \*\*\*\*= $p < 0.0001$ . Blots are representative of  $n=3$  independent experiments.

### **3.3.20 Supplementation with nonessential amino acids and $\alpha$ -ketoglutarate rescues the inhibition on TGF- $\beta_1$ -induced collagen synthesis in AOAA-treated pHLFs.**

Having shown that alanine rescued AOAA-inhibited TGF- $\beta_1$ -induced mTORC1 activation, I next sought to assess the implications of this for TGF- $\beta_1$ -induced collagen I deposition. However, alanine supplementation, while able to rescue the inhibitory effects of AOAA on mTORC1 activation, was not able to alleviate the inhibition of TGF- $\beta_1$ -enhanced collagen I deposition (Fig. 3.43). As AOAA may affect the synthesis of other amino acids, I also assessed the impact of supplementing the cell media with a cocktail of nonessential amino acids (glutamate, asparagine, aspartate, proline, alanine, serine and glycine). However, this did not rescue the inhibition in TGF- $\beta_1$ -stimulated collagen I deposition induced by AOAA treatment. These results indicate that AOAA likely impacts on a non-amino acid biosynthesis function that was essential for supporting TGF- $\beta_1$ -enhanced levels of collagen I.

AOAA is an inhibitor for many aminotransferases, which mediate the reversible reaction of transferring an amino group from glutamate to an oxo-acid, forming an amino acid and  $\alpha$ -ketoglutarate. I then questioned whether the generation of  $\alpha$ -ketoglutarate was an important function of aminotransferases in meeting the enhanced collagen deposition requirements in response to TGF- $\beta_1$  stimulation. Notably, addition of  $\alpha$ -ketoglutarate to AOAA-treated pHLFs in a media supplemented with nonessential amino acids fully restore TGF- $\beta_1$ -induced collagen synthesis (Fig. 3.44). Addition of  $\alpha$ -ketoglutarate and alanine also provided a significant rescue of around 41% of TGF- $\beta_1$ -stimulated levels ( $n < 0.0001$ ,  $n = 3$ ). Interestingly, addition of  $\alpha$ -ketoglutarate alone was not able to rescue the AOAA-inhibited TGF- $\beta_1$ -induced collagen I response, highlighting a need for both  $\alpha$ -ketoglutarate and nonessential amino acids in order to mount a full TGF-beta response.

Collectively, these results identify a critical role for aminotransferases in supporting enhanced collagen synthesis, likely through the generation of  $\alpha$ -ketoglutarate and nonessential amino acids.

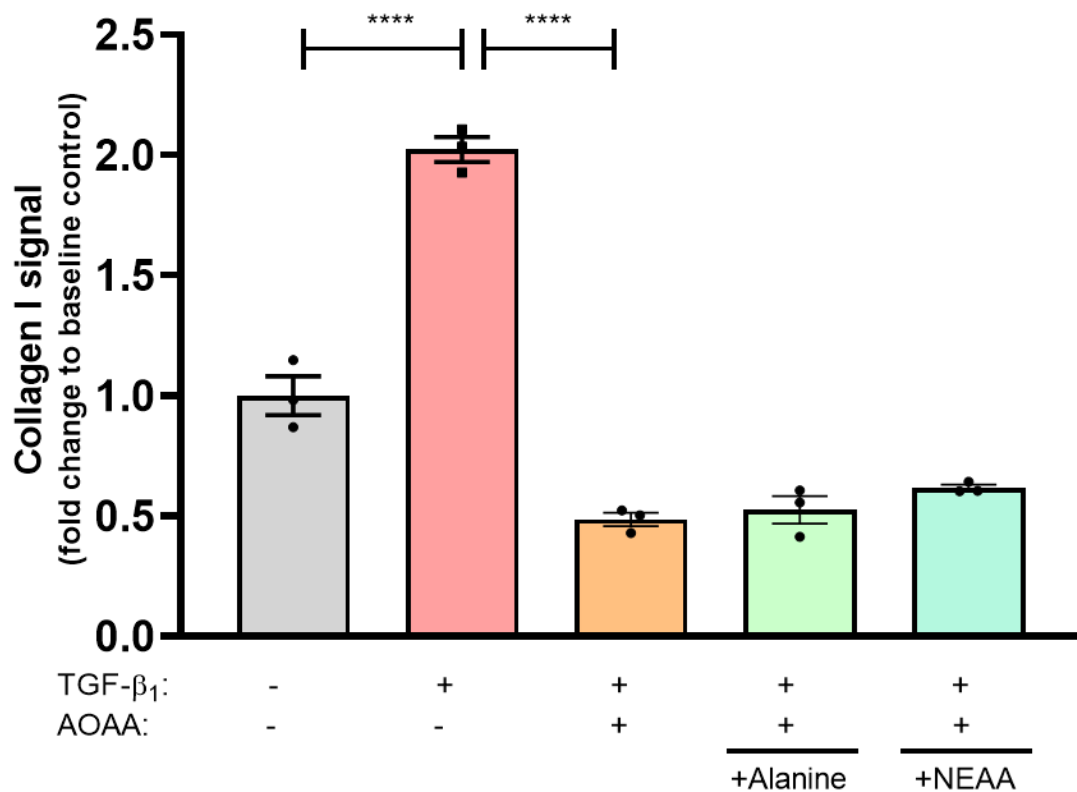


**Figure 3. 43. Alanine and nonessential amino acid supplementation do not impact on AOAA-treated TGF- $\beta_1$ -induced collagen I deposition.**

pHLFs were serum-starved 24 hours prior to pre-treatment with 1mM AOAA and indicated metabolite supplement (500 $\mu$ M alanine or 250 $\mu$ M nonessential amino acids (NEAA)) and TGF- $\beta_1$  (1ng/ml) stimulation under macromolecular crowding conditions for 48 hours, prior to fixation and staining for collagen I and with DAPI. The mean fluorescent intensity and cell count per well (n=4 reads per well) was calculated and data expressed as mean  $\pm$  SEM of n=3 replicate wells. Comparisons between groups were performed by two-way ANOVA followed by Tukey post-hoc test. In all cases, p<0.05 was considered statistically significant. Data are presented as mean  $\pm$  S.E.M. of n=3 biological replicates \* =p<0.05, \*\* =p<0.01, \*\*\* =p<0.001, \*\*\*\* =p<0.0001.

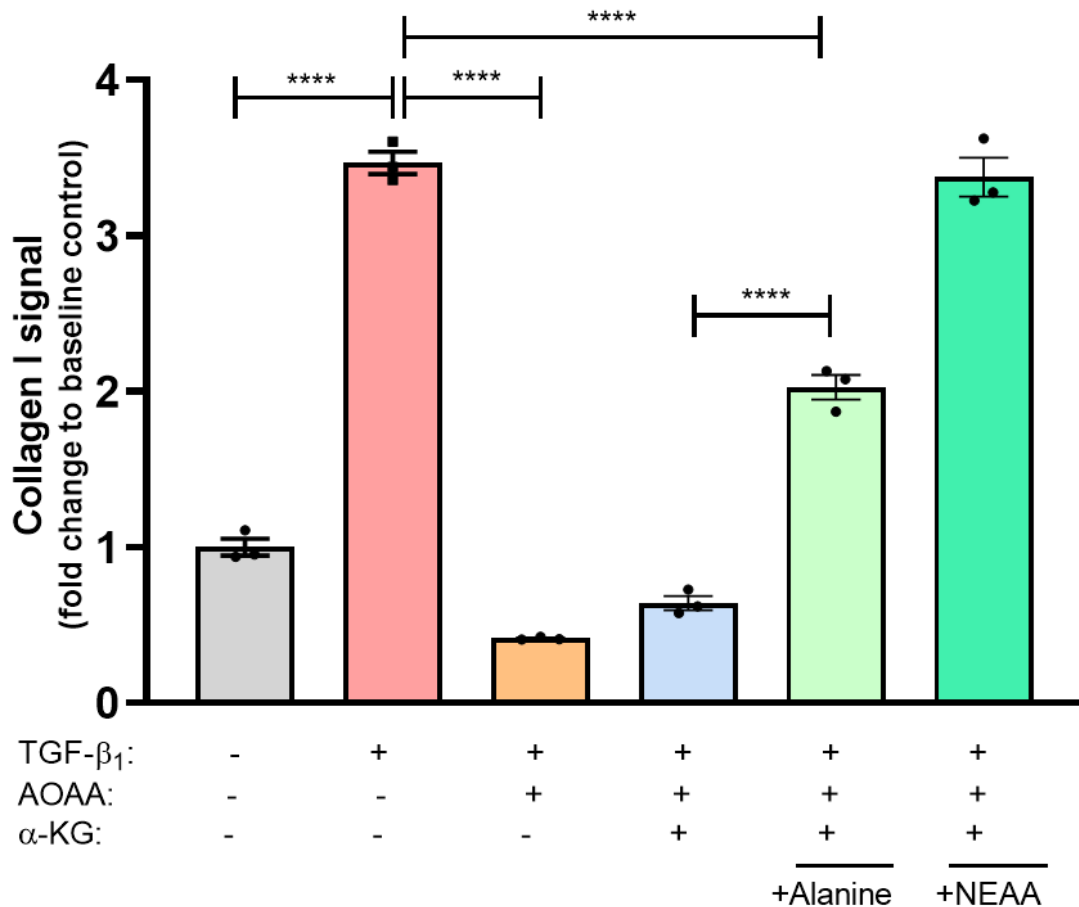


**Figure 3. 44. Nonessential amino acid supplementation with  $\alpha$ -ketoglutarate rescues AOAA-treated TGF- $\beta_1$ -induced collagen I deposition.**

pHLFs were serum-starved 24 hours prior to pre-treatment with 1mM AOAA and indicated metabolite supplement (500 $\mu$ M alanine, 250 $\mu$ M nonessential amino acids (NEAA) or 4mM  $\alpha$ -ketoglutarate) and TGF- $\beta_1$  (1ng/ml) stimulation under macromolecular crowding conditions for 48 hours, prior to fixation and staining for collagen I and with DAPI. The mean fluorescent intensity and cell count per well (n=4 reads per well) was calculated and data expressed as mean  $\pm$  SEM of n=3 replicate wells. Comparisons between groups were performed by two-way ANOVA followed by Tukey post-hoc test. In all cases, p<0.05 was considered statistically significant. Data are presented as mean  $\pm$  S.E.M. of n=3 biological replicates \*\*\*\*=p<0.0001.

### 3.2.21 Summary.

The results described in this section explore the functional role(s) of glutamine metabolism in supporting TGF- $\beta_1$ -enhanced collagen synthesis. TGF- $\beta_1$  was found to increase the rate of glutamine consumption and the expression of key glutamine transporters and glutaminolysis enzymes. Glutamate synthesis via GLS1 was critical for TGF- $\beta_1$ -induced collagen deposition and rescuable by addition of  $\alpha$ -ketoglutarate, which regenerated intracellular levels of glutamate, alanine and proline. TGF- $\beta_1$  increased the expression of glutamate-utilizing GPT2 which was essential for enhanced collagen synthesis via generating alanine. GPT2 protein expression was required for TGF- $\beta_1$ -induced mTORC1 activation via a Rags-independent mechanism. Targeting of GPT2 may yield anti-fibrotic effects as the alanine availability in a fibrotic focus are unknown. Lastly, the aminotransferase family to which GPT2 belongs was required for TGF- $\beta_1$ -induced collagen deposition for functions exceeding solely alanine (or nonessential amino acids) synthesis. Addition of both nonessential amino acids and  $\alpha$ -ketoglutarate rescued aminotransferase enzymatic inhibition, suggesting another enzyme(s) other than GPT2 in regulating collagen synthesis.

Taken together, these findings identify a two-way model where aminotransferases modulate TGF- $\beta_1$ -enhanced collagen I deposition through GPT2-derived alanine supporting mTORC1 activation and through their biosynthesis functions of producing nonessential amino acids and  $\alpha$ -ketoglutarate. Targeting of this family of enzymes and deeper understanding of the functions the biosynthetic pathways of these amino acids play may yield novel approaches for treating lung fibrosis and other fibrotic conditions.

## Chapter 4: Discussion

### Overview:

Idiopathic pulmonary fibrosis is a progressive fibrotic disease of the lung which leads to destruction of lung architecture, lung failure and ultimately death. While its name defines it as a disease with unknown aetiology, it is becoming increasingly accepted that repetitive epithelial injury promotes dysregulation in epithelial-mesenchymal cell crosstalk leading to the development of fibrosis in genetically susceptible and aged individuals. A key pro-fibrotic component of this crosstalk is the pleiotropic cytokine TGF- $\beta_1$  which promotes fibroblast differentiation into highly contractile and synthetic myofibroblasts, the key effector cells in IPF. In reaching this differentiated state, fibroblasts exhibit stark metabolic alterations which suggests a shift in nutrient requirements to meet the biosynthetic demand for increased protein synthesis.

Increasing evidence supports the therapeutic strategy of targeting these metabolic changes to prevent myofibroblasts from reaching the capacity to synthesize pathological levels of ECM components which drives disease progression. At the start of this thesis, transcriptional analyses of human lung fibroblasts *in vitro* highlighted many metabolic pathways which were modulated following TGF- $\beta_1$  stimulation [81].

This thesis therefore examined the hypothesis that **the metabolic alterations induced by TGF- $\beta_1$  promote fibrogenesis by supporting the biosynthetic demands for enhanced collagen synthesis in human lung fibroblasts.**

The data presented in this thesis presents evidence for a role in TGF- $\beta_1$ -induced changes in the biosynthesis of the nonessential amino acids serine, glycine, glutamate and alanine in supporting enhanced collagen synthesis. Using siRNA-targeted approaches, the enzymes PSAT1, GLS1 and GPT2 are shown to play a critical role in mediating TGF- $\beta_1$ -induced collagen synthesis. Additionally, using a pharmacological small molecule inhibitor, the family of aminotransferases which mediate the biosynthesis of many nonessential amino acids, including serine and alanine, are shown to be an important set of enzymes for supporting TGF- $\beta_1$ -induced collagen synthesis. These metabolic enzymes may represent potential therapeutic targets for the treatment of lung fibrosis and other fibrotic conditions.

## 4.1 The role of the serine-glycine biosynthetic axis in mediating the pro-fibrotic effects of TGF- $\beta_1$ in pHLFs.

### 4.1.1 Introduction.

Serine can be converted to glycine via the single enzymatic reaction catalysed by the mitochondrial enzyme SHMT2. Serine can be taken up by the cell or synthesized *de novo* via a linear three-enzyme pathway involving PHGDH, PSAT1 and PSPH.

Serine biosynthesis requires glucose, glutamine and NAD<sup>+</sup> while glycine biosynthesis requires serine and THF (see figure 1.2). PSAT1 and SHMT2 are both dependent on PLP as a co-factor and thus both biosynthetic arms require vitamin B<sub>6</sub> to function. Serine biosynthesis furthermore produces  $\alpha$ -ketoglutarate, NADH and inorganic phosphate (P<sub>i</sub>) while glycine biosynthesis regenerates THF-CH<sub>2</sub> for folate metabolism. Due to these numerous bioenergetic and biomolecular functions, it is therefore not surprising that these enzymes are frequently overexpressed in numerous cancer types including breast, melanoma, glioma and colon [97, 191-193]. The pro-tumorigenic effects of amplifying these pathways have frequently been attributed to amino acid synthesis which helps support the increased biosynthetic demands of highly proliferative cancer cells. In other cancer models, PHGDH inhibition was shown to limit cell proliferation yet with no effect on intracellular serine concentrations, revealing a serine-independent pro-tumorigenic function [107, 194-196]. Serine-independent functions that have been identified include  $\alpha$ -ketoglutarate generation and nucleotide biosynthesis [96, 97]. As serine biosynthesis depletes the glycolytic intermediate 3-PG, leading to a potential decrease in pyruvate for lactate and ATP production, the effects of this pathway influence the larger metabolome. Indeed, a recent study demonstrated limited serine and  $\alpha$ -ketoglutarate changes upon PHGDH inhibition but with global effects on carbon metabolic outputs such as purine and pyrimidine levels [96]. In the present study, the expression profiles of the serine-glycine biosynthesis enzymes and the role of this pathway in mediating enhanced collagen synthesis following TGF- $\beta_1$  stimulation were evaluated.

This thesis reports that serine biosynthesis genes (*PHGDH*, *PSAT1* & *PSPH*) and glycine biosynthesis (*SHMT2*) were all observed to be transcriptionally upregulated

by TGF- $\beta_1$  in pHLFs (Fig. 3.0). These changes were furthermore found to be dependent on the multi-functional kinase, mTOR which was pharmacologically inhibited with AZD8055. mTOR is the central catalytic unit to the two complexes mTORC1 and mTORC2 which regulate a host of biological processes such as protein translation, autophagy, metabolism, proliferation and motility.

#### **4.1.2 TGF- $\beta_1$ -enhanced collagen synthesis and sensitivity to mTOR inhibition is maintained in physiological media.**

The mTOR complexes regulate a host of cellular processes such as protein translation, autophagy, cytoskeletal remodelling, glucose and lipid metabolism and nucleotide biosynthesis. The critical role of mTOR in lung fibroblast fibrogenesis has been extensively investigated within the host centre and additionally shown to play a role in the collagen responses of dermal fibroblasts (skin fibrosis) and liver hepatic stellate cells (HSCs) (liver fibrosis) [30, 68]. Overactivation of mTOR has also been detected in HSCs and shown to aggravate liver fibrosis induced by CCl<sub>4</sub>- treatment [197]. Whilst the wide-ranging functions of mTOR make it difficult to identify specific players in mediating a fibrogenic response, these studies have demonstrated that mTOR activation confers increased resistance to apoptotic cues in fibroblasts and promotes myofibroblast differentiation which may both accentuate the development of fibrotic lesions. The RNA sequencing analysis (see Fig 3.0) which originally highlighted the TGF- $\beta_1$ -modulated and mTOR-dependent serine-glycine biosynthetic pathway was performed in pHLFs grown in standard DMEM which consisted of supraphysiological glucose (25mM compared to ~5mM) and glutamine (2mM compared to ~0.7mM). As these two nutrients are required for serine biosynthesis, their large excess available extracellularly may disrupt or mask biological effects by overwhelming the system above the conditions seen *in vivo*. In cancer cells, glucose uptake is significantly enhanced and supports increased serine synthesis which promotes cell proliferation [198]. Thus, excessive glucose availability may lead to a heightened uptake of this sugar and drive serine synthesis under non-physiological conditions. Additionally, a study found that growing cancer cell lines in low glucose concentrations which better match the microenvironment availability subjected them to an increased sensitivity to inhibitors of oxidative phosphorylation to limit their

excessive proliferation [199]. Therefore, we shifted media formulation to adopt physiological parameters for glucose and glutamine. As foundation experiments for this new media, I measured TGF- $\beta_1$  responsiveness in terms of collagen I deposition in pHLFs and evaluated the anti-fibrotic effect of mTOR inhibition, an effect the host lab has reported on [30, 68, 81].

As expected, TGF- $\beta_1$  produced a concentration-dependent increase in collagen I deposition which reached a plateau from onwards of 300 pg/ml, indicating a maximal TGF- $\beta_1$  response. All subsequent experiments were performed with 1ng/ml TGF- $\beta_1$  to ensure a full collagen response and to not over-saturate the receptors, potentially activating low-affinity receptors which may not be physiologically relevant *in vivo*. The collagen I threshold observed for TGF- $\beta_1$  stimulation may indicate maximal TGF- $\beta_1$  engagement of receptors, which are internalized following ligand binding to regulate intracellular TGF- $\beta_1$  signalling [200]. Another possibility exists in the maximal rate at which collagen I is deposited as a restraint of the experimental method and collagen crosslinking rate.

The central role of mTOR in supporting TGF- $\beta_1$ -induced collagen I synthesis was confirmed and the sigmoidal concentration-dependent decrease in collagen deposition was consistent with pharmacological engagement by AZD8055. As expected, mTOR inhibition had no effect on cell counts. Unstimulated pHLFs treated with AZD8055 displayed minimal changes in baseline collagen deposition which confirmed engagement of a TGF- $\beta_1$ -specific pathway which is critical for cells to produce enhanced collagen synthesis. Recent work from the host centre has established this effect to be through mTORC1-mediated phosphorylation of its downstream substrate, 4E-BP1 [30].

#### **4.1.3 TGF- $\beta_1$ increases the protein levels of the serine-glycine biosynthesis enzymes through an mTOR-dependent mechanism.**

The overexpression of the serine-glycine biosynthetic pathway is frequently observed in the oncology setting and pharmacological inhibition of PHGDH has shown to decrease proliferation in breast and melanocyte cancer cells *in vitro* models [97, 192, 196, 201]. Figure 3.3 shows that the protein levels of PHGDH,

PSAT1, PSPH and SHMT2 were increased by TGF- $\beta_1$ , an effect found to be entirely dependent on mTOR activity. An unexpected increase in SHMT2 protein levels was observed in cells treated with the mTOR inhibitor, AZD8055 alone. The reasons for this observation were not pursued further but as metabolic networks are highly dynamic and often modulated to compensate for non-physiological changes, it is possible that mTOR inhibition impacts on a metabolic axis which regulates the constitutive expression of SHMT2. In neuronal cells, it was found that dampened proline metabolism via *PYCR2* deletion led to an increase in the mRNA and protein levels of SHMT2 [202]. In our RNA sequencing dataset, we observed *PYCR1* to be mTOR-dependent and TGF- $\beta_1$ -upregulated (GEO identifier: GSE102674). Therefore, it is a possibility that AZD8055-induced downregulation of *PYCR1* expression leads to an upregulation of SHMT2. Furthermore, proline biosynthesis produces NAD(P)<sup>+</sup>, which protects against ROS that can stabilise HIF-1 $\alpha$ , a proven regulator of SHMT2 expression [203, 204]. Additionally, as mTOR inhibition prevents cap-dependent translation, this suggests that SHMT2 is translated via a cap-independent mechanism [205]. Interestingly, HIF-1 $\alpha$  and c-myc (another regulator of SHMT2 expression) both contain internal ribosome entry sites (IRES) which allow their mRNAs to be translated independently of eIF4E sequestered by 4E-BP1 and thus mTOR-independent [206]. As TGF- $\beta_1$  increased SHMT2 protein levels alone, this may suggest that the mechanism employed by TGF- $\beta_1$  and the mechanism employed by mTOR inhibition to increase SHMT2 protein levels are not the same. Lastly, dual treatment with TGF- $\beta_1$  and AZD8055 significantly reduced SHMT2 protein levels as well as PHGDH, PSAT1 and PSPH.

Together, these data show the protein levels of the serine-glycine biosynthetic pathway to be increased by TGF- $\beta_1$  and this effect to be mTOR-dependent.

#### **4.1.4 TGF- $\beta_1$ increases ATF4 expression through an mTOR-independent and Smad3-dependent mechanism.**

ATF4 is a member of the cAMP response element-binding protein (CREB)-2 transcription factor family that regulates a host of stress-responsive genes, including the serine and glycine biosynthetic enzymes [122, 207]. In the studies presented in this thesis, ATF4 was localised in the chromatin-bound cell protein fraction and

induced by TGF- $\beta_1$  from 8 hours following stimulation, suggesting potential early active transcription. Figure 3.4 shows that ATF4 was increased at the protein and mRNA levels following TGF- $\beta_1$  stimulation yet only the protein increase was found to be dependent on mTOR activity. To ensure this effect at the protein level was due to mTOR inhibition and not an off-target effect of the compound, the well-described dual mTORC1 and mTORC2 inhibitor torin-1 was used and showed a replication of the effects of AZD8055. siRNA-mediated knockdown experiments showed the transcriptional upregulation of *ATF4* was further dependent on canonical TGF- $\beta_1$  signalling via Smad3. The siRNA approach was controlled using siNT from the manufacturing company (Horizon Discovery) which were “designed and microarray tested for minimal targeting of human...genes”. Additionally, the siRNA for SMAD3 consisted of a pool of 4 siRNA sequences which have the antisense strands modified to minimize seed-related off-targeting and the sense strands to prevent interaction with RNA-induced silencing complex (RISC) [208]. However, deconvoluting the pool of 4 different siRNA sequences and assessing individual function would confirm target specificity and that the effect is indeed SMAD3-driven. Additionally, deconstructing the pool and assessing individual knockdown and effect on ATF4 mRNA levels would highlight potential off-target effects exhibited by using the collective pool. These steps would apply to all subsequent siRNA experiments in this thesis to ensure target specificity and limited off-target effects. This finding suggests that either *ATF4* is directly transcribed by the Smads via Smad binding element (SBE) regions or the Smads induce the expression of a factor which then leads to increased *ATF4* mRNA levels. In silico analysis from the host lab of the *ATF4* promoter revealed likely Smad3 binding elements which made the former option more likely [81]. Indeed, a recent study using ChIP-Seq showed that Smad2/3 binds and regulates *ATF4* transcription in the breast cancer cell line, BT459 [209]. There is furthermore an apparent disconnect between the relatively moderate increase in *ATF4* mRNA levels compared to the intense induction observed in protein abundance via immunoblotting, suggesting the regulation is pre-dominantly post-transcriptional.

The classical pathway leading to ATF4 protein stability involves the integrated stress response (ISR)-mediated phosphorylation of eIF2 $\alpha$ , which decreases global protein synthesis and allows for selective translation of stress-responsive proteins which

upstream open reading frames (uORFs), including ATF4 and its target genes. Phosphorylation of eIF2 $\alpha$  occurs via four known stress-induced kinases and this event decreases methionine-tRNA availability for the initiation complex required in translation [210]. However, work in the host lab has shown no eIF2 $\alpha$  phosphorylation following TGF- $\beta$ <sub>1</sub> stimulation [81]. Additionally, recent work has demonstrated that silencing of the ER stress response factor, PERK, and of the amino acid deprivation factor, GCN2, which both independently lead to eIF2 $\alpha$  phosphorylation, had no effect on TGF- $\beta$ <sub>1</sub>-induced ATF4 protein levels in HLFs [211]. Therefore, these results identify a stress-independent mechanism for ATF4 mRNA translation. A recently identified mechanism identifies growth factor-induced mTORC1 activity as the mechanism for ATF4 protein abundance via 4E-BP1, which is independent of the ISR pathway [212]. It is therefore likely to be how TGF- $\beta$ <sub>1</sub> increases ATF4 protein abundance in pHLFs which was found to be ISR-independent and mTOR-dependent. Indeed, a recent study showed that inhibition of the ISR did not affect TGF- $\beta$ <sub>1</sub>-induced ATF4 expression in breast cancer cells [209]. Moreover, ATF4 is known to regulate 4E-BP1 expression and its regulation via mTORC1 thus represents a feedback loop in TGF- $\beta$ <sub>1</sub>-stimulated pHLFs [213].

In summary, TGF- $\beta$ <sub>1</sub> regulates ATF4 transcriptionally via direct Smad3-binding to the ATF4 promoter and translationally via mTORC1 activation (mechanism still unknown) which utilizes 4E-BP1 to allow for ATF4 mRNA translation via its uORF independently of the ISR pathway.

#### **4.1.5 siRNA-mediated ATF4 silencing leads to cell death.**

Ongoing work in the host centre found that silencing of ATF4 abolished the TGF- $\beta$ <sub>1</sub>-induced increases in protein levels of the serine-glycine biosynthesis enzymes shown in figure 3.3 [81]. Therefore, the next step was to evaluate whether ATF4 silencing would decrease TGF- $\beta$ <sub>1</sub>-enhanced collagen synthesis to investigate the hypothesis that decreased serine-glycine biosynthesis would lead to sub-optimal amino acid levels required for increased protein synthesis. Figure 3.7 shows a total loss of ATF4 protein following siRNA treatment in pHLFs. However, siRNA-mediated loss of ATF4 protein levels led to a substantial decrease in cell count in both TGF- $\beta$ <sub>1</sub>-stimulated and unstimulated cells. As a master regulator of the cellular stress

response, it might not be surprising that loss of ATF4 leads to a reduced capacity of survival in cells grown *in vitro*. There are several cellular stresses which may lead to cell death in siATF4-treated cells as sustained activation of the ISR-eIF2 $\alpha$  axis without resolution has been shown to lead to apoptosis [214]. Growth media changes during the experiment may cause amino acid availability fluctuations, leading to GCN2 activation and eIF2 $\alpha$  phosphorylation. Additionally, oxidative stress and hypoxic pathways are sensed by protein kinase R (PKR) or PERK, two other kinases capable of phosphorylating eIF2 $\alpha$  [215]. It was noticed that confluency could be reached in siATF4 cells if grown for a longer period following siRNA treatment. However, the efficiency in knockdown was uncertain as siRNA is not a permanent knockdown strategy. To solve this issue, pHLFs were gene edited using CRISPR-Cas9 to knockout ATF4 gene expression, an experimental process which takes two weeks to complete. This length of time allowed the crATF4 cells to adapt to not having ATF4 and to reach confluency for the subsequent experiment which showed ATF4 silencing blunted the upregulation in protein levels of PHGDH, PSAT1, PSPH and SHMT2 [81].

#### **4.1.6 Pharmacological inhibition of PHGDH attenuates TGF- $\beta$ <sub>1</sub>-induced collagen I deposition.**

To date, there are no pharmacological tools against ATF4 and thus the role of the serine biosynthetic pathway in TGF- $\beta$ <sub>1</sub>-induced collagen I deposition was interrogated directly using an inhibitor for PHGDH, NCT-503. Treatment with this compound resulted in a complete inhibition of TGF- $\beta$ <sub>1</sub>-induced collagen I deposition. The serine-glycine biosynthetic pathway has multiple metabolite outputs and is in close proximity to glucose and glutamine metabolic pathways. Therefore, the precise mechanism(s) of action of this pathway in supporting TGF- $\beta$ <sub>1</sub>-induced collagen deposition was not identified in this thesis. Recent work in the oncology setting have identified several mechanisms by which PHGDH inhibition has shown promising antiproliferative effects. These include disruption of the biosynthesis of serine, glycine, nucleotides and  $\alpha$ -ketoglutarate [93, 96, 196]. Further experiments are therefore required to identify the precise mechanism involved in NCT-503-treated pHLFs. A recent study has shown PHGDH inhibition causes an unexpected

disruption in the levels of central carbon metabolites, including glycolytic intermediates, TCA cycle intermediates, pentose phosphate pathway intermediates and purine and pyrimidine biosynthesis intermediates [96]. Therefore, a metabolomics approach to encompass these potential changes may provide data to aid in identifying the mechanism(s) of action of NCT-503 in TGF- $\beta_1$ -stimulated pHLFs.

While producing a complete inhibition of TGF- $\beta_1$ -increased collagen I levels at 30 $\mu$ M, the concentration-curve for NCT-503 did not follow the expected concentration-dependent sigmoidal curve with a low Hill coefficient. Instead, the percentage inhibition in TGF- $\beta_1$ -induced collagen by NCT-503 increased from 0% to 100% in the narrow range of 10-30 $\mu$ M, a 3-fold window whereas usual inhibitors replicate this inhibition in 100-fold concentration windows [216]. The inhibitory range, however, is consistent with the cell-free IC<sub>50</sub> value for NCT-503 of 2.5 $\mu$ M, which is generally 10-fold lower than the calculated cell-based IC<sub>50</sub> [98].

There are several potential mechanisms which may lead to steep concentration-response curves. Certain compounds can phase-transition upon passing a concentration threshold which leads to precipitation or colloid formation and may produce non-specific inhibition of a wide-range of enzymes, leading to a sudden inhibition and potentially artefactual conclusion [216]. However, I did not visually detect phase transitioning throughout the experimental process. Additionally, NCT-503 was given at concentrations upwards of 100 $\mu$ M to cancer cell lines in preliminary compound-discovery experiments and this showed differential cytotoxicity depending on high or low PHGDH expression of the cell lines used with no report of phase transitioning. Steep dose-response curves can also be produced when both the concentration of the enzyme and the dissociation constant (K<sub>d</sub>) of the inhibitor are very high or if multi-site binding of the enzyme occurs. The tetrameric nature of PHGDH may well be an unusual characteristic driving this steep response curve as it may require four NCT-503 molecules to inhibit the activity of one PHGDH active unit. Further experiments are merited to confirm the role pharmacological inhibition of PHGDH plays in TGF- $\beta_1$ -induced collagen I deposition. Additionally, 30 $\mu$ M of NCT-503 had no significant effect on unstimulated levels of collagen I, implying that the mechanism of action of this compound is likely through a TGF- $\beta_1$ -specific enzyme,

likely PHGDH. These results highlight the value of concentration curves when assessing new compounds and not simply measuring the effects of one concentration as is very commonly observed in the literature.

NCT-503 decreased *COL1A1* mRNA levels by approximately 50%. This suggests that the effect at the collagen protein level may partly be a consequence of decreased mRNA levels. How inhibition of PHGDH leads to reduced collagen I mRNA levels remains to be elucidated. A possibility exists in a recent study which found significantly decreased levels of the purine and pyrimidine biosynthetic intermediates R5P, IMP and carbamoyl-aspartate following PHGDH inhibition [96]. Therefore, PHGDH inhibition by NCT-503 may influence the global transcriptome by decreasing purine and pyrimidine availability. Furthermore, this effect may be more pronounced when measuring large transcripts whose syntheses may be more impeded by reduced nucleotide levels, such as collagen I.

#### **4.1.7 TGF- $\beta_1$ -increased intracellular glycine levels are mTOR and SHMT2 dependent.**

The data shown in this thesis strongly suggested a TGF- $\beta_1$ -dependent increase in the synthesis of glycine, a major constituent of collagen, via the serine-glycine biosynthetic pathway. Previous amino acid quantification was limited to hydroxyproline, a secondary amino acid which reacts preferentially to the derivatization agent NBD-Cl used for HPLC absorbance detection (see Fig. 3.9-3.10). I therefore optimised the methodology for hydroxyproline detection and quantification to include glycine in addition to the the nonessential amino acids glutamine, glutamate, aspartate, proline and alanine. NBD-Cl is capable of reacting with these primary amino acids but at a slower rate [217]. Therefore, the derivatization time was extended from 20 minutes to 60 minutes. The elution gradient also had to be changed extensively in terms of duration and rate of organic solvent introduction. The polarities of the amino acids except for aspartate and glutamate (which are much more acidic) were very similar and thus would elute at the same time. To counter this, the rate of introduction of the organic buffer was extended from 0-15 minutes to 0-50 minutes, allowing for a slower rate these amino

acids passed through the column. Additionally, the concentration of acetonitrile in the organic buffer was reduced from 8 to 2% to further decrease the rate the derivatized amino acids passed through the C18 column. These changes yielded an appropriate separation of the peaks of these amino acids, which was confirmed through standard curves showing linearity between concentration and peak AUC.

Intracellular glycine levels were then quantified and found to be significantly increased by TGF- $\beta_1$ , which was attenuated by pharmacological inhibition of mTOR using AZD8055 or silencing of SHMT2 using siRNA. This increase in intracellular glycine was replicated in another study performed at the same time in TGF- $\beta_1$ -stimulated HLFs [188]. As SHMT2 protein abundance was found to be reduced with AZD8055 treatment following TGF- $\beta_1$  stimulation, it is likely that the mechanism of action by which mTOR inhibition decreases glycine levels is through diminished SHMT2 protein levels. However, the reduction in intracellular glycine levels with AZD8055 treatment was greater than with siSHMT2 treatment, indicating a further mechanism of action by which mTOR may regulate intracellular glycine levels. A likely mechanism may be glycine uptake through cell surface amino acid transporters. From our RNA sequencing data, the gene expression of a key glycine transporter, *SLC6A9* was found to be TGF- $\beta_1$ -increased and this effect entirely mTOR-dependent (GEO identifier: GSE102674). Additionally, mTOR has been shown to regulate the expression of a host of cell surface amino acid transporters [212, 218].

A surprising finding was that PHGDH silencing did not affect TGF- $\beta_1$ -stimulated intracellular glycine levels. Since *de novo* serine biosynthesis is entirely dependent on the PHGDH/PSAT1/PSPH pathway, this suggested that SHMT2 must use exogenously derived serine to synthesize glycine. However, it is possible that silencing of SHMT2 may lead to expression changes in cell surface glycine transporters and the reduction in intracellular glycine levels may not be due to impairment of *de novo* glycine biosynthesis. To further interrogate this observation, radiolabelling of extracellular serine and glycine could be used to track intracellular levels of these amino acids following siSHMT2 treatment.

Since intracellular glycine levels were unchanged following siPHGDH treatment, this finding further suggests that the PHGDH inhibitor, NCT-503 affects TGF- $\beta_1$ -induced

collagen I deposition through a glycine-independent mechanism as discussed in section 4.1.6.

#### **4.1.8 Potential role for PSAT1 in TGF- $\beta_1$ -induced collagen synthesis.**

This thesis revealed a key role for PSAT1 in TGF- $\beta_1$ -increased collagen I synthesis. The failure to rescue siPSAT1-inhibited TGF- $\beta_1$ -induced collagen levels by exogenous addition of the products of the serine biosynthetic pathway indicates that PSAT1 supports TGF- $\beta_1$ -enhanced collagen synthesis via a serine-independent mechanism. However, it is worth noting that intracellular levels of serine and glycine were not measured in siPSAT-treated cells following exogenous addition of these two amino acids. Therefore, it remains to be confirmed if supplementing the media with these amino acids leads to a subsequent increase in their intracellular levels. The modulated form of  $\alpha$ -ketoglutarate used in supplementation experiments contains two methyl groups which highly increases its cell permeability and has been shown to rescue  $\alpha$ -ketoglutarate-impaired processes in several studies at a concentration of 4mM [219-221].

Whilst unanticipated, the seemingly unique role of PSAT1 and its serine-independent function(s) have been recently observed in several other contexts. Independent of its enzymatic functions, PSAT1 was shown to impact on cell cycle progression via regulating cyclin D1 and retinoblastoma protein (Rb) levels in three independent studies performed in NSCLC cells, oestrogen receptor (ER)-negative breast cancer cells and colorectal cancer cells [99, 101, 222]. Therefore, it is possible that no metabolite combination may rescue an impairment in cell cycle progression induced by PSAT1 silencing which may be having a role in regulating TGF- $\beta_1$ -induced collagen I synthesis. Additionally, a similar study concluded that the mechanism of action of siPSAT1 on TGF- $\beta_1$ -stimulated HLFs was through glycine generation as  $C^{13}$  from radiolabelled glucose was found in collagen I [188]. However, the data presented in this thesis shows that when PHGDH is silenced, pHLFs are still able to synthesize glycine, likely through increased consumption of extracellular serine which is then cleaved by SHMT2, whose knockdown reduced glycine levels.

Therefore, the mechanism of action of siPSAT1 in the context of TGF- $\beta$ <sub>1</sub>-induced collagen I synthesis remains to be determined. Understanding the impact of PSAT1 silencing on the metabolome would further help clarify the role this enzyme plays outside of the serine biosynthetic pathway.

## **4.2 Effect of extracellular serine, glycine, glucose and glutamine on TGF- $\beta$ <sub>1</sub>-induced collagen I deposition.**

### **4.2.1 Introduction.**

The biomolecular requirements for pHLFs to mount a TGF- $\beta$ <sub>1</sub>-enhanced collagen response are far from understood. The previous section discussed the likelihood that TGF- $\beta$ <sub>1</sub> modulated the intracellular levels of glycine, an amino acid whose synthesis is dependent on serine which, in turn, is dependent on glucose and glutamine for its synthesis. The therapeutic approach of limiting the availability of specific metabolites is well documented in the oncology setting. Intravenous administration of the enzyme asparaginase, which depletes serum asparagine levels, is a highly effective treatment in acute lymphoblastic leukaemia (ALL), increasing 9.4-year survival from 31% to 71%. Therefore, understanding the metabolic requirements for pHLFs to synthesize TGF- $\beta$ <sub>1</sub>-induced levels of ECM components may provide insight into similar therapeutic approaches. The next step in this thesis was to further investigate the potential role the extracellular metabolites involved in *de novo* serine and glycine biosynthesis (serine, glycine, glutamine and glucose) play in mediating TGF- $\beta$ <sub>1</sub>-induced collagen I deposition.

### **4.2.2 Extracellular glycine is required for a full TGF- $\beta$ <sub>1</sub>-induced collagen I response.**

Figures 3.15-3.16 showed a full TGF- $\beta$ <sub>1</sub>-enhanced collagen I response when the media contained at least 200 $\mu$ M glycine. Removal of glycine from the media led to a significant decrease in TGF- $\beta$ <sub>1</sub>-induced collagen deposition. However, the media contained 0.4% FBS which was not dialyzed and thus was not completely void of glycine and may have softened the reduction in collagen deposition measured.

Extracellular serine in the media was dispensable for TGF- $\beta_1$ -induced collagen I deposition if glycine was present. This was a surprising observation given that serine can generate glycine. However, as serine is synthesized first via the *de novo* pathway, a portion of the intracellular pool must be lost for *de novo* glycine synthesis via SHMT2 (see figure 3.12). Therefore, the presence of glycine in the media may allow for a retained intracellular serine pool and additionally allow the cells a metabolic shortcut bypassing PHGDH, PSAT1 and PSPH if the role of the pathway for TGF- $\beta_1$ -induced collagen deposition is for glycine synthesis.

The observation that pHLFs can mount a TGF- $\beta_1$ -enhanced collagen I response when grown in media containing glycine and not serine seemingly contradicts findings of consumption of these two amino acids in cancer cells [223, 224]. CRC cell proliferation was shown to be decreased when these cells are grown in media lacking serine, as the capacity for *de novo* serine synthesis was not sufficient for cell growth and glycine was generated from serine which lost one-carbon units and therefore reduced nucleotide levels [225]. However, there is a recent contradictory study showing a preference for glycine consumption in cancer cells to support nucleotide biosynthesis and cell growth [224]. Additionally, TGF- $\beta_1$ -stimulated pHLFs may not face the same high bioenergetic and biomolecular requirements as cancer cells to produce collagen I. Furthermore, TGF- $\beta_1$  was shown in this thesis to upregulate the expression of the serine biosynthetic pathway and therefore it is possible that pHLFs rely solely on *de novo* serine biosynthesis to support collagen I synthesis.

Together, these results show that extracellular glycine and not serine is required for supporting TGF- $\beta_1$ -induced collagen I synthesis.

#### **4.2.3 Role of extracellular glutamine and glucose in TGF- $\beta_1$ -induced collagen I deposition.**

The serine-glycine biosynthetic axis is dependent on both glucose for the initiating glycolytic intermediate, 3-PG and glutamine which provides the amino group to synthesize phosphoserine. The concentration of these two nutrients vary greatly between media compositions ranging from 0.6-2 mM glutamine and 5-25 mM

glucose. Glucose and glutamine are important carbon sources and support biomolecular and bioenergetic pathways in the cell. Glutamine is additionally a source of nitrogen, able to support nucleotide and nonessential amino acid synthesis. Therefore, it can be speculated that glutamine may compensate for glucose withdrawal to allow pHLFs to synthesize TGF- $\beta_1$ -induced collagen I levels. As the measured output of collagen I deposition is largely dependent on protein synthesis, it is possible that glutamine, which is required in the synthesis of nonessential amino acids, contributes greater to polypeptide synthesis than glucose by maintaining the appropriate levels of amino acids required for TGF- $\beta_1$ -induced collagen synthesis. These findings would agree with a recent flux balance analysis showing that glutamine is as important as glucose for supporting cell proliferation and energy production in the context of cancer cell proliferation [226].

Extracellular glutamine was found to be critical for TGF- $\beta_1$ -induced collagen I deposition, suggesting a critical role for glutamine metabolism in supporting enhanced collagen synthesis. Cells were only able to mount a TGF- $\beta_1$  collagen I response in the absence of glutamine if glucose concentrations reached 25 mM, which are well above the normal physiological range for glucose in circulation (4.4-6.1 mM) [227]. This result suggested that excessive amounts of glucose may lead to the synthesis of certain metabolites normally dependent on glutamine which are required for TGF- $\beta_1$ -induced collagen I synthesis. However, the consequences of supraphysiological glucose may be more wide-ranging than just metabolomic effects as glucose is a regulator of mTORC1, a critical kinase for TGF- $\beta_1$ -induced transcriptional changes [30, 228].

Figure 3.17 shows that pHLFs grown in media containing supraphysiological levels of glucose (25 mM) and glutamine (2 mM) had significantly higher resting levels of glutamine, glutamate and proline. Additionally, these resting amino acid levels were similar to those measured in pHLFs grown in physiological media containing 5mM glucose and 0.7 mM glutamine. A recent study reported that glucose concentrations impacted on glutamine metabolism via modulating the expression of SIRT4, a negative regulator of glutamine metabolism [229]. Therefore, in supraphysiological media, pHLFs may exhibit reduced SIRT4 expression and heightened glutamine metabolism, as evidenced by higher intracellular glutamate and proline levels.

Additionally, supraphysiological glutamine concentrations may simply promote a heightened synthetic rate of glutamine-dependent amino acids such as glutamate and proline. This may be evidenced by the retained intracellular pool of glutamine in cells grown in supraphysiological media in both TGF- $\beta_1$ -stimulated and unstimulated cells. Moreover, the significant decrease in intracellular glutamine levels (see Fig 3.17A) following TGF- $\beta_1$  stimulation in physiological media was observed in similar human lung fibroblast studies [186, 187] but not in a study which used DMEM with 25mM glucose and 6mM glutamine [188].

In the work presented in this thesis, intracellular glycine levels were found to be consistent in both DMEM compositions, supporting that increased glutamine and glucose availability does not drive increased *de novo* glycine synthesis. Additionally, the concentration of extracellular glycine and serine are fixed between the two medias (400  $\mu$ M for both) which may further decrease the influence of glucose and glutamine in the intracellular levels of glycine.

In summary, glutamine is a critical component in growth media for TGF- $\beta_1$ -induced collagen I deposition and its metabolic pathways may represent potential targets for therapeutic intervention.

## **4.3 Role of glutamine metabolism in TGF- $\beta$ <sub>1</sub>-induced pro-fibrotic parameters.**

### **4.3.1 Introduction.**

Investigations into the role of glutamine metabolism in the pro-fibrotic functions of TGF- $\beta$ <sub>1</sub> in HLFs are recent and limited in numbers. In tandem with this thesis, data highlighted critical roles for glutamine-derived nonessential amino acids and the anaplerotic substrate  $\alpha$ -ketoglutarate in mediating collagen synthesis. However, the roles of these metabolites and the role of glutamine metabolism in TGF- $\beta$ <sub>1</sub> signalling remain unclear. Competing conclusions have been drawn on the function of glutamine metabolism in supporting TGF- $\beta$ <sub>1</sub>-induced collagen synthesis and these discrepancies may be explained by differences in media compositions, which vary among laboratories. As highlighted in the previous section, glucose and glutamine are often present at non-physiological concentrations and their impact on intracellular metabolic networks is increasingly becoming apparent. A strength of the work presented in this thesis in terms of translational potential is that all experiments were performed using primary cells which were cultured in physiological concentrations of glucose and glutamine.

### **4.3.2 TGF- $\beta$ <sub>1</sub> increases extracellular glutamine depletion and glutamine transporter gene expression in pHLFs.**

The work presented in section 3.2 of this thesis highlighted the important role of extracellular glutamine in supporting TGF- $\beta$ <sub>1</sub>-enhanced collagen I deposition. To further investigate the pro-fibrotic functions of glutamine in pHLFs, extracellular glutamine concentrations were measured over a time-course using the HPLC amino acid quantification methodology described in section 4.1.7. This experiment showed TGF- $\beta$ <sub>1</sub> increased the rate of depletion of extracellular glutamine compared to unstimulated cells. This finding coupled with the intracellular glutamine and glutamate data shown in figure 3.17 supported the notion of TGF- $\beta$ <sub>1</sub>-enhanced glutamine metabolism, whereby increased glutamine consumption did not lead to

increase intracellular glutamine levels as these were likely rapidly metabolised to glutamate, which was increased by TGF- $\beta_1$ . These observations are frequently observed in cancer cells, which are referred to as being 'glutamine addicted' due to their high glutamine consumption and generation of glutamine-derived metabolites, such as glutamate [230]. There are many similarities between cancerous and fibrotic processes, possibly due to the increased demand for protein synthesis where one supports growth and proliferation (cancer) and the other ECM component synthesis (fibrosis). Cancer cells have been shown to have increased expression of glutamine transporters, such as SLC1A5, to mediate their enhanced consumption of glutamine [231]. Other transporters known to facilitate the import of extracellular glutamine include SLC38A1, SLC38A2 and SLC38A5 [232-234]. In the work presented in this thesis, the mRNA levels of all these transporters but SLC38A2 were significantly up-regulated at 24 hours post-TGF- $\beta_1$  stimulation.

These results suggested that glutamine consumption was enhanced by TGF- $\beta_1$ -modulation of the transporters *SLC1A5*, *SLC38A1* and *SLC38A5* and further experiments aimed at decoupling the contribution to the intracellular glutamine pool of these individual transporters would aid in answering this possibility.

#### **4.3.3 TGF- $\beta_1$ increases the expression of the glutaminolysis pathway.**

The previous section strongly suggested that under TGF- $\beta_1$ , pHLFs glutamine uptake was increased and its catabolism to produce glutamate was also increased. This reaction is predominantly facilitated by GLS1, which is the first enzyme in glutaminolysis and is overexpressed in many cancers and its expression correlates with increased mortality [235]. As GLUL facilitates the inverse reaction of assimilating ammonia and glutamate to synthesize glutamine, it is interesting that TGF- $\beta_1$  upregulated GLS1 expression and downregulated GLUL expression, potentially skewing the pathway more towards glutaminolysis. Furthermore, these changes were found at 3 hours following TGF- $\beta_1$  stimulation at the mRNA level, suggesting an early need for glutaminolysis to support the end-functions of TGF- $\beta_1$  signalling and a potential role for the canonical early Smad proteins in regulating

*GLS1* and *GLUL* mRNA levels. Recent work indeed showed an inhibition of TGF- $\beta_1$ -induced GLS1 protein levels when Smad3 was silenced in HLFs [186]. However, this was measured at 48 hours following TGF- $\beta_1$  stimulation and thus it is not known if a secondary Smad3-dependent factor leads to the upregulation in *GLS1* gene expression at 3 hours in the present study. A recent study additionally measured TGF- $\beta_1$ -induced GLS1 mRNA levels over a time-course but did not report a significant increase at 3 hours [236]. However, this experiment was performed in AKR-2B cells and data using pHLFs showed a TGF- $\beta_1$ -induced increase in GLS1 but at 24 hours. This study furthermore describes a TGF- $\beta_1$ -induced downregulation of SIRT7 via increased FOXO4 acetylation which negatively regulates GLS1 expression. This decrease in SIRT7, however, was only observed at 9 hours following TGF- $\beta_1$  stimulation and may therefore not explain the mechanism by which GLS1 gene expression is increased at 3 hours in the present study. Additionally, two studies using the PI3K inhibitor, LY294002 have shown GLS1 and, in reference to previous sections, PHGDH, PSAT1 and ATF4 expression to be PI3K-dependent [211, 236]. However, as a first generation PI3K inhibitor, LY294002 has shown specificity for other kinases, particularly mTOR [237]. LY294002 was used at 20 $\mu$ M to show PI3K-dependent GLS1 expression, a concentration within the IC<sub>50</sub> range for mTOR kinase function (1-30 $\mu$ M) [238]. Therefore, the role of the PI3K/mTOR pathway in regulating GLS1 expression requires further investigation.

The data reported here shows that TGF- $\beta_1$  increased GPT2 but decreased GLUD1 and GOT2 expression, three mitochondrial enzymes which compete for the same substrate, glutamate. The decrease in GOT2 may also help explain the increase in GOT1, the cytosolic aspartate aminotransferase to cover the biosynthesis of aspartate for the cell. Therefore, it is tempting to speculate that the decrease in GLUD1 and GOT2 expression may allow for an increased pool of glutamate for GPT2 by reducing other glutamate-utilizing enzymes. These expression profiles have also been linked to those in proliferating cells, where aminotransferases such as GPT2 and GOT1 are upregulated but GOT2 is downregulated [163]. GPT2 is the main enzyme responsible for *de novo* alanine biosynthesis and has been shown to promote cancer growth through its  $\alpha$ -ketoglutarate consuming and generating functions [159, 160]. Whilst the temporal expression profiles of these enzymes would suggest GLS1-derived glutamate is preferentially used by GPT2 to synthesize

alanine and  $\alpha$ -ketoglutarate, enzyme kinetic assays would have to be performed to evaluate this further.

#### **4.3.4 TGF- $\beta$ <sub>1</sub>-induced GLS1-derived glutamate is critical for enhanced collagen I deposition.**

During the course of this PhD, the critical role of GLS1 in TGF- $\beta$ <sub>1</sub>-induced collagen synthesis has been reported in several studies and inhibition of GLS1 shown to reduce bleomycin-induced lung fibrosis in mouse models [155]. The data presented in this thesis describe a potential compensatory mechanism where  $\alpha$ -ketoglutarate supplementation to GLS1-inhibited cells using CB-839 led to regenerated TGF- $\beta$ <sub>1</sub>-induced intracellular glutamate levels (Fig. 3.26). This highlights the plastic nature of metabolism and the need to fully consider the impact of a rescue metabolite on the levels of other metabolites which may in turn be lead to the observed phenotype. Indeed, a lung fibrosis study concluded that  $\alpha$ -ketoglutarate generation via GLS1 was the mechanism of action TGF- $\beta$ <sub>1</sub> employed to increase the expression of the anti-apoptotic protein survivin and XIAP [239]. However, this rescue effect may be due to increased glutamate levels which can have global cellular effects due to its many functions, such as glutathione and nonessential amino acid synthesis. Furthermore, another lung fibrosis study showed  $\alpha$ -ketoglutarate supplementation increased collagen I abundance in unstimulated HLFs and concluded it was linked to the role  $\alpha$ -ketoglutarate plays in proline hydroxylation, which is critical for collagen polypeptide stability [187]. Whilst this is possible, it does not rule out accessory functions of glutamate, such as proline synthesis, which is in itself critical for collagen I synthesis, particularly when these cells are entirely reliant on *de novo* synthesis of proline when grown in DMEM. Additionally, this thesis shows collagen I deposition was not significantly increased at any concentration of  $\alpha$ -ketoglutarate examined. The differing results of  $\alpha$ -ketoglutarate treatment modulating collagen I synthesis in unstimulated fibroblasts could be explained by the different approaches taken to quantify collagen I. The reported study measured intracellular collagen using immunoblotting which does not capture crucial post-translational modifications and secretion mechanisms that the immunofluorescence and macromolecular crowding assay employed by this study captures. This suggests that whilst  $\alpha$ -ketoglutarate

supplementation may increase collagen I peptide abundance, this is not reflected extracellularly following cross-linking and deposition.

Previous studies have shown GLUD1 as a chief enzyme for  $\alpha$ -ketoglutarate generation in cancer cells and this deamination reaction of glutamate is reversible and dependent on substrate concentrations [240]. Therefore, it is possible that GLUD1 facilitates the regeneration of glutamate following  $\alpha$ -ketoglutarate supplementation to GLS1-inhibited pHLFs. Other mechanisms for glutamate regeneration involve the aminotransferases, though this would consume intracellular supplies of aspartate and alanine which are not found in the media. GLUD1 silencing and pharmacological inhibition both failed to attenuate TGF- $\beta_1$ -induced collagen I deposition. Therefore, if  $\alpha$ -ketoglutarate generation is a requirement for TGF- $\beta_1$ -induced collagen synthesis then it may be facilitated by the aminotransferases during GLUD1 inhibition. Furthermore, the dispensable role for GLUD1 in TGF- $\beta_1$ -stimulated collagen synthesis has been shown in a recent study using siRNA silencing [188]. In the data presented in this thesis, pharmacological inhibition of GLUD1 with the small-molecule inhibitor, R162 showed a significant increase in both unstimulated and stimulated collagen I deposition at a concentration of 100 $\mu$ M. The immunoblotting data from figure 3.33 shows GLUD1 protein abundance is decreased with TGF- $\beta_1$ . Therefore, decreasing GLUD1 activity may promote pro-fibrotic effects independently of TGF- $\beta_1$  stimulation by decreasing a glutamate-consuming process and increasing glutamate levels for proline and alanine synthesis. R162 treatment in TGF- $\beta_1$ -stimulated cells may further compound the decreased expression of GLUD1 and lead to even higher mitochondrial glutamate abundance.

Together, the data presented highlights a critical role for TGF- $\beta_1$ -induced GLS1-derived glutamate in supporting enhanced collagen I deposition.

#### **4.3.5 Alanine is conditionally essential for TGF- $\beta_1$ -induced collagen I deposition.**

To further understand the rescue to collagen I deposition of  $\alpha$ -ketoglutarate supplementation to GLS1-inhibited and TGF- $\beta_1$ -stimulated pHLFs (see Fig. 3.26), the intracellular levels of the three amino acids whose biosynthesis is dependent on

mitochondrial glutamate (aspartate, alanine and proline) were measured. Supplementation with  $\alpha$ -ketoglutarate not only regenerated intracellular glutamate levels but also those of alanine and proline. Together, these three amino acids make up approximately 33% of the collagen I polypeptide (glutamate: 5%; alanine: 10%; proline: 18%) and highlight the need for tracing experiments when attempting to establish mechanisms of action of metabolites [241]. Similarly, addition of exogenous alanine, which rescued GLS1-inhibited TGF- $\beta$ <sub>1</sub>-induced collagen I deposition levels, increased intracellular proline levels. Whilst tracing studies would effectively show how alanine supplementation leads to increased proline levels, it is likely that alanine is deaminated by GPT2 to produce glutamate, which can then feed into *de novo* proline biosynthesis. In a HLFs study, it was found that the incorporation of glutamine-derived carbon into proline was increased nearly 7-fold by TGF- $\beta$ <sub>1</sub>, highlighting proline biosynthesis as a major destination of glutaminolysis [170]. Glutamate-dependent proline biosynthesis has also been shown to be critical for TGF- $\beta$ <sub>1</sub>-induced collagen synthesis and therefore the supply of alanine-derived glutamate may be sufficient to mount a full TGF- $\beta$ <sub>1</sub> collagen response [188].

In contrast, intracellular aspartate levels were not changed significantly by TGF- $\beta$ <sub>1</sub> stimulation. Whilst aspartate levels were severely reduced following GLS1 inhibition, these levels were not rescued by  $\alpha$ -ketoglutarate supplementation. This suggests that GOT1/2 regulate intracellular aspartate levels using GLS1-derived glutamate but under the collagen rescue conditions induced by  $\alpha$ -ketoglutarate supplementation, the regenerated glutamate may not lead back to aspartate synthesis. This may be explained by the different oxoacid substrates used by GPT2 and GOT2, with the former using more readily available pyruvate and the latter using oxaloacetate which is necessary for the first step in the TCA cycle through its condensation with acetyl-coA to form citrate. Oxidative phosphorylation and TCA cycle intermediates have been shown to be increased by TGF- $\beta$ <sub>1</sub> in HLFs, suggesting a higher activity rate for the TCA cycle and thus a potentially limiting availability of oxaloacetate for aspartate synthesis [81, 186]. Additionally, figure 3.30 showed no significant increase in aspartate levels with TGF- $\beta$ <sub>1</sub> at 48 hours, suggesting that increased aspartate biosynthesis may not be a requirement for TGF- $\beta$ <sub>1</sub>-induced collagen I deposition.

The data in this thesis show for the first time that TGF- $\beta_1$  increases intracellular alanine levels, an effect dependent on GPT2 activity. It further demonstrates that silencing of GPT2 attenuates TGF- $\beta_1$ -induced collagen synthesis, an effect rescued by exogenous supplementation of alanine. Interestingly, a study also investigated the effect of siGPT2 on collagen I protein abundance and found no changes on TGF- $\beta_1$ -induced collagen I abundance [188]. In addition to the collagen quantification techniques being different as described in the previous section, cells were also grown in different medias. The study used DMEM with 25mM glucose, 6mM glutamine and 1mM pyruvate. In reference to the discussion in section 4.2.3, it is likely that under these supraphysiological conditions, intracellular alanine levels were already at the concentration required to rescue GPT2 silencing. Therefore, silencing of GPT2 may not have enough time to produce an effect on collagen synthesis as alanine abundance remained sufficient. Additionally, data from this thesis showed that pyruvate supplementation was enough to produce a significant alleviation in siGPT2-inhibited collagen levels (see Fig 3.35) and may therefore further allow the HLFs in this study to cope with silencing of GPT2. How pyruvate supplementation can produce a moderate rescue of TGF- $\beta_1$ -induced collagen synthesis in siGPT2 pHLFs remains to be elucidated. It is possible that in the course of collagen synthesis the functional role of GPT2 may change to consume alanine for pyruvate generation. Additionally, pyruvate was supplemented at 1mM which is nearly 30-fold higher than what is physiologically available in the blood and may therefore increase the kinetic rate of remaining GPT2 enzymes through excess substrate availability and lead to increased alanine synthesis [242]. However, this is quite speculative and understanding the metabolomic effect of GPT2 silencing would help better understand this effect.

In summary, GPT2 is essential for collagen synthesis in cells growing in an environment with limited alanine availability. At the end of this thesis, a study was published which identified GPT2 as a conditionally essential gene for cancer cells through its alanine-generating function which was shown to support protein synthesis and cell growth under conditions of extracellular alanine restriction [243]. In the data presented in this thesis, TGF- $\beta_1$  maintained its upregulation of GPT2 protein levels even in the presence of extracellular alanine, indicating GPT2 is intrinsically tied to the TGF- $\beta_1$  signalling program. As a therapy, regionally blocking alanine

biosynthesis in fibrotic lungs via GPT2 inhibition may effectively starve fibroblasts of a key amino acid required for synthesizing collagen. While alanine is highly present in the blood, there is evidence that the extensive ECM present in fibrotic diseases such as in fibroblastic foci impedes tissue perfusion thereby potentially reducing myofibroblast access to blood components [244]. However, whether an increased density of ECM in the fibrotic lung alters alanine availability is unknown and amino acid labelling studies in a bleomycin-induced lung fibrosis mouse model may aid in further understanding this. It is therefore possible to consider a therapeutic approach targeting alanine biosynthesis localised to the lung which, in partnership with a potential inaccessibility to serum alanine may limit the synthetic capacity of these cells to produce the excessive amounts of collagen driven TGF- $\beta_1$  stimulation. Furthermore, there may be structural similarities between dense fibroblastic foci found in IPF and a developing tumour, both of which may be poorly perfused and have differential availability of blood nutrients. The concept of 'metabolic zonation' is well established in the oncology setting and describes spatial cellular metabolic heterogeneity in a tumour as a function of its proximity to a blood vessel [245, 246]. A recent study found intracellular levels of the essential amino acid leucine were lower the further the cell was from the vasculature [247]. As leucine cannot be synthesized and can only be sourced from the blood, it may act as a proxy marker for perfusion status in certain cases. In IPF, fibroblastic foci have been shown to push alveolar capillaries by approximately 100 $\mu$ m in their development and have been observed to display increased hypoxic markers, possibly an indication of reduced oxygenation as a result of blood vessel distance [244, 248]. Therefore, the case for targeting GPT2 in the disease setting may yield beneficial therapeutic effects as the extracellular and reliable supply of serum alanine has not been investigated. Additionally, GPT2 inhibition has been shown to be synergistic with GLS1 inhibition in NSCLC models, which highlights the compensatory nature of GPT2-derived glutamate (utilizing extracellular alanine) under GLS1-inhibited conditions [249]. Therefore, dual targeting of the glutaminolysis pathway may yield prominent anti-fibrotic effects by depriving myofibroblasts of the metabolites necessary for excessive ECM component synthesis.

#### **4.3.6 Alanine modulates TGF- $\beta$ <sub>1</sub>-induced mTORC1 activation via a Rags-independent mechanism.**

In the data presented in this thesis, the GPT2 inhibitor, AOAA, reduced intracellular alanine to undetectable levels in both TGF- $\beta$ <sub>1</sub>-stimulated and unstimulated pHLFs. AOAA further showed a complete inhibition of TGF- $\beta$ <sub>1</sub>-induced 4E-BP1<sup>S65</sup> phosphorylation, an effect rescuable by alanine supplementation (see Fig 3.38). This was a surprising rescue result as AOAA is an inhibitor for vitamin B<sub>6</sub>/PLP-dependent reactions which are involved in the biosynthesis of a host of amino acids including serine, glycine, aspartate and glutamate [250]. Therefore, the sole addition of alanine producing a complete rescue highlights its unique role in mediating mTORC1 activity following TGF- $\beta$ <sub>1</sub> stimulation. Furthermore, dual silencing of GOT1 and GOT2 which are the sole enzymes capable of synthesizing aspartate (an amino acid also not present extracellularly) had no effect on TGF- $\beta$ <sub>1</sub>-induced mTORC1 activation, further highlighting the unique role of GPT2 in regulating mTORC1 activity. Amino acids like leucine and glutamine have been shown to impact on mTORC1 activity in various cell types, yet other amino acids have failed to show as strong of a modulation, with alanine being described as a priming amino acid for mTORC1 activation [251]. A very recent paper was the first to demonstrate that GPT2 knockout breast cancer cells have impaired mTORC1 activity via assessing phosphorylation of P70-S6K [252]. This study further showed that GPT2-KO cells have increased autophagy, an effect induced by reduced mTORC1 activity and as a potential mechanism to overcome the limitations in alanine levels.

The classical mechanism for amino acid sensing by mTORC1 involves the Rag-GTPases which interact with various distinct amino acid-binding proteins [253]. As dual siRNA-mediated silencing of RagA and RagB produced no decrease in TGF- $\beta$ <sub>1</sub>-induced 4E-BP1<sup>S65</sup> phosphorylation, it may be possible that alanine does not use the Rags to signal to mTORC1. However, complete loss of protein abundance of both RagA or RagB was not achieved and therefore the possibility remains that the unaffected protein levels may be sufficient to facilitate mTORC1 activation. A study showed that alanine addition following amino acid starvation was able to activate previously inhibited levels of pS6K, an effect prevented by RagA/RagB-KO [254]. This study showed that only glutamine and asparagine were able to activate

mTORC1 in RagA/RagB-KO cells, describing a Rags-independent amino acid sensing mechanism. However, as glutamine can lead to *de novo* alanine synthesis, it is unknown whether dual alanine and glutamine are required for this effect and therefore whether sole alanine supplementation is a valid experimental approach to investigating its Rags-dependency or not. Measuring TGF- $\beta_1$ -induced mTORC1 activation following alanine supplementation in pHLFs treated with siRNA for GPT2, RagA and RagB would help further understand how alanine levels are sensed by mTORC1.

In summary, the data presented in this thesis identify GPT2 as a conditionally essential gene for TGF- $\beta_1$ -induced collagen synthesis via its alanine-synthesizing function. Furthermore, GPT2-derived alanine is critical for TGF- $\beta_1$ -induced mTORC1 activation in conditions of extracellular alanine restriction.

#### **4.3.7 Aminotransferase-derived $\alpha$ -ketoglutarate and nonessential amino acids are both required for TGF- $\beta_1$ -induced collagen I deposition.**

The data presented in figure 3.29 showed that  $\alpha$ -ketoglutarate was a critical output for glutaminolysis due to its effect in regenerating glutamate levels and leading to a rescue in CB-839-attenuated collagen I levels. This regenerative event may be facilitated via the aminotransferases or GLUD1, which use  $\alpha$ -ketoglutarate for glutamate synthesis, and vice versa. Interestingly, it is likely that both  $\alpha$ -ketoglutarate and nonessential amino acids are critical outputs of glutaminolysis for supporting TGF- $\beta_1$ -induced collagen synthesis (see Fig. 3.43). In aminotransferase-inhibited cells via AOAA, however, the rescue effect of  $\alpha$ -ketoglutarate can be more conclusive as most of the metabolic pathways utilizing  $\alpha$ -ketoglutarate are inhibited. If glutamate regeneration in this instance was a rescuing event, then the addition of nonessential amino acids without  $\alpha$ -ketoglutarate should have rescued AOAA-inhibited levels of TGF- $\beta_1$ -induced collagen I deposition, which it did not. Other  $\alpha$ -ketoglutarate-utilizing pathways are less metabolically flexible, such as its role in demethylation, hydroxylation or the TCA cycle, all of which convert  $\alpha$ -ketoglutarate to succinate. A recent study, however, showed that silencing of the enzyme which

converts  $\alpha$ -ketoglutarate to succinate in the TCA cycle,  $\alpha$ -ketoglutarate dehydrogenase ( $\alpha$ KDH), had no impact on TGF- $\beta_1$ -induced collagen I abundance [188]. It is therefore a likely possibility that the rescuing effect of  $\alpha$ -ketoglutarate on collagen I deposition are not through its TCA cycle functions but through hydroxylation of the proline residues of collagen which is critical for quaternary structure stabilisation and secretion. As such, it may be even more appropriate to adopt quantification techniques for collagen past this crucial processing stage to fully capture the potential impact on collagen deposition that  $\alpha$ -ketoglutarate may be having.

As a weak acid,  $\alpha$ -ketoglutarate is found in low concentrations in the blood of around  $7\mu\text{M}$  [242]. This is several orders of magnitude lower than the  $4\text{mM}$  of  $\alpha$ -ketoglutarate required to rescue the antifibrotic effects of AOAA and therefore endogenous rescuing from blood availability of a potential aminotransferase inhibition strategy for an antifibrotic therapy would not be expected. Furthermore, targeting the TGF- $\beta_1$ -specific mechanism which leads to the  $\alpha$ -ketoglutarate levels required for proline hydroxylation may avoid potential systemic effects of targeting all collagen prolyl hydroxylases. The levels of  $\alpha$ -ketoglutarate have been shown to be increased by TGF- $\beta_1$  in HLFs and measuring its levels following silencing of specific aminotransferases may yield promising results for therapies in helping to identify the pathways leading to this increase [187].

Very recently, the antifibrotic effects of AOAA on TGF- $\beta_1$ -induced collagen I synthesis *in vitro* were reported by a group [188]. This study suggested the mechanism of action of AOAA in regulating TGF- $\beta_1$ -induced collagen I synthesis was through its targeting of PSAT1, which the researchers had identified previously in connection to enhanced glycine biosynthesis in lung fibrosis. The data presented in this thesis, however, may not fully agree with this analysis given that the effects on collagen I synthesis of AOAA were not able to be rescued with glycine and serine supplementation. Additionally, AOAA was rescued with  $\alpha$ -ketoglutarate and nonessential amino acids supplementation but these same conditions did not alter siPSAT1-treated collagen levels. To date, data on the specificity of AOAA to PSAT1 was not found yet if AOAA does effectively inhibit PSAT1, the data presented in this thesis suggest an enzyme-independent function of PSAT1 for TGF- $\beta_1$ -induced

collagen synthesis. Interestingly, a recent study found that PSAT1 promoted metastasis in lung cancer cells via a non-enzymatic modulation of IFN- $\gamma$ /IRF1 signalling [100]. Non-enzymatic functions of metabolic enzymes, or moonlighting functions, are well described in the literature and it may be possible that PSAT1 regulates TGF- $\beta_1$ -induced collagen synthesis via a non-serine biosynthesis pathway function [255]. Further understanding the amino acid requirements for rescuing AOAA-inhibited collagen I levels and the disconnect seen in PSAT1 silencing (see Fig. 3.13) and pharmacological inhibition (see Fig. 3.43) would help elucidate the chokepoints in these metabolic pathways and help lead to more specific target identification for fibrotic therapies.

As a standalone therapy, AOAA may not be suitable as a treatment for lung fibrosis or any fibrotic conditions due to its global inhibition of aminotransferases, which make up nearly 4% of all classified metabolic reactions [256]. Furthermore, a study into AOAA as a treatment for Huntington disease found it induced toxic symptoms in all patients which caused a premature end to the trial [257]. Therefore, further understanding the mechanism of action of AOAA in TGF- $\beta_1$ -induced collagen synthesis would help lead to the identification of potentially more promising and specific targets.

## 4.4 Conclusion.

This thesis examined the hypothesis that the changes in amino acid metabolism induced by TGF- $\beta_1$  are required for primary human lung fibroblasts to synthesize TGF- $\beta_1$ -induced levels of collagen. The work presented herein reports that the metabolic pathways for serine, glutamine, alanine and  $\alpha$ -ketoglutarate are critical for TGF- $\beta_1$ -induced collagen I deposition.

The present study supports a model (Figure 4.1) whereby TGF- $\beta_1$  upregulates the expression of serine, glycine and glutamine metabolic pathways which are critical for TGF- $\beta_1$ -induced collagen synthesis. TGF- $\beta_1$ -induced ATF4 is post-transcriptionally regulated by mTORC1 and regulates the expression of the serine-glycine biosynthetic axis, particularly PSAT1 which is required for TGF- $\beta_1$ -enhanced

collagen synthesis independent of its enzymatic function. TGF- $\beta_1$  increases consumption of glutamate and synthesis of glutamate, which is used by aminotransferases to provide nonessential amino acids and  $\alpha$ -ketoglutarate which support enhanced collagen synthesis. Alanine, synthesized by the aminotransferase GPT2, is critical for TGF- $\beta_1$ -enhanced collagen synthesis and TGF- $\beta_1$ -induced mTORC1 activation via a Rags-independent mechanism.

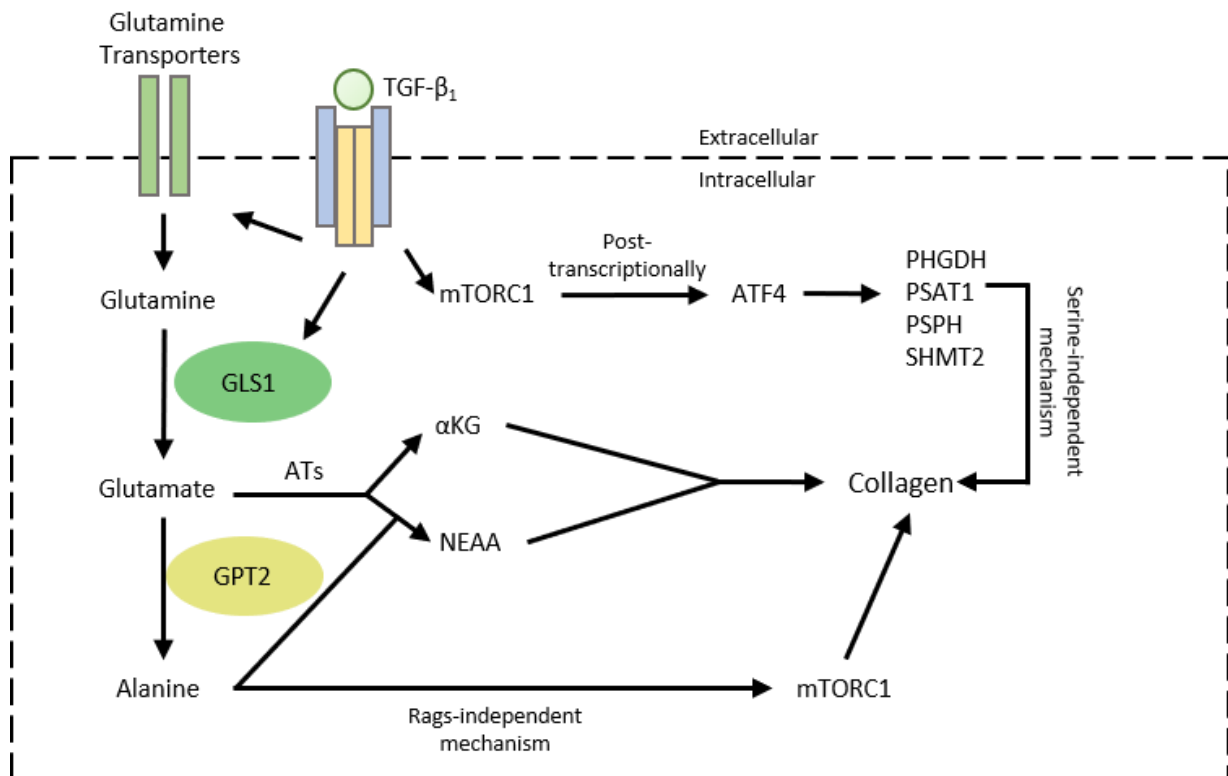


**Figure 4. 1. Proposed mechanism by which TGF- $\beta_1$  regulates collagen synthesis via metabolic pathways.**

The present study suggests that TGF- $\beta_1$  enhances the expression of glutamine transporters which leads to increased glutamine uptake. Glutaminase 1 (GLS1)-derived glutamate from glutamine supports  $\alpha$ -ketoglutarate ( $\alpha$ -KG) and nonessential amino acid (NEAA) synthesis via the aminotransferases (ATs) which is required for TGF- $\beta_1$ -induced collagen synthesis. One of these ATs, Glutamic-pyruvic transaminase 2 (GPT2) uses glutamate to synthesize alanine, which is required for TGF- $\beta_1$ -induced mTORC1 activation via a Rags GTPase independent mechanism. TGF- $\beta_1$ -induced mTORC1 activation then regulates through a post-transcriptional mechanism Activating transcription factor 4 (ATF4), which in turn regulates the expression of the serine-glycine biosynthetic axis genes; PHGDH, PSAT1, PSPH and SHMT2. PSAT1 is critical for enhanced collagen synthesis independently of its capacity to generate serine.

## 4.6 Future work.

The present study highlights the importance in composition of cell culture media in modulating metabolic pathways. Certain metabolites found in human circulation are entirely absent in common medias, such as DMEM. This absence may place excessive pressure on the pathways which produce these metabolites and potentially help establish an unphysiological and artefactual metabolome that does not match that found in the disease. Future work would attempt to grow pHLFs in a more physiologically relevant media and evaluate the TGF- $\beta_1$ -induced changes reported in this thesis. For example, the excessive glutamine consumption of tumour cells grown *in vitro* was found to be a consequence of the supraphysiological concentrations of cystine in the media which promoted glutamate efflux, thus driving glutamine catabolism to replenish secreted glutamate stocks [258].

The question remains whether preventing the transcriptional upregulation of *ATF4* by TGF- $\beta_1$  would then limit ATF4 protein abundance, leading to a downregulating of the serine-glycine biosynthetic axis and thereby potentially preventing TGF- $\beta_1$ -induced collagen synthesis. Investigating the factor which leads to the upregulation in *ATF4* gene expression may provide insight into the early signalling pathways which lead to the metabolic reprogramming exhibited by TGF- $\beta_1$ -stimulated pHLFs. On this axis, the role of PSAT1 remains unclear and assessing the consequences on the metabolome and transcriptome following PSAT1 knockdown may help elucidate the mechanism by which PSAT1 regulates TGF- $\beta_1$ -induced collagen synthesis.

There remains the possibility that TGF- $\beta_1$ -stimulated cells rely on a singular glutamine transporter to facilitate the enhanced consumption of glutamine required to support collagen synthesis. Therefore, a selective silencing approach may help answer this possibility or reveal a compensatory network whereby silencing of one transporter leads to an enhancement or compensation of another transporter.

The mechanism by which alanine regulates mTORC1 activity remains unsolved and the data in this thesis suggests it is independent of the Rag-GTPases. Thus far, only glutamine has been shown to be sensed by mTORC1 in a Rags-independent manner. Investigating the identified Rags-independent pathways and whether their inhibition limits the reactivation of mTORC1 activity following a period of alanine withdrawal may help reveal the sensing mechanism for alanine.

Lastly, future work could examine the metabolic fates of *de novo* biosynthesized amino acids and  $\alpha$ -ketoglutarate which help support the bioenergetic and biomolecular demands for TGF- $\beta_1$ -induced collagen synthesis. Whether alanine mediates collagen synthesis, in addition to its role in maintaining mTORC1 activation (which is critical for TGF- $\beta_1$ -enhanced collagen synthesis), through its function as a component of the collagen polypeptide remains unanswered.

## References.

1. Gribbin, J., et al., *Incidence and mortality of idiopathic pulmonary fibrosis and sarcoidosis in the UK*. Thorax, 2006. **61**(11): p. 980-5.
2. Raghu, G., et al., *Diagnosis of Idiopathic Pulmonary Fibrosis. An Official ATS/ERS/JRS/ALAT Clinical Practice Guideline*. Am J Respir Crit Care Med, 2018. **198**(5): p. e44-e68.
3. Glassberg, M.K., *Overview of idiopathic pulmonary fibrosis, evidence-based guidelines, and recent developments in the treatment landscape*. Am J Manag Care, 2019. **25**(11 Suppl): p. S195-S203.
4. Nakamura, Y. and T. Suda, *Idiopathic Pulmonary Fibrosis: Diagnosis and Clinical Manifestations*. Clin Med Insights Circ Respir Pulm Med, 2015. **9**(Suppl 1): p. 163-71.
5. Galioto, F., et al., *Complications in Idiopathic Pulmonary Fibrosis: Focus on Their Clinical and Radiological Features*. Diagnostics (Basel), 2020. **10**(7).
6. Zhang, Y., et al., *Histopathological and molecular analysis of idiopathic pulmonary fibrosis lungs from patients treated with pirfenidone or nintedanib*. Histopathology, 2019. **74**(2): p. 341-349.
7. Nicholson, A.G., et al., *The relationship between individual histologic features and disease progression in idiopathic pulmonary fibrosis*. Am J Respir Crit Care Med, 2002. **166**(2): p. 173-7.
8. Izumi, S., M. Iikura, and S. Hirano, *Prednisone, azathioprine, and N-acetylcysteine for pulmonary fibrosis*. N Engl J Med, 2012. **367**(9): p. 870; author reply 870-1.
9. Kaarteenaho, R., *The current position of surgical lung biopsy in the diagnosis of idiopathic pulmonary fibrosis*. Respir Res, 2013. **14**: p. 43.
10. Flaherty, K.R., et al., *Safety of nintedanib added to pirfenidone treatment for idiopathic pulmonary fibrosis*. Eur Respir J, 2018. **52**(2).
11. Hajari Case, A. and P. Johnson, *Clinical use of nintedanib in patients with idiopathic pulmonary fibrosis*. BMJ Open Respir Res, 2017. **4**(1): p. e000192.
12. Schaefer, C.J., et al., *Antifibrotic activities of pirfenidone in animal models*. Eur Respir Rev, 2011. **20**(120): p. 85-97.
13. Naqvi, M., *A comparison of pirfenidone versus nintedanib for the management of idiopathic pulmonary fibrosis*. European Respiratory Journal, 2018.
14. Heukels, P., et al., *Inflammation and immunity in IPF pathogenesis and treatment*. Respir Med, 2019. **147**: p. 79-91.
15. Morawiec, E., et al., *Exacerbations of idiopathic pulmonary fibrosis treated with corticosteroids and cyclophosphamide pulses*. Eur Respir J, 2011. **38**(6): p. 1487-9.
16. Cerri, S., et al., *Occurrence of idiopathic pulmonary fibrosis during immunosuppressive treatment: a case report*. J Med Case Rep, 2016. **10**: p. 127.
17. Wolters, P.J., et al., *Time for a change: is idiopathic pulmonary fibrosis still idiopathic and only fibrotic?* Lancet Respir Med, 2018. **6**(2): p. 154-160.
18. Mathai, S.K. and D.A. Schwartz, *Taking the "I" out of IPF*. Eur Respir J, 2015. **45**(6): p. 1539-41.
19. Camelo, A., et al., *The epithelium in idiopathic pulmonary fibrosis: breaking the barrier*. Front Pharmacol, 2014. **4**: p. 173.
20. Chilosi, M., et al., *Epithelial stem cell exhaustion in the pathogenesis of idiopathic pulmonary fibrosis*. Sarcoidosis Vasc Diffuse Lung Dis, 2010. **27**(1): p. 7-18.
21. Schafer, M.J., et al., *Cellular senescence mediates fibrotic pulmonary disease*. Nat Commun, 2017. **8**: p. 14532.

22. Zank, D.C., et al., *Idiopathic Pulmonary Fibrosis: Aging, Mitochondrial Dysfunction, and Cellular Bioenergetics*. *Front Med (Lausanne)*, 2018. **5**: p. 10.
23. Lawson, W.E., et al., *Endoplasmic reticulum stress in alveolar epithelial cells is prominent in IPF: association with altered surfactant protein processing and herpesvirus infection*. *Am J Physiol Lung Cell Mol Physiol*, 2008. **294**(6): p. L1119-26.
24. Borie, R., et al., *The MUC5B variant is associated with idiopathic pulmonary fibrosis but not with systemic sclerosis interstitial lung disease in the European Caucasian population*. *PLoS One*, 2013. **8**(8): p. e70621.
25. Joyce Lee, E.D., Alani Estrella, Alex Schulick, Ivana Yang, Paul Wolters, David Schwartz, *MUC5B is expressed by bronchoalveolar epithelia and is associated with ER stress in idiopathic pulmonary fibrosis and rheumatoid arthritis associated interstitial lung disease*. *European Respiratory Journal* 2018. **52**: PA3711.
26. Jin, Y., L.Q. Peng, and A.L. Zhao, *Hyperoxia induces the apoptosis of alveolar epithelial cells and changes of pulmonary surfactant proteins*. *Eur Rev Med Pharmacol Sci*, 2018. **22**(2): p. 492-497.
27. Tanjore, H., T.S. Blackwell, and W.E. Lawson, *Emerging evidence for endoplasmic reticulum stress in the pathogenesis of idiopathic pulmonary fibrosis*. *Am J Physiol Lung Cell Mol Physiol*, 2012. **302**(8): p. L721-9.
28. Garcia, C.K., *Idiopathic pulmonary fibrosis: update on genetic discoveries*. *Proc Am Thorac Soc*, 2011. **8**(2): p. 158-62.
29. Allen, R.J., et al., *Genome-Wide Association Study of Susceptibility to Idiopathic Pulmonary Fibrosis*. *Am J Respir Crit Care Med*, 2020. **201**(5): p. 564-574.
30. Woodcock, H.V., et al., *The mTORC1/4E-BP1 axis represents a critical signaling node during fibrogenesis*. *Nat Commun*, 2019. **10**(1): p. 6.
31. White, E.S., *Lung extracellular matrix and fibroblast function*. *Ann Am Thorac Soc*, 2015. **12** **Suppl 1**: p. S30-3.
32. Nho, R.S., et al., *Pathological alteration of FoxO3a activity promotes idiopathic pulmonary fibrosis fibroblast proliferation on type I collagen matrix*. *Am J Pathol*, 2011. **179**(5): p. 2420-30.
33. Mehrad, B., M.D. Burdick, and R.M. Strieter, *Fibrocyte CXCR4 regulation as a therapeutic target in pulmonary fibrosis*. *Int J Biochem Cell Biol*, 2009. **41**(8-9): p. 1708-18.
34. Onder, T.T., et al., *Loss of E-cadherin promotes metastasis via multiple downstream transcriptional pathways*. *Cancer Res*, 2008. **68**(10): p. 3645-54.
35. Nieto, M.A., et al., *Emt: 2016*. *Cell*, 2016. **166**(1): p. 21-45.
36. Yao, L., et al., *Paracrine signalling during ZEB1-mediated epithelial-mesenchymal transition augments local myofibroblast differentiation in lung fibrosis*. *Cell Death Differ*, 2019. **26**(5): p. 943-957.
37. Rock, J.R., et al., *Multiple stromal populations contribute to pulmonary fibrosis without evidence for epithelial to mesenchymal transition*. *Proc Natl Acad Sci U S A*, 2011. **108**(52): p. E1475-83.
38. Xu, Y.D., et al., *Release of biologically active TGF-beta1 by alveolar epithelial cells results in pulmonary fibrosis*. *Am J Physiol Lung Cell Mol Physiol*, 2003. **285**(3): p. L527-39.
39. Last, J.A., A.D. Siefkin, and K.M. Reiser, *Type I collagen content is increased in lungs of patients with adult respiratory distress syndrome*. *Thorax*, 1983. **38**(5): p. 364-8.
40. Madri, J.A. and H. Furthmayr, *Collagen polymorphism in the lung. An immunochemical study of pulmonary fibrosis*. *Hum Pathol*, 1980. **11**(4): p. 353-66.
41. Tatler, A.L. and G. Jenkins, *TGF-beta activation and lung fibrosis*. *Proc Am Thorac Soc*, 2012. **9**(3): p. 130-6.
42. Di Lullo, G.A., et al., *Mapping the ligand-binding sites and disease-associated mutations on the most abundant protein in the human, type I collagen*. *J Biol Chem*, 2002. **277**(6): p. 4223-31.

43. Wolters, P.J., H.R. Collard, and K.D. Jones, *Pathogenesis of idiopathic pulmonary fibrosis*. *Annu Rev Pathol*, 2014. **9**: p. 157-79.
44. Marinkovic, A., F. Liu, and D.J. Tschumperlin, *Matrices of physiologic stiffness potentially inactivate idiopathic pulmonary fibrosis fibroblasts*. *Am J Respir Cell Mol Biol*, 2013. **48**(4): p. 422-30.
45. Gelse, K., E. Poschl, and T. Aigner, *Collagens--structure, function, and biosynthesis*. *Adv Drug Deliv Rev*, 2003. **55**(12): p. 1531-46.
46. Xia, H., et al., *Pathological integrin signaling enhances proliferation of primary lung fibroblasts from patients with idiopathic pulmonary fibrosis*. *J Exp Med*, 2008. **205**(7): p. 1659-72.
47. Khalil, N., et al., *TGF-beta 1, but not TGF-beta 2 or TGF-beta 3, is differentially present in epithelial cells of advanced pulmonary fibrosis: an immunohistochemical study*. *Am J Respir Cell Mol Biol*, 1996. **14**(2): p. 131-8.
48. Yue, X., B. Shan, and J.A. Lasky, *TGF-beta: Titan of Lung Fibrogenesis*. *Curr Enzym Inhib*, 2010. **6**(2).
49. Branton, M.H. and J.B. Kopp, *TGF-beta and fibrosis*. *Microbes Infect*, 1999. **1**(15): p. 1349-65.
50. Varga, J. and B. Pasche, *Antittransforming growth factor-beta therapy in fibrosis: recent progress and implications for systemic sclerosis*. *Curr Opin Rheumatol*, 2008. **20**(6): p. 720-8.
51. Tarantal, A.F., et al., *Overexpression of transforming growth factor-beta1 in fetal monkey lung results in prenatal pulmonary fibrosis*. *Eur Respir J*, 2010. **36**(4): p. 907-14.
52. Leivonen, S.K., et al., *TGF-beta-elicited induction of tissue inhibitor of metalloproteinases (TIMP)-3 expression in fibroblasts involves complex interplay between Smad3, p38alpha, and ERK1/2*. *PLoS One*, 2013. **8**(2): p. e57474.
53. Liu, Y., et al., *Transforming growth factor-beta (TGF-beta)-mediated connective tissue growth factor (CTGF) expression in hepatic stellate cells requires Stat3 signaling activation*. *J Biol Chem*, 2013. **288**(42): p. 30708-19.
54. Jenkins, R.G., et al., *Ligation of protease-activated receptor 1 enhances alpha(v)beta6 integrin-dependent TGF-beta activation and promotes acute lung injury*. *J Clin Invest*, 2006. **116**(6): p. 1606-14.
55. Sun, K.H., et al., *alpha-Smooth muscle actin is an inconsistent marker of fibroblasts responsible for force-dependent TGFbeta activation or collagen production across multiple models of organ fibrosis*. *Am J Physiol Lung Cell Mol Physiol*, 2016. **310**(9): p. L824-36.
56. Derynck, R. and Y.E. Zhang, *Smad-dependent and Smad-independent pathways in TGF-beta family signalling*. *Nature*, 2003. **425**(6958): p. 577-84.
57. Hayes, S., A. Chawla, and S. Corvera, *TGF beta receptor internalization into EEA1-enriched early endosomes: role in signaling to Smad2*. *J Cell Biol*, 2002. **158**(7): p. 1239-49.
58. Verrecchia, F. and A. Mauviel, *Transforming growth factor-beta signaling through the Smad pathway: role in extracellular matrix gene expression and regulation*. *J Invest Dermatol*, 2002. **118**(2): p. 211-5.
59. Flanders, K.C., *Smad3 as a mediator of the fibrotic response*. *Int J Exp Pathol*, 2004. **85**(2): p. 47-64.
60. Zhang, L., et al., *Smad2 protects against TGF-beta1/Smad3-mediated collagen synthesis in human hepatic stellate cells during hepatic fibrosis*. *Mol Cell Biochem*, 2015. **400**(1-2): p. 17-28.
61. Zhu, H., et al., *A SMAD ubiquitin ligase targets the BMP pathway and affects embryonic pattern formation*. *Nature*, 1999. **400**(6745): p. 687-93.
62. Zhang, Y.E., *Non-Smad pathways in TGF-beta signaling*. *Cell Res*, 2009. **19**(1): p. 128-39.
63. Jhanwar-Uniyal, M., et al., *Diverse signaling mechanisms of mTOR complexes: mTORC1 and mTORC2 in forming a formidable relationship*. *Adv Biol Regul*, 2019. **72**: p. 51-62.
64. Laplante, M. and D.M. Sabatini, *mTOR signaling in growth control and disease*. *Cell*, 2012. **149**(2): p. 274-93.

65. Chen, C.Y., et al., *PTEN: Tumor Suppressor and Metabolic Regulator*. Front Endocrinol (Lausanne), 2018. **9**: p. 338.
66. Populo, H., J.M. Lopes, and P. Soares, *The mTOR signalling pathway in human cancer*. Int J Mol Sci, 2012. **13**(2): p. 1886-918.
67. Qin, X., B. Jiang, and Y. Zhang, *4E-BP1, a multifactor regulated multifunctional protein*. Cell Cycle, 2016. **15**(6): p. 781-6.
68. Mercer, P.F., et al., *Exploration of a potent PI3 kinase/mTOR inhibitor as a novel anti-fibrotic agent in IPF*. Thorax, 2016. **71**(8): p. 701-11.
69. Zhang, X.L., et al., *PI3K/Akt signaling is involved in the pathogenesis of bleomycin-induced pulmonary fibrosis via regulation of epithelial-mesenchymal transition*. Mol Med Rep, 2016. **14**(6): p. 5699-5706.
70. Xu, F., et al., *Roles of the PI3K/AKT/mTOR signalling pathways in neurodegenerative diseases and tumours*. Cell Biosci, 2020. **10**: p. 54.
71. Yi, J.Y., I. Shin, and C.L. Arteaga, *Type I transforming growth factor beta receptor binds to and activates phosphatidylinositol 3-kinase*. J Biol Chem, 2005. **280**(11): p. 10870-6.
72. Dan, H.C., et al., *Akt-dependent activation of mTORC1 complex involves phosphorylation of mTOR (mammalian target of rapamycin) by IkkappaB kinase alpha (IKKalpha)*. J Biol Chem, 2014. **289**(36): p. 25227-40.
73. Angarola, B. and S.M. Ferguson, *Weak membrane interactions allow Rheb to activate mTORC1 signaling without major lysosome enrichment*. Mol Biol Cell, 2019. **30**(22): p. 2750-2760.
74. Manning, B.D., et al., *Identification of the tuberous sclerosis complex-2 tumor suppressor gene product tuberlin as a target of the phosphoinositide 3-kinase/akt pathway*. Mol Cell, 2002. **10**(1): p. 151-62.
75. Shang, C., et al., *Iron chelation inhibits mTORC1 signaling involving activation of AMPK and REDD1/Bnip3 pathways*. Oncogene, 2020. **39**(29): p. 5201-5213.
76. Anandapadamanaban, M., et al., *Architecture of human Rag GTPase heterodimers and their complex with mTORC1*. Science, 2019. **366**(6462): p. 203-210.
77. Brady, O.A., H.I. Diab, and R. Puertollano, *Rags to riches: Amino acid sensing by the Rag GTPases in health and disease*. Small GTPases, 2016. **7**(4): p. 197-206.
78. Sancak, Y., et al., *Ragulator-Rag complex targets mTORC1 to the lysosomal surface and is necessary for its activation by amino acids*. Cell, 2010. **141**(2): p. 290-303.
79. Gu, X., et al., *SAMTOR is an S-adenosylmethionine sensor for the mTORC1 pathway*. Science, 2017. **358**(6364): p. 813-818.
80. Shen, K. and D.M. Sabatini, *Ragulator and SLC38A9 activate the Rag GTPases through noncanonical GEF mechanisms*. Proc Natl Acad Sci U S A, 2018. **115**(38): p. 9545-9550.
81. Selvarajah, B., et al., *mTORC1 amplifies the ATF4-dependent de novo serine-glycine pathway to supply glycine during TGF-beta1-induced collagen biosynthesis*. Sci Signal, 2019. **12**(582).
82. Pavlova, N.N. and C.B. Thompson, *The Emerging Hallmarks of Cancer Metabolism*. Cell Metab, 2016. **23**(1): p. 27-47.
83. Hewitson, T.D. and E.R. Smith, *A Metabolic Reprogramming of Glycolysis and Glutamine Metabolism Is a Requisite for Renal Fibrogenesis-Why and How?* Front Physiol, 2021. **12**: p. 645857.
84. Henderson, J., et al., *Metabolic reprogramming of glycolysis and glutamine metabolism are key events in myofibroblast transition in systemic sclerosis pathogenesis*. J Cell Mol Med, 2020. **24**(23): p. 14026-14038.
85. Tsukamoto, H., *Metabolic reprogramming and cell fate regulation in alcoholic liver disease*. Pancreatology, 2015. **15**(4 Suppl): p. S61-5.
86. Wei, Q., et al., *Glycolysis inhibitors suppress renal interstitial fibrosis via divergent effects on fibroblasts and tubular cells*. Am J Physiol Renal Physiol, 2019. **316**(6): p. F1162-F1172.

87. Gao, G., B. Gong, and W. Shen, *Meta-analysis of the additional value of integrated 18FDG PET-CT for tumor distant metastasis staging: comparison with 18FDG PET alone and CT alone*. *Surg Oncol*, 2013. **22**(3): p. 195-200.
88. Groves, A.M., et al., *Idiopathic pulmonary fibrosis and diffuse parenchymal lung disease: implications from initial experience with 18F-FDG PET/CT*. *J Nucl Med*, 2009. **50**(4): p. 538-45.
89. Zhao, Y.D., et al., *Metabolic heterogeneity of idiopathic pulmonary fibrosis: a metabolomic study*. *BMJ Open Respir Res*, 2017. **4**(1): p. e000183.
90. Bargagli, E., et al., *Metabolic Dysregulation in Idiopathic Pulmonary Fibrosis*. *Int J Mol Sci*, 2020. **21**(16).
91. Yang, M. and K.H. Vousden, *Serine and one-carbon metabolism in cancer*. *Nat Rev Cancer*, 2016. **16**(10): p. 650-62.
92. Amelio, I., et al., *Serine and glycine metabolism in cancer*. *Trends Biochem Sci*, 2014. **39**(4): p. 191-8.
93. Vandekeere, S., et al., *Serine Synthesis via PHGDH Is Essential for Heme Production in Endothelial Cells*. *Cell Metab*, 2018. **28**(4): p. 573-587 e13.
94. Mullarky, E., et al., *Inhibition of 3-phosphoglycerate dehydrogenase (PHGDH) by indole amides abrogates de novo serine synthesis in cancer cells*. *Bioorg Med Chem Lett*, 2019. **29**(17): p. 2503-2510.
95. DeBerardinis, R.J., *Serine metabolism: some tumors take the road less traveled*. *Cell Metabolism*, 2012.
96. Reid, M.A., et al., *Serine synthesis through PHGDH coordinates nucleotide levels by maintaining central carbon metabolism*. *Nat Commun*, 2018. **9**(1): p. 5442.
97. Possemato, R., et al., *Functional genomics reveal that the serine synthesis pathway is essential in breast cancer*. *Nature*, 2011. **476**(7360): p. 346-50.
98. Pacold, M.E., et al., *A PHGDH inhibitor reveals coordination of serine synthesis and one-carbon unit fate*. *Nat Chem Biol*, 2016. **12**(6): p. 452-8.
99. Wang, H., et al., *Overexpression of PSAT1 regulated by G9A sustains cell proliferation in colorectal cancer*. *Signal Transduct Target Ther*, 2020. **5**(1): p. 47.
100. Chan, Y.C., et al., *Overexpression of PSAT1 promotes metastasis of lung adenocarcinoma by suppressing the IRF1-IFN $\gamma$  axis*. *Oncogene*, 2020. **39**(12): p. 2509-2522.
101. Yang, Y., et al., *PSAT1 regulates cyclin D1 degradation and sustains proliferation of non-small cell lung cancer cells*. *Int J Cancer*, 2015. **136**(4): p. E39-50.
102. Vie, N., et al., *Overexpression of phosphoserine aminotransferase PSAT1 stimulates cell growth and increases chemoresistance of colon cancer cells*. *Mol Cancer*, 2008. **7**: p. 14.
103. Liu, M., et al., *A cluster of metabolism-related genes predict prognosis and progression of clear cell renal cell carcinoma*. *Sci Rep*, 2020. **10**(1): p. 12949.
104. Hwang, I.Y., et al., *Psat1-Dependent Fluctuations in alpha-Ketoglutarate Affect the Timing of ESC Differentiation*. *Cell Metab*, 2016. **24**(3): p. 494-501.
105. Herzfeld, A., M.A. Legg, and O. Greengard, *Human colon tumors: enzymic and histological characteristics*. *Cancer*, 1978. **42**(3): p. 1280-3.
106. Pollari, S., et al., *Enhanced serine production by bone metastatic breast cancer cells stimulates osteoclastogenesis*. *Breast Cancer Res Treat*, 2011. **125**(2): p. 421-30.
107. Park, S.M., et al., *Phosphoserine Phosphatase Promotes Lung Cancer Progression through the Dephosphorylation of IRS-1 and a Noncanonical L-Serine-Independent Pathway*. *Mol Cells*, 2019. **42**(8): p. 604-616.
108. Bachelor, M.A., Y. Lu, and D.M. Owens, *L-3-Phosphoserine phosphatase (PSPH) regulates cutaneous squamous cell carcinoma proliferation independent of L-serine biosynthesis*. *J Dermatol Sci*, 2011. **63**(3): p. 164-72.
109. Liao, L., et al., *PSPH Mediates the Metastasis and Proliferation of Non-small Cell Lung Cancer through MAPK Signaling Pathways*. *Int J Biol Sci*, 2019. **15**(1): p. 183-194.

110. Stover, P. and V. Schirch, *Serine hydroxymethyltransferase catalyzes the hydrolysis of 5,10-methenyltetrahydrofolate to 5-formyltetrahydrofolate*. J Biol Chem, 1990. **265**(24): p. 14227-33.
111. Giardina, G., et al., *How pyridoxal 5'-phosphate differentially regulates human cytosolic and mitochondrial serine hydroxymethyltransferase oligomeric state*. FEBS J, 2015. **282**(7): p. 1225-41.
112. Giardina, G., et al., *The catalytic activity of serine hydroxymethyltransferase is essential for de novo nuclear dTMP synthesis in lung cancer cells*. FEBS J, 2018. **285**(17): p. 3238-3253.
113. Appaji Rao, N., et al., *Structure-function relationship in serine hydroxymethyltransferase*. Biochim Biophys Acta, 2003. **1647**(1-2): p. 24-9.
114. Walden, M., et al., *Metabolic control of BRISC-SHMT2 assembly regulates immune signalling*. Nature, 2019. **570**(7760): p. 194-199.
115. Melendez-Hevia, E. and P.D. Paz-Lugo, *Branch-point stoichiometry can generate weak links in metabolism: the case of glycine biosynthesis*. J Biosci, 2008. **33**(5): p. 771-80.
116. Gonen, N. and Y.G. Assaraf, *Antifolates in cancer therapy: structure, activity and mechanisms of drug resistance*. Drug Resist Updat, 2012. **15**(4): p. 183-210.
117. Ning, S., et al., *SHMT2 Overexpression Predicts Poor Prognosis in Intrahepatic Cholangiocarcinoma*. Gastroenterol Res Pract, 2018. **2018**: p. 4369253.
118. Garcia-Canaveras, J.C., et al., *SHMT inhibition is effective and synergizes with methotrexate in T-cell acute lymphoblastic leukemia*. Leukemia, 2020.
119. Ducker, G.S., et al., *Human SHMT inhibitors reveal defective glycine import as a targetable metabolic vulnerability of diffuse large B-cell lymphoma*. Proc Natl Acad Sci U S A, 2017. **114**(43): p. 11404-11409.
120. Dash, S., Y. Aydin, and T. Wu, *Integrated stress response in hepatitis C promotes Nrf2-related chaperone-mediated autophagy: A novel mechanism for host-microbe survival and HCC development in liver cirrhosis*. Semin Cell Dev Biol, 2020. **101**: p. 20-35.
121. B'Chir, W., et al., *The eIF2alpha/ATF4 pathway is essential for stress-induced autophagy gene expression*. Nucleic Acids Res, 2013. **41**(16): p. 7683-99.
122. DeNicola, G.M., et al., *NRF2 regulates serine biosynthesis in non-small cell lung cancer*. Nat Genet, 2015. **47**(12): p. 1475-81.
123. Ye, J., et al., *The GCN2-ATF4 pathway is critical for tumour cell survival and proliferation in response to nutrient deprivation*. EMBO J, 2010. **29**(12): p. 2082-96.
124. Zhang, P., et al., *The GCN2 eIF2alpha kinase is required for adaptation to amino acid deprivation in mice*. Mol Cell Biol, 2002. **22**(19): p. 6681-8.
125. Pathria, G., et al., *Targeting the Warburg effect via LDHA inhibition engages ATF4 signaling for cancer cell survival*. EMBO J, 2018. **37**(20).
126. Zhao, E., et al., *KDM4C and ATF4 Cooperate in Transcriptional Control of Amino Acid Metabolism*. Cell Rep, 2016. **14**(3): p. 506-519.
127. Ding, J., et al., *The histone H3 methyltransferase G9A epigenetically activates the serine-glycine synthesis pathway to sustain cancer cell survival and proliferation*. Cell Metab, 2013. **18**(6): p. 896-907.
128. Tonelli, C., I.I.C. Chio, and D.A. Tuveson, *Transcriptional Regulation by Nrf2*. Antioxid Redox Signal, 2018. **29**(17): p. 1727-1745.
129. Thimmulappa, R.K., et al., *Identification of Nrf2-regulated genes induced by the chemopreventive agent sulforaphane by oligonucleotide microarray*. Cancer Res, 2002. **62**(18): p. 5196-203.
130. Robledinos-Anton, N., et al., *Activators and Inhibitors of NRF2: A Review of Their Potential for Clinical Development*. Oxid Med Cell Longev, 2019. **2019**: p. 9372182.
131. Ye, P., et al., *Nrf2- and ATF4-dependent upregulation of xCT modulates the sensitivity of T24 bladder carcinoma cells to proteasome inhibition*. Mol Cell Biol, 2014. **34**(18): p. 3421-34.

132. Sarcinelli, C., et al., *ATF4-Dependent NRF2 Transcriptional Regulation Promotes Antioxidant Protection during Endoplasmic Reticulum Stress*. *Cancers (Basel)*, 2020. **12**(3).
133. Solis, L.M., et al., *Nrf2 and Keap1 abnormalities in non-small cell lung carcinoma and association with clinicopathologic features*. *Clin Cancer Res*, 2010. **16**(14): p. 3743-53.
134. Xia, Y., et al., *Metabolic Reprogramming by MYCN Confers Dependence on the Serine-Glycine-One-Carbon Biosynthetic Pathway*. *Cancer Res*, 2019. **79**(15): p. 3837-3850.
135. Sun, L., et al., *cMyc-mediated activation of serine biosynthesis pathway is critical for cancer progression under nutrient deprivation conditions*. *Cell Res*, 2015. **25**(4): p. 429-44.
136. Sullivan, M.R., et al., *Increased Serine Synthesis Provides an Advantage for Tumors Arising in Tissues Where Serine Levels Are Limiting*. *Cell Metab*, 2019. **29**(6): p. 1410-1421 e4.
137. Choi, Y.K. and K.G. Park, *Targeting Glutamine Metabolism for Cancer Treatment*. *Biomol Ther (Seoul)*, 2018. **26**(1): p. 19-28.
138. Chan, W.K., et al., *Glutaminase Activity of L-Asparaginase Contributes to Durable Preclinical Activity against Acute Lymphoblastic Leukemia*. *Mol Cancer Ther*, 2019. **18**(9): p. 1587-1592.
139. Hensley, C.T., A.T. Wasti, and R.J. DeBerardinis, *Glutamine and cancer: cell biology, physiology, and clinical opportunities*. *J Clin Invest*, 2013. **123**(9): p. 3678-84.
140. Hulsewe, K.W., et al., *Pulmonary glutamine production: effects of sepsis and pulmonary infiltrates*. *Intensive Care Med*, 2003. **29**(10): p. 1833-6.
141. Mohiuddin, S.S. and D. Khattar, *Biochemistry, Ammonia*, in *StatPearls*. 2020: Treasure Island (FL).
142. Spinelli, J.B., et al., *Metabolic recycling of ammonia via glutamate dehydrogenase supports breast cancer biomass*. *Science*, 2017. **358**(6365): p. 941-946.
143. Lane, A.N. and T.W. Fan, *Regulation of mammalian nucleotide metabolism and biosynthesis*. *Nucleic Acids Res*, 2015. **43**(4): p. 2466-85.
144. Kodama, M., et al., *A shift in glutamine nitrogen metabolism contributes to the malignant progression of cancer*. *Nat Commun*, 2020. **11**(1): p. 1320.
145. Loffler, M., et al., *Pyrimidine pathways in health and disease*. *Trends Mol Med*, 2005. **11**(9): p. 430-7.
146. Robitaille, A.M., et al., *Quantitative phosphoproteomics reveal mTORC1 activates de novo pyrimidine synthesis*. *Science*, 2013. **339**(6125): p. 1320-3.
147. Nakashima, A., et al., *Association of CAD, a multifunctional protein involved in pyrimidine synthesis, with mLST8, a component of the mTOR complexes*. *J Biomed Sci*, 2013. **20**: p. 24.
148. Ahmed, N.K., R.C. Haggitt, and A.D. Welch, *Enzymes of salvage and de novo pathways of synthesis of pyrimidine nucleotides in human colorectal adenocarcinomas*. *Biochem Pharmacol*, 1982. **31**(15): p. 2485-8.
149. Del Cano-Ochoa, F., et al., *Characterization of the catalytic flexible loop in the dihydroorotase domain of the human multi-enzymatic protein CAD*. *J Biol Chem*, 2018. **293**(49): p. 18903-18913.
150. Altman, B.J., Z.E. Stine, and C.V. Dang, *From Krebs to clinic: glutamine metabolism to cancer therapy*. *Nat Rev Cancer*, 2016. **16**(11): p. 749.
151. Lopez de la Oliva, A.R., et al., *Nuclear Translocation of Glutaminase GLS2 in Human Cancer Cells Associates with Proliferation Arrest and Differentiation*. *Sci Rep*, 2020. **10**(1): p. 2259.
152. Cassago, A., et al., *Mitochondrial localization and structure-based phosphate activation mechanism of Glutaminase C with implications for cancer metabolism*. *Proc Natl Acad Sci U S A*, 2012. **109**(4): p. 1092-7.
153. Curthoys, N.P. and M. Watford, *Regulation of glutaminase activity and glutamine metabolism*. *Annu Rev Nutr*, 1995. **15**: p. 133-59.
154. Lampa, M., et al., *Glutaminase is essential for the growth of triple-negative breast cancer cells with a deregulated glutamine metabolism pathway and its suppression synergizes with mTOR inhibition*. *PLoS One*, 2017. **12**(9): p. e0185092.

155. Cui, H., et al., *Inhibition of Glutaminase 1 Attenuates Experimental Pulmonary Fibrosis*. Am J Respir Cell Mol Biol, 2019. **61**(4): p. 492-500.
156. Du, K., et al., *Increased Glutaminolysis Marks Active Scarring in Nonalcoholic Steatohepatitis Progression*. Cell Mol Gastroenterol Hepatol, 2020. **10**(1): p. 1-21.
157. Gowda, S., et al., *A review on laboratory liver function tests*. Pan Afr Med J, 2009. **3**: p. 17.
158. Smith, B., et al., *Addiction to Coupling of the Warburg Effect with Glutamine Catabolism in Cancer Cells*. Cell Rep, 2016. **17**(3): p. 821-836.
159. Cao, Y., et al., *Glutamic Pyruvate Transaminase GPT2 Promotes Tumorigenesis of Breast Cancer Cells by Activating Sonic Hedgehog Signaling*. Theranostics, 2017. **7**(12): p. 3021-3033.
160. Kim, M., et al., *Mitochondrial GPT2 plays a pivotal role in metabolic adaptation to the perturbation of mitochondrial glutamine metabolism*. Oncogene, 2019. **38**(24): p. 4729-4738.
161. Sun, W., et al., *Aspulvinone O, a natural inhibitor of GOT1 suppresses pancreatic ductal adenocarcinoma cells growth by interfering glutamine metabolism*. Cell Commun Signal, 2019. **17**(1): p. 111.
162. Feld, F.M., et al., *GOT1/AST1 expression status as a prognostic biomarker in pancreatic ductal adenocarcinoma*. Oncotarget, 2015. **6**(6): p. 4516-26.
163. Coloff, J.L., et al., *Differential Glutamate Metabolism in Proliferating and Quiescent Mammary Epithelial Cells*. Cell Metab, 2016. **23**(5): p. 867-80.
164. Smith, H.Q., et al., *Glutamate Dehydrogenase, a Complex Enzyme at a Crucial Metabolic Branch Point*. Neurochem Res, 2019. **44**(1): p. 117-132.
165. Plaitakis, A., et al., *The Glutamate Dehydrogenase Pathway and Its Roles in Cell and Tissue Biology in Health and Disease*. Biology (Basel), 2017. **6**(1).
166. Kim, A.Y. and E.J. Baik, *Glutamate Dehydrogenase as a Neuroprotective Target Against Neurodegeneration*. Neurochem Res, 2019. **44**(1): p. 147-153.
167. Chen, R., et al., *Hominoid-specific enzyme GLUD2 promotes growth of IDH1R132H glioma*. Proc Natl Acad Sci U S A, 2014. **111**(39): p. 14217-22.
168. Wu, G., et al., *Proline and hydroxyproline metabolism: implications for animal and human nutrition*. Amino Acids, 2011. **40**(4): p. 1053-63.
169. Tanner, J.J., S.M. Fendt, and D.F. Becker, *The Proline Cycle As a Potential Cancer Therapy Target*. Biochemistry, 2018. **57**(25): p. 3433-3444.
170. Schworer, S., et al., *Proline biosynthesis is a vent for TGFbeta-induced mitochondrial redox stress*. EMBO J, 2020. **39**(8): p. e103334.
171. Waitkus, M.S., B.H. Diplas, and H. Yan, *Biological Role and Therapeutic Potential of IDH Mutations in Cancer*. Cancer Cell, 2018. **34**(2): p. 186-195.
172. Goitre, L., et al., *Up-regulation of NADPH oxidase-mediated redox signaling contributes to the loss of barrier function in KRIT1 deficient endothelium*. Sci Rep, 2017. **7**(1): p. 8296.
173. Arner, E.S. and A. Holmgren, *Physiological functions of thioredoxin and thioredoxin reductase*. Eur J Biochem, 2000. **267**(20): p. 6102-9.
174. Kattih, B., et al., *IDH1/2 mutations in acute myeloid leukemia patients and risk of coronary artery disease and cardiac dysfunction-a retrospective propensity score analysis*. Leukemia, 2020.
175. Aref, S., et al., *Prevalence and Clinical Effect of IDH1 and IDH2 Mutations Among Cytogenetically Normal Acute Myeloid Leukemia Patients*. Clin Lymphoma Myeloma Leuk, 2015. **15**(9): p. 550-5.
176. Jezek, P., *2-Hydroxyglutarate in Cancer Cells*. Antioxid Redox Signal, 2020. **33**(13): p. 903-926.
177. Lu, C. and C.B. Thompson, *Metabolic regulation of epigenetics*. Cell Metab, 2012. **16**(1): p. 9-17.

178. Biggar, K.K. and S.S. Li, *Non-histone protein methylation as a regulator of cellular signalling and function*. Nat Rev Mol Cell Biol, 2015. **16**(1): p. 5-17.
179. Long, L.H. and B. Halliwell, *Artefacts in cell culture: alpha-Ketoglutarate can scavenge hydrogen peroxide generated by ascorbate and epigallocatechin gallate in cell culture media*. Biochem Biophys Res Commun, 2011. **406**(1): p. 20-4.
180. Andrianifahanana, M., et al., *Profibrotic up-regulation of glucose transporter 1 by TGF-beta involves activation of MEK and mammalian target of rapamycin complex 2 pathways*. FASEB J, 2016. **30**(11): p. 3733-3744.
181. Yin, X., et al., *Hexokinase 2 couples glycolysis with the profibrotic actions of TGF-beta*. Sci Signal, 2019. **12**(612).
182. Xie, N., et al., *Glycolytic Reprogramming in Myofibroblast Differentiation and Lung Fibrosis*. Am J Respir Crit Care Med, 2015. **192**(12): p. 1462-74.
183. Hamanaka, R.B., et al., *Inhibition of Phosphoglycerate Dehydrogenase Attenuates Bleomycin-induced Pulmonary Fibrosis*. Am J Respir Cell Mol Biol, 2018. **58**(5): p. 585-593.
184. Jung, M.Y., et al., *Fatty acid synthase is required for profibrotic TGF-beta signaling*. FASEB J, 2018. **32**(7): p. 3803-3815.
185. Donald McCarthy , A.K.S., Arnold Ha , Kamran Atabai ,, *Loss of Fatty Acid Synthase Increases the Severity of Lung Fibrosis by Preventing Collagen Resorption*. American Thoracic Society International Conference Abstracts, 2016.
186. Bernard, K., et al., *Glutaminolysis is required for transforming growth factor-beta1-induced myofibroblast differentiation and activation*. J Biol Chem, 2018. **293**(4): p. 1218-1228.
187. Ge, J., et al., *Glutaminolysis Promotes Collagen Translation and Stability via alpha-Ketoglutarate-mediated mTOR Activation and Proline Hydroxylation*. Am J Respir Cell Mol Biol, 2018. **58**(3): p. 378-390.
188. Hamanaka, R.B., et al., *Glutamine Metabolism Is Required for Collagen Protein Synthesis in Lung Fibroblasts*. Am J Respir Cell Mol Biol, 2019. **61**(5): p. 597-606.
189. Gross, M.I., et al., *Antitumor activity of the glutaminase inhibitor CB-839 in triple-negative breast cancer*. Mol Cancer Ther, 2014. **13**(4): p. 890-901.
190. Jin, L., et al., *Glutamate dehydrogenase 1 signals through antioxidant glutathione peroxidase 1 to regulate redox homeostasis and tumor growth*. Cancer Cell, 2015. **27**(2): p. 257-70.
191. Yoon, S., et al., *Clinical Implication of Serine Metabolism-Associated Enzymes in Colon Cancer*. Oncology, 2015. **89**(6): p. 351-9.
192. Mullarky, E., et al., *PHGDH amplification and altered glucose metabolism in human melanoma*. Pigment Cell Melanoma Res, 2011. **24**(6): p. 1112-5.
193. Liu, J., et al., *Phosphoglycerate dehydrogenase induces glioma cells proliferation and invasion by stabilizing forkhead box M1*. J Neurooncol, 2013. **111**(3): p. 245-55.
194. Li, A.M. and J. Ye, *The PHGDH enigma: Do cancer cells only need serine or also a redox modulator?* Cancer Lett, 2020. **476**: p. 97-105.
195. Chen, J., et al., *Phosphoglycerate dehydrogenase is dispensable for breast tumor maintenance and growth*. Oncotarget, 2013. **4**(12): p. 2502-11.
196. Locasale, J.W., et al., *Phosphoglycerate dehydrogenase diverts glycolytic flux and contributes to oncogenesis*. Nat Genet, 2011. **43**(9): p. 869-74.
197. Shan, L., et al., *mTOR Overactivation in Mesenchymal cells Aggravates CCl4- Induced liver Fibrosis*. Sci Rep, 2016. **6**: p. 36037.
198. Tedeschi, P.M., et al., *Contribution of serine, folate and glycine metabolism to the ATP, NADPH and purine requirements of cancer cells*. Cell Death Dis, 2013. **4**: p. e877.
199. Birsoy, K., et al., *Metabolic determinants of cancer cell sensitivity to glucose limitation and biguanides*. Nature, 2014. **508**(7494): p. 108-12.
200. Chen, Y.G., *Endocytic regulation of TGF-beta signaling*. Cell Res, 2009. **19**(1): p. 58-70.

201. Nguyen, M.Q., et al., *Targeting PHGDH Upregulation Reduces Glutathione Levels and Resensitizes Resistant NRAS-Mutant Melanoma to MAPK Kinase Inhibition*. *J Invest Dermatol*, 2020. **140**(11): p. 2242-2252 e7.
202. Escande-Beillard, N., et al., *Loss of PYCR2 Causes Neurodegeneration by Increasing Cerebral Glycine Levels via SHMT2*. *Neuron*, 2020. **107**(1): p. 82-94 e6.
203. Ye, J., et al., *Serine catabolism regulates mitochondrial redox control during hypoxia*. *Cancer Discov*, 2014. **4**(12): p. 1406-17.
204. Krishnan, N., M.B. Dickman, and D.F. Becker, *Proline modulates the intracellular redox environment and protects mammalian cells against oxidative stress*. *Free Radic Biol Med*, 2008. **44**(4): p. 671-81.
205. Shatsky, I.N., et al., *Cap-Independent Translation: What's in a Name?* *Trends Biochem Sci*, 2018. **43**(11): p. 882-895.
206. Stine, Z.E., et al., *MYC, Metabolism, and Cancer*. *Cancer Discov*, 2015. **5**(10): p. 1024-39.
207. Pitale, P.M., O. Gorbatyuk, and M. Gorbatyuk, *Neurodegeneration: Keeping ATF4 on a Tight Leash*. *Front Cell Neurosci*, 2017. **11**: p. 410.
208. Jackson, A.L., et al., *Position-specific chemical modification of siRNAs reduces "off-target" transcript silencing*. *RNA*, 2006. **12**(7): p. 1197-205.
209. Gonzalez-Gonzalez, A., et al., *Activating Transcription Factor 4 Modulates TGFbeta-Induced Aggressiveness in Triple-Negative Breast Cancer via SMAD2/3/4 and mTORC2 Signaling*. *Clin Cancer Res*, 2018. **24**(22): p. 5697-5709.
210. Baird, T.D. and R.C. Wek, *Eukaryotic initiation factor 2 phosphorylation and translational control in metabolism*. *Adv Nutr*, 2012. **3**(3): p. 307-21.
211. O'Leary, E.M., et al., *TGF-beta Promotes Metabolic Reprogramming in Lung Fibroblasts via mTORC1-dependent ATF4 Activation*. *Am J Respir Cell Mol Biol*, 2020. **63**(5): p. 601-612.
212. Park, Y., et al., *mTORC1 Balances Cellular Amino Acid Supply with Demand for Protein Synthesis through Post-transcriptional Control of ATF4*. *Cell Rep*, 2017. **19**(6): p. 1083-1090.
213. Yamaguchi, S., et al., *ATF4-mediated induction of 4E-BP1 contributes to pancreatic beta cell survival under endoplasmic reticulum stress*. *Cell Metab*, 2008. **7**(3): p. 269-76.
214. Xia, X., et al., *GCN2 controls the cellular checkpoint: potential target for regulating inflammation*. *Cell Death Discov*, 2018. **4**: p. 20.
215. Way, S.W. and B. Popko, *Harnessing the integrated stress response for the treatment of multiple sclerosis*. *Lancet Neurol*, 2016. **15**(4): p. 434-43.
216. Shoichet, B.K., *Interpreting steep dose-response curves in early inhibitor discovery*. *J Med Chem*, 2006. **49**(25): p. 7274-7.
217. Yang, C., et al., *Analysis of free amino acids in islets of Langerhans by high-performance liquid chromatography using pre-column derivatization with 4-chloro-7-nitrobenzo-2-oxa-1,3-diazole*. *J Sep Sci*, 2007. **30**(18): p. 3154-63.
218. Rosario, F.J., et al., *Mammalian target of rapamycin signalling modulates amino acid uptake by regulating transporter cell surface abundance in primary human trophoblast cells*. *J Physiol*, 2013. **591**(3): p. 609-25.
219. Baracco, E.E., et al., *alpha-Ketoglutarate inhibits autophagy*. *Aging (Albany NY)*, 2019. **11**(11): p. 3418-3431.
220. Gaglio, D., et al., *Oncogenic K-Ras decouples glucose and glutamine metabolism to support cancer cell growth*. *Mol Syst Biol*, 2011. **7**: p. 523.
221. Ulanet, D.B., et al., *Mesenchymal phenotype predisposes lung cancer cells to impaired proliferation and redox stress in response to glutaminase inhibition*. *PLoS One*, 2014. **9**(12): p. e115144.
222. Gao, S., et al., *PSAT1 is regulated by ATF4 and enhances cell proliferation via the GSK3beta/beta-catenin/cyclin D1 signaling pathway in ER-negative breast cancer*. *J Exp Clin Cancer Res*, 2017. **36**(1): p. 179.

223. Maddocks, O.D., et al., *Serine starvation induces stress and p53-dependent metabolic remodelling in cancer cells*. *Nature*, 2013. **493**(7433): p. 542-6.
224. Jain, M., et al., *Metabolite profiling identifies a key role for glycine in rapid cancer cell proliferation*. *Science*, 2012. **336**(6084): p. 1040-4.
225. Labuschagne, C.F., et al., *Serine, but not glycine, supports one-carbon metabolism and proliferation of cancer cells*. *Cell Rep*, 2014. **7**(4): p. 1248-58.
226. Mazat, J.P. and S. Ransac, *The Fate of Glutamine in Human Metabolism. The Interplay with Glucose in Proliferating Cells*. *Metabolites*, 2019. **9**(5).
227. Sharma, A., et al., *Fasting Blood Glucose Levels Provide Estimate of Duration and Progression of Pancreatic Cancer Before Diagnosis*. *Gastroenterology*, 2018. **155**(2): p. 490-500 e2.
228. Lepruvier, G. and B. Rotblat, *How does mTOR sense glucose starvation? AMPK is the usual suspect*. *Cell Death Discov*, 2020. **6**: p. 27.
229. Wang, L., et al., *Molecular link between glucose and glutamine consumption in cancer cells mediated by CtBP and SIRT4*. *Oncogenesis*, 2018. **7**(3): p. 26.
230. Still, E.R. and M.O. Yuneva, *Hopefully devoted to Q: targeting glutamine addiction in cancer*. *Br J Cancer*, 2017. **116**(11): p. 1375-1381.
231. Yoo, H.C., et al., *Glutamine reliance in cell metabolism*. *Exp Mol Med*, 2020. **52**(9): p. 1496-1516.
232. Yamada, D., et al., *Inhibition of the glutamine transporter SNAT1 confers neuroprotection in mice by modulating the mTOR-autophagy system*. *Commun Biol*, 2019. **2**: p. 346.
233. Morotti, M., et al., *Increased expression of glutamine transporter SNAT2/SLC38A2 promotes glutamine dependence and oxidative stress resistance, and is associated with worse prognosis in triple-negative breast cancer*. *Br J Cancer*, 2021. **124**(2): p. 494-505.
234. Bhutia, Y.D. and V. Ganapathy, *Glutamine transporters in mammalian cells and their functions in physiology and cancer*. *Biochim Biophys Acta*, 2016. **1863**(10): p. 2531-9.
235. Xiang, L., et al., *Glutaminase 1 expression in colorectal cancer cells is induced by hypoxia and required for tumor growth, invasion, and metastatic colonization*. *Cell Death Dis*, 2019. **10**(2): p. 40.
236. Choudhury, M., et al., *SIRT7-mediated modulation of glutaminase 1 regulates TGF-beta-induced pulmonary fibrosis*. *FASEB J*, 2020. **34**(7): p. 8920-8940.
237. Cleary, J.M. and G.I. Shapiro, *Development of phosphoinositide-3 kinase pathway inhibitors for advanced cancer*. *Curr Oncol Rep*, 2010. **12**(2): p. 87-94.
238. Brunn, G.J., et al., *Direct inhibition of the signaling functions of the mammalian target of rapamycin by the phosphoinositide 3-kinase inhibitors, wortmannin and LY294002*. *EMBO J*, 1996. **15**(19): p. 5256-67.
239. Bai, L., et al., *Glutaminolysis Epigenetically Regulates Antiapoptotic Gene Expression in Idiopathic Pulmonary Fibrosis Fibroblasts*. *Am J Respir Cell Mol Biol*, 2019. **60**(1): p. 49-57.
240. Abla, H., et al., *The multifaceted contribution of alpha-ketoglutarate to tumor progression: An opportunity to exploit?* *Semin Cell Dev Biol*, 2020. **98**: p. 26-33.
241. Eriksen, H.A., et al., *Type I and type III collagen synthesis and composition in the valve matrix in aortic valve stenosis*. *Atherosclerosis*, 2006. **189**(1): p. 91-8.
242. Buckle, R.M., *Blood Pyruvic and Alpha-Ketoglutaric Acids in Thiamine Deficiency*. *Metabolism*, 1965. **14**: p. 141-9.
243. Holmes, D.L., D.T. Vogt, and M. Lagunoff, *A CRISPR-Cas9 screen identifies mitochondrial translation as an essential process in latent KSHV infection of human endothelial cells*. *Proc Natl Acad Sci U S A*, 2020. **117**(45): p. 28384-28392.
244. Aquino-Galvez, A., et al., *Dysregulated expression of hypoxia-inducible factors augments myofibroblasts differentiation in idiopathic pulmonary fibrosis*. *Respir Res*, 2019. **20**(1): p. 130.
245. Virga, F., M. Ehling, and M. Mazzone, *Blood Vessel Proximity Shapes Cancer Cell Metabolism*. *Cell Metab*, 2019. **30**(1): p. 16-18.

246. Carmona-Fontaine, C., et al., *Metabolic origins of spatial organization in the tumor microenvironment*. Proc Natl Acad Sci U S A, 2017. **114**(11): p. 2934-2939.
247. Kumar, S., et al., *Intra-Tumoral Metabolic Zonation and Resultant Phenotypic Diversification Are Dictated by Blood Vessel Proximity*. Cell Metab, 2019. **30**(1): p. 201-211 e6.
248. Yamaguchi, M., et al., *Fibroblastic foci, covered with alveolar epithelia exhibiting epithelial-mesenchymal transition, destroy alveolar septa by disrupting blood flow in idiopathic pulmonary fibrosis*. Lab Invest, 2017. **97**(3): p. 232-242.
249. Caiola, E., et al., *Glutaminase Inhibition on NSCLC Depends on Extracellular Alanine Exploitation*. Cells, 2020. **9**(8).
250. Shang, W., X. Wei, and W. Ying, *Malate-aspartate shuttle inhibitor aminooxyacetic acid blocks lipopolysaccharides-induced activation of BV2 microglia*. Int J Physiol Pathophysiol Pharmacol, 2017. **9**(2): p. 58-63.
251. Dyachok, J., et al., *Amino Acids Regulate mTORC1 by an Obligate Two-step Mechanism*. J Biol Chem, 2016. **291**(43): p. 22414-22426.
252. Mitra, D., et al., *Abrogating GPT2 in triple-negative breast cancer inhibits tumor growth and promotes autophagy*. Int J Cancer, 2020.
253. Shimobayashi, M. and M.N. Hall, *Multiple amino acid sensing inputs to mTORC1*. Cell Res, 2016. **26**(1): p. 7-20.
254. Meng, D., et al., *Glutamine and asparagine activate mTORC1 independently of Rag GTPases*. J Biol Chem, 2020. **295**(10): p. 2890-2899.
255. Snaebjornsson, M.T. and A. Schulze, *Non-canonical functions of enzymes facilitate cross-talk between cell metabolic and regulatory pathways*. Exp Mol Med, 2018. **50**(4): p. 1-16.
256. Percudani, R. and A. Peracchi, *A genomic overview of pyridoxal-phosphate-dependent enzymes*. EMBO Rep, 2003. **4**(9): p. 850-4.
257. Perry, T.L., et al., *Failure of aminooxyacetic acid therapy in Huntington disease*. Neurology, 1980. **30**(7 Pt 1): p. 772-5.
258. Muir, A., et al., *Environmental cystine drives glutamine anaplerosis and sensitizes cancer cells to glutaminase inhibition*. Elife, 2017. **6**.



